

509401
166 PG

chapter **1**

N92-15431

POLAR OZONE

Coordinator

S. Solomon (USA)

Principal Authors

W. L. Grose (USA)

R. L. Jones (UK)

M. P. McCormick (USA)

M. J. Molina (USA)

A. O'Neill (UK)

L. R. Poole (USA)

K. P. Shine (UK)

S. Solomon (USA)

Other Contributors

R.A. Plumb (USA)

V. Pope (UK)

Chapter 1.

POLAR OZONE

TABLE OF CONTENTS

1.0	INTRODUCTION	1
1.1	CLIMATOLOGY OF THE OZONE TRENDS IN POLAR REGIONS	1
1.1.1	Ozone Measurements and Trend Detection	1
1.1.2	The Seasonal and Latitudinal Variability of Total Ozone	2
1.1.3	Observed Trends in the Total Ozone Column Content in Antarctica and Southern Mid-Latitudes	7
1.1.4	Suggested Explanations for the Antarctic Ozone Hole	15
1.1.5	Observed Trends in the Vertical Distribution of Ozone above Antarctica	17
1.1.6	Trends in Northern Hemisphere Ozone	20
1.2	CLIMATOLOGY OF POLAR STRATOSPHERIC CLOUDS (PSCs) IN BOTH POLAR REGIONS	23
1.2.1	Physical Characteristics	23
1.2.2	Seasonal Behavior of PSCs	27
1.2.3	Long-Term Trends in PSC Frequency and Intensity	33
1.2.4	Effect of PSCs on the Radiative Budget	36
1.3	PHYSICAL PROPERTIES OF POLAR STRATOSPHERIC CLOUDS	38
1.3.1	Laboratory Studies	39
1.3.2	Direct Supporting Evidence from Field Experiments	40
1.4	HETEROGENEOUS CHEMISTRY	43
1.5	GAS PHASE CHEMISTRY	45
1.5.1	Photochemical Processes of Importance in Polar Ozone Depletion	46
1.5.2	Laboratory Kinetics and Photochemistry	50
1.6	PHOTOCHEMISTRY OF THE ANTARCTIC SPRING	54
1.6.1	Reactive and Reservoir Chlorine	54
1.6.2	Reactive and Reservoir Nitrogen	62
1.6.3	Other Chemical Species	68
1.6.4	Modeling Studies of the Composition and Photochemistry	74

1.7	DYNAMICAL PROCESSES	82
1.7.1	Differences in Climatology Between the Two Hemispheres and Their Relationship to Observed Ozone Amounts	82
1.7.2	Role of Synoptic-Scale Disturbances	105
1.7.3	Processing of Antarctic Air	108
1.7.4	The Dilution Effect	110
1.8	TEMPERATURE TRENDS—CAUSES AND EFFECTS	117
1.8.1	Resume of Work Discussed by OTP (1989)	117
1.8.2	Other Recent Work	119
1.8.3	Causes of Temperature Trends	124
1.9	CALCULATED AND OBSERVED CHANGES IN ULTRAVIOLET RADIATION AT THE GROUND	127
1.10	ARCTIC PHOTOCHEMISTRY	130
1.10.1	Observations Prior to the 1988-1989 Arctic Winter	131
1.10.2	Conclusions from 1989 Research	138
1.11	PRINCIPAL CONCLUSIONS AND OUTSTANDING ISSUES	142
	REFERENCES AND BIBLIOGRAPHY	145

1.0 INTRODUCTION

The observation and interpretation of an unexpected, large ozone depletion over Antarctica (the ozone hole) has changed the international scientific view of stratospheric chemistry. The observations demonstrating the veracity, seasonal nature, and vertical structure of the Antarctic ozone hole are presented in Section 1.1, along with a brief description of the theoretical ideas first advanced to explain the phenomenon. Evidence for Arctic and mid-latitude ozone loss is also discussed. The chemical theory for Antarctic ozone depletion centers around the widespread occurrence of polar stratospheric clouds (PSCs) in Antarctic winter and spring; the climatology and radiative properties of these clouds represent the subject of Section 1.2. The clouds are believed to be of central importance in Antarctic ozone depletion because they provide a surface upon which important chemical reactions can take place that are not possible in the gas phase, and which greatly perturb the composition of the polar stratosphere. Laboratory studies of the physical properties of PSCs and the chemical reactions that likely take place upon them are described in Sections 1.3 and 1.4. Related gas phase chemical processes that subsequently influence ozone depletion are discussed in Section 1.5. Observations and interpretation of the chemical composition of the Antarctic stratosphere are described in Section 1.6, where it is shown that the observed, greatly enhanced abundances of chlorine monoxide in the Antarctic lower stratosphere are sufficient to explain much if not all of the Antarctic ozone decrease. The dynamic meteorology of both polar regions is the subject of Section 1.7, where important interannual and interhemispheric variations in dynamical processes are outlined and their likely roles in ozone depletion are discussed. Observations and interpretation of temperature trends in polar regions are reviewed in Section 1.8. Observations and calculations of changes in the penetration of ultraviolet radiation due to Antarctic ozone depletion are presented in Section 1.9. The photochemistry of the Arctic stratosphere in spring is described in Section 1.10, where the similarities and differences between the polar regions of the two hemispheres are explored. Finally, in Section 1.11 a summary is given of both the current state of understanding and outstanding issues.

1.1 CLIMATOLOGY OF THE OZONE TRENDS IN POLAR REGIONS

In this Section, ozone trends in polar regions are briefly reviewed; a more detailed and updated review of global ozone trends is the subject of Chapter 2 of this document. The distribution of total ozone deduced prior to the advent of the Antarctic ozone hole is first described and the primary processes that control the distribution of ozone in polar regions are identified. Such an understanding is critical to defining the background against which changes such as those associated with polar ozone trends must be evaluated and understood. Observations of the trends of total ozone in Antarctica are then summarized. It is shown that the Antarctic ozone hole originally detected by Farman et al. (1985a) has been confirmed with a broad range of studies from several international Antarctic stations as well as from satellite data. The observation of a dramatic hole in Antarctic ozone led to several important theories aimed at understanding its origin. These are briefly described in Section 1.1.4. Smaller observed trends at southern mid-latitudes may provide important clues regarding the mechanisms responsible for Antarctic ozone depletion, and are of interest in terms of the possible dilution of polar ozone decreases to lower latitudes (see Section 1.7). Observations of changes in the vertical distribution of Antarctic ozone and possible ozone changes in the Arctic and northern mid-latitudes are also discussed.

1.1.1 Ozone Measurements and Trend Detection

Worldwide ozone monitoring nominally began during the International Geophysical Year (IGY) in 1957, but only a very few stations have continuous records from 1957 to the present day. Ground-based total ozone monitoring is largely carried out using the ultraviolet absorption technique pioneered by Dobson.

POLAR OZONE

Satellite monitoring of total ozone began in 1970, and continuous global coverage dates back only to 1978. Satellite measurements of total ozone are principally based on detection of ultraviolet light backscattered from the troposphere (although research is underway to evaluate total ozone using infrared sensing methods). Thus, both routine ground-based and satellite observations are largely limited to those latitudes and seasons when the sun is above the horizon.

Detection of long-term trends is complicated by many factors including: a) natural variability, which must be estimated based on the available history of measurements and b) characterization of the long-term stability of the calibration of the instruments used. The absolute calibration of ground-based measurements can be tested and checked periodically. However, ground-based data from particular stations can be strongly influenced by natural fluctuations associated with variability in local dynamic conditions; these increase the variance of the data and therefore complicate attempts to deduce trends. In polar regions, local variability is particularly large due to steep latitudinal gradients in total ozone and large amplitudes of atmospheric waves (see Figure 1.1.2-3 below and Section 1.7). The extensive spatial coverage afforded by satellite data alleviates much of the local variability associated with single station measurements, but the absolute calibrations of many of the satellite instruments are subject to drift, which has not been measured while the instruments have been in space (a notable exception is the SAGE measurement technique, which is relatively insensitive to the absolute calibration). The shorter time history of the satellite ozone data as compared to some ground-based records also implies that less extensive temporal variability has been sampled (e.g., the variability associated with the 11-year solar cycle and its fluctuations from one cycle to another cannot be evaluated with a record as brief as 9 years). Use of both satellite and ground-based data sets in concert can greatly strengthen confidence in the trends evaluated from either in isolation, as discussed in detail by the International Ozone Trends Panel report (hereafter referred to as OTP, 1989).

1.1.2 The Seasonal and Latitudinal Variability of Total Ozone

Interest in atmospheric ozone was originally sparked by the work of Dobson and his collaborators, who correctly identified many of the factors that influence the column abundance and vertical distribution of atmospheric ozone. The relative magnitudes and changing roles of photochemical production, loss, and transport processes all play major roles in determining the ozone distribution. Figure 1.1.2-1 displays estimates of the time scale for photochemical destruction of ozone as a function of latitude and height for winter solstice from model calculations including a reasonably complete formulation of gas-phase photochemistry. Heterogeneous reactions and the subsequent photochemistry (see Sections 1.3–1.5) will markedly decrease the photochemical lifetime in polar regions in winter and spring, especially in the presence of polar stratospheric clouds and for anthropogenically perturbed chlorine abundances. Nevertheless, this figure provides useful insight into the behavior of the unperturbed stratosphere. Note the large seasonal differences in photochemical loss rates in polar regions, which are related to the seasonal cycle in solar illumination there.

Stratospheric ozone is produced primarily from photolysis of molecular oxygen, and its mixing ratio maximum occurs near 30–40 km, depending on season and latitude. The ozone concentration maximum is found at lower, denser levels near 15–30 km. In the lower stratosphere (below about 25 km), photochemical production of ozone is very slow due to the limited ultraviolet penetration to these levels, and the ozone densities there are dependent principally on a balance between downward transport from higher levels and local photochemical loss. Natural photochemical destruction of stratospheric ozone takes place mainly through catalytic cycles involving nitrogen and hydrogen free radicals (see for example, Brasseur and Solomon, 1984).

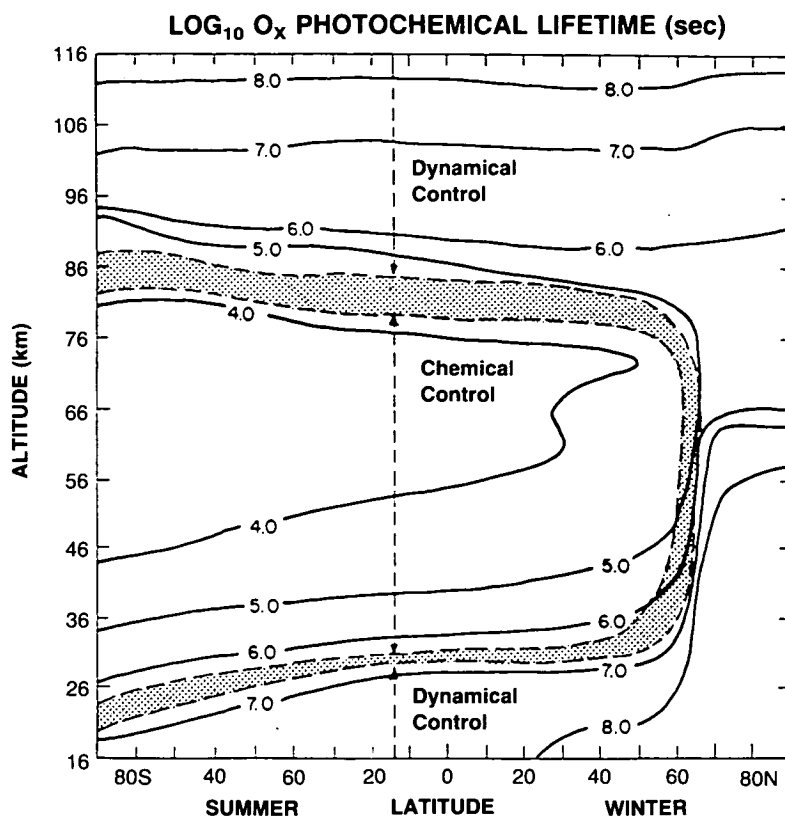


Figure 1.1.2-1 Logarithm of the computed lifetime of the odd oxygen family in Northern Hemisphere winter versus latitude and height, from the Garcia-Solomon two-dimensional model (from Garcia and Solomon, 1985). Regions dominated by chemical and dynamical processes are indicated.

The basic features of the seasonal evolution of total ozone in the northern and southern polar regions were first elucidated by Dobson and co-workers, who compared the earliest ground-based total ozone measurements from Halley Bay, Antarctica, to those from the Arctic station at Spitzbergen. Figure 1.1.2-2 displays the measured annual cycles of total ozone at the two stations. Dobson noted that these differences are indicative of fundamental asymmetries in the atmospheric dynamics of the Northern and Southern Hemispheres, which will be explored below and in more detail in Section 1.7. This natural difference in winter and spring ozone abundances between the two hemispheres should not be confused with the ozone hole.

Dobson et al. (1928) pointed out that total ozone minima are observed at tropical latitudes due largely to upward motion there, while ozone maxima are obtained in polar regions as a result of downward, poleward transport. Figure 1.1.2-3 displays the distribution of total ozone as a function of season and latitude as inferred from observations prior to the 1980s. A fall minimum of about 280–300 Dobson units (DU) is observed in both the northern and southern polar regions. Figure 1.1.2-1 suggests that photochemical destruction of ozone extends to very low altitudes in the summer season at high latitudes (Farman et al., 1985b). Thus, rapid chemical destruction of ozone is the primary cause of the observed fall minimum, and it is therefore not surprising that the two hemispheres exhibit similar values. However, as already noted, the interhemispheric differences in total ozone obtained in winter and spring attest to the important role

POLAR OZONE

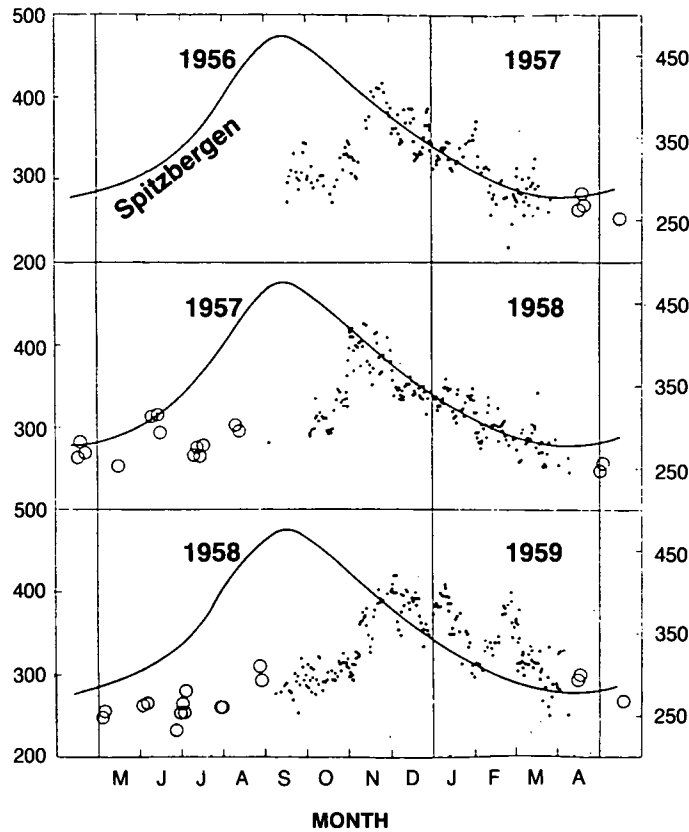


Figure 1.1.2-2. The first 3 years of ozone data from the Dobson instrument at Halley Bay, Antarctica, compared to average values observed at Spitzbergen (shifted by 6 months). Open circles indicate lunar Dobson measurements; closed circles are direct sun measurements (from Dobson, 1968).

played by atmospheric transport processes in determining the abundance of total ozone during those seasons, when photochemical processes are normally slow.

Examination of the temperature structure of the two hemispheres provides useful insights into the origin of the differences in the natural ozone distributions in the north and south polar regions. Figures 1.1.2-4 and 1.1.2-5 display observed seasonal cycles of the monthly and zonally averaged 50-mb temperature and total ozone abundances for 60°N, 60°S, 80°N, and 80°S, based on satellite data (Barnett and Corney, 1985; Keating and Young, 1985). The total ozone values are based on observations from about 1979 to 1982, when the Antarctic ozone hole was beginning to be detectable (see next section). The 50-mb level is located near the region of maximum ozone concentration at these latitudes. The temperatures near 50 mb are influenced by radiative heating and cooling as well as by dynamical heating and cooling associated with the mean meridional circulation. During winter when solar heat sources are absent, temperature increases are related, at least in part, to downward motion and associated warming by compression. Such downward transport will increase the total ozone abundance. The winter and spring dynamics of the two hemispheres (in particular, the observed behavior in 1987–1989) will be discussed in much greater detail in Section 1.7. Detailed reviews are also given by Koshelkov (1987), Koshelkov et al. (1987) and Tarasenko (1988). Here we seek only to establish a very general basis for understanding the natural distribution of total ozone as a framework for discussion of possible trends and their causes.

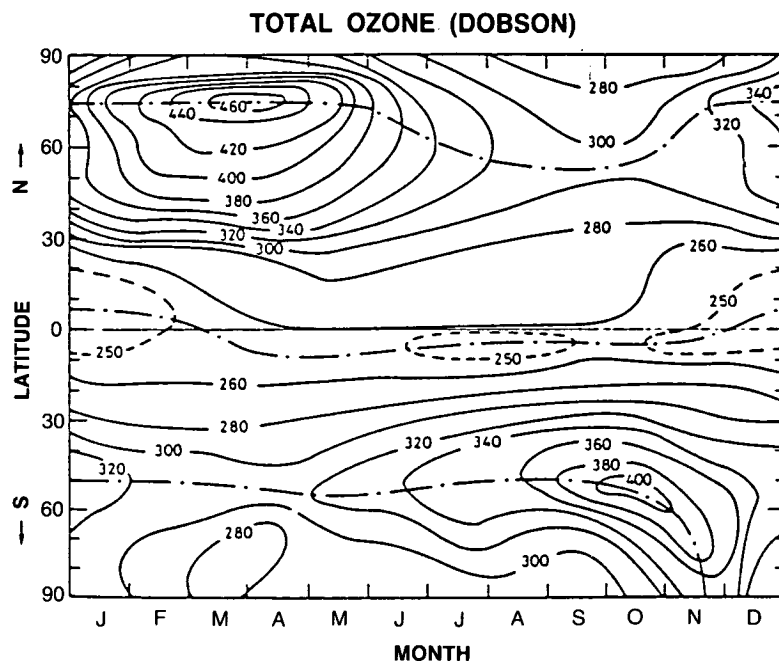


Figure 1.1.2-3. Observed global variation of total ozone with latitude and season, based largely on Dobson data (from London, 1980).

Figure 1.1.2-4 shows that the total ozone abundances observed at 60°N from about May through October are very similar to those observed at 60°S in the conjugate months from November to April. The temperatures are nearly the same in the two hemispheres during these summer and early fall months as well. Temperature and ozone differences begin to increase in early winter (Nov-Dec in the Northern Hemisphere as compared to May-June in the Southern Hemisphere), and very large differences of about 12 K and 50–100 DU, respectively, are obtained by early spring. The differences both in ozone and in temperature reflect the greater planetary wave activity and stronger downward transport characteristic of the Northern Hemisphere winter.

The Southern Hemisphere temperatures remain cold much later in the spring season than those in the Northern Hemisphere. The total ozone increase observed in October at 60°S is associated with a rapid rise in temperature. It is therefore likely to be the result of rapid poleward transport of ozone associated with the final stratospheric warming and should be expected to vary from one year to another in association with the timing and characteristics of stratospheric warmings. The seasonal variations of total ozone and temperature at 80°N and 80°S , and the differences between them, display similar features to those obtained at 60°N and 60°S . Temperatures and total ozone abundances in the two hemispheres are comparable in summer and fall. The total ozone abundance drops to about 300 DU in both hemispheres by fall. In the Southern Hemisphere, zonally averaged winter temperatures drop to a minimum near 185–190 K in winter and spring, and the total ozone remains relatively constant at about 250–300 DU until the temperatures rise dramatically in late spring, when the total ozone also increases. Because of greater wave activity in the Northern Hemisphere, temperatures are on average warmer and ozone levels higher than those of the Southern Hemisphere. Such variations in total ozone are reproduced rather well by three-dimensional models such as the one by Cariolle et al. (1986) and in two-dimensional simulations including for example, that of Stordal et al. (1985).

POLAR OZONE

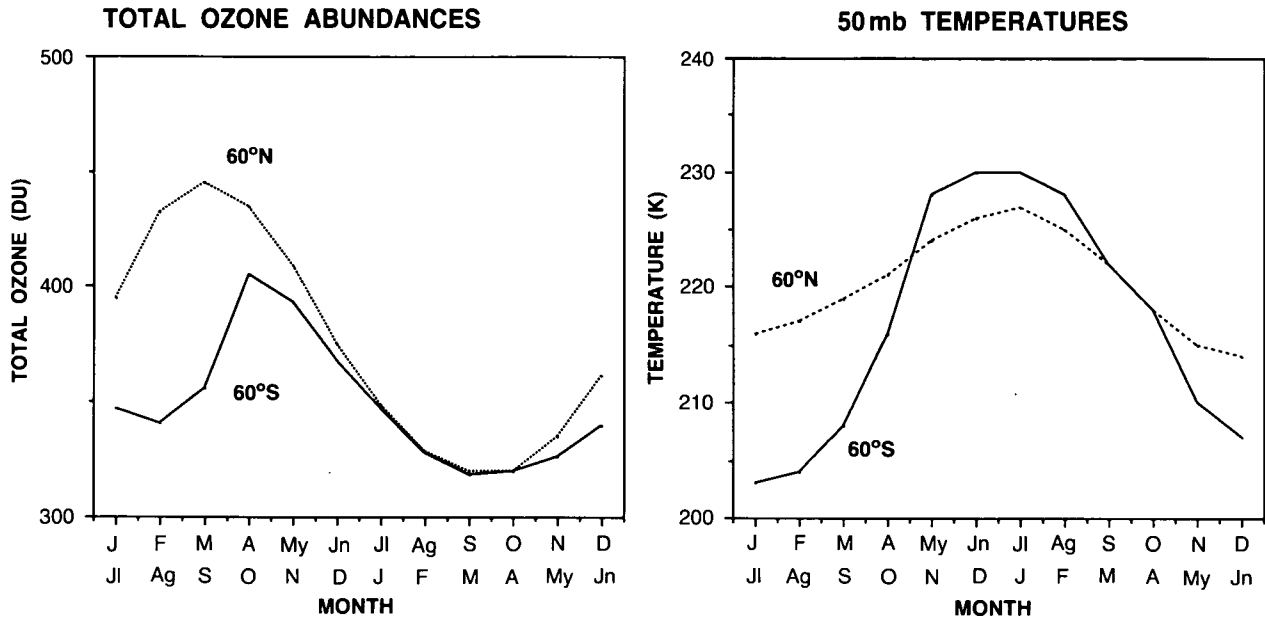


Figure 1.1.2-4. Seasonal cycles of total ozone and 50 mb temperatures at 60°N (January-December) and 60°S (July-June). The total ozone is taken from Keating and Young (1985) and is based upon satellite observations from 1979-1982, while the temperature data are taken from the climatology compiled by Barnett and Corney (1985).

Although the data are limited in the polar night region, Figure 1.1.2-3 suggests that the total ozone abundances in both hemispheres decrease towards the pole. This latitudinal gradient does not necessarily indicate destruction of ozone. Rather, the center of the winter polar vortex should be expected to be very cold in both hemispheres, due in part to slower downward transport than that of the surrounding region.

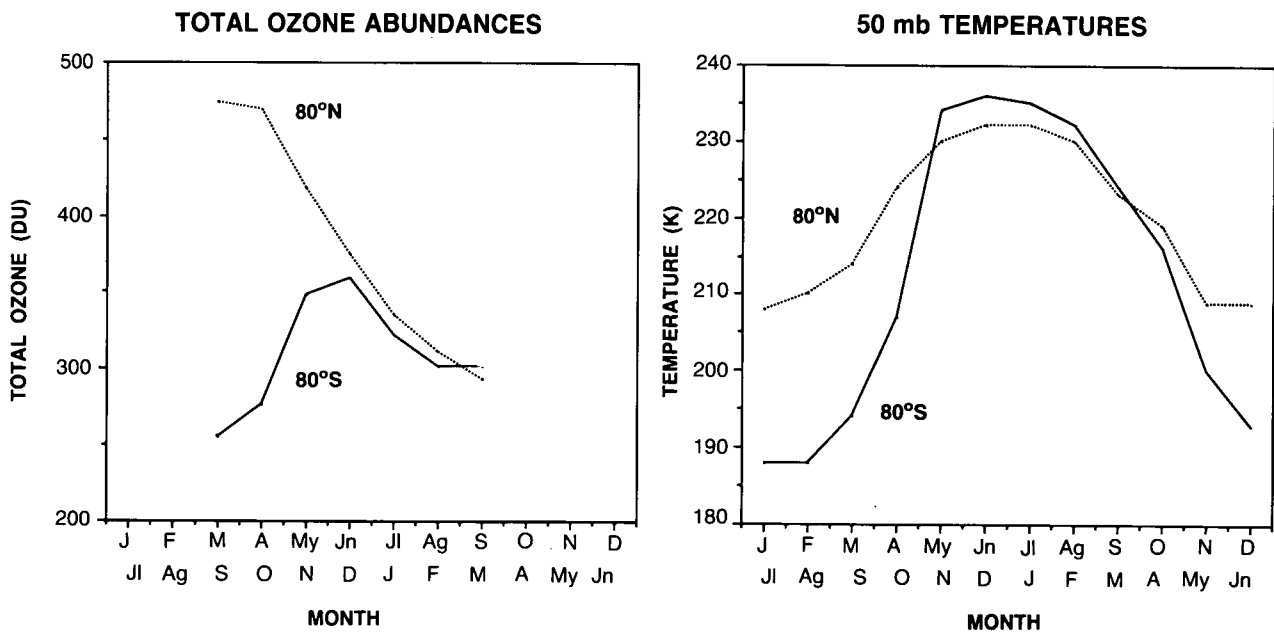


Figure 1.1.2-5. As in Figure 1.1.2-4, but for 80°N (January-December) and 80°S (July-June).

Further, any horizontal transport of ozone from lower latitudes will reach the vortex later than the surrounding sub-polar latitudes. Near the heart of the cold winter polar vortex, ozone levels can therefore remain comparable to the low values obtained in fall (following the chemical destruction obtained in that season), while the surrounding “collar” region is likely to exhibit higher ozone levels due to transport processes. Note that zonally and monthly averaged temperatures and total ozone values may not reflect those of the core of the vortex, especially in the Northern Hemisphere where the vortex is often centered far from the geographic pole.

In summary, polar total ozone in the Southern Hemisphere exhibits the following natural annual cycle: a summer and early fall minimum due primarily to photochemical destruction, then followed by fairly constant low values in winter and early spring associated with very cold temperatures, culminating in a rapid spring increase associated with downward poleward transport during and after the final stratospheric spring warming. In the Northern Hemisphere, warmer winter temperatures indicate greater planetary wave activity and mean descent and hence are associated with larger, increasing total ozone levels through the winter (at least for latitudes equatorward of the heart of the polar vortex). The timing and nature of the spring warming play an important role in determining the springtime ozone increases in both hemispheres.

1.1.3 Observed Trends in the Total Ozone Column Content in Antarctica and Southern Mid-Latitudes

The British Antarctic Survey station at Halley Bay is one of the few worldwide ozone monitoring stations whose record extends back to the late 1950s. Farman et al. (1985a) presented observations of total ozone from Halley Bay (76°S) and the Argentine Islands (66°S) which showed that the total ozone abundance had dropped noticeably over both stations during the period from about the mid-1970s to the mid-1980s, although a small decrease may have occurred even earlier. The changes were much larger at Halley Bay than over the Argentine Islands, and were most pronounced in October, when the total ozone levels above Halley Bay in 1984 were only about 60% as large as those obtained in the late 1950s and early 1960s. A much smaller decrease (5–10%) was also apparent in summer. The strong seasonal asymmetry in the apparent trend suggested that it was unlikely to be a result of calibration errors.

Other observations quickly confirmed the veracity of this remarkable ozone trend. Stolarski et al. (1986) presented total ozone measurements from 1978 through 1986 from the TOMS (Total Ozone Mapping Spectrometer) instrument, displaying the same general trend and seasonal structure. They also pointed out that the ozone changes apparently took place largely in September rather than in October and that the ozone actually decreased rapidly during that month. Thus it was clear that the ozone trend was not due to lower abundances at the end of fall or winter, but was actually characterized by relatively “normal” levels at the end of winter followed by a rapid spring decrease. It is this spring decrease that is now clearly identified with the Antarctic ozone hole. They also noted that polar ozone levels were apparently influenced by the tropical Quasi-Biennial Oscillation (QBO), such that easterly (westerly) phase years exhibited larger (smaller) mean levels of total ozone. The dynamics of the QBO and further discussion of the QBO signal in ozone measurements will be presented in Section 1.7.1.

Chubachi (1984; 1986) and Sekiguchi (1986) showed that the Japanese Antarctic research station at Syowa (69°S) displayed a comparable trend in October, and Komhyr et al. (1986) demonstrated that large October decreases in total ozone had also been obtained at the South Pole.

POLAR OZONE

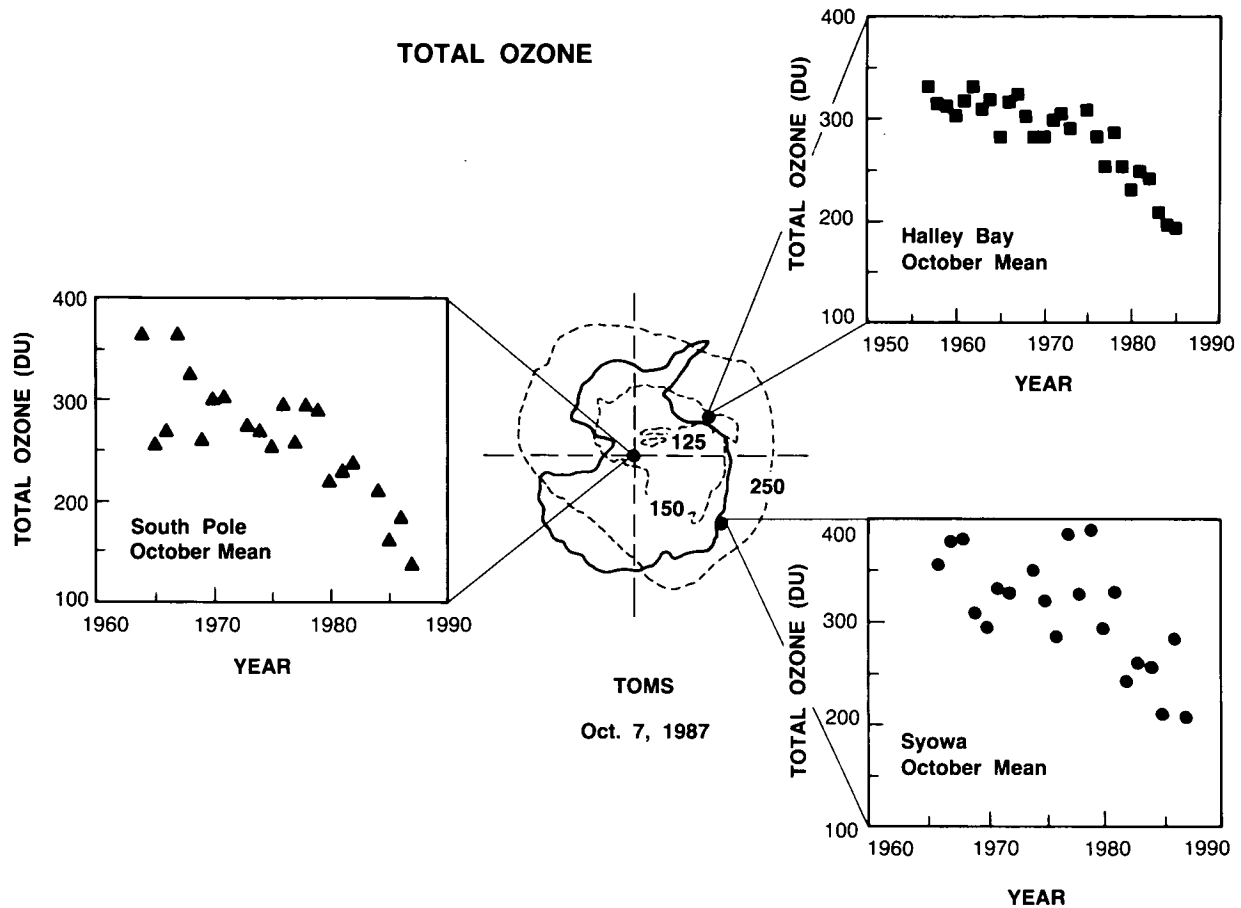


Figure 1.1.3-1. Observed long-term trends in total ozone from the ground-based Antarctic stations at Syowa, Halley Bay, and the South Pole.

Figure 1.1.3-1 is a composite of long-term total column observations in October from Syowa, Halley Bay, and the South Pole. It is clear that all three stations exhibit a substantial decrease in total ozone beginning sometime in the late 1970s or early 1980s. Underlying the station observations is a TOMS map of total ozone obtained in early October 1987, when the Antarctic ozone hole was extremely pronounced. The very low minimum values of total ozone below 125 DU can be compared with levels of about 250 DU observed in 1979, although the data from Halley Bay and later discussion presented here suggest that 300 DU may be more representative of the “undisturbed” value.

Figure 1.1.3-2 displays the monthly mean minimum October total ozone values obtained from TOMS satellite data, along with measurements of the Singapore zonal wind speeds at 30 mb, illustrating the QBO fluctuation. Garcia and Solomon (1987) showed that the minimum temperatures within the polar vortex were strongly modulated by the QBO (with the westerly phase years being colder by some 5–8 K) and summarized evidence for a substantial QBO signal in Antarctic ozone and in the ozone trend. Angell (1988a) showed that the association between the QBO and Antarctic ozone is statistically significant in the long-term record (from the mid-1960s) using ground-based data. Many other authors have also commented on the association between extra-tropical ozone and the QBO. The mechanism is not at all well understood, but the apparent correlation is particularly strong in Antarctica.

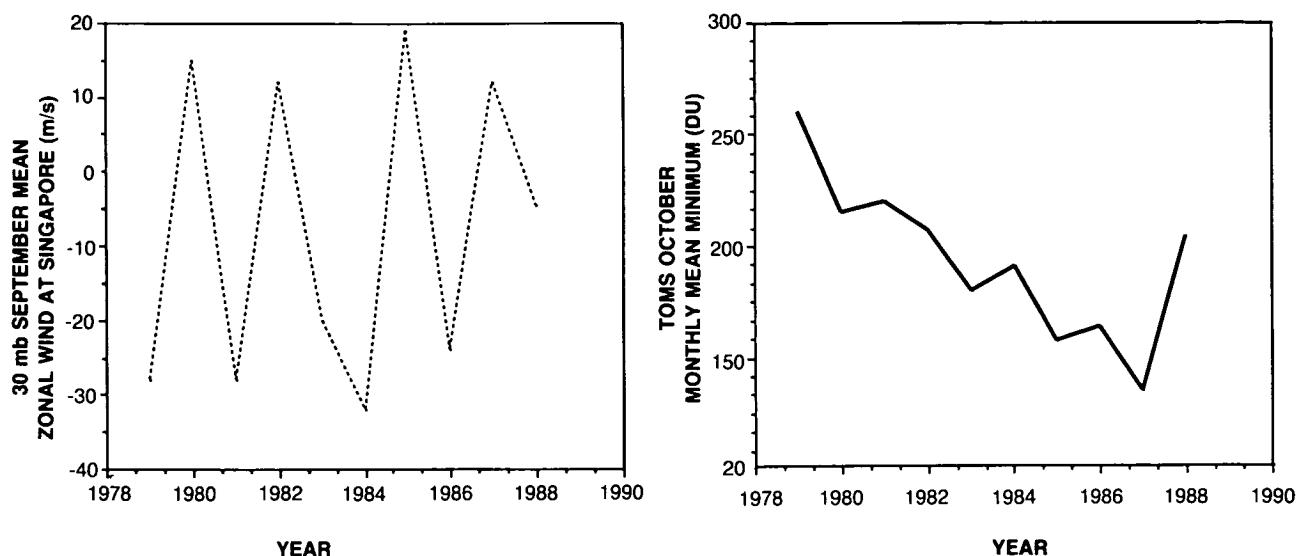


Figure 1.1.3-2. TOMS October monthly mean minimum total ozone measurements along with equatorial zonal wind speeds. Periods of strong westerly QBO phase are indicated (adapted from Garcia and Solomon, 1987).

The association of the QBO with temperature variations suggests that the QBO modulates the meridional circulation and thus the transport of ozone. It is also true that any temperature-dependent destruction processes should be influenced by the observed temperature fluctuations (see Sections 1.3 and 1.4). Regardless of the mechanism, the correlation between ozone and the QBO phase is quite strong and apparently plays a major role in modulating Antarctic ozone abundances in spring. It is worthy of note that the mean period of the QBO is about 28 months (Naujokat, 1986) rather than 24 months, so that the cycle does not necessarily alternate from one austral spring to the next. While October 1987 was an unusually cold month in south polar regions and one of strong westerly QBO phase, 1988 was considerably warmer and the QBO phase was easterly near 10 to 30 mb. The next westerly phase period should be expected to occur after the 1989 austral spring if the mean period of 28 months is followed, so that relatively high ozone levels may also be anticipated in austral spring 1989, with the next cold, westerly phase austral spring likely to occur in 1990. Note that both sets of years of like phase exhibit long-term decreases (i.e., a trend is seen in the easterly phase years of 1979, 1982, 1984, 1986, and 1988, as well as in the westerly phase years of 1980, 1983, 1985, and 1987). If the past correlation between the QBO and the ozone hole continues, then the ozone depletion ought to be relatively modest in 1989 but quite deep in 1990 (note, however, that the QBO period can vary by as much as 8 months). The next few years should therefore provide an excellent test of the relationship between the QBO and the Antarctic ozone hole.

All of the measurements indicated in Figure 1.1.3-1 were obtained with ultraviolet absorption methods, as already noted. While this is the sole historical means of measurement of total ozone, it must also be asked whether there is any possibility that the apparent trends might arise from instrumental effects (e.g., changes in the propagation of ultraviolet radiation associated with enhanced particulate matter or other interfering agents). Observations of the vertical profile of ozone obtained with ozonesondes provide a partial check on the ultraviolet absorption measurements, as will be shown in the Section 1.1.5. However, ozonesondes do not measure the total profile and are sometimes normalized to Dobson measurements of the total column, so that the two methods may not provide independent information. Observations of the rate of decline in total ozone obtained in a particular season in the contemporary Antarctic atmosphere

POLAR OZONE

place a further important check on possible measurement errors, since they have been carried out with a variety of techniques including infrared and visible absorption, as well as ozonesondes. Such measurements also place important constraints on the rates of processes responsible for the ozone hole.

Figure 1.1.3-3 shows observations of the total column abundance above McMurdo Station (78S) in September and October 1986. Large local fluctuations are apparent as noted earlier. These were clearly associated with warm air advected from lower latitudes (Mount et al., 1987). The measurements by TOMS, ozonesondes, infrared and visible absorption are all in fairly good agreement with one another, and display values below 200 DU by late October. Figure 1.1.3-4 shows a similar comparison for 1987, when the dynamical conditions above McMurdo were somewhat less variable, along with measurements of the TOMS minimum ozone within the vortex. These data show that a rapid decline in total ozone is observed in September (days 244 through 273) with four independent methods, eliminating any possibility that its origin is instrumental. It is clear that the overall levels are generally larger at McMurdo than they are at the ozone minimum, but the observed rate of decrease is comparable, about 1%/day, showing that the maximum rate of decline is not confined to the ozone minimum. The observed trends occur over a broad region extending throughout much of the polar region. The latitude dependence of the trends will be discussed quantitatively below. Stolarski et al. (1986) noted that the rate of decline of the ozone minimum in September 1983 was 0.6%/day. This and the more detailed study by Lait et al. (1989) suggest that the rate of ozone loss may have increased, a topic which will be discussed further below.

The observations from Halley Bay suggest that historical levels of springtime total ozone were about 300 DU in October. Gardiner and Shanklin (1986) also noted that the historical total ozone levels averaged from 1957 through 1973 at Halley Bay for September 1-5, 6-10, 11-15, 16-20, 21-25, and 26-30 were 294,

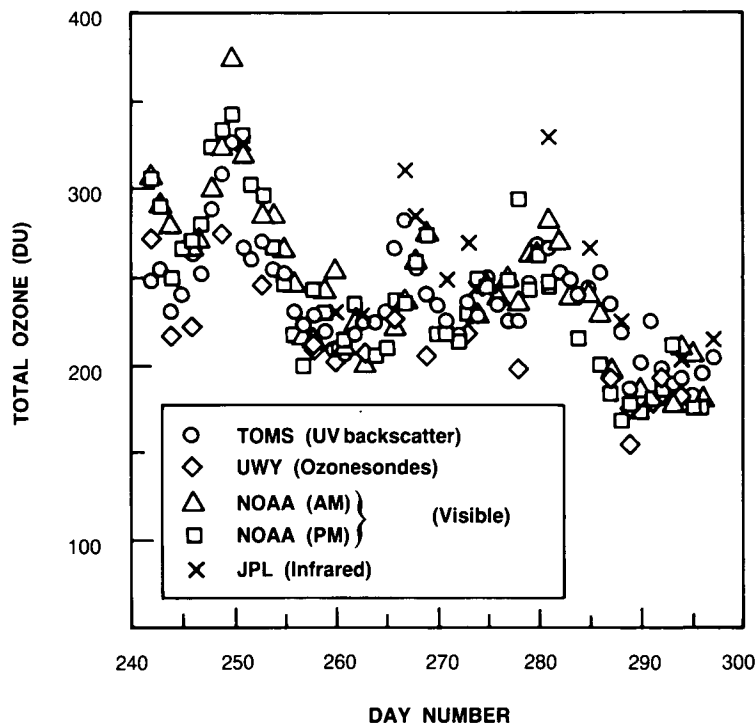


Figure 1.1.3-3. Seasonal decline in total ozone above McMurdo Station in 1986 as deduced by visible, ultraviolet, and infrared spectroscopy, as well as from (unnormalized) ozonesonde observations.

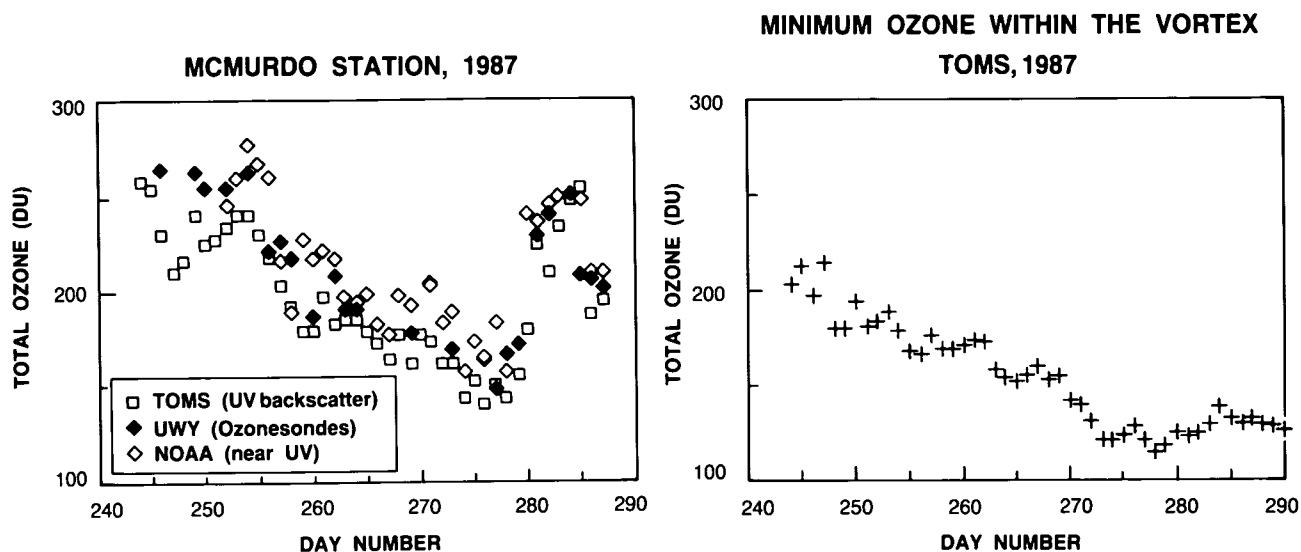


Figure 1.1.3-4. (Left) Same as Figure 1.1.3-3, but for 1987. (Right) Seasonal decline in the daily TOMS ozone minimum during 1987.

282, 306, 299, 299, and 302 DU, respectively. Thus the ozone did not decline during September in historical years. It is therefore critical to note that the ozone hole has been associated with a fundamental change not just in the magnitude of October ozone abundances, but in the character of the ozone seasonal cycle in Antarctica.

The Halley Bay ozone measurements indicate a small decrease in summer compared to historical data, by perhaps 10–20 DU. These data taken together with historical Halley Bay and South Pole ozone measurements in October and September imply that estimation of the depth of the ozone hole in any particular year in the present day atmosphere should be based on comparison to 300 DU, rather than to the contemporary values observed in late August (since these may reflect a partial depletion). It is important to consider whether the smaller summertime Antarctic ozone changes represent a residual of the spring changes or are associated with some other mechanism. This issue will be discussed somewhat further in Sections 1.7 and 1.8.

We now consider the latitude dependence of the ozone trends in somewhat greater detail. The number of ground-based stations in the Southern Hemisphere is quite limited outside Antarctica, and the local dynamics influencing the region of maximum ozone at southern mid-latitudes can influence the trends derived from single-station measurements. The analysis by Bojkov (1986) suggested no apparent trend in Southern Hemisphere total ozone records, but the study of TOMS data presented in the OTP report suggested that this may be due to changes in the location (but not necessarily the magnitude) of the ozone maximum.

Figure 1.1.3-5 presents a contour plot of the percent changes versus month and latitude band from TOMS measurements over the period from 1979 to 1988 based on a linear trend analysis. The TOMS data have been corrected for a long-term drift, based on comparison with ground-based data (OTP, 1989). The correction is about 3.5% from 1978 to 1987. The possibility of latitude dependence in the correction factor is also important, but has not been evaluated quantitatively. Analyses of Northern Hemisphere ground-

POLAR OZONE

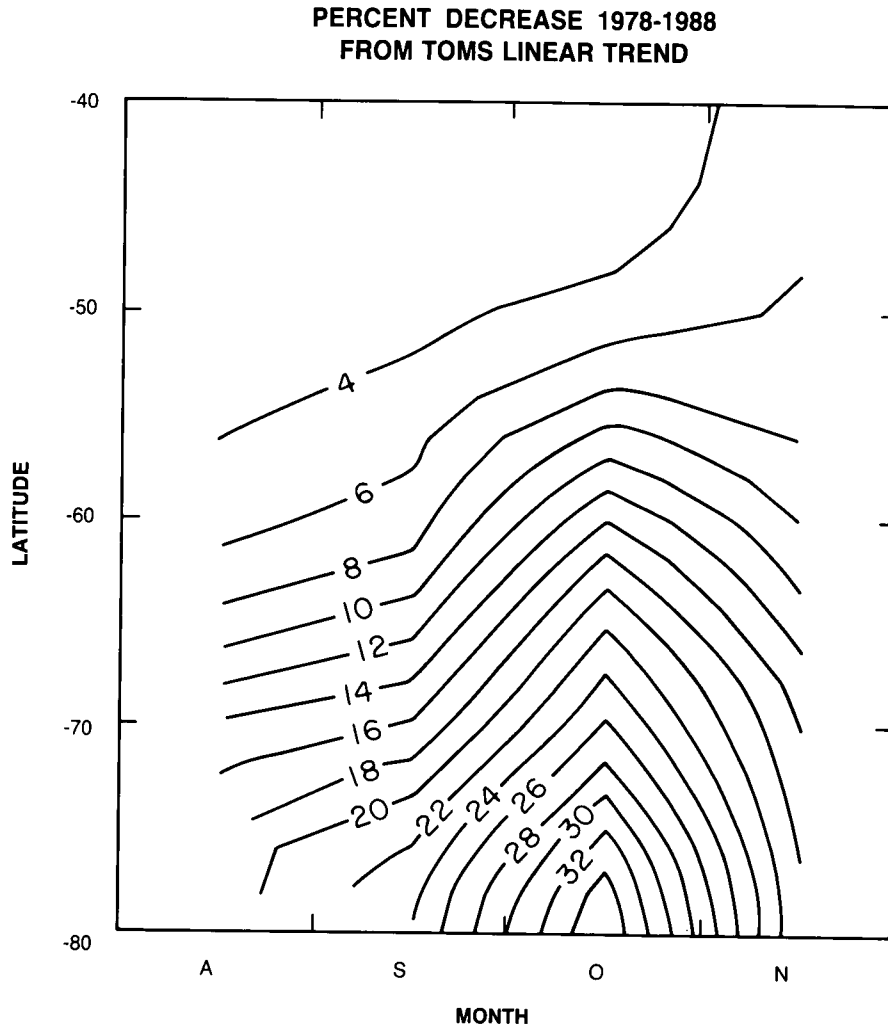


Figure 1.1.3-5. Contour plot of the ozone decrease obtained from 1978-1988 derived from a linear trend analysis of the TOMS measurements (Stolarski, personal communication, 1989).

based data suggest that the 11-year solar cycle is likely to cause a downward trend in total ozone of at most a few percent over this period (Angell, 1988a; OTP, 1989), much smaller than the measured decreases in polar regions. The seasonal variations in these trends are of particular importance with regard to their possible causes. The largest trend of about -34% is deduced near 80°S for the month of October. The magnitude and timing of the trend near 60°S suggests that it may largely be due to spreading, or dilution, of the high latitude depletion. Figure 1.1.3-5 suggests that a good deal of the trend obtained at 50°S in October may also be due to dilution of the polar depletion. Atkinson et al. (1989) pointed out that unusually low ozone abundances obtained over Australia and New Zealand in December 1987 appeared to be linked to transport of air that had been severely depleted in ozone from Antarctica to lower latitudes, especially in association with the final stratospheric warming. It has been suggested that flow of air through the vortex and out to lower latitudes can occur not only in association with vortex breakup, but perhaps throughout the winter and spring (see Section 1.7). Under these circumstances, the ozone trend at latitudes as far equatorward as 50°S could well occur earlier in the spring season than that in the center of the polar vortex

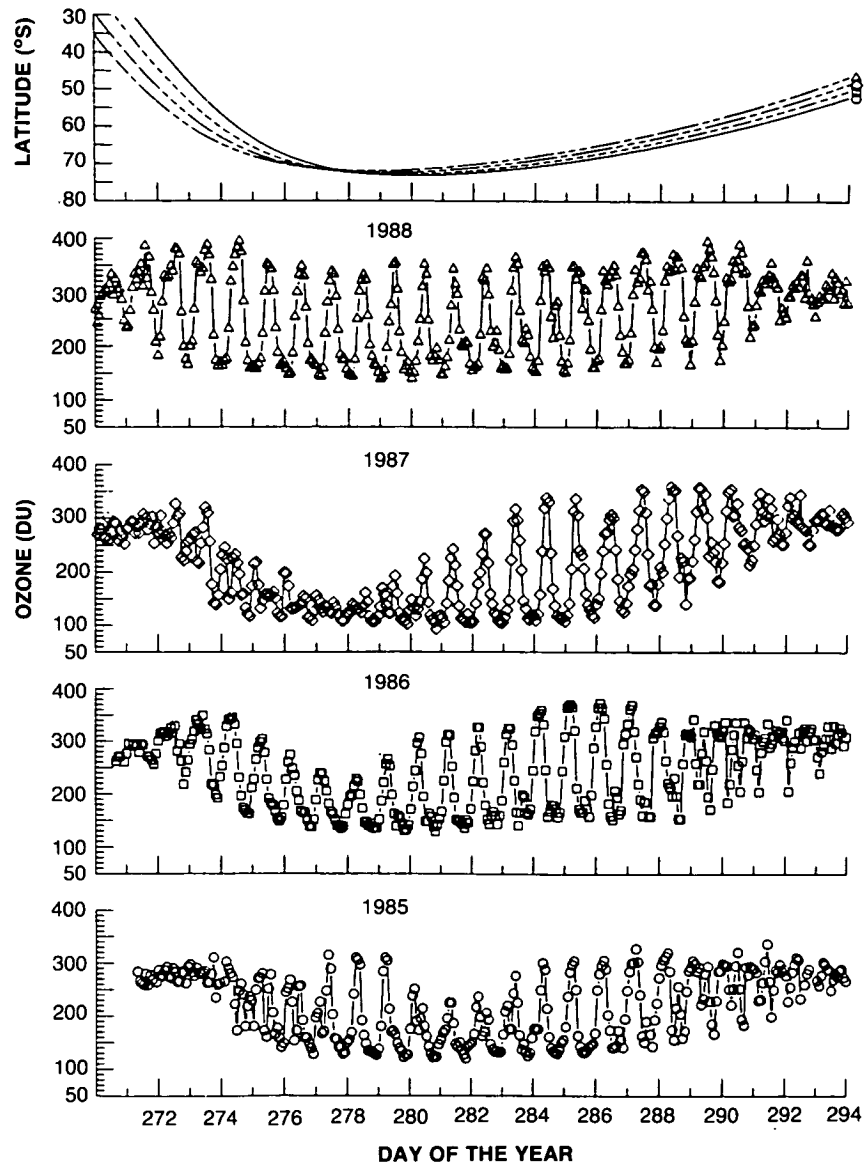


Figure 1.1.3-6. SAGE II total column ozone above 100 mb for all measurement events from day 270 through 293 (September 27- October 20, 1985, 1986, and 1987; September 26-October 19, 1988). Latitude coverage is shown in the top panel for each year. Minimum total ozone ranged from 120 to 126 DU in 1985, 128 to 135 DU in 1986, 101 to 109 DU in 1987, and 140 to 145 DU in 1988 (an update of Figure 2 in McCormick and Larsen, 1988).

and would not necessarily appear as a spreading with a time delay. It is clear, however, that a substantial fraction of the trend at lower latitudes (40°S and 50°S) does not lag those observed in the polar regions; a decrease of the order of 3–4% is indicated even in August and September. Thus, the possible spread of Antarctic ozone depletion to lower latitudes appears difficult to quantify with present observations.

Satellite measurements of ozone have also been obtained by the Stratospheric Aerosol and Gas Experiment II (SAGE II) since October 24, 1984, using a solar occultation technique. Description of the

SAGE II OZONE HOLE OBSERVATIONS
O₃ (DU)

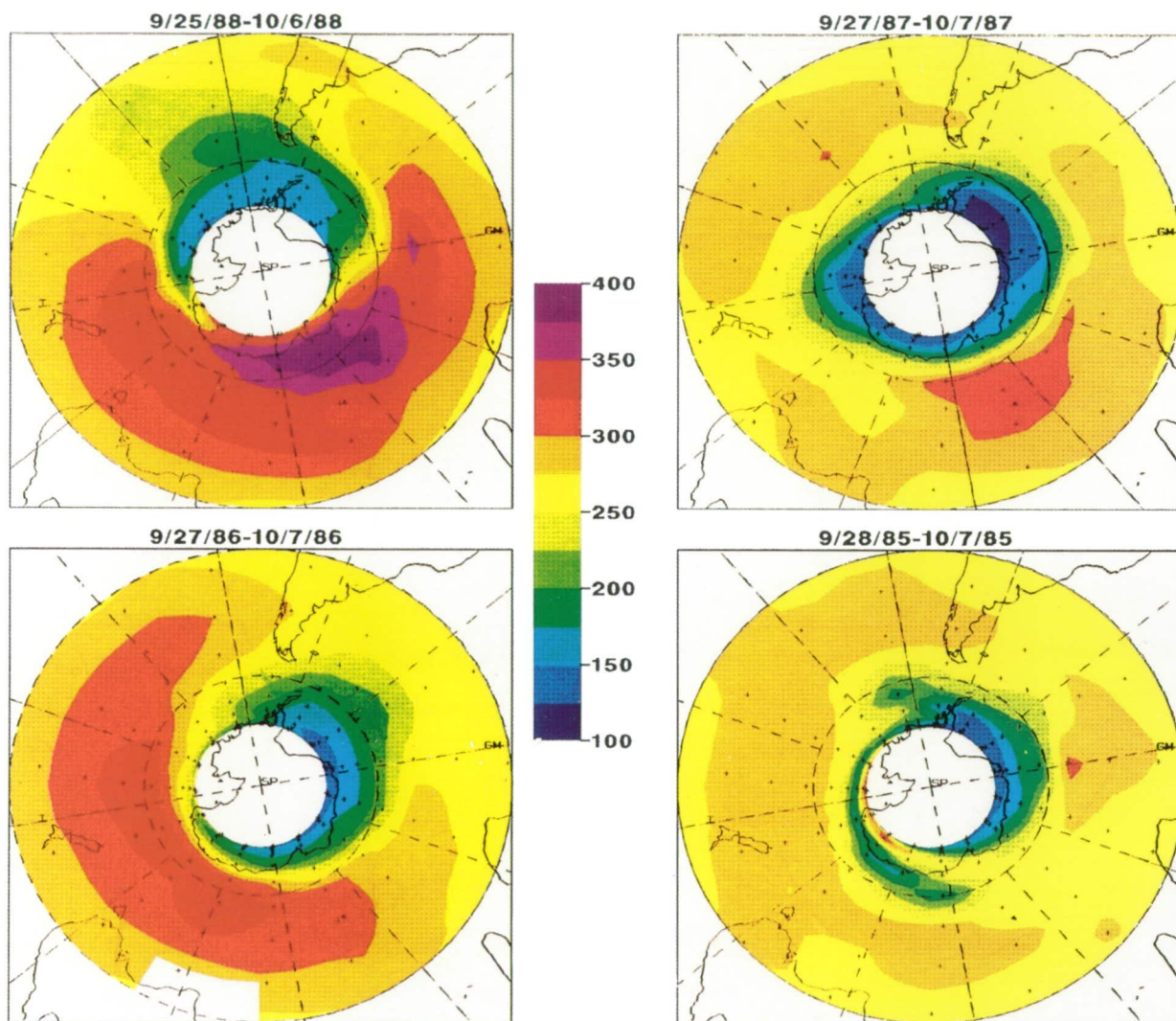


Figure 1.1.3-7. False color images of SAGE II total column ozone above 100 mb for 1985 through 1988. The images are built up as the SAGE II measurement latitude circle moves southward from 30°S in late September to 72°S in the first week of October. The +’s in each figure indicate measurement locations. The ozone ridge and chemical depletion region are quite evident in these images and display a QBO-type response from year to year. Although short-term distortions of the vortex can drastically change the areal extent of the depletion region, the year-to-year trend in ozone depletion minimums and ridge maximums are in agreement with other reported measurements.

ORIGINAL PAGE
COLOR PHOTOGRAPH

instrument, inversion algorithm, and error analysis may be found in Chu et al. (1989) and references therein.

Figure 1.1.3-6, an update of Figure 2 in McCormick and Larsen (1988), shows the variation of total column ozone above 100 mb along a sunset measurement sweep into and out of the Antarctic region for 1985, 1986, 1987, and 1988 in early October. Distortions and displacements of the vortex from the pole allow SAGE II to obtain measurements from the ozone ridge to near the center of the vortex, thus producing the cyclical variations in total ozone apparent in Figure 1.1.3-6. Low total ozone is generally associated with the colder temperatures inside the vortex. Figure 1.1.3-7 shows that in 1985 the minimum total ozone above 100 mb fell in the range of 120 to 126 DU, while in 1986 it ranged from 128 to 135 DU. The greatest ozone depletion to date was for 1987, with most minimum values falling in the 101 to 109 DU range and one profile displaying 93 DU. The 1987 measurements also show the smallest variation from profile to profile, suggesting a depletion region larger areally and more symmetric about the pole. In 1988, however, ozone minima increased to levels of 140 to 145 DU. These data also show the strong depletion of Antarctic ozone, and suggest significant correlation of the depletion with the phase of the QBO as discussed above.

Figure 1.1.3-7 displays gridded SAGE II total column ozone distributions above 100 mb for years 1985 through 1988. The measurements start at 30°S in late September and finish at 72°S in early October. Low levels of total ozone in the region of the polar vortex are produced by ozone depletion occurring from mid-August through the first week of October. The ozone map also displays a ridge of high ozone that is produced by transport from mid-latitudes and minimal horizontal mixing across the vortex edge. The QBO signal is evident in both the minimum level within the chemical depletion region and the ridge values outside the vortex. A long-term trend in Antarctic ozone was also clearly detected by SAGE measurements (OTP, 1989).

In summary, there is no question that a pronounced change in springtime Antarctic ozone has occurred, based on a broad range of satellite and ground-based measurements employing a variety of instrumental techniques. The ozone decrease occurs rapidly during the month of September. Sources of natural variability (such as the QBO) must be considered and do influence year-to-year fluctuations.

1.1.4 Suggested Explanations for the Antarctic Ozone Hole

The discovery and verification of the Antarctic ozone hole quickly prompted theoretical studies aimed at understanding its origin. The fact that the ozone hole was largely confined to Antarctica provided some important guidelines for possible mechanisms, but also meant that the available data to test and verify theoretical notions were sorely lacking. Indeed, apart from the observation that ozone itself had declined precipitously, little else was known about the chemical composition of the Antarctic stratosphere. Meteorological data, while less extensive than those available at other latitudes, did suggest that there had been a significant cooling in the austral spring (Angell, 1986; see Section 1.8 for a detailed discussion). The paucity of detailed observations led to the inception of three very different and, in some respects, contradictory hypotheses to explain the Antarctic ozone decline. In this section, the basic elements of the three theories will be briefly described. The theories will be discussed further in the context of the data that allowed discrimination between them in the later sections of this chapter.

Tung et al. (1986) and Tung (1986) considered the forcing of the Antarctic mean circulation. They noted that the Antarctic stratosphere reaches temperatures approaching radiative equilibrium in late winter and spring. As the lower stratosphere cools, the infrared cooling rate approaches zero, so that the net heating is given by ultraviolet heating alone. They suggested that the return of sunlight to polar regions

POLAR OZONE

could then lead to net upward motion, bringing ozone-poor air from lower altitudes up to the heart of the ozone layer and causing the seasonal decline. Mahlman and Fels (1986) also examined the possibility of upward motion in spring, and pointed out that reduced wintertime planetary scale wave activity might lead to reduced downward transport of ozone during winter and spring. This in turn would be expected to lead to a colder polar stratosphere at the end of the polar night, and thus a greater tendency for springtime upward motion. These dynamical theories thus rested primarily on the extreme coldness of the Antarctic stratosphere to explain the appearance of the ozone hole uniquely in Antarctica, and required a temporal trend in Antarctic dynamics to explain the decadal trend. Possible sources for such a decadal trend included the influence of volcanic aerosols on the radiative balance (Tung et al., 1986) and/or dynamical factors influencing the dynamical forcing of the Antarctic circulation, such as changes in sea surface temperatures or tropospheric dynamics (Mahlman and Fels, 1986; Nagatani and Miller, 1987; Dunkerton, 1988).

It was clear that the seasonal evolution of the ozone depletion and any associated lower stratospheric temperature trends were important elements in these dynamical theories. If the ozone decrease were caused by upward motion, then a temperature decline should be expected to occur before, or simultaneously with, the ozone decline (i.e., if the ozone declines in September then the temperature decline must precede or accompany it). When the dynamical theories were first suggested, little information was available on the temporal evolution of the ozone decline; it was not known whether the observed Halley Bay ozone trend actually occurred during October, or earlier in the spring season. Later studies established that the decline occurs largely in September (Section 1.1.3), providing an important observational constraint against which any theory should be tested.

It is also important to note that ozone provides the primary source of solar heating to the Antarctic lower stratosphere. Thus, a decline in ozone should be expected to result in a decline in temperature somewhat later in the spring season (Shine, 1986). This underscores the importance of identifying not only the existence of any temperature trends, but also their timing relative to the ozone trend. It is the timing (phase lag or phase lead) that is a critical component in distinguishing whether any observed temperature trends constitute a cause or an effect.

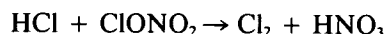
Two fundamentally different chemical theories were also proposed to explain the ozone decline. Figure 1.1.2-1 shows that photochemical processes are expected to take place only very slowly under normal conditions in the polar winter and spring. Therefore, any photochemical means of destroying ozone in this region must rely upon a dramatic change in photochemical time scales.

Callis and Natarajan (1986) considered the production of reactive nitrogen (NO_x) in the upper atmosphere. They noted that the intense solar maximum that occurred near 1980 might have produced large amounts of NO_x in the mesosphere and lower thermosphere. If this NO_x could be transported to the stratosphere, it could potentially deplete ozone photochemically following the spring return of sunlight to polar regions. Such transport would occur primarily in the polar night (since NO_x is rapidly destroyed in the sunlit mesosphere) and might be expected to be most effective in the relatively isolated Antarctic polar vortex as compared to the Arctic. Thus, this theory rested on the importance of solar activity in producing NO_x , its downward transport to the stratosphere in the polar night, and the subsequent destruction of ozone following the return of sunlight to the polar cap. Callis and Natarajan (1986) discussed satellite observations that indicated that a temporal increase in NO_2 might have occurred from about 1979 to 1983.

Several authors considered the possibility that chlorine chemistry and/or the coupling between chlorine and bromine chemistry might be responsible for the ozone decline. As noted by Farman et al. (1985a), the clear increase in chlorine abundances that occurred over the time scale during which the ozone hole

developed (late 1970s to early 1980s) suggests that chlorine chemistry should be considered as a possible mechanism.

Solomon et al. (1986) and McElroy et al. (1986a) noted that the extreme cold temperatures of the Antarctic winter and spring had been shown by McCormick et al. (1982) to lead to greatly enhanced polar stratospheric cloud (PSC) occurrences. They suggested that heterogeneous reactions such as



would both enhance the level of reactive chlorine at the expense of the reservoir species, HCl and ClONO₂, and suppress the abundance of reactive nitrogen (NO_x) in favor of the HNO₃ reservoir. The suppression of reactive nitrogen is quite important, since it impedes the reformation of ClONO₂, allowing the liberated reactive chlorine to remain active (see Section 1.5 for a detailed discussion of the coupling between nitrogen and chlorine chemistry). Ozone depletion could then be expected to occur in the spring, when sunlight is again available to drive photochemical effects following such chemical perturbations due to PSCs. McElroy et al. (1986a) also emphasized the importance of coupled chlorine-bromine chemistry in depleting ozone in such an environment. Molina and Molina (1987) noted that the reaction of ClO with itself to produce the ClO dimer (Cl₂O₂) might be expected to lead to particularly efficient ozone loss under such conditions.

It should be emphasized that both an enhancement in ClO_x and a suppression of NO_x is needed in order for chlorine and/or bromine to effectively destroy ozone in the lower stratosphere. O. B. Toon et al. (1986), Crutzen and Arnold (1986), and McElroy et al. (1986b) noted that the clouds might themselves be composed of nitric acid. Toon et al. (1986) also emphasized that sedimentation of sufficiently large PSC cloud particles could “denitrify” the stratosphere. These processes would further lower the abundance of reactive nitrogen, allowing the chlorine chemistry to destroy ozone still more effectively.

As in the dynamical theory, the extreme cold temperatures of Antarctica and the return of sunlight to the polar regions were essential elements in the chemical hypotheses. The vertical profiles of the ozone changes implied by the three theories were, however, quite different (measured vertical profiles of the ozone change are presented in Section 1.1.5). The solar activity theory suggested large changes in the ozone vertical profile at high altitudes, with decreasing changes below, while the dynamical and halogen chemical theories implied that the ozone profile changes would be largest where temperatures are coldest (around 10–20 km). The halogen chemical theory was also in direct contradiction to the one suggested by Callis and Natarajan insofar as the chemical composition of the Antarctic stratosphere was concerned, since low rather than high levels of reactive nitrogen were hypothesized. Clearly, measurements of reactive nitrogen and chlorine compounds in Antarctica were badly needed. Observations of dynamical tracers and temperature trends were also critical to a fuller understanding of the mechanisms responsible for the ozone decline. Laboratory studies of heterogeneous phase chemistry and thermodynamics of the HNO₃/H₂O/HCl system were key to understanding the possible role of PSC activity in modifying polar chemistry (Sections 1.3 and 1.4).

1.1.5 Observed Trends in the Vertical Distribution of Ozone above Antarctica

The data base of long-term ozonesonde observations from Antarctica is considerably more limited than the total column observations. Historical measurements are only available from Syowa and from the South Pole. More recent data can be used to evaluate the seasonal evolution of the vertical distribution associated with the observed seasonal depletion.

POLAR OZONE

Figure 1.1.5-1 presents observations of the historical change in October total ozone profiles from Syowa and the South Pole, along with the seasonal changes reported at McMurdo and Halley Bay (see original publications of Kondoh et al., 1987; Komhyr et al., 1988; Hofmann et al., 1989c; Gardiner, 1988). Recent observations from the Indian station at Dakshin Gangotri (70°S, 12°E) are also shown (A. P. Mitra, private communication, 1989) as well as measurements from the Soviet station at Molodezhnaya (67°S,

OZONE VERTICAL PROFILES

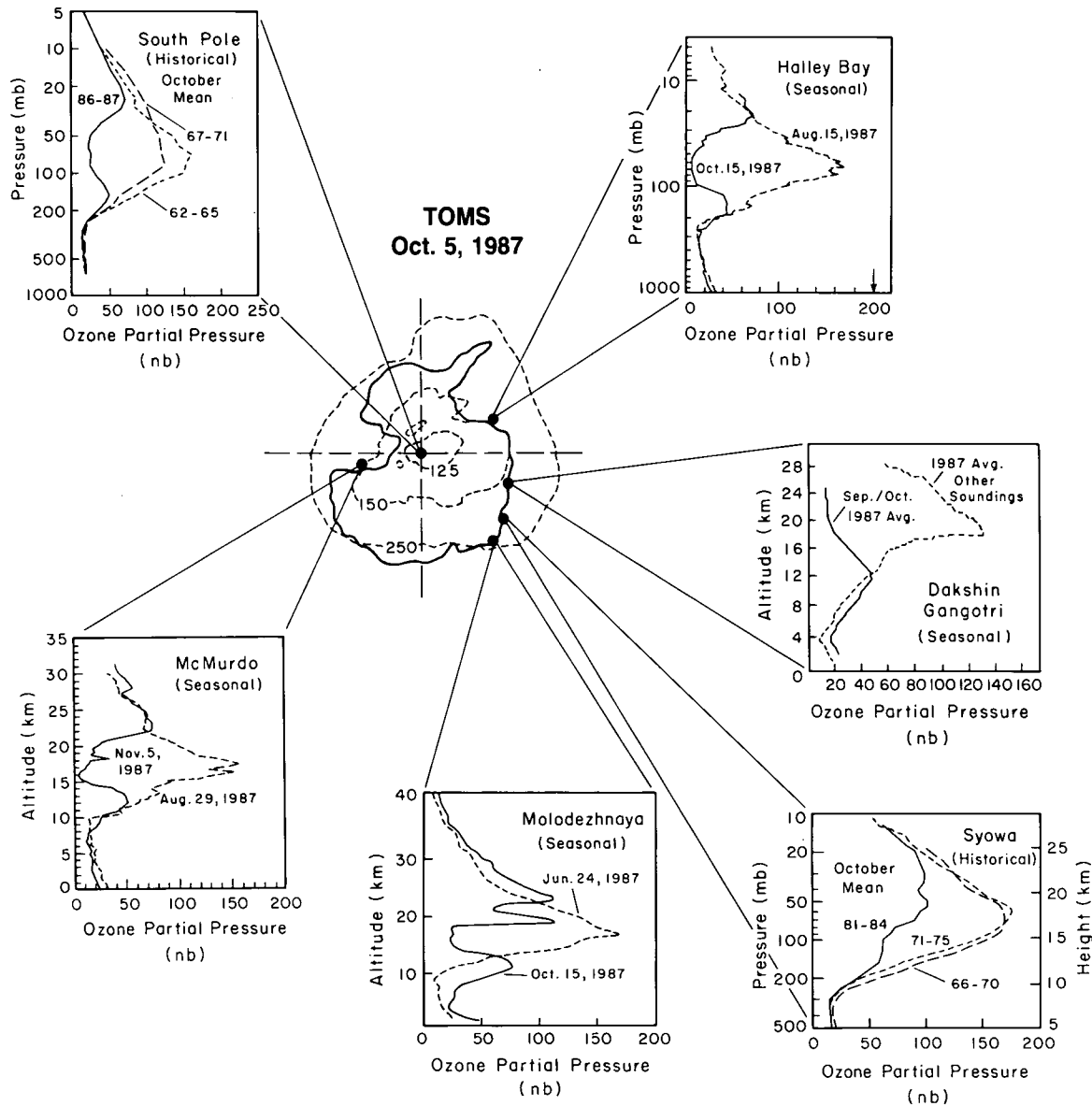


Figure 1.1.5-1. Observations of the change in the vertical profile of ozone as measured by ozone-sondes. At Syowa and the South Pole, historical data show the changes in October mean profiles measured in the 1960s and 1970s as compared to more recent observations. At Halley Bay, McMurdo, Molodezhnaya, and Dakshin Gangotri, similar changes in the vertical profile are revealed in seasonal measurements.

45°E). The Soviet data were obtained with rocketsondes, and hence allow examination of the vertical structure of the ozone profile to levels at and above 35 km, where no ozone depletion is apparent (Kokin et al., 1989). Gernandt (1987) presented evidence for similarly depleted October ozone profiles from the German Democratic Republic's Antarctic research base at 71°S. All of the stations show that the vertical profile of ozone has changed markedly in October. McCormick and Larsen (1986) and McPeters et al. (1986) have shown similar ozone depletions using observations from the SAGE II and SBUV satellite instruments. Figure 1.1.5-2 (left) presents average vertical profiles of summertime ozone from February 1-10 over the latitude region from about 61.5°S to 73°S for various years from SAGE II measurements. These should be contrasted with the right panel in this figure, which depicts the most severely depleted profiles observed in various years from both SAGE I (1981) and SAGE II (1985-1988). Both the ground-based and satellite data show that the ozone decreases are largely limited to the altitude range from 200 to 20 mb (about 10 to 25 km), where local depletions as large as 95% were obtained in 1987. This implies that the maximum local Antarctic ozone depletion cannot get much more severe than it was in 1987 unless the affected altitude range increases. However, the depleted region could expand horizontally, causing larger decreases away from that part of the Antarctic stratosphere suffering the maximum local depletion. Both the ground-based and satellite data reveal the gradual temporal evolution of the profile above Antarctica since about 1980.

Hofmann et al. (1987a) and Hofmann (1989a) noted the occurrence of sharp notches in the ozone profile, and suggested that these may be related to the sharp vertical structure of PSCs that deplete ozone, perhaps through heterogeneous mechanisms beyond those presently understood (see Section 1.4). While the apparent ozone depletion averaged over several kilometers in 1986 was on the order of 50%, the local depletion in such layers appears to be as large as 95%. Thus, the observation of sharply layered depletions places additional constraints on the rates of processes that remove it (see Section 1.6.4). However, it is also important to note that vertical and horizontal wind shear will influence the vertical structure observed at any particular location and may well introduce structure into observed balloon profiles.

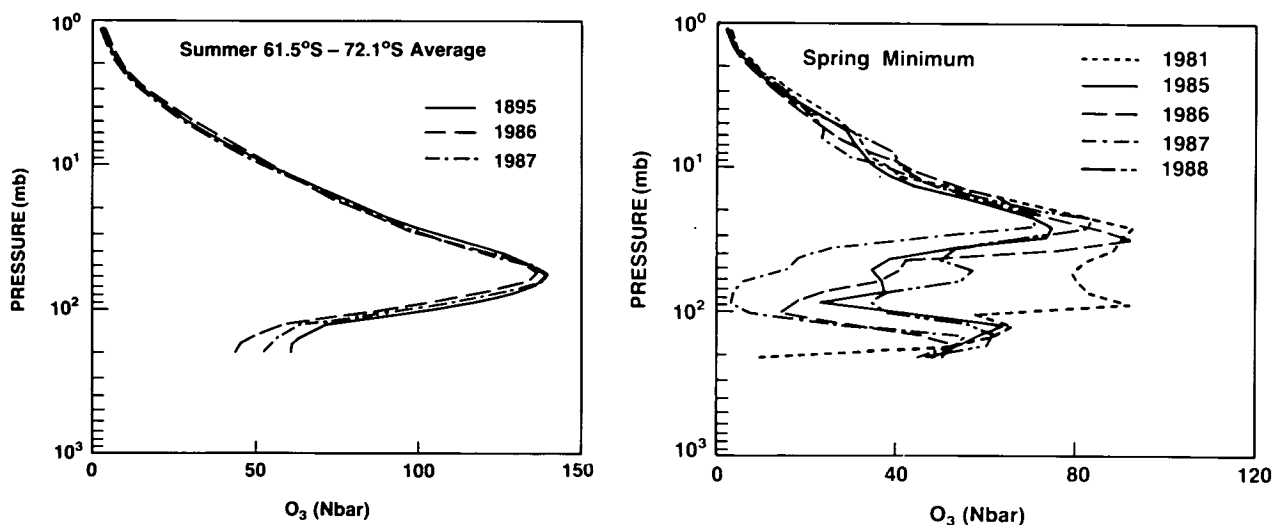


Figure 1.1.5-2. (Left) Average vertical profiles of summertime ozone from February 1-10 over the latitude region from about 61.5°S to 73°S for various years from SAGE II measurements. (Right) The most severely depleted profiles observed in various years from both SAGE I (1981) and SAGE II (1985-1988).

POLAR OZONE

Figure 1.1.5-3 shows the time evolution of ozone at the 18-km level (in the heart of the region of maximum depletion as shown in 1.1.5-1) observed at McMurdo Station in 1986 and 1987 (Hofmann et al., 1989c). Although local fluctuations are evident, a large, systematic decrease is also observed over the months of August and September in both years. It is clear that the rate of decline was appreciably faster in 1987 than that obtained in 1986. A similar increase in the depletion rate near 20 km was measured with South Pole ozonesondes (Komhyr et al., 1989a). Poole et al. (1989) suggest that these differences may be related to observed differences in the frequency of polar stratospheric cloud sightings in the 2 years (see Section 1.2), which in turn are probably a reflection of temperature changes. Differences in the chemistry and dynamics of the Antarctic spring seasons of 1987 and 1986 will be discussed further in Sections 1.6 and 1.7.

1.1.6 Trends in Northern Hemisphere Ozone

The OTP report presented a detailed study of the ozone trends reported in Arctic regions based upon both ground-based and satellite data. The accuracy of calibration procedures at individual total ozone observing stations was carefully considered, and the comparison between TOMS and ground-based data was evaluated at each station. The influence of the 11-year solar cycle and the QBO in modulating total ozone was also evaluated. In this section, the conclusions regarding trends in Arctic ozone that were deduced from the OTP report are briefly summarized. A detailed discussion of Arctic observations of chemical species and dynamical tracers that can provide insight as to the causes of Arctic ozone trends will be the subject of Section 1.10.

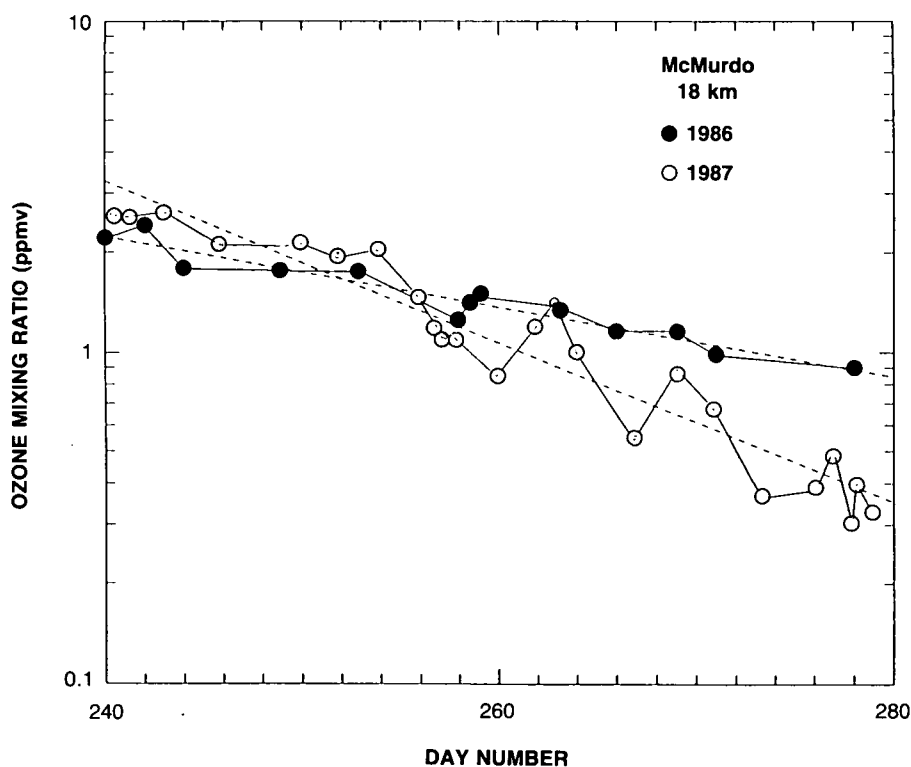


Figure 1.1.5-3. Trend in total ozone at 18 km observed from ozonesondes at McMurdo Station in 1986 and 1987 (from Hofmann et al., 1989a).

One approach taken to evaluating ozone trends using ground-based data was to average over two consecutive solar cycles (1965–1975 as compared to 1976–1986). This approach is expected to alleviate (but probably not eliminate) trends due to the solar cycle and the QBO. Variations between one solar (and/or QBO) cycle and another may still influence the apparent trends, and processes such as the sporadic (approximately 4-year) El Niño Southern Oscillation may also exert an influence. Table 1.1.6-1 displays the results of this analysis for each station considered. The decreases are largest in Arctic latitudes, and are far greater in winter than in summer. Poleward of about 50°N, winter ozone decreases of 2.5–4.7% were reported. These values are larger than model-predicted decreases of 0.9 to 1.1% for 60°N (OTP, 1989).

Table 1.1.6-1. Changes in average total ozone abundances, as measured at individual Dobson stations over the 22-year period, 1965–1986, inclusive (Percentage Differences for 1976–1986 Compared to 1965–1975; from Ozone Trends Panel report, 1989)

North Latitude	Station	Winter ^a	Summer ^b	Annual
74.7	Resolute (Canada)	-1.4 ± 1.8 ^c	-0.8 ± 0.9	-1.6 ± 1.0
64.1	Reykjavik (Iceland)	-2.5 ± 2.2	+1.7 ± 1.3	+0.1 ± 2.4
60.2	Lerwick (Scotland)	-3.8 ± 2.0	-0.9 ± 0.9	-1.6 ± 1.0
58.8	Churchill (Canada)	-4.2 ± 0.9	-1.4 ± 0.8	-2.5 ± 0.7
53.6	Edmonton (Canada)	-4.7 ± 1.3	+0.8 ± 0.9	-1.8 ± 0.8
53.3	Goose Bay (Canada)	-2.4 ± 1.3	-0.1 ± 1.1	-0.8 ± 0.9
51.8	Belsk (Poland)	-3.2 ± 0.8	+1.2 ± 1.0	-1.2 ± 0.9
50.2	Hradec Kralove (Czech.)	-4.7 ± 2.0	±1.1 ± 0.9	-1.8 ± 1.1
47.8	Hohenpeissenberg (FRG)	-1.8 ± 1.7	+0.2 ± 0.9	-1.0 ± 0.9
46.9	Caribou (Maine, U.S.)	-2.8 ± 1.5	-0.6 ± 0.8	-1.8 ± 0.9
46.8	Arosa (Switzerland)	-3.0 ± 1.3	-1.1 ± 1.0	-2.0 ± 0.9
46.8	Bismarck (N. Dak., U.S.)	-3.0 ± 1.2	-1.4 ± 1.0	-2.0 ± 0.7
43.8	Toronto (Canada)	-1.3 ± 1.2	-1.3 ± 0.8	-1.2 ± 0.7
43.1	Sapporo (Japan)	-0.6 ± 1.4	-0.1 ± 0.9	-0.3 ± 0.6
42.1	Vigna di Valle (Italy)	-2.9 ± 1.2	+0.7 ± 0.9	-0.9 ± 0.9
40.0	Boulder (Colorado, U.S.)	-3.9 ± 1.3	-3.1 ± 0.7	-3.3 ± 0.8
39.3	Cagliari (Italy)	-2.5 ± 1.7	-0.7 ± 1.1	-1.1 ± 1.2
36.3	Nashville (Tennessee, U.S.)	-1.8 ± 1.4	-3.3 ± 0.7	-2.4 ± 0.8
36.1	Tateno (Japan)	-0.7 ± 1.6	-0.5 ± 0.8	-0.4 ± 0.7
31.6	Kagoshima (Japan)	+0.9 ± 1.7	+0.5 ± 1.0	+0.9 ± 0.8
30.4	Tallahassee (Florida, U.S.)	-1.7 ± 1.9	-0.2 ± 1.1	-1.3 ± 1.4
30.2	Quetta (Pakistan)	-1.1 ± 1.6	+0.1 ± 0.8	-0.7 ± 0.8
25.5	Varanasi (India)	-0.3 ± 1.4	+0.4 ± 0.9	-0.2 ± 0.9
19.5	Mauna Loa (Hawaii, U.S.)	-1.5 ± 1.7	0.0 ± 0.6	-0.9 ± 0.6
30°N to 60°N		-2.5 ± 1.0	-0.5 ± 0.6	-1.4 ± 0.7
40°N to 60°N		-3.0 ± 0.9	-0.4 ± 0.5	-1.6 ± 0.6
30°N to 39°N		-1.2 ± 1.5	-0.7 ± 1.0	-0.8 ± 1.1

^aWinter = Dec., Jan., Feb., March.

^bSummer = May, June, July, August.

^cResolute is above the Arctic Circle, so that only less accurate moonlight measurements are available during actual winter. These "winter" data are the averages for the months of March and April.

POLAR OZONE

An alternate approach was to attempt to evaluate the magnitude of known sources of variability such as the QBO, solar cycle, etc., using the full record of ground-based ozone data averaged into latitude bands, and then to evaluate any residual long-term trend. Table 1.1.6-2 presents the results of this analysis. While the observed summer decreases are consistent with model estimates including increasing trace gases (chlorofluorocarbons, methane, nitrous oxide, and carbon dioxide), the winter values exceed theoretical expectations. The changes are again largest in winter at high latitudes, where values as large as 8.3% were deduced.

The satellite data were also used in analysis of global ozone trends. The long-term satellite instrument degradation was derived by comparison between satellite and ground-based data, and was estimated at $3.5 \pm 0.5\%$ from October 1978 to October 1987. The TOMS data were then corrected for this drift and the remaining trends were evaluated. Table 1.1.6-3 presents the results of this analysis. It should be noted that an ozone trend of perhaps 1% should be expected over the period from 1978 to 1987 due to the decline in the phase of the 11-year solar cycle during this period. Nevertheless, the TOMS data suggest residual trends of at least 2–3% in the Northern Hemisphere as an annual average.

Table 1.1.6-2. Coefficients of Multiple Regression Statistical Analysis of re-analyzed Dobson measurements of total ozone concentrations collected into latitudinal band averages. (Data are expressed in total percent changes for the period 1969–1986; From Ozone Trends Panel Report, 1989)

Month	Latitude Band		
	53–64°N	40–52°N	30–39°N
January	-8.3 ± 2.2	-2.6 ± 2.1	-2.2 ± 1.5
February	-6.7 ± 2.8	-5.0 ± 2.2	-1.2 ± 1.9
March	-4.0 ± 1.4	-5.6 ± 2.3	-3.5 ± 1.9
April	-2.0 ± 1.4	-2.5 ± 1.7	-1.7 ± 1.3
May	-2.1 ± 1.2	-1.3 ± 1.1	-1.7 ± 0.9
June	$+1.1 \pm 0.9$	-1.8 ± 1.0	-3.3 ± 1.0
July	$+0.0 \pm 1.1$	-2.2 ± 1.0	-1.3 ± 1.0
August	$+0.2 \pm 1.2$	-2.4 ± 1.0	-1.0 ± 1.0
September	$+0.2 \pm 1.1$	-2.9 ± 1.0	-1.0 ± 0.9
October	-1.1 ± 1.2	-1.5 ± 1.5	-0.9 ± 0.8
November	$+1.5 \pm 1.8$	-2.4 ± 1.3	-0.1 ± 0.8
December	-5.8 ± 2.3	-5.5 ± 1.7	-2.1 ± 1.1
Annual Average	-2.3 ± 0.7	-3.0 ± 0.8	-1.7 ± 0.7
Winter Average	-6.2 ± 1.5	-4.7 ± 1.5	-2.3 ± 1.3
Summer Average (a) JJA	$+0.4 \pm 0.8$	-2.1 ± 0.7	-1.9 ± 0.8
(b) MJJA	-0.2 ± 0.8	-1.9 ± 0.7	-1.9 ± 0.8
QBO*	-2.0 ± 0.6	-1.3 ± 0.6	$+1.9 \pm 0.6$
Solar*	$+1.8 \pm 0.6$	$+0.8 \pm 0.7$	$+0.1 \pm 0.6$

*Percent changes per cycle, minimum-to-maximum. All uncertainties are expressed with one statistical significance.

Average of monthly ozone trends in Dobson units per year and percent change in 17 years:

DU/yr:	-0.5 ± 0.16	-0.63 ± 0.17	-0.32 ± 0.14
Percent/17 yrs:	-2.3 ± 0.7	-3.0 ± 0.8	-1.7 ± 0.7

Uniform trend in ozone change assumed throughout the year, in Dobson units per year and percent change in 17 years:

DU/yr:	-0.14 ± 0.13	-0.47 ± 0.13	0.17 ± 0.11
Percent/17 yrs:	-0.7 ± 0.6	-2.3 ± 0.7	-0.9 ± 0.6

Table 1.1.6-3. Percentage changes in total column ozone (measured by TOMS on Nimbus 7, calibrated by comparison with ground-based measurements; from Ozone Trends Panel report, 1989)

Latitude Band	Total Change from 11/1978 to 10/1985	Total Change from 11/1978 to 11/1987
Global, except high latitudes (53°S–53°N)	-2.6 ± 0.5	-2.5 ± 0.6
Hemispheric		
0–53°S	-2.6 ± 0.9	-2.9 ± 0.9
0–53°N	-2.1 ± 1.5	-1.8 ± 1.4
Bands		
53°S–65°S	-0.9 ± 1.8	-10.6 ± 1.6
39°S–53°S	-5.0 ± 1.8	-4.9 ± 1.8
29°S–39°S	-3.2 ± 2.4	-2.7 ± 2.1
19°S–29°S	-2.5 ± 1.9	-2.6 ± 1.5
0–19°S	-1.1 ± 0.8	-2.1 ± 0.8
0–19°N	-1.1 ± 1.5	-1.6 ± 1.3
19°N–29°N	-3.5 ± 2.2	-3.1 ± 1.9
29°N–39°N	-3.7 ± 2.0	-2.5 ± 1.7
39°N–53°N	-2.7 ± 1.7	-1.2 ± 1.5
53°N–65°N	-2.4 ± 1.6	-1.4 ± 1.4

(Linear trends with an autoregressive model through TOMS data, with uncertainties at the one-sigma level of significance.)

In summary, analysis of both ground-based and satellite data has indicated significant (and, more importantly, consistent) trends in Arctic ozone. The trends are far smaller than those obtained in the Antarctic, but exhibit some important common features. Most notably, summer trends were small or zero, while winter trends were much larger, and were greatest at high latitudes (5–10%).

1.2 CLIMATOLOGY OF POLAR STRATOSPHERIC CLOUDS (PSCs) IN BOTH POLAR REGIONS

As noted in Section 1.1.4, several theories advanced to explain the Antarctic ozone hole depend critically on the persistence and characteristics of polar stratospheric clouds. In this section, the physical characteristics of these clouds, their seasonal occurrence frequencies (in both hemispheres) and interannual variability will be discussed. It has also been suggested that radiative effects of the clouds may play a particularly important role in the heat budget of the lower stratosphere and hence in the stratospheric circulation.

1.2.1 Physical Characteristics

Visible sightings of bright clouds in the winter polar lower stratosphere date back to at least the late 1800s (see Stanford and Davis, 1974 for a review). They were dubbed “mother-of-pearl” clouds due to their often very brilliant coloration. Sometimes also referred to as nacreous clouds, it was recognized that these clouds were generally rather localized in extent and tied to surface orography.

McCormick et al. (1982) reported that abnormally high visible extinction values had often been observed in the stratosphere by the SAM II satellite sensor during Arctic and Antarctic winters. While nacreous clouds represent a portion of the cloud population believed to be detected by the satellite sensor,

POLAR OZONE

the satellite observations allow sensitivity far beyond that of the human eye, and thus sample a range of cloud optical depths. Noting that the high extinction events were closely correlated with very cold temperatures, the authors named the phenomenon polar stratospheric clouds (PSCs). Based on a comparison of measured and theoretical extinction coefficient trends by Steele et al. (1983), it was thought that PSCs were H₂O ice particles which formed on frozen stratospheric aerosol nuclei at temperatures below the frost point (≈ 188 K at the 50-mb level assuming 5 ppmv of H₂O). Papers by Solomon et al. (1986) and McElroy et al. (1986a), which suggested that heterogeneous processes involving PSCs might be a major cause of the Antarctic ozone hole, provided the impetus for new studies of the physical characteristics of the clouds. Recent papers that present remote sensing observations of PSCs, balloon-borne particle size and ancillary meteorological measurements, and theoretical PSC microphysics calculations will be discussed in this section. Direct measurements of PSC properties from the airborne and ground-based polar investigations will be discussed briefly below and in Sections 1.3.2 and 1.10.2.

Seminal studies by O. B. Toon et al. (1986), Crutzen and Arnold (1986), and McElroy et al. (1986b) suggested that PSCs might begin to form at temperatures above the frost point as (probably frozen) binary mixtures of HNO₃ and H₂O. Such a mechanism would suppress reactive gaseous nitrogen species (NO_x), which normally counteract chlorine-catalyzed ozone destruction (see Section 1.5). Further, as noted by Toon et al. (1986), such particles might remove reactive nitrogen irreversibly ("denitrify") from the polar stratosphere through sedimentation of large PSC particles containing HNO₃.

Iwasaka et al. (1985a) reported lidar measurements of Antarctic PSCs indicating two distinct cloud particle classes. Alekseev et al. (1988) also presented airborne lidar soundings of lower stratospheric aerosols in the arctic. Poole (1987) and Poole and McCormick (1988a) reported dual-polarization airborne lidar measurements of Arctic PSCs from 1984 and 1986 which support a two-stage PSC formation process. At temperatures from 2–6 K above the frost point, they found that particulate backscatter significantly exceeded that of the background aerosol, but that accompanying depolarization ratios were very small, a signature indicative of (Type 1) PSC particles having radii on the order of the laser wavelength (0.5–0.7 μm). At temperatures near the frost point, they found much larger backscatter enhancements as well as depolarization ratios which were typical of larger, cirrus-like ice crystals (Type 2 PSCs). Clear signatures of Type 1 PSCs were also seen in more recent Arctic PSC lidar measurements by Poole et al. (1988a) and in the analysis of 1987 SAM II Antarctic PSC data by Poole et al. (1988b). The latter study also made the important point that the threshold temperature for Antarctic Type 1 PSC formation was some 5 K colder in October 1987 than in May. The pronounced drop in the temperatures required for PSC formation indicates that irreversible loss of HNO₃ and H₂O vapor occurred during the winter.

Balloon-borne optical particle counter measurements during Antarctic winter and spring were first performed at McMurdo in 1986 and reported by Hofmann et al. (1986, 1987a) and Rosen et al. (1988a). Although conditions were nominally favorable for PSC formation on several occasions, identifiable PSC particles were absent in the two size classes discriminated ($r > 0.15$ μm and $r > 0.25$ μm). This observation led Rosen et al. to speculate that PSCs may be quasi-cirrus clouds composed of large ice particles ($r > 5$ μm) in very low concentrations (< 0.01 cm^{-3}). Balloon-borne particle size measurements were made at McMurdo again in 1987 with an optical counter having additional particle discrimination in the 1–2 μm radius range (Hofmann et al., 1988a). These were supplemented by frost-point hygrometer measurements and ground-based lidar PSC observations (Rosen et al., 1988b). The 1987 measurements showed clear evidence of (Type 1) PSCs at temperatures above the frost point, consistent with the anticipated thermodynamic stability of nitric acid trihydrate (HNO₃/3H₂O). Particle size distributions in these instances were distinctly bimodal, with the larger (1–2 μm) particles having concentrations generally between 0.01 and 0.001 cm^{-3} . Higher concentrations (0.1–2.0 cm^{-3}) of the larger particles were measured in association with

nacreous clouds. Results from McMurdo in September 1988 (Hofmann et al., 1989b) again showed significant particle enhancement at temperatures above the frost point. For example, the concentration of particles with $r > 0.2 \mu\text{m}$ were ten times the normal level at 12 km, and large particles with a modal radius near $0.8 \mu\text{m}$ and a concentration of 0.3 cm^{-3} were also observed. It should be noted, however, that such observations may not represent the particle size distribution characteristic of their formation. Watterson and Tuck (1989) suggest that inflow to the Antarctic vortex occurs preferentially near the Palmer Peninsula, leading to enhanced formation of PSCs in that sector. Adiabatic cooling associated with orographic effects of the peninsula are also likely to play a particularly important role in cloud formation (Watterson and Tuck, 1989; McKenna et al., 1989a; Cariolle et al., 1989a). Watterson and Tuck suggest that sedimentation of large particles in that sector may remove condensables there. This suggests that observations over stations well away from the peninsula (such as McMurdo) may exhibit fewer PSCs in winter and spring due to removal of condensates, and emphasizes the need for general caution in interpreting any locally observed PSC size distribution without detailed consideration of the meteorological conditions.

Recent measurements by Hofmann (1989a) in the Arctic during January 1989 showed in one case a 3-km thick PSC layer near 21 km at temperatures from 186–187 K in which roughly half of the available condensation nuclei grew to radii $> 0.2 \mu\text{m}$, about 1 in 10 grew to radii $> 1.0 \mu\text{m}$, and none grew to radii $> 5.0 \mu\text{m}$. The absence of large ice crystals implied that the observed PSC particles were of the Type 1 class. On a second occasion, thin (300-m thick) PSC layers were observed near 25 km at temperatures near 191 K which consisted predominantly of particles in the 1–2 μm radius range. Further interpretation of these and similar Antarctic data has been presented by Hofmann (1989b), who noted that the small particle mode ($r \leq 0.5 \mu\text{m}$) appeared to be associated with fast cooling events such as those due to mountain lee waves or tropospheric anticyclones. In contrast, the thin layers of larger particles contained only a few percent of the available condensation nuclei and were apparently associated with even more rapid cooling events. Both modes are illustrated in Figure 1.2.1-1. Salawitch et al. (1989) note that sedimentation of the

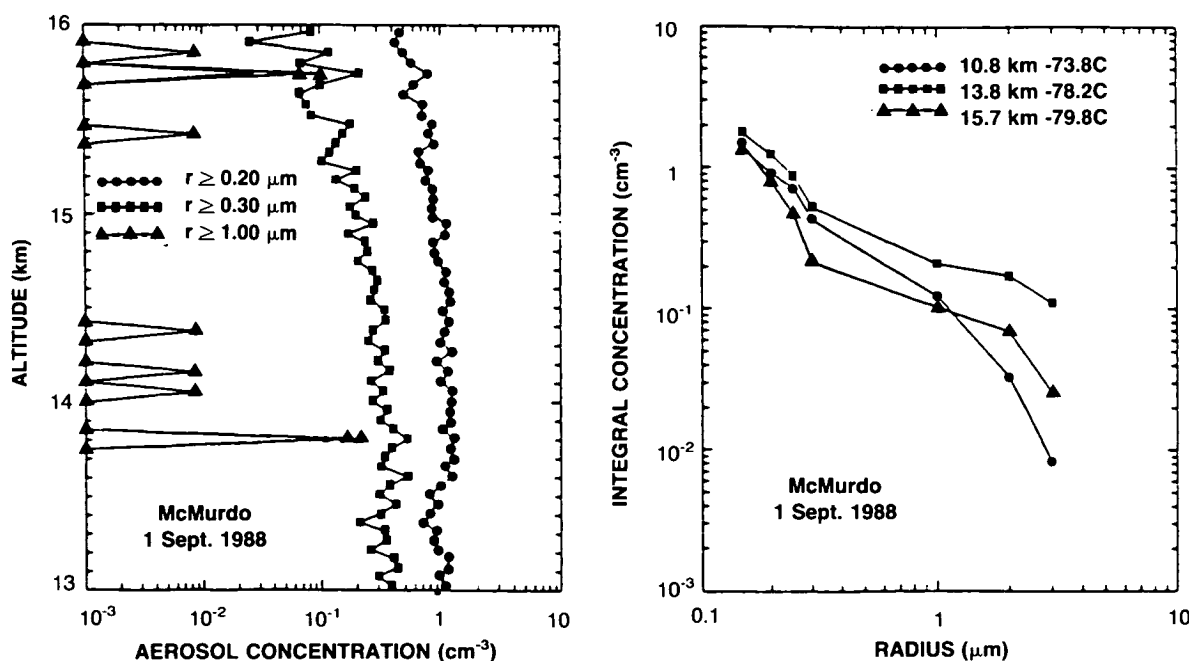


Figure 1.2.1-1. (Left) Vertical profiles of cloud particles observed during balloon soundings at McMurdo Station in September, 1988. Note the thin layers of few large particles observed, for example, near 13.8 km. (Right) Particle size distributions at various altitudes from the same sounding (from Hofmann, 1989b).

POLAR OZONE

large particle mode could significantly denitrify the polar stratosphere without much accompanying dehydration if these particles are composed of nitric acid trihydrate (in contrast to water ice clouds, which could presumably both denitrify and dehydrate the stratosphere). However, Hofmann (1989b) emphasized that such thin layers could not survive long (hours to days) and pointed out that current understanding of cloud microphysics cannot explain their formation. Understanding the formation, composition, and sedimentation of cloud particles is critical to an understanding of the processes responsible for the observed gas-phase composition of the polar stratosphere (see Sections 1.6 and 1.10).

Poole (1987) and Poole and McCormick (1988b) presented calculations from a two-stage PSC microphysics model which assumed that Type 1 PSCs form above the frost point as $\text{HNO}_3/3\text{H}_2\text{O}$ deposited on frozen background aerosol nuclei, and that Type 2 PSCs form subsequently (below the frost point) as H_2O ice deposited on Type 1 nuclei. They used vapor pressure relationships extrapolated from laboratory measurements of liquid $\text{HNO}_3\text{-H}_2\text{O}$ mixtures and assumed that no barrier to cloud particle nucleation existed other than the Kelvin vapor pressure elevation factor. Results showed that for slow cooling conditions (0.5 K/day), only a fraction (5%) of the background aerosol population would be activated as PSC particles, resulting in a bimodal particle size distribution. For typical Antarctic vapor mixing ratios, the authors reported Type 1 modal radii on the order of $1\ \mu\text{m}$ and Type 2 radii near $4\ \mu\text{m}$ and suggested that sedimentation of these larger Type 2 particles might lead to irreversible removal of HNO_3 from the Antarctic stratosphere. Calculated optical properties for Type 1 PSCs generally agreed well with lidar and SAM II observations. Theoretical calculations of the growth of Type 1 PSCs from the background aerosol were also reported by Hamill et al. (1988), who noted that Type 1 particle radii vary inversely (and markedly) with the fraction of aerosol activated into PSC particles.

The formation and growth of Type 2 PSCs has been discussed in recent papers by Ramaswamy (1988) and O. B. Toon et al. (1989). Ramaswamy specifically addressed the role played by Type 2 PSCs in the dehydration of the Antarctic stratosphere during winter, assuming that the particles form by deposition of H_2O ice directly onto the background aerosol and that the Kelvin effect is the only barrier to particle activation. Although not focusing on particle size, Ramaswamy found that Type 2 particles of radii $2\text{-}3\ \mu\text{m}$ formed over the course of several days with temperature decreases below the frost point, and that such a process could lead to extensive irreversible removal of H_2O vapor in the Antarctic. O. B. Toon et al. (1989) presented calculations on the size and lifetime of Type 2 particles forming on Type 1 PSC nuclei assumed to have a modal radius of $0.5\ \mu\text{m}$. The authors found that an energy barrier to ice nucleation (particle activation) akin to that observed in tropospheric cirrus was necessary in order to explain the dependence of observed Type 2 PSC properties on cooling rate. For cooling rates of several degrees K/day, inclusion of the nucleation barrier led to Type 2 particle radii on the order of $20\ \mu\text{m}$, which could rapidly dehydrate the Antarctic stratosphere through sedimentation.

In summary, there is agreement among the various measurements and calculations that Type 1 PSCs do exist at temperatures above the frost point (by as much as $5\text{-}7\ \text{K}$). This temperature regime is consistent with laboratory measurements of the stability of nitric acid trihydrate (Hanson and Mauersberger, 1988a,b), although the presence of super-cooled liquid $\text{HNO}_3\text{-H}_2\text{O}$ solutions, non-stoichiometric solid solutions with compositions near that of the trihydrate, or ternary $\text{H}_2\text{SO}_4\text{-HNO}_3\text{-H}_2\text{O}$ solutions cannot be ruled out. There is little doubt that predominantly water ice Type 2 clouds form at temperatures below the frost point. Recent laboratory vapor pressure measurements (see Section 1.3.1) imply that both PSC classes also likely contain trace amounts of HCl. The notion of a typical particle size for either Type 1 or Type 2 PSCs, on the other hand, appears to be an open question. Theory suggests that PSC particle sizes should depend strongly on the number of nuclei activated into cloud particles, which in turn is a very sensitive function of the physical properties of the nuclei themselves as well as the dynamical environment in which the

clouds form (e.g., the temperature history and the available vapor pressures of condensables). Additional in-situ measurements and more sophisticated modeling calculations are required to address these uncertainties.

1.2.2 Seasonal Behavior of PSCs

In this section, observations of PSC frequency with respect to season and year for both hemispheres will be discussed. This analysis is similar in content to that presented in McCormick et al. (1982) based upon only the first observations of PSCs. Although quantitative details presented herein differ from those of McCormick et al. (1982), the general conclusions regarding the seasonal variation, vertical extent, and hemispheric differences in PSC frequency are largely unchanged from the pioneering study of McCormick et al. The seasonal evolution of PSCs in both hemispheres can be examined by searching the weekly SAM II extinction data base (and ancillary temperature data) for those events which can clearly be distinguished from the background stratospheric aerosol as PSCs. In the study described here, the extinction characteristics of the unperturbed background atmosphere were identified using more detailed information than in previous work (see Poole et al., 1989). The selection criteria employed are likely to allow better discrimination between cloudy and clear conditions, particularly for relatively optically thin cloud events.

It would be desirable to search the SAM II data base for occurrences of Type 2 (predominantly H₂O ice) PSCs. Since the potential for growth to large sizes is much greater for Type 2 particles than for their Type 1 counterparts, Type 2 particles are the more likely to experience rapid sedimentation, which can irreversibly remove condensed HNO₃ from the polar stratosphere. They are therefore likely to play a particularly important role in denitrification. However, there are difficulties in choosing meaningful criteria to identify Type 2 PSCs in the SAM II record:

- (a) SAM II extinction coefficient measurements necessarily represent a spatial average over the instrument's line of sight, a distance on the order of 200 km. Thus, it is impossible to distinguish between patchy Type 2 PSCs and a continuous Type 1 PSC "haze" layer.
- (b) The potential for PSC extinction enhancement relative to that of the background aerosol (the PSC nuclei) depends quite critically on the initial characteristics (size and number density) of the aerosol. Aerosol characteristics are known to vary markedly with height in mid-latitudes, and are not well defined in the winter polar regions.
- (c) Theoretical models of PSC formation and growth have not matured to the stage at which they can provide unambiguous guidelines for differentiation of PSCs by Type.

Due to these unresolved issues in the interpretation of SAM II measurements, only the general trends in cloud occurrence frequency will be discussed here, without regard to intensity or Type.

The latitudinal coverage of SAM II is dependent on the orbit of the satellite and on the position of the sun (since the measurements are carried out by solar occultation; hence, there are no measurements in the polar night region). The latitude of SAM II observations varies from 64° (N or S) at the solstices to 80° (N or S) at the equinoxes. Thus, it is unknown whether seasonal patterns that are discernable from the SAM II data base are representative of actual PSC occurrences over the entire polar region.

The background aerosol population at a given altitude changes over the course of the winter in both polar regions, presumably due to subsidence and particle sedimentation. Therefore, temporally varying

POLAR OZONE

background extinction values were used as the basis for the PSC search described by Poole et al. (1989). These variations are normally quite subtle in the Arctic and are easily quantified, since many SAM II measurements during the winter are of the background aerosol alone (not PSCs). Calculated individual monthly average background extinction ratios and standard deviations were defined for November through February in each winter, while the February values were used as bases for March and April as well. SAM II observations of the Antarctic background aerosol show that a dramatic change occurs between May and October, but the details of the temporal variation are often obscured by the prevalence of very low temperatures and (hence) pervasive PSC sightings during the winter. However, in most years, the background aerosol extinction ratio is believed to remain relatively constant from May through July. Therefore, the temporal trend for each Antarctic winter was approximated by using average background extinction ratios (and standard deviations) from (a) the May monthly ensemble, for May–July; (b) the October monthly ensemble, for October; and (3) a linear interpolation between the May and October monthly ensembles, for August–September.

SAM II PSC observations for altitudes from 14–24 km at 2-km intervals are presented below. All data periods from November 1978 through April 1989 were included, with the exception of observations in 1983, which were omitted due to contamination by El Chichon volcanic aerosols.

Histograms of weekly SAM II PSC sightings in the Antarctic are shown in Figures 1.2.2-1 and 1.2.2-2 for the years 1979–1982 and 1984, at 14, 16, 20, 22, and 24 km. Corresponding figures for 1985–1988 are presented in Figures 1.2.2-3 and 1.2.2-4. Arctic PSC sightings are shown for the 1978–1979 through 1988–1989

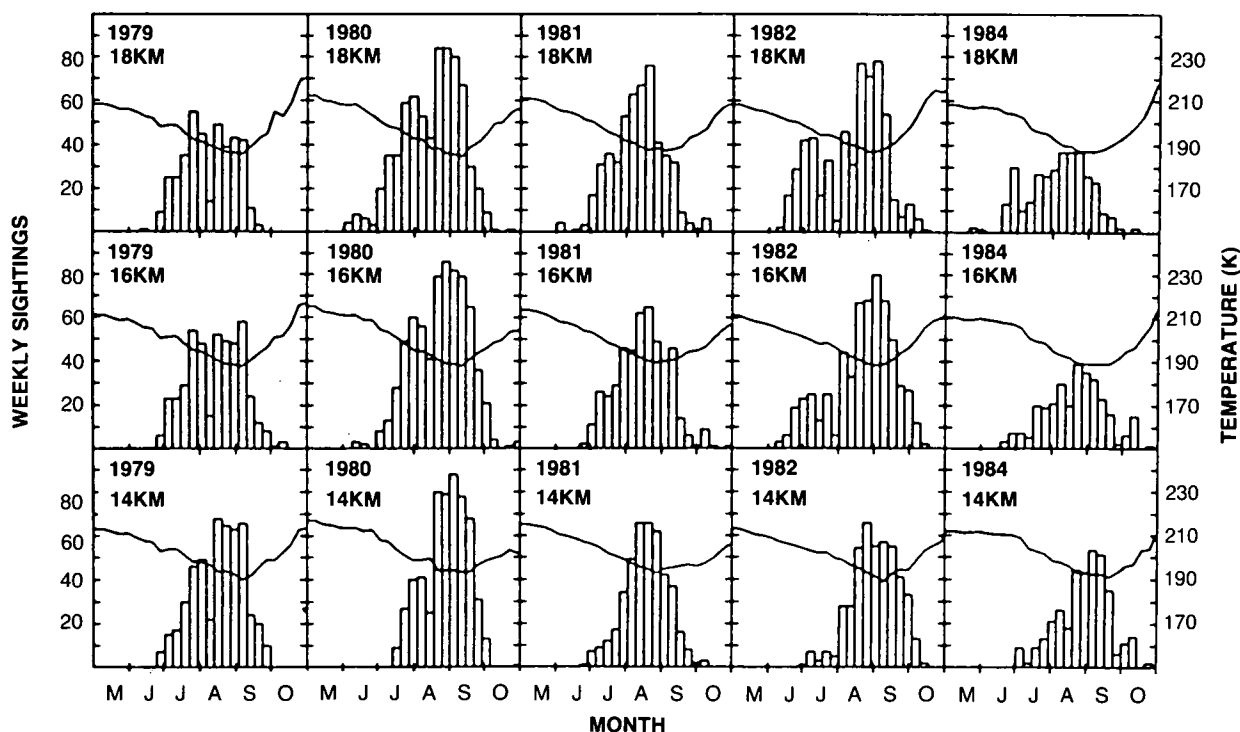


Figure 1.2.2-1. Observations of PSC sightings (per week) from SAM II during 1979, 1980, 1981, 1982, and 1984 for May through October in the Southern Hemisphere vortex (south of the 50 mb polar night jet). Sightings at the 14, 16, and 18 km levels are shown. The solid line indicates the corresponding average temperature for all polar SAM II measurements at each level as a function of time.

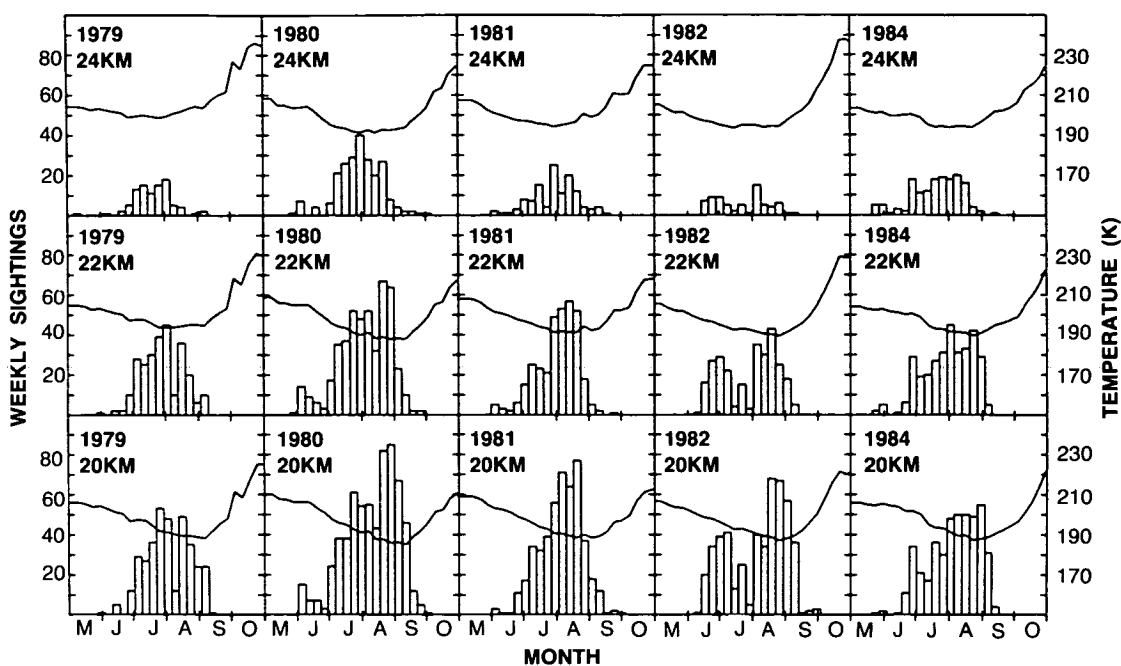


Figure 1.2.2-2. As in figure 1.2.2-1, but for 20, 22, and 24 km.

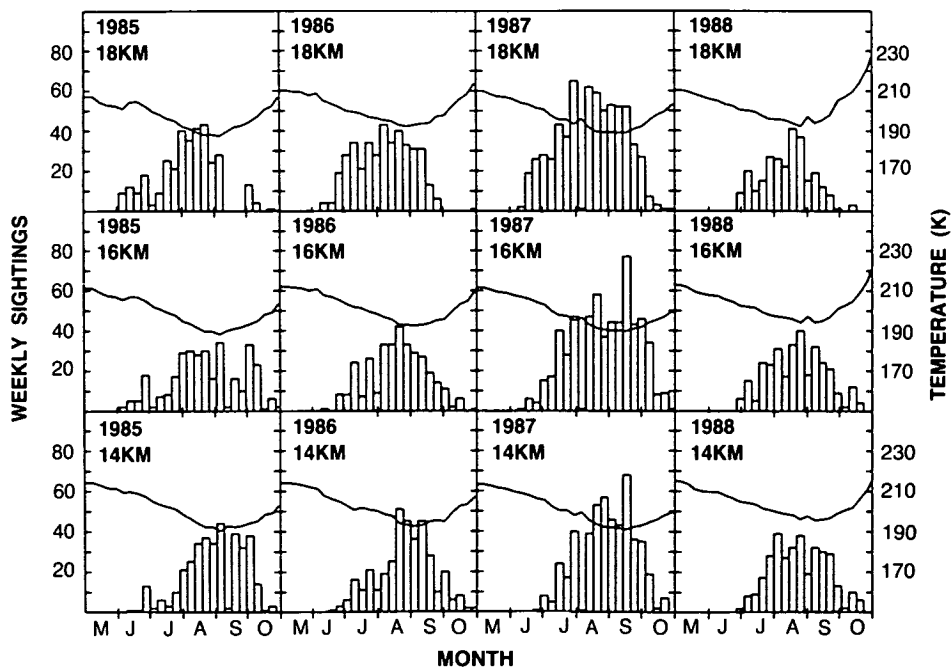


Figure 1.2.2-3. As in Figure 1.2.2-1, but for 1985 through 1988.

POLAR OZONE

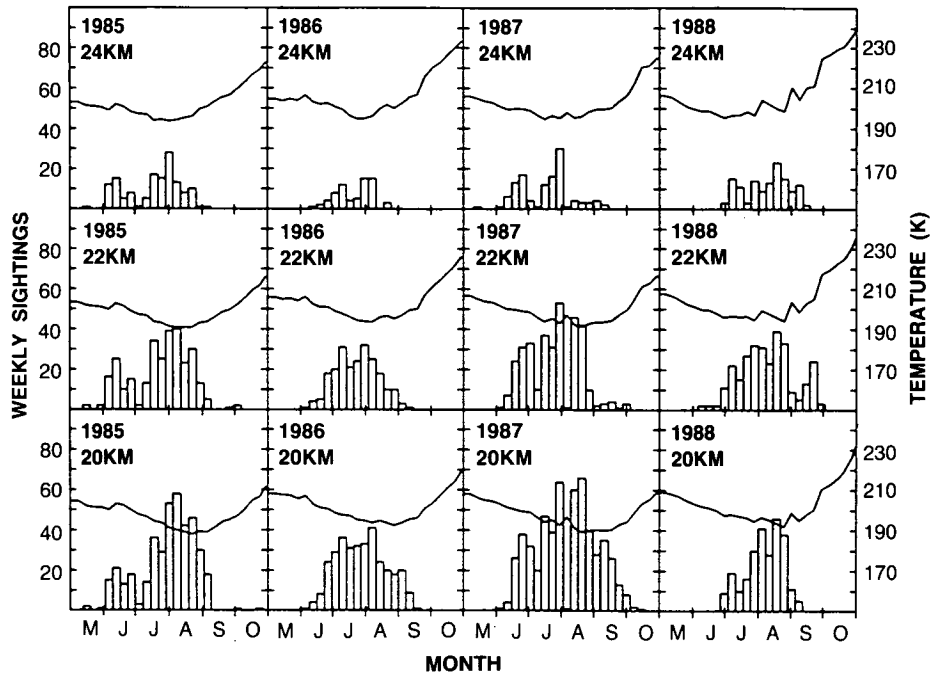


Figure 1.2.2-4. As in Figure 1.2.2-3, but for 20, 22, and 24 km.

winters excluding 1982–1983 in Figures 1.2.2-5 to 1.2.2-8. Also included in each frame is a plot of the weekly average temperature (solid line) for all SAM II measurements (PSC and non-PSC, both inside and outside of the vortex). By inspection and comparison of individual histograms, several general features can be noted:

- (a) At all altitudes and in all years, many more PSCs were observed in the Antarctic than in the Arctic. When totaled over a season, the ratio of Antarctic to Arctic sightings varied considerably with altitude and year, but typically ranged between 10 and 100.
- (b) During a given year in the Antarctic, the maximum number of PSCs was usually seen in the 16–18 km altitude range. The maximum number of Arctic PSCs was usually seen in the 20–22 km altitude range.
- (c) In the Arctic, the vast majority of PSC sightings occurred in January and February. However, there were some sightings in December and even a few in November and March. No Arctic PSCs were sighted in April. As expected, maxima in PSC sightings generally coincided with minimum temperatures. Since the temperatures shown are weekly averages at all SAM II locations including those at which PSCs were not observed, they are somewhat higher than the values at which PSCs are thermodynamically stable, but provide a rough indication of the relationship between the seasonal progression of temperature and PSC formation.
- (d) In the Antarctic, there were occasional PSC sightings in May and quite a few sightings in June, especially at the higher altitudes. The number of sightings generally increased during the winter months at all altitudes, with the temporal peak occurring in late August or early September at altitudes below 18 km and somewhat earlier at higher altitudes. As was seen in the Arctic, maxima in PSC sightings generally coincided with minimum weekly average temperatures. At all altitudes below

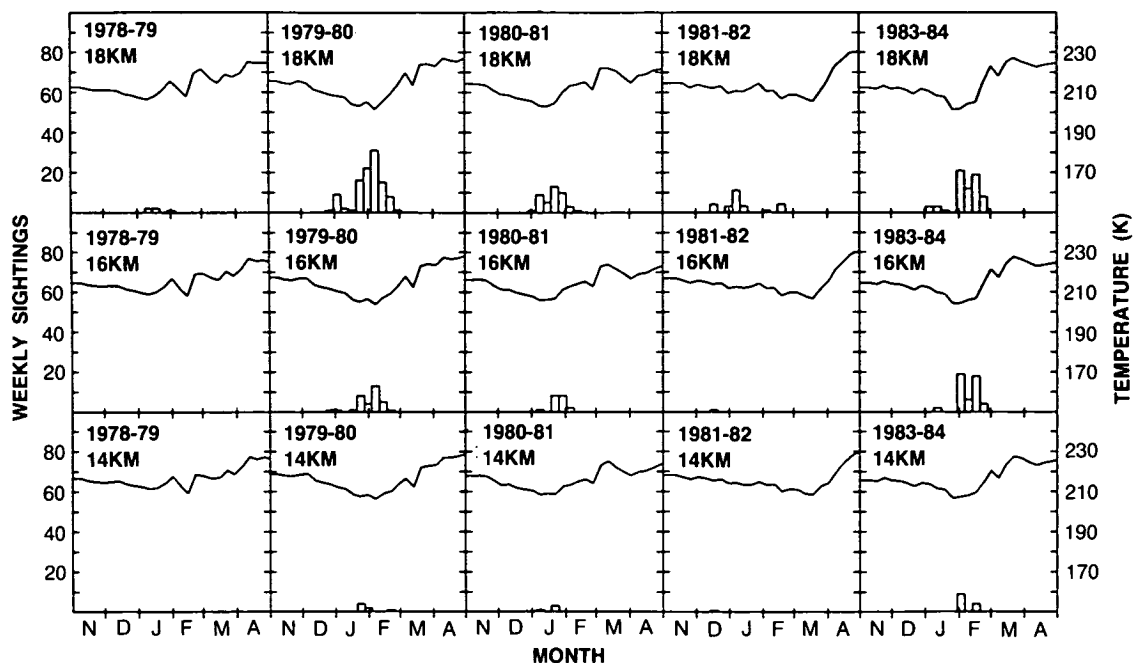


Figure 1.2.2-5. As in Figure 1.2.2-1, but for November through April in the Northern Hemisphere vortex (north of the 50 mb polar night jet) for the 1978-1979, 1979-1980, 1980-1981, 1981-1982, and 1983-1984 winter seasons.

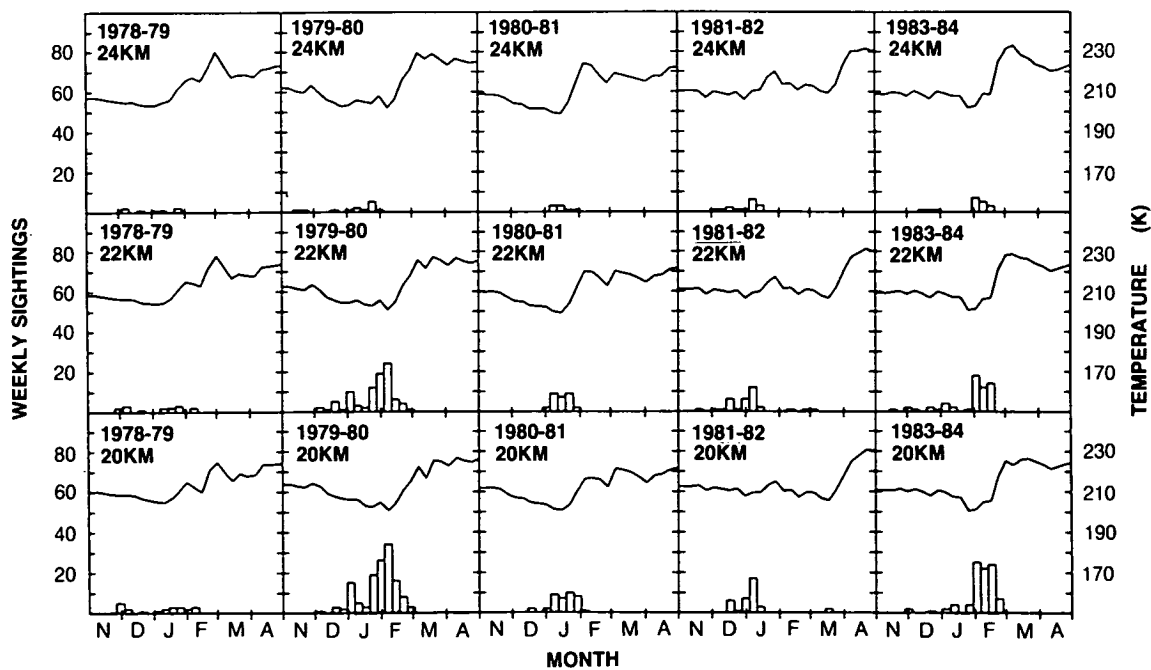


Figure 1.2.2-6. As in Figure 1.2.2-5, but for 20, 22, and 24 km.

POLAR OZONE

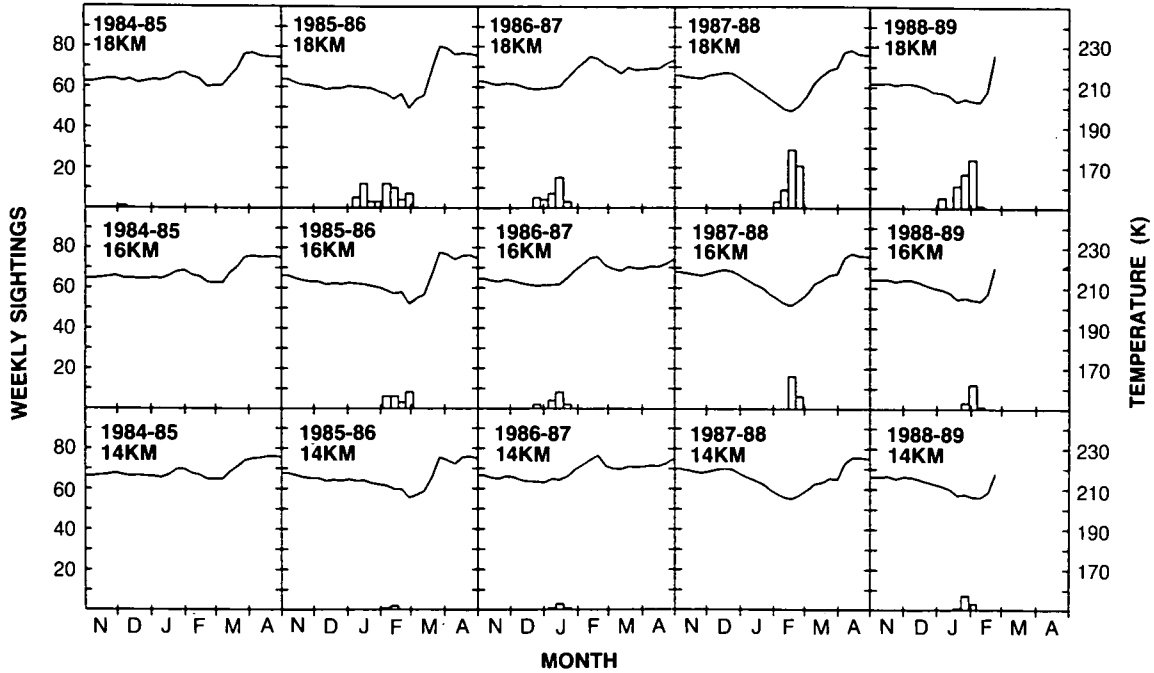


Figure 1.2.2-7. As in Figure 1.2.2-5, but for 1984-1985 through 1988-1989.

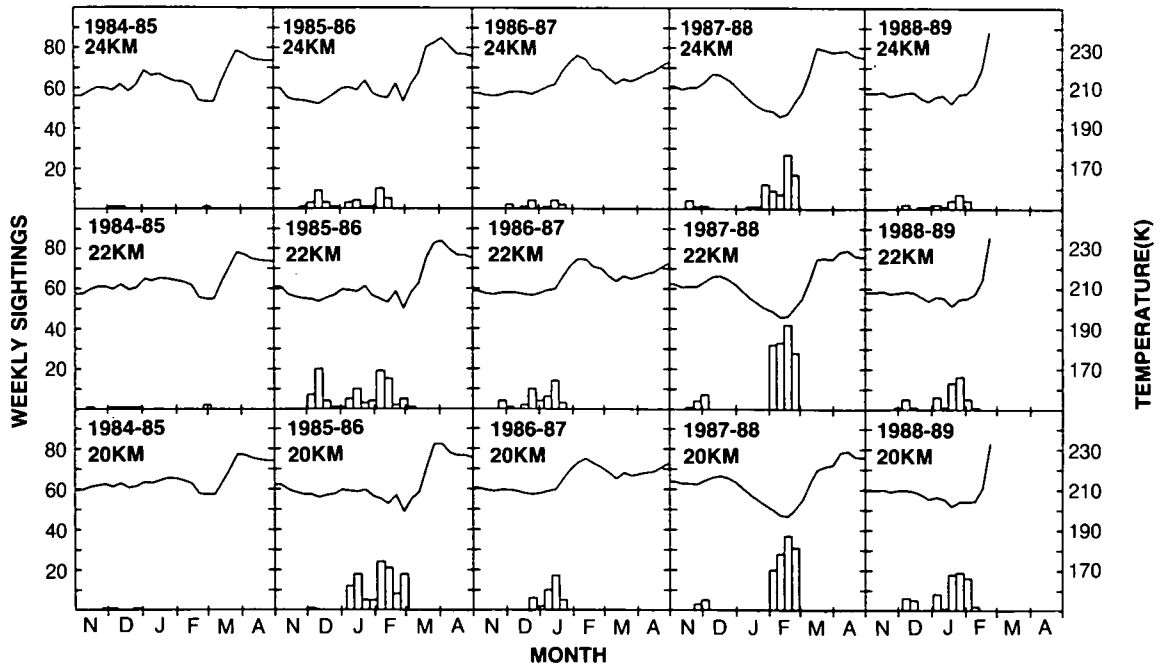


Figure 1.2.2-8. As in Figure 1.2.2-7, but for 20, 22, and 24 km.

20 km, PSCs were generally abundant in September and, in many years, were seen through the middle of October.

The comparison between Arctic and Antarctic PSC sightings thus reveals important differences both in the frequency of PSC sightings and in their duration, especially in spring. PSCs are far more prevalent in the colder Antarctic stratosphere as compared to the Arctic. While PSCs are generally observed in Antarctica in September and often in October, they are only seldom observed in the conjugate Northern Hemisphere Arctic data in March, and never in April in the years for which data are available. The seasonal PSC differences appear related to differences in spring temperatures between the two hemispheres. As discussed in Sections 1.6 and 1.10.2, these hemispheric variations in temperature and PSC duration in early spring months likely lead to large hemispheric differences in ozone depletion.

1.2.3 Long-Term Trends in PSC Frequency and Intensity

The SAM II data base also can be used to examine long-term trends in PSC frequency and intensity. A first-order approach to the entire data base is to integrate weekly averaged extinction coefficient measurements over altitude to form a temporal optical depth record. Observed optical depth records integrated from 2 km above the tropopause to 30 km for both hemispheres for the 1979–87 period are shown in Figure 1.2.3-1. The dates of major volcanic eruptions which injected aerosol into the stratosphere are also indicated.

The occurrence of PSCs in the Antarctic appears every year in the optical depth record as a marked third-quarter maximum, although (as mentioned in Section 1.2.2) the presence of aerosol injected by El Chichon obscures the maxima in 1983–1985. It is also interesting to note that the yearly minimum in

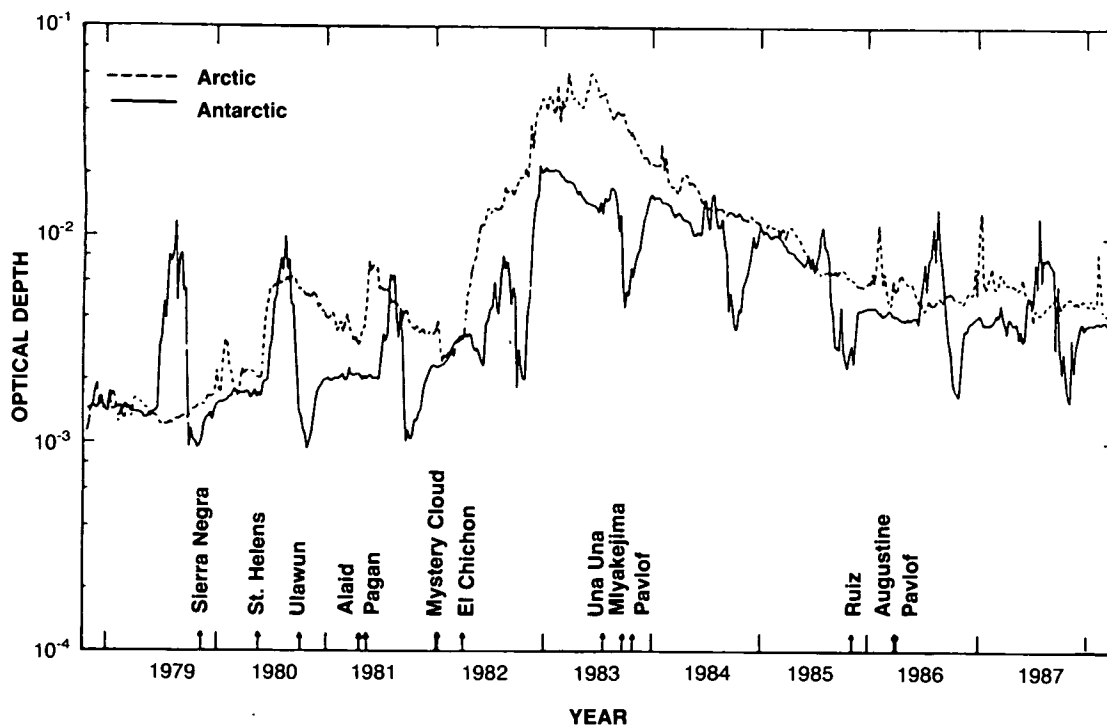


Figure 1.2.3-1. SAM II optical depth integrated from 2 km above the tropopause to 30 km, for the Northern and Southern Hemispheres. Major volcanic eruptions are indicated (after McCormick and Trepte, 1987).

POLAR OZONE

Antarctic optical depth immediately follows the maximum. This may indicate that particulate matter in the Antarctic stratosphere is redistributed downward during winter by subsidence or sedimentation (see Hofmann et al., 1988). The occurrence of PSCs in the Arctic appears (in most years) as a smaller, yet pronounced first-quarter maximum in optical depth. No clear trend for an abrupt minimum in optical depth following the PSC maximum can be seen in the Arctic. Figure 1.2.3-1 certainly establishes that PSCs have been recurrent seasonal phenomenon for the last decade, but reveals no obvious trend in either PSC frequency or intensity.

Another approach to analysis of PSC temporal trends is suggested by the work of Garcia and Solomon (1987), who reported a possible relationship between the quasi-biennial oscillation (QBO) and observed interannual variability in the October minima of mean TOMS total ozone values for Antarctica and of 100-mb temperatures inside the Antarctic vortex. The particular sensitivity of October temperatures to the QBO and the fact that Antarctic vortex temperatures in that month generally lie very close to the expected saturation over the nitric acid trihydrate suggests that the occurrence of PSCs during October might be particularly sensitive to both QBO and longer term trends in Antarctic temperatures. Calculated monthly sums of SAM II Antarctic PSC sightings (defined in Poole et al., 1989) in October for altitudes from 14–24 km (at 2-km intervals) from 1979–1987 are presented in Figure 1.2.3-2, while those for September are shown in Figure 1.2.3-3 (again excluding 1983 due to the masking effects of El Chichon aerosol). The phase of the QBO at 30 mb in tropical regions is also indicated. Results for 14–18 km show pronounced peaks in September and October PSC sightings in 1985 and 1987, with additional peaks in 1980 and 1982 at some

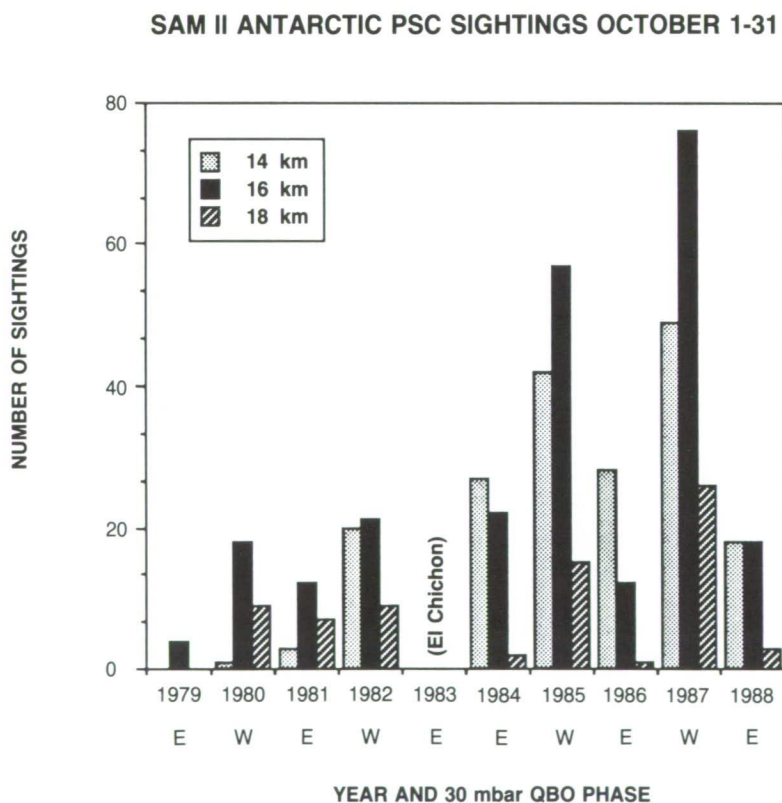


Figure 1.2.3-2. Observations of SAM II PSC sightings for Antarctica from 1979 through 1988 at 14, 16, and 18 km, during the month of October. The QBO phase at 30 mb is also indicated for each year (from Poole et al., 1989).

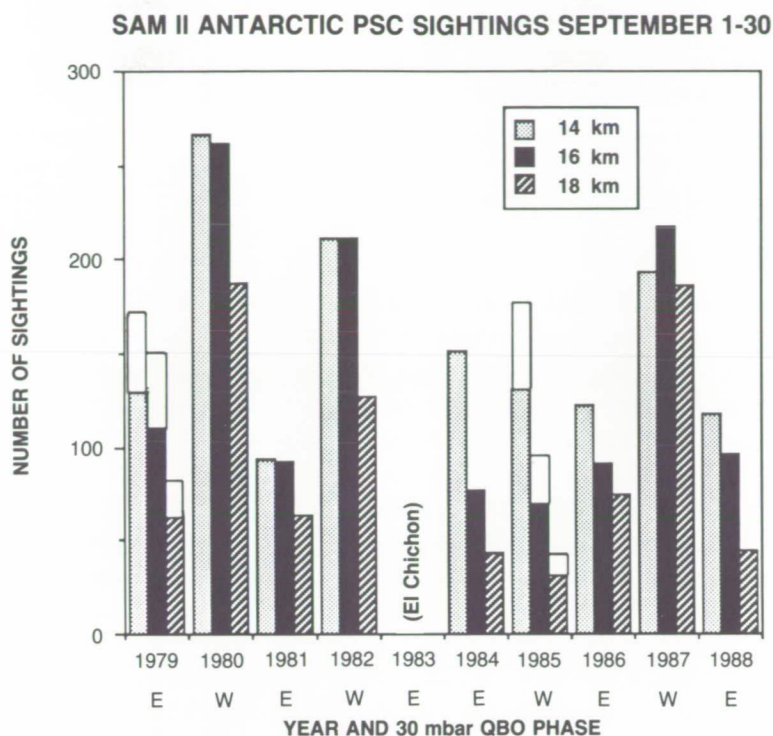


Figure 1.2.3-3. As in Figure 1.2.3-2, but for September.

altitudes. Years in which the Antarctic spring coincides with the strong westerly (easterly) phase of the QBO generally show September and October maxima (minima) in PSC sightings.

Figure 1.2.3-2 also suggests that the trend over the last decade has been towards an increase in PSC sightings at 14 and 16 (and possibly 18) km in the westerly phase years during October but not in September. It is important to emphasize that the determination of the long-term trend is complicated by the strong influence of El Chichon aerosol in 1983. The tallies for 1984–85 are likely low due to the masking influence of El Chichon aerosol remnants. However, Hofmann et al. (1987b) noted that the influence of El Chichon aerosol in the Antarctic vortex was negligible by austral spring of 1986.

The apparent trend is broadly consistent with observed long-term decreases in October temperatures discussed in Section 1.8. The PSC occurrence, temperatures, and ozone loss are expected to be closely interconnected, since ozone provides the source of heat to the stratosphere and the observed changes in temperature probably result in part from the ozone loss (see Section 1.8). Particularly in 1987, for example, the near-complete removal of ozone in the altitude region from about 10 to 24 km during September (Section 1.1) is believed to have substantially decreased temperatures in the lower stratosphere and hence likely played a role in enhancing the time during which PSCs persisted into the spring season.

The QBO and long-term trends in PSC occurrence in October clearly have important implications for heterogeneous chemistry and its effects on ozone. In particular, the apparent QBO modulation of PSCs in September may affect the rates of ozone removal in westerly as compared to easterly years. Further, the long-term trend in PSC frequency in October during westerly phase years should be expected to lengthen the time during which heterogeneous reactions are most effective at suppressing reactive nitrogen levels

POLAR OZONE

and enhancing reactive chlorine, thus leading to subsequent ozone loss (see Poole et al., 1989). The decadal trend in PSCs is likely to feed back into the decadal trend in total ozone and suggests a means of amplifying the expected long-term depletion of total ozone beyond that anticipated from the known growth in total chlorine content. This issue will be discussed further in Section 1.6.

1.2.4 Effect of PSCs on the Radiative Budget

Quantitative calculations of the evolution of the climate of the polar lower stratosphere must consider whether PSCs can significantly alter the radiative budget. As noted for example, by Tung et al. (1986), radiative cooling or heating by PSCs could have a substantial effect on the net radiative heating rate in the lower spring Antarctic stratosphere and hence on the mean meridional circulation and any possible ozone depletion due to uplifting. Further, as discussed in Section 1.7, downwelling may also be of considerable importance in tracer transport in the polar vortex.

The two most detailed studies of the impact of PSCs on the radiation budget (Blanchet, 1985; Pollack and McKay, 1985) were both performed prior to the announcement of the discovery of the ozone hole. Since then, much attention has been focused on the properties of PSCs, both observational and theoretical, and there have been significant changes in our understanding of the clouds (see Section 1.2.1).

Blanchet (1985) and Pollack and McKay (1985) reach fundamentally different conclusions about the sign of the effect of PSC cloud particles on the thermal infrared radiation budget. This is because the impact of the PSCs is critically dependent on the upwelling radiation from the underlying troposphere. Pollack and McKay assume a rather extreme cloudless troposphere with surface temperatures of 195 K; the increase in absorption of the upwelling radiation as a consequence of the PSCs does not balance the increased emission and the cloud particles cause a cooling. Blanchet assumes a rather warmer troposphere, and in this case, the increased absorption dominates, and the clouds cause a warming. Blanchet shows that his results are similar to Pollack and McKay's when similar temperature profiles are used. Hence, while the magnitude of the impact of the clouds is generally determined by such properties as the cloud particle size and number concentration, the net effect is dependent on conditions remote from the clouds.

Another fundamental difference between the two studies is that Pollack and McKay consider the effect of decreased water vapor mixing ratio, as a result of water tied up in the cloud particles. Since water vapor acts to cool the stratosphere by emission in the thermal infrared, its loss leads to a relative warming. For a wide range of conditions, Pollack and McKay show that the effect of loss of water vapor dominates the effect of the cloud particles, and hence the net effect of the particles is to cause a warming. This effect is not considered in Blanchet's work.

Pollack and McKay (1985) calculate the effect of a cloud of extinction coefficient (at a wavelength of 1 μm) of 0.01 km^{-1} , a value based on observations from SAM II. Standard calculations are based on a particle radius of 1 μm , but other radii, ranging from 0.056 to 18 μm are also considered. The effect of the 1 μm particles is very small; they cause a cooling of no more than 0.01 K/day, a value dominated by the relative warming due to loss of water vapor, which can exceed 0.08 K/day. At the extremes of the range of particle sizes used in the calculations, more significant effects are found. For a radius of 0.1 μm , a cooling of about 0.24 K/day is found, while for large particles (10 μm) the cooling reaches 0.12 K/day.

Blanchet (1985) considered the effect of PSC particles growing from 0.0725 μm to 2 μm ; for a case with a number concentration of 6 cm^{-3} , Blanchet considered the effect of increasing particle size (i.e., the extinction coefficient is not held constant as in Pollack and McKay's calculation). Particles with a radius

of $0.5 \mu\text{m}$ (representing an extinction of 0.02 km^{-1} at $1 \mu\text{m}$) give a mild heating of about 0.3 K/day at the cloud base, with smaller coolings towards the cloud top. Particle radii of $1 \mu\text{m}$ cause a peak heating of about 0.2 K/day . Increasing the particle radii to $2.0 \mu\text{m}$ (with a corresponding increase in extinction coefficient of 0.1 km^{-1}) does generate significant heating rates of 1.0 K/day . Blanchet proposed that under normal conditions such particle sizes could not be reached, as such large heating rates would act as a limiting factor in the cloud's development.

Less work has been performed on the effects of PSCs on solar radiation, principally because of the limited sunlight available at times when PSCs are normally presented. Nevertheless, Shi et al. (1986) show that heating rates of about 0.2 K/day are possible in late September and that the solar heating of the particles dominates over effects in the thermal infrared. This is for a case with a total stratospheric optical depth of 0.02 at $1 \mu\text{m}$, a value close to those observed during springtime in the Antarctic. Akiyoshi et al. (1988) performed similar calculations using extinction data derived from SAGE II observations during 1985. These authors do not discuss the extinction coefficients derived from the measurements. They find that the aerosols always act to warm the lower stratosphere in the thermal infrared as well as at solar wavelengths. However, on no occasion is the net heating due to the aerosols greater than 0.1 K/day .

As noted earlier, *in situ* balloonsonde measurements indicate that PSC clouds sometimes consist of particles of radii between $1\text{--}10 \mu\text{m}$, with concentrations of 0.0001 to 0.001 cm^{-3} (Rosen et al., 1988a; Hofmann et al., 1987a,b; Hofmann, 1989a,b). Such low concentrations of particles would, on the basis of the calculations described earlier, have a negligible effect on the diabatic heating.

Kinne and Toon (1989) provide a preliminary report of calculations of the radiative effects of PSCs based on measurements of cloud properties near the Palmer Peninsula from the AAOE experiment. Calculations for PSC Types 1 and 2 were performed for a cold south polar profile for 19 September 1987 (surface temperature about -60°C) both with and without high level ($10\text{--}14 \text{ km}$) cirrus. Their Type 1 PSCs (with an optical thickness of 0.002 and typical particle radii of $0.8 \mu\text{m}$) have an insignificant effect in the absence of cirrus and cause only a slight (-0.09 K/day) cooling with cirrus. The Type 2 PSCs (with an optical thickness of 0.05 and typical particle radius of $15 \mu\text{m}$) have a much larger effect. The thermal infrared cooling (0.3 K/day at cloud top) dominates the solar heating (0.12 K/day at cloud top). In the presence of cirrus the IR cooling rate reaches 1 K/day .

A further set of calculations were performed for optically thick "mountain-PSCs" associated with forced adiabatic ascent such as that present during "mini-hole" episodes (see Section 1.7.2). These calculations are for far warmer Palmer Peninsula profiles (for 21 August 1987 surface temperatures are about -9°C and for 9 September 1987 they are about -3°C). The mountain-PSCs have an optical thickness of 1 and a typical particle radius of $1 \mu\text{m}$. Again the infrared effects dominate over solar heating, although it should be noted that Kinne and Toon use the same solar zenith angle for both days (84°) and do not attempt an integration over daylength. The role of cirrus in modulating the net heating is, however, very dramatic and is shown in Figure 1.2.4-1. In the absence of cirrus, the PSCs cause a strong heating in the thermal infrared, which reaches 8 K/day at cloud base. In the presence of cirrus the net effect is one of cooling, which exceeds 7 K/day at cloud top.

In summary, in the absence of cirrus, thermal infrared radiation reaching the cloud base is principally emitted from the surface and lower troposphere, which are far warmer than the cloud base; hence the cloud base is receiving more radiation than it emits and heats. The addition of the optically thick cirrus blocks the radiation from the lower troposphere; the radiation now reaching the PSC base is from the cold cirrus top, causing the PSC layer above to yield a net cooling. The calculations shown in Figure 1.2.4-1

POLAR OZONE

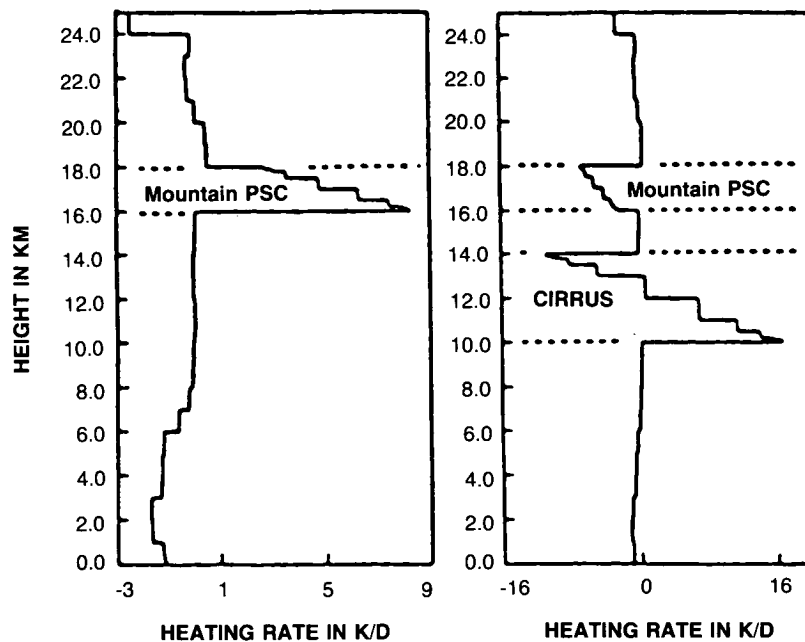


Figure 1.2.4-1. Changes in net heating caused by mountain-PSCs with and without cirrus. The calculations are for a temperature profile from Palmer Peninsula Station for 9 September 1987 (from Kinne and Toon, 1989).

suggest that radiative effects due to clouds may be extremely important under some conditions and clearly demonstrate the importance of accurate specification of the state of the underlying atmosphere.

A full assessment of the impact of PSCs on the radiative budget of the entire polar vortex needs to be performed as considerable uncertainties still remain. Such a calculation would need to include a representative range of tropospheric temperature and cloud conditions, as experienced in the Antarctic during winter and early spring. Clearly the impact of water passing from the vapor to the liquid/ice phase, and possibly out of the lower stratosphere altogether, would need to be incorporated. Perhaps the most important aspect of the radiative properties of PSCs lies in the possibility that some PSCs may lead to very large cooling rates in the lower stratosphere. These in turn could result in substantial downward motion, with attendant effects on the dynamics of the vortex and its ability to work as a "processor" for ozone depletion (see Tuck, 1989, and Section 1.7).

1.3 PHYSICAL PROPERTIES OF POLAR STRATOSPHERIC CLOUDS

The goal of this section is to present laboratory and field studies aimed at understanding the chemical composition of PSCs and their physical properties. In Section 1.3.1, laboratory studies of the co-condensation of HNO_3 and H_2O will be briefly described, and the nature of the interaction of HCl with such surfaces will be summarized. In Section 1.3.2, field observations of chemical species in the particulate phase will be reviewed. It will be shown that both the laboratory and field investigations support the notion that the nitric acid trihydrate is the dominant component of Type 1 PSCs (Toon et al., 1986; Crutzen and Arnold, 1986). Trace amounts of HCl are also expected to be present in such particles based on laboratory and field measurement studies and likely play a particularly important role in heterogeneous chemistry as discussed in Section 1.4.

1.3.1 Laboratory Studies

Co-condensation of HNO_3 with H_2O leads to the formation of PSCs at temperatures above the frost point of water, as concluded by Crutzen and Arnold (1986), McElroy et al. (1986) and Toon et al. (1987) from extrapolations of $\text{HNO}_3/\text{H}_2\text{O}$ vapor pressure data near room temperature.

The physical chemistry of the $\text{H}_2\text{O}-\text{HNO}_3$ system under conditions pertinent to the polar stratosphere has been investigated in the laboratory only very recently (Hanson and Mauersberger, 1988a,b). These authors measured the vapor pressures of both components using high-sensitivity mass spectrometry. The results show that for solids with bulk compositions close to those of the nitric acid trihydrate ($\text{HNO}_3-3\text{H}_2\text{O}$) or the monohydrate ($\text{HNO}_3-\text{H}_2\text{O}$), these crystalline phases can indeed be prepared by co-condensation of gaseous $\text{H}_2\text{O}-\text{HNO}_3$ mixtures with the appropriate composition; bounds on their vapor pressures can be established by extrapolation of vapor pressures of the liquid solutions to the freezing point temperatures, using the Clausius-Clapeyron equation. Furthermore, the results have been shown to agree with the Gibbs-Duhem relationship (Poole, private communication, 1989), which yields the vapor pressure of one of the components in the binary system as a function of the vapor pressure of the other component and of the composition of the condensed phase. These laboratory results corroborate that PSCs consisting of nitric acid trihydrate crystals may form at temperatures several degrees above the frost point of water (see Section 1.2).

The interaction of HCl vapor with water-ice has been studied in the past few years by several groups. Molina et al. (1987) found that HCl has a significant affinity for ice crystals; that it readily diffuses within the surface layers and grain boundaries of such crystals; and that the "sticking" coefficient around 200 K is close to unity, i.e., 0.1 or larger. This coefficient is the probability per collision with the surface that the gas molecule will be incorporated into the condensed phase (assuming a collision frequency given by gas kinetic theory). Similarly high sticking coefficient values were obtained by Tolbert et al. (1987), by M.-T. Leu (1988a) and by Kolb et al. (personal communication, 1988). Molina et al. (1987) and Wofsy et al. (1988) first interpreted their results in terms of a high solubility of HCl in the ice matrix, analogous (but not as large as) that in liquid water. More recent laboratory experiments with a variety of ice substrates, including large single crystals as well as ice frosts, have shown that this affinity of HCl vapor for ice (and the high mobility) are confined to a surface layer that is at least several hundred angstroms deep (Molina et al., 1989). The amounts of HCl absorbed can be orders of magnitude larger than required for the formation of a monolayer at the surface. This behavior is most likely associated with crystal defects, which are known from previous work on ice to be present in layers extending hundreds of angstroms from the surface. Thus, the laboratory observation of a high affinity of HCl vapor for ice frosts is indeed relevant to the behavior of PSCs, since both systems have similarly high surface-to-volume ratios.

In contrast to these results, Wolff et al. (1989) concluded that the solubility of HCl in ice is negligible, and suggested that melting at the surface was responsible for the above observations. Wolff et al. based their conclusions on scanning electron microscopy studies of ice crystals grown by freezing aqueous HCl solutions. It is clear, though, that efficient absorption of HCl vapor by ice can occur readily under conditions where no liquid phase is present, that is, at temperatures below 180 K (Molina et al., 1989).

There is little experimental information on the ternary system $\text{H}_2\text{O}/\text{HNO}_3/\text{HCl}$ at temperatures leading to the formation of solid phases. Tolbert and coworkers (Tolbert, private communication, 1989) have measured a sticking coefficient value of about 0.07 for HCl vapor on nitric acid trihydrate at 190 K. Hanson and Mauersberger (1989a,b) reported vapor pressures of HCl over nitric acid trihydrate at 200 K, with values in the 10^{-8} to 10^{-6} torr range corresponding to compositions in the solid phase in the 0.1 to 2% HCl

POLAR OZONE

range. According to these studies, HCl is significantly more soluble in the trihydrate than in pure water-ice. Work in progress in other laboratories (Molina et al., 1989) corroborates that there is a significant affinity of the trihydrate for HCl. This work indicates that around 180 K, pure water-ice absorbs HCl vapor efficiently only when the HCl partial pressure is above about 10^{-5} torr. The absorption occurs apparently by the growth of HCl hexahydrate crystals, but the hexahydrate is not expected to form at the reduced abundances of HCl present in the stratosphere. Clearly, one of the most difficult aspects of these studies is the proper characterization of the solid substrate, and additional quantitative HCl vapor pressure measurements are clearly needed for various ice substrates.

1.3.2 Direct Supporting Evidence from Field Experiments

Recent field investigations have shed a great deal of light on the composition of polar stratospheric clouds. As noted earlier, a number of studies of PSCs have revealed that the clouds begin to form at temperatures far above the frost point (by as much as 8 K), strongly suggesting condensation of trace species other than water. This was first pointed out by Austin et al. (1986a) based on LIMS observations of anomalous infrared radiance, and studied in detail by Poole and McCormick (1988a,b) using SAM II observations of PSC extinction. Hofmann (1989a,b) and Rosen et al. (1988a) also noted the formation of PSCs at temperatures well above the frost point. Arnold and Knop (1989) reported measurements of HNO_3 in the Arctic that set an upper limit for HNO_3 cloud formation temperatures at 195 K at 23 km, well below the frost point. The optical and physical characteristics of the clouds observed were discussed in Section 1.2. Measurements of particles and gases during the Airborne Antarctic Ozone Experiment (AAOE) and Airborne Arctic Stratosphere Experiment (AASE) provide particularly detailed information on cloud particles and accompanying chemistry.

The observations of total reactive nitrogen (NO_y) by Fahey et al. (1989a,b) also provide important insights into the composition of PSCs. The measurements of NO_y are somewhat difficult to interpret in the presence of PSC particles, because the instrument has a greater sampling efficiency for NO_y in large particulates than for NO_y in the gas phase. This can lead to substantial, particle size-dependent NO_y enhancements when large amounts of NO_y -containing particles are present. These enhancements complicate interpretation of the gas-phase component of the signal but also provide important insights to the particle composition, especially when coupled with concurrent observations of the particle size distribution so that their effects can be quantitatively evaluated (see Fahey et al., 1989b).

Figure 1.3.2-1 shows measurements of NO_y , total water vapor, temperature, pressure, and cloud particles as a function of time on August 17, 1987 from Fahey et al. (1989b). These observations demonstrate that cloud particle formation occurred well above the frost point of water vapor. These observations permit identification of cloud "edges," although it should be emphasized that the past temperature history of air parcels also plays a role in determining the onset of cloud formation and should be examined in a detailed analysis. Nonetheless, it is clear that the observed condensation point was far warmer than the frost point, and in general agreement with expectations based on the thermodynamics of the nitric acid trihydrate as proposed by O. B. Toon et al. (1986) and quantified by the laboratory study of Hanson and Mauersberger (1988a,b). Further, the dramatic NO_y enhancement directly confirms that the particles contain a substantial amount of nitrate. This set of observations therefore provides strong evidence that condensation of HNO_3 plays a critical role in PSC cloud formation.

Observations by Gandrud et al. (1989) support and extend this picture. Gandrud et al. conducted filter sampler measurements of cloud composition during the AAOE experiment. Using a dual filter system,

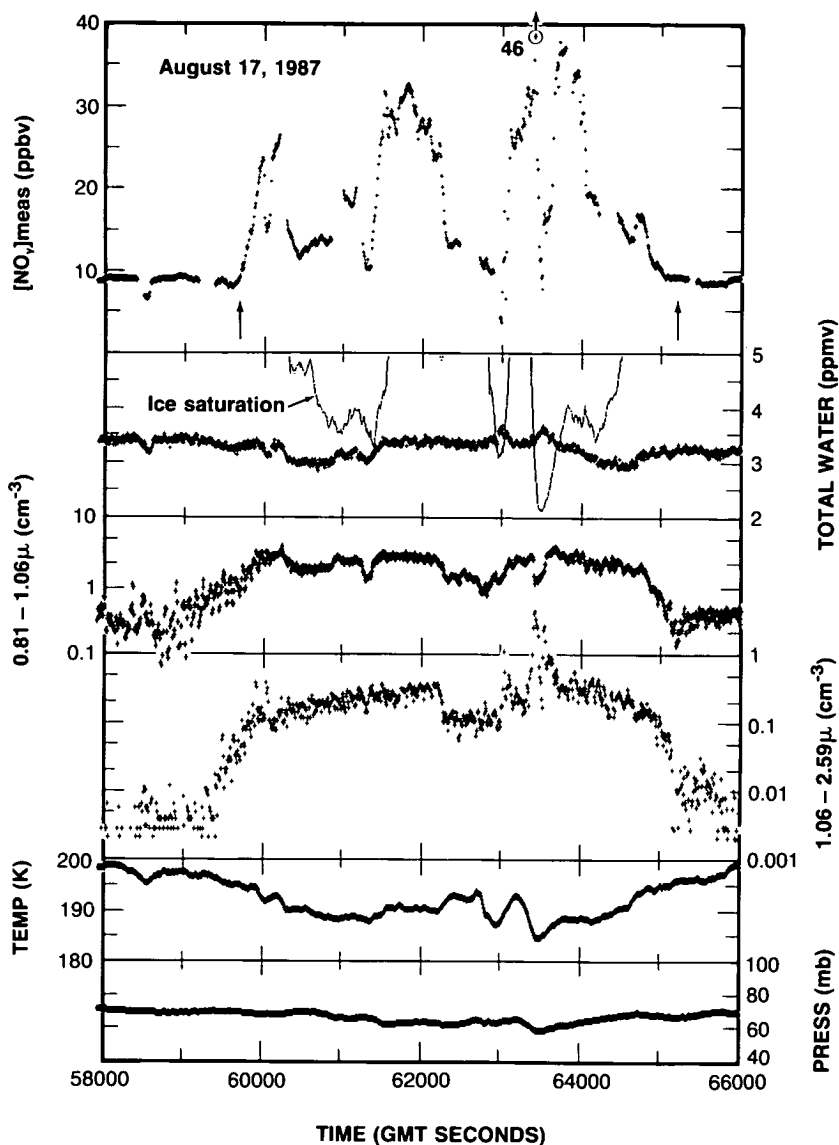


Figure 1.3.2-1. Plot of the flight track data for the encounter with a PSC event on August 17, 1987. The gaps in the NO_y data are caused by instrument calibration checks. The ice saturation mixing ratio is calculated from the observed pressure and temperature using the Smithsonian Meteorological Tables. The cloud edge times are noted by the arrows (from Fahey et al., 1989b).

Gandrud et al. (1989) deduced the amount of nitrate in both the particulate and gas phases. The instrument is sensitive to HNO_3 , ClONO_2 , N_2O_5 , and particulate nitrate. Total acidic chloride (from HCl and ClONO_2) is also observed in both the gas and particulate phases, along with total acidic fluoride. Figure 1.3.2-2 shows the time behavior of the measured percentage of total nitrate in particulates along with other relevant parameters derived for the flight of 4 September, 1987. Note that the most poleward point (about 72°S) was reached at roughly GMT time 61,000 seconds, the temperature at this point was 190 K, and the largest values were obtained during the aircraft "dip" to near 16 km. The data for this flight clearly suggest that a

POLAR OZONE

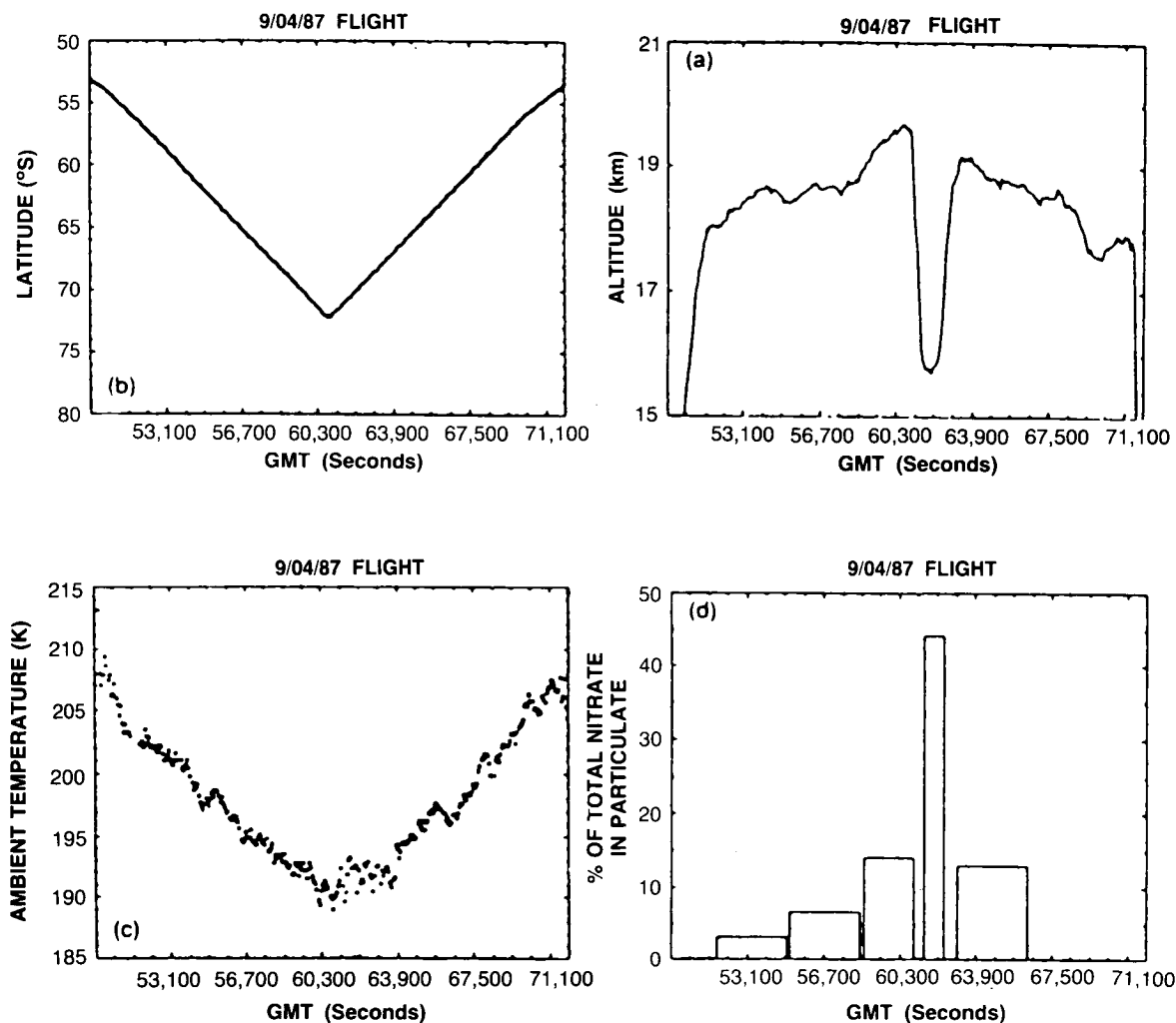


Figure 1.3.2-2. Observations of the percent of total observed nitrate in the particulate phase as a function of time along the AAOE flight track for September 4, 1987 along with observed temperature, latitude and altitude (from Gandrud et al., 1989).

substantial fraction of the available nitrate had been taken up on particles. In contrast, no chloride was observed in the particulate phase on any of the flights, nor were substantial particulate nitrate levels observed outside of the chemically perturbed region. The detection limit for chloride was estimated at 0.08 to 0.16 ppbv Cl. Assuming that the total inorganic chlorine is about 2.5–3.0 ppbv, this corresponds to at most 6.4% of the total chloride, in good agreement with laboratory studies showing that only a few percent of available HCl condenses on ice surfaces (e.g., Molina et al., 1987; Hanson and Mauersberger, 1989a). Similarly, the upper limit for particulate fluoride was only 4–5% of the total acidic fluoride. As discussed in further detail in later sections of this report, the possible removal of nitrate, fluoride, and chloride through sedimentation of large particles can influence the photochemistry of the polar lower stratosphere. The small abundances of chloride and fluoride in the particulate phase strongly suggest that “dechlorination” or “defluorination” will be far less effective than denitrification.

Pueschel et al. (1989) collected aerosol particles during the same aircraft experiments using a wire impactor technique and subsequently analyzed them for nitrate and chloride. Their results revealed a sharp dependence of condensed nitrate on temperature: nitrate-containing aerosols began to form at temperatures below about 193 K, in general agreement with expectations based on the thermodynamics of Type 1 nitric acid trihydrate particles. Pueschel et al. (1989) also concluded that the mass of HCl condensed in the particles was only 3% of the sulfuric acid mass, suggesting that only a small fraction of the available chloride is incorporated into the particles.

As expected from theoretical and laboratory studies, *in situ* measurements of total NO_y and gas and particulate phase nitrate confirm that PSC particles often contain a large amount of nitrate and form at roughly the temperatures expected for the HNO₃/3H₂O system. The formation of nitrate-containing PSC Type 1 clouds is likely to affect the chemistry of the polar lower stratosphere in two important ways: by removing reactive nitrogen from the gas phase (and hence affecting the photochemical balance, at least temporarily), and by allowing for cloud formation at significantly warmer temperatures than the frost point. While the observations are consistent with suggestions regarding irreversible removal of reactive nitrogen via incorporation into particles and subsequent sedimentation, there is no evidence for substantial removal of chloride or fluoride in PSC particles. However, the observations also suggest that a few percent of the available HCl is in the particulate phase (which could drive important heterogeneous processes), consistent with laboratory studies.

1.4 HETEROGENEOUS CHEMISTRY

Heterogeneous chemical processes in the atmosphere involve a reaction between a gaseous species and a solid or liquid particle. These processes occur in several steps: diffusion of the gaseous molecule to the surface; absorption or adsorption at the surface; diffusion on the surface or into the particle; chemical reaction, etc. For atmospheric systems there is usually not enough information to characterize each of these steps, whose rate may depend not only on the type of particle but also on its temperature, composition, size, shape, etc. On the other hand, the overall reaction rate can be approximated in terms of a single parameter, the "reaction probability *g*," defined as the probability that a collision of a gas molecule with the surface will result in the net chemical reaction in question. This parameter *g* has often been labeled a "sticking coefficient," but this term should be restricted to steps or processes not involving chemical reactions (see Section 1.3).

Molina et al. (1987), using FTIR spectroscopy and gas chromatography, showed that gaseous chlorine nitrate (ClONO₂) reacts efficiently with HCl-doped ice producing molecular chlorine (Cl₂), which is immediately released to the gas phase, and nitric acid (HNO₃), which remains in the solid phase:



These authors measured reaction probability values in the 0.02 to 0.1 range for ice containing HCl at up to 1% mole levels (see Table 1.4-1). Similarly, large reaction probabilities were reported for the same system by Tolbert et al. (1987), who employed a Knudsen cell reactor attached to a mass spectrometer, and by Leu (1988a), who used a fast flow reactor with mass spectrometric detection. In the absence of HCl, the reaction probabilities measured by these groups were somewhat smaller, the gaseous product being HOCl, which has an affinity for ice intermediate between that of Cl₂ and that of HCl:



POLAR OZONE

Table 1.4-1. Reaction probabilities on water-ice

Gaseous Reactant	Temperature (K)	HCl (mole fraction × 100)	Reaction Probability	Reference
ClONO ₂	200	—	0.02	Molina et al. (1987)
ClONO ₂	200	0.03–1.0	0.05–0.1	Molina et al. (1987)
ClONO ₂	185	—	>0.01	Tolbert et al. (1987)
ClONO ₂	185	0–13	>0.01	Tolbert et al. (1987)
ClONO ₂	200	—	0.06	Leu (1988a)
ClONO ₂	200	0.23–7.1	0.11–0.27	Leu (1988a)
N ₂ O ₅	185	—	>0.001	Tolbert et al. (1988a)
N ₂ O ₅	190	—	0.03	Tolbert et al. (1988b)
N ₂ O ₅	190	^a	0.02	Tolbert et al. (1988b)
N ₂ O ₅	190	^b	<0.001	Tolbert et al. (1988b)
N ₂ O ₅	185	7–14	>0.003	Tolbert et al. (1988b)
N ₂ O ₅	195	—	0.028	Leu (1988b)
N ₂ O ₅	195	1.5–4	0.05–0.07	Leu (1988b)

^aOn nitric acid trihydrate.

^bOn nitric acid monohydrate.

Reactions analogous to (1.4.1) and (1.4.2) in which ClONO₂ is replaced by dinitrogen pentoxide (N₂O₅) have been studied in the laboratory by Tolbert et al. (1988b) and by Leu (1988b):



A summary of the reported reaction probabilities is listed in Table 1.4-1. Both because of its apparently large reaction probability and because two chlorine containing reservoir species are affected by it, reaction (1.4.1) is believed to be of particular importance in polar photochemistry (see Section 1.6).

It is likely that nitric acid trihydrate crystals will behave in a manner analogous to water-ice in promoting reactions (1.4.1) to (1.4.4), but this remains to be confirmed in the laboratory. Another issue which requires additional studies involves the competition between water and HCl as heterogeneous reactants, that is, between reactions (1.4.1) or (1.4.3), and (1.4.2) or (1.4.4); the key factor is the concentration of HCl on the surface of the particle. A related question concerns the amount of HCl that will be incorporated into PSCs, and the corresponding concentrations at the surface of the crystals (see Section 1.3.1).

Experiments by Leu (1988b) have indicated a sticking coefficient value greater than about 0.01 for ClO on ice. This system should be studied further to establish whether chemical reactions occur in this process; it might have significant consequences in the polar stratosphere.

The heterogeneous reactions discussed in this section are likely to proceed through an ionic mechanism, without a significant activation energy. The pulsed experiments carried out by Molina et al. (1987) indicated that ClONO₂ remains on the surface of the HCl-doped ice crystals for, at most, a fraction of a second before releasing gaseous Cl₂. Additional studies should be carried out to elucidate the mechanism

of these reactions at a molecular level, particularly considering that there was essentially no precedent in the literature for ice-induced chemistry until its importance in the polar stratosphere became apparent.

For atmospheric modeling purposes (to estimate, for example, the rate at which chlorine is converted to its active form in the polar stratosphere by the reaction between ClONO_2 and HCl on ice), one needs to compute a collision frequency for ClONO_2 vapor with the surface of the PSC particles, to be multiplied by the reaction probability g . The former depends on the abundance and the size of the particles, which can come from atmospheric observations or, in principle, from detailed considerations of cloud microphysics. These considerations, in turn, require information on nucleation rates, vapor pressures, sticking coefficients, etc. The concentration of HCl on the surface of the PSC particles also needs to be estimated, since it affects the reaction probability g . This can be done, assuming complete equilibration in the atmosphere, from laboratory measurements of the HCl surface concentration as a function of temperature, and of the HCl partial pressure in the gas phase (i.e., the thermodynamics of the HCl/ice system). The sticking coefficient for HCl vapor on ice would also be needed if one wants to estimate the time scale for HCl vapor to be absorbed by the PSCs, rather than assuming thermodynamic equilibrium. The desorption rate would then also be needed: it can be obtained from laboratory measurements, or in principle, it can be calculated given the sticking coefficients, the equilibrium vapor pressure, and by taking into account diffusion rates within the particle.

At present even the functional dependencies for many of the relevant parameters are not clear: does the HCl vapor pressure depend linearly on the HCl concentration in the particles? Does the reaction probability for ClONO_2 or N_2O_5 colliding with nitric acid trihydrate crystals depend significantly on whether the crystals are water-rich or nitric acid-rich? How large need the particles be before it matters where the HCl is absorbed, i.e., surface layers vs. bulk solid? Clearly, much additional work remains to be done.

Sulfuric acid aerosols may also promote important heterogeneous chemical reactions in the stratosphere, analogous to those discussed above (Hofmann and Solomon, 1989). However, the chemical reaction rates are uncertain at present. Tolbert et al. (1988a) have shown that ClONO_2 vapor reacts readily with HCl dissolved in aqueous sulfuric acid solutions. For this system, however, measurements of the HCl vapor pressure as a function of temperature and composition are needed, so that the chemical rate experiments can be carried out with a concentration of HCl in the condensed phase that corresponds to stratospheric conditions. Only trace amounts of stratospheric HCl will dissolve in the typical mid-latitude sulfuric acid aerosols (Molina et al., 1989; Watson et al., 1989), which contain less than about 40% by weight of water. In regions at lower temperatures, these aerosols absorb more water (Steele et al., 1983), and may freeze to form sulfuric acid hydrates. As discussed in Section 1.2, at sufficiently low temperature these aerosols grow to form PSCs. It is likely, though, that they become chemically active even before reaching the PSC stage.

1.5 GAS PHASE CHEMISTRY

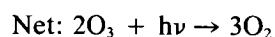
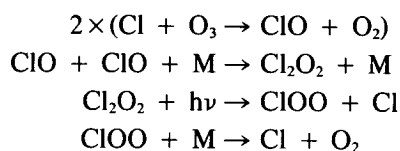
In this section, the gas phase photochemistry relevant to polar ozone depletion will be reviewed. As indicated in Section 1.1.4, it was suggested that heterogeneous reactions on PSCs could lead to enhanced levels of reactive chlorine in the polar lower stratosphere, leading to possible ozone loss through some arguably unusual catalytic cycles. The possible catalytic cycles considered are delineated in Section 1.5.1, and the importance of coupling between reactive nitrogen and reactive chlorine is emphasized. In Section 1.5.2, several aspects of relevant polar photochemistry and their uncertainties are discussed. Finally, photolysis rates for a number of molecules of possible importance in the polar lower stratosphere in winter and spring are presented and their implications for ozone depletion are explored.

POLAR OZONE

1.5.1 Photochemical Processes of Importance in Polar Ozone Depletion

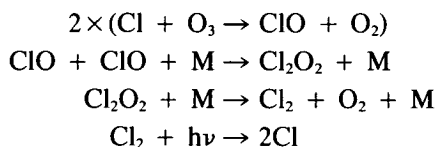
There are several catalytic chemical and photochemical processes that can contribute to Antarctic ozone depletion. Modeling studies that seek to evaluate and compare these cycles insofar as their role in Antarctic ozone depletion is concerned will be discussed in Section 1.6.4.

Molina and Molina (1987) emphasized the importance of ClO dimer formation and photolysis:



The formation of the ClO dimer and its photolysis provides a pathway for ozone loss whose rate is proportional to the square of the ClO abundance, leading to a strong non-linearity in possible ozone depletion. As will be shown in Section 1.6, observations of ClO and detailed modeling studies have shown that this catalytic cycle likely played a dominant role in the intense Antarctic ozone depletion observed during austral spring, 1987.

Molina and Molina (1987) noted that thermal decomposition of the ClO dimer might also lead to ozone loss at cold temperatures:



However, the products of thermal decomposition of the ClO dimer are subject to debate at present. If thermal decomposition of Cl_2O_2 leads to 2ClO rather than to the products indicated above, then significant ozone loss will not occur through ClO dimer formation whenever temperatures are warm enough for thermal decomposition to dominate over photolysis (in effect, a “do-nothing” cycle is obtained rather than ozone destruction). This is a particularly important issue insofar as Northern Hemisphere ozone depletion is considered. Figure 1.5.1-1 illustrates the rate of thermal decomposition of the ClO dimer as a function of temperature based on present best-estimates of kinetic rates, compared to the range of its photolysis rate for solar zenith angles between about 70 and 90 degrees. In examining this figure in order to determine whether photolysis or thermal decomposition is likely to be the dominant fate of any Cl_2O_2 formed, the fraction of the day that is sunlit must be considered along with the local temperatures. During Antarctic late winter and early spring in the lower stratosphere, temperatures generally remain well below 210 K at least until mid-October, so that Cl_2O_2 photolysis is expected to dominate its loss rate. Hence, ozone loss through the photolysis cycle will occur upon formation of the dimer. In the Arctic, stratospheric warmings often raise lower stratospheric temperatures well above 210 K, at least by late February. These warmer temperatures favor thermal decomposition of the dimer and hence are likely to mitigate ozone loss if the products of the thermal decomposition process are 2ClO , even if greatly elevated levels of ClO are present.

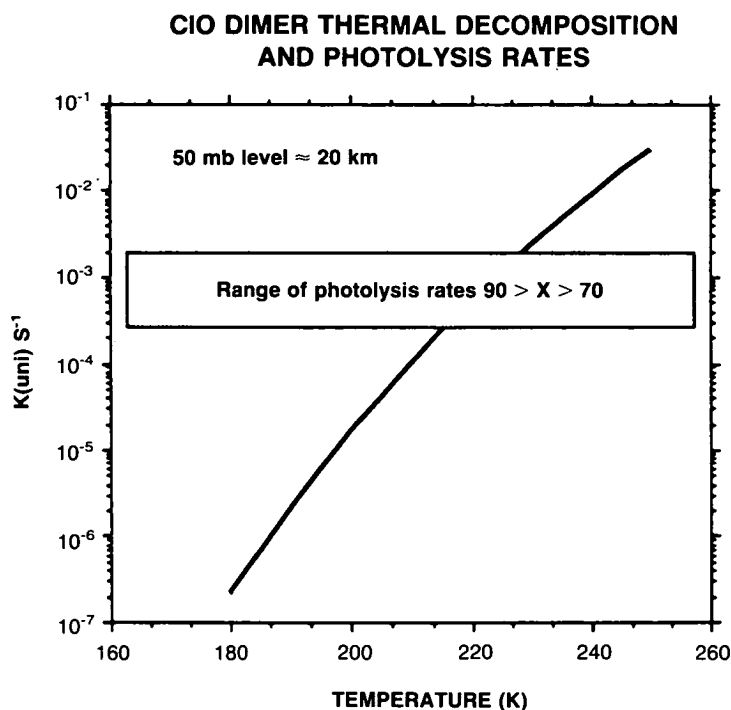
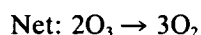
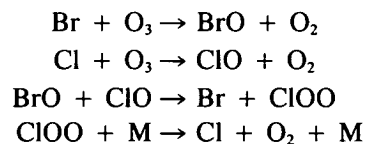


Figure 1.5.1-1. Thermal decomposition rate of Cl_2O_2 near 50 mb (calculated from the equilibrium constant measurements of Hayman and Cox (private communication, 1989) and the forward rate constant of Sander et al. (1989) along with the range of photolysis rates at that level for solar zenith angles from 70 to 90 degrees.

Further studies of the products of Cl_2O_2 thermal decomposition are needed to address this issue, which may represent a significant element in determining inter-hemispheric differences in ozone destruction rates.

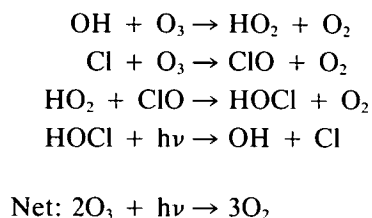
McElroy et al. (1986a), Tung et al. (1986), and Rodriguez et al. (1986) emphasized the catalytic destruction of ozone via the interaction of ClO and BrO:



It is important to note that the reaction between ClO and BrO has three product channels, which influence the diurnal variations of BrO and hence limit its ability to destroy ozone to the sunlit atmosphere. Other channels and their branching ratios are discussed below. The rate of ozone loss due to this catalytic cycle is dependent on the abundances of ClO and BrO in the polar lower stratosphere. Both species have been measured in the Arctic and Antarctic lower stratospheres, as discussed in Sections 1.6 and 1.10. The bromine-catalyzed destruction of ozone can be extremely effective in destroying ozone in the lower stratosphere even at relatively modest enhancements of ClO, leading to a high ozone depletion potential for bromine species (which is believed to play a particularly important role in Arctic ozone depletion due in part to relatively warm temperatures in spring as noted above).

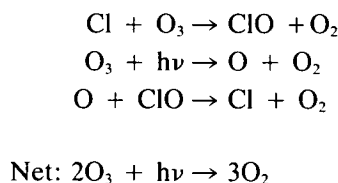
POLAR OZONE

Solomon et al. (1986) and Crutzen and Arnold (1986) also discussed the possibility of the HO_x-ClO_x catalytic destruction of ozone:



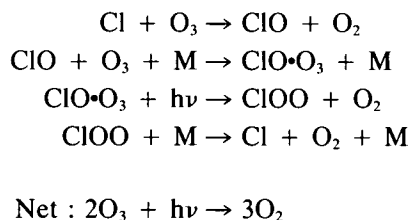
Measurements of HOCl (Toon and Farmer, 1989) in the Antarctic stratosphere discussed in Section 1.6 suggest that this cycle is unlikely to contribute significantly to the observed ozone loss there (but see below for further kinetic studies of relevance).

Finally, the well-known ClO_x-O_x catalytic cycle should be mentioned among currently accepted chemical schemes:

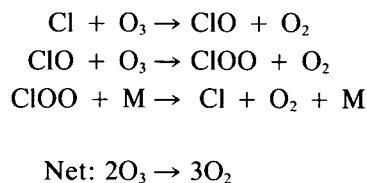


The competition between these cycles in destroying Antarctic ozone depends on the relative abundances of ClO, BrO, reactive hydrogen, atomic oxygen, temperature, the required wavelengths of the indicated photodissociation processes, and the relevant kinetic rate constants.

Some additional potentially important chemical cycles have recently been delineated by Anderson et al. (1989):



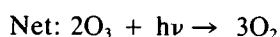
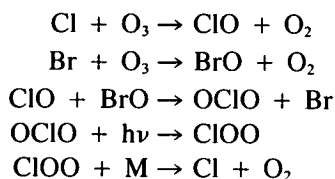
and



Although the current estimated upper limit for the bimolecular reaction between ClO and O₃ is $1.0 \times 10^{-18} \text{ cm}^3 \text{ s}^{-1}$ (DeMore et al., 1987), this reaction could be important if the rate constant is as fast as $1.0 \times 10^{-17} \text{ cm}^3 \text{ s}^{-1}$, and the reaction rate is extremely difficult to determine accurately in the laboratory due to secondary

reactions of the Cl atoms. As will be shown in Section 1.6.4, some studies suggest that additional catalytic cycles such as those indicated by Anderson et al. (1989) may be needed to explain the observed rate of Antarctic ozone depletion, while other studies disagree that any additional losses are needed.

Vaida et al. (1989) propose another possible ozone loss mechanism involving photoisomerization of OCIO. If OCIO photolysis leads to ClO + O, no ozone loss is obtained through OCIO formation. If, on the other hand, OCIO photoisomerizes to ClOO, the following catalytic ozone-destroying cycle is obtained in the sunlit atmosphere:

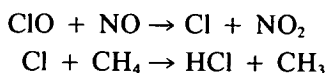


The efficiency of this cycle depends on the rate constant of the reaction between ClO and BrO, the branching ratio for OCIO production, and the quantum yield for OCIO photoisomerization. The latter parameter requires further study in the laboratory.

The interaction between nitrogen- and chlorine-containing species is a critical element in polar ozone depletion. Section 1.4 described heterogeneous reactions that liberate reactive chlorine at the expense of the reservoir species, HCl and ClONO₂. The reactive chlorine can form ClO in the presence of sunlight and go on to participate in the catalytic cycles delineated above. However, the time scale during which the ClO so formed remains available to destroy ozone depends critically on the abundances of the nitrogen oxides, NO and NO₂, which control the rate of reformation of both HCl and ClONO₂ from ClO. In the case of ClONO₂, the reaction leading to its formation is:



so that the rate of reformation of ClONO₂ is directly controlled by the NO₂ abundance. The reactive nitrogen species also play an important role in HCl formation by the more indirect route:



so that nitrogen oxide abundances strongly influence the loss rate of any chlorine radicals liberated by heterogeneous processes. The abundances of gas-phase nitrogen oxide species are reduced by the same heterogeneous reactions responsible for chlorine release (1.4.1–1.4.4). These reactions convert relatively short-lived nitrogen compounds such as N₂O₅ into HNO₃ (a much longer-lived nitrogen reservoir) and hence reduce the abundances of NO and NO₂. Furthermore, the HNO₃ product apparently remains in the particulate phase, and sedimentation of large particles may even remove nitrogen from the stratosphere altogether (denitrification). These processes greatly lengthen the photochemical lifetime of ClO and hence increase the ozone loss rate. Figure 1.5.1-2 illustrates the strong effect of denitrification on the time scale for ClO recovery. In the particular case shown, the abundance of ClO obtained nine days after a notional PSC event is doubled when severe denitrification is assumed as compared to a non-denitrified case.

POLAR OZONE

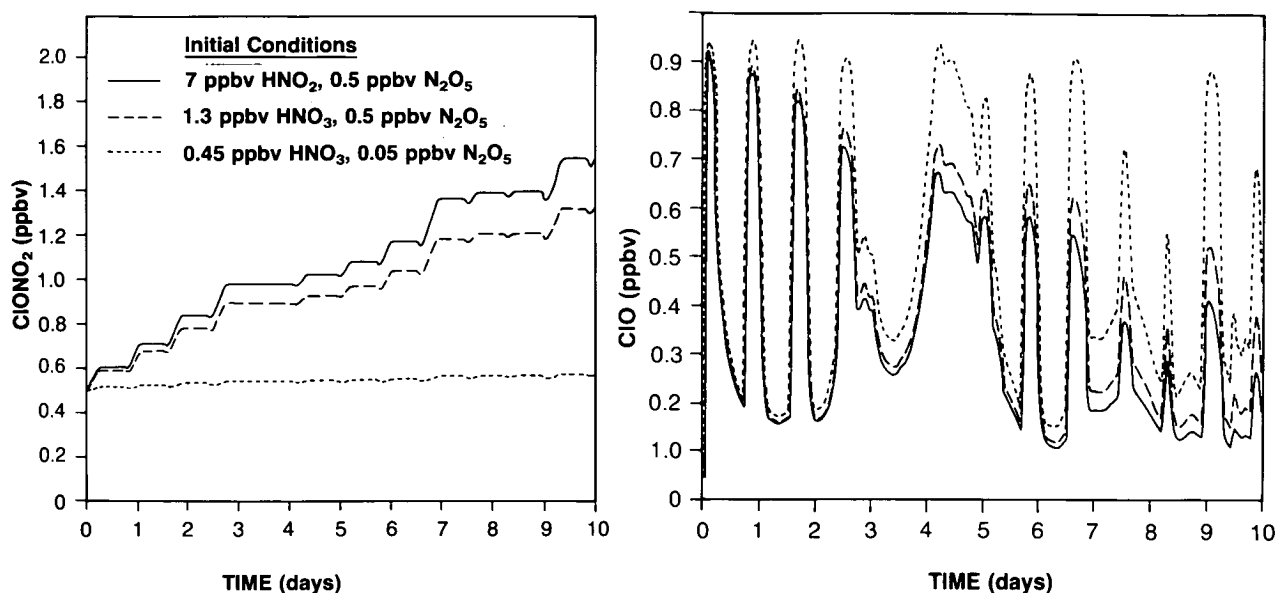


Figure 1.5.1-2. Calculated time behavior of ClONO₂ and ClO during Arctic spring for three different cases, illustrating the importance of the reactive nitrogen content in determining the time scale for photochemical recovery following PSC exposure.

1.5.2 Laboratory Kinetics and Photochemistry

The importance of species such as Cl₂O₂ in the polar stratosphere has been recognized only recently, and the chemistry and photochemistry of this compound had not been investigated earlier. In contrast, the rates of elementary reactions such as Cl + O₃ or ClO + NO₂ had been measured years ago, although not under conditions directly applicable to the polar stratosphere, where they are also important. However, their rates under polar stratospheric conditions can be estimated by extrapolation, for which there exists a theoretical framework (see, e.g., DeMore et al., 1987). In general, though, the uncertainties in the measurements increase at the lower temperatures, and much laboratory work remains to be carried out to ensure the validity of these extrapolations and also to further elucidate polar stratospheric chemistry. This work is challenging, since existing techniques often cannot be readily implemented at the relatively low temperatures and high pressures of interest. Also, there are potentially important reactions—homogeneous and heterogeneous—involving bromine-containing species, higher oxides of chlorine, etc., that should be investigated.

Much progress has been achieved in terms of understanding the physical chemistry of Cl₂O₂, the ClO dimer, since it was first suggested as an intermediate in a catalytic ozone destruction cycle (Molina and Molina, 1987). The infrared and ultraviolet spectra, as well as the structure of this species, which is the symmetrical chlorine peroxide, ClOOC1, are now reasonably well established. The two compounds originally assigned by Molina and Molina (1987) as isomers of Cl₂O₂ are now known to be the symmetric peroxide and Cl₂O₃, which is formed by addition of ClO to OClO, in agreement with the findings of Hayman et al. (1986). These authors reported a measurement of the UV spectrum of ClOOC1, which has subsequently been verified with good agreement by Burkholder et al. (1989), Friedl and Sander (1988), Molina (1989), DeMore and Roux (private communication, 1989), and Vogt, Parmien, and Schindler (private communication, 1989). Figure 1.5.2-1 shows a ClOOC1 spectrum, which is a smoothed average of the results of Hayman et al. (1986), DeMore and Roux (private communication, 1989), and Vogt et al. (private commu-

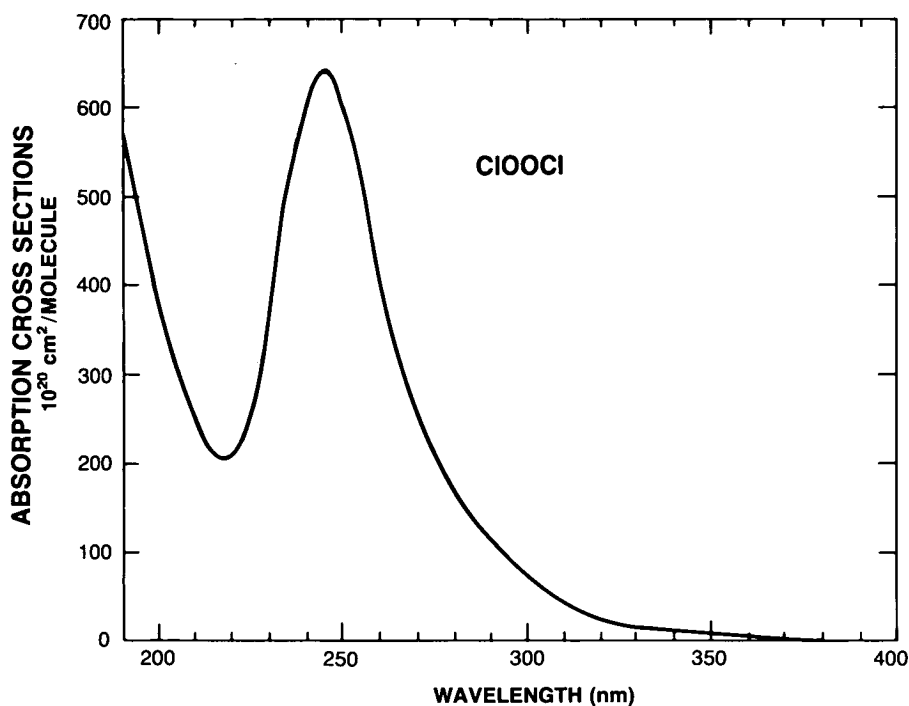


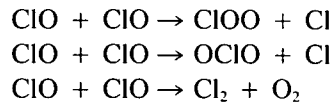
Figure 1.5.2-1. Absorption cross sections of ClOOCl: smoothed average of the results of Hayman et al. (1986), DeMore and Roux (private communication, 1989), and Vogt et al. (private communication, 1989).

nication, 1989). The cross section data of Burkholder et al. are about 35% larger around 280 nm. More accurate data are needed, particularly in the long wavelength tail beyond 300 nm, in order to better estimate the atmospheric photodissociation rates. The long-wavelength tail is of particular importance, since it controls the photolysis rate at the large solar zenith angle characteristic of the polar spring (see the discussion of Figure 1.5.2-3 below). The infrared spectra of ClOOCl and of Cl₂O₃ have also been characterized (Burkholder et al., 1989; Friedl and Sander, 1989; Molina, 1989; Cheng and Lee, 1989). Cheng and Lee noted that their observed infrared spectrum for ClOOCl was in excellent agreement with the predictions of McGrath et al. (1988), and found no evidence for formation of ClOCIO. Furthermore, the thermal stability of these species has been investigated by Cox and Hayman (1988) and Hayman et al. (1986): they conclude that the dimer is bound by 17 kcal/mole, and Cl₂O₃ by about 15 kcal/mole. Ab-initio quantum mechanical calculations have further corroborated the higher stability of ClOOCl relative to that of ClOCIO and ClClO₂, which are other plausible isomeric forms (Toohey et al., 1987; McGrath et al., 1988). More recently, high-resolution microwave spectra of the product of the ClO self reaction have clearly established that it is indeed the non-planar ClOOCl (Birk et al., 1989); furthermore, these authors were able to infer high-accuracy bond lengths and angles for this molecule.

The primary photodissociation products in the photolysis of ClOOCl need to be determined. There are indications from experiments reported by Margitan (1983) that Cl atoms are produced, and this is the channel expected for photolysis at the atmospherically important wavelengths, namely around 310 nm. By analogy with other species such as ClONO₂, absorption of a photon at those wavelengths promotes a non-bonding electron in the Cl atoms to a repulsive electronic state which falls apart by breaking the Cl atom bond. The weaker ClO-OCl peroxide bond is not likely to be affected at those wavelengths.

POLAR OZONE

The self-reaction of the ClO radical has been under investigation since the 1950s: there are three channels for the pressure independent component, which is rather slow:



The pressure-dependent channel yields the dimer, whose existence had been merely postulated in the early studies:



At the temperatures and pressures characteristic of the polar stratosphere, this appears to be the only channel of importance. The rate constant for this pressure-dependent step has been measured by Cox and Hayman (1988), who employed a molecular modulation technique; very recent studies using the more direct flash-photolysis approach have yielded rate constant values that are smaller by up to a factor of two at the temperatures and pressures appropriate to the polar stratosphere (Sander et al., 1989; Trolrier et al., 1989). The 194 K results are shown in Figure 1.5.2-2; the rate increases by a little more than a factor of two between 250 K and 190 K.

The reaction between ClO and BrO also has a complex mechanism with several channels:

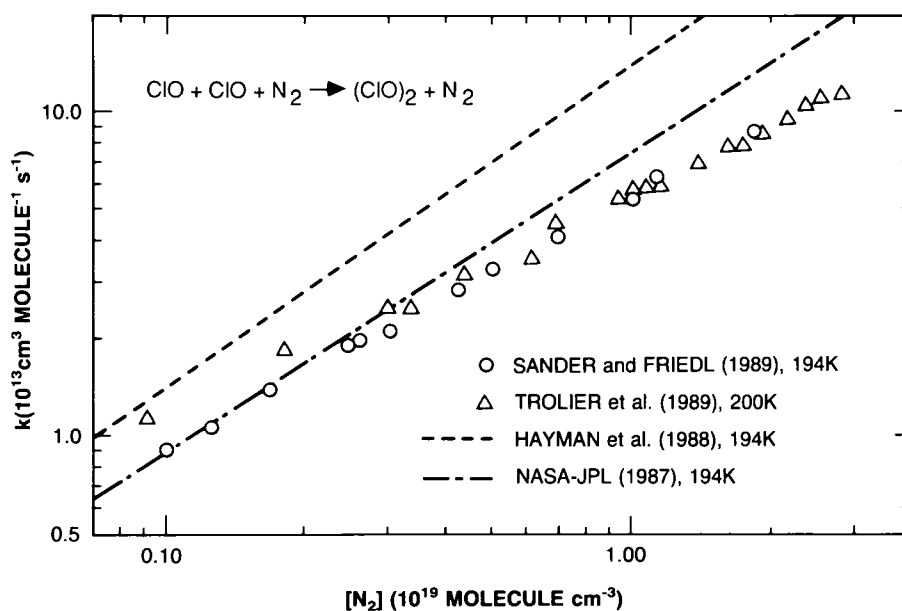
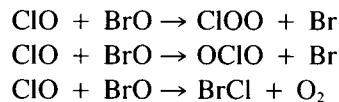


Figure 1.5.2-2. Rate constants for the $\text{ClO} + \text{ClO} + \text{M} \rightarrow \text{Cl}_2\text{O}_2 + \text{M}$ reaction, with N_2 as the third body M.

Several recent studies of this complex reaction have been carried out. The results for the overall rate constant are summarized in Table 1.5.2-1: at room temperature, the older number of Clyne and Watson (1977) is in good agreement with Toohy et al. (1988) and Sander and Friedl (1988), while the value reported by Hills et al. (1987) is about 40% smaller. Also, in this latter work no significant temperature dependence is reported, while Sander and Friedl find that the overall rate constant increases by about a factor of two for a temperature change between 400 K and 220 K.

In terms of the partitioning to the different product channels, all these authors agree that production of ClOO and OCIO are about equally fast; BrCl production appears to be only about 8% of the total, according to Sander and Friedl (1988). This is, however, an important channel, because it provides a means of sequestering BrO during the night, reducing the magnitude of the diurnal OCIO variation. (See Friedl and Sander, 1988; and Sander and Friedl, 1988, for a more detailed description of this work.) As discussed in Section 1.6, OCIO has been measured both at night and during the day in Antarctica.

Although the importance of OCIO as an atmospheric species has only been recognized recently (Rodriguez et al., 1986; McElroy et al., 1986a; S. Solomon et al., 1987), its chemistry and photochemistry had been the subject of many earlier laboratory studies (see, e.g., DeMore et al., 1987). In particular, the absorption spectrum in the near UV, which is highly structured, has been carefully reexamined, since it is needed for the interpretation of atmospheric measurements (Wahner et al., 1987). The upper electronic states are strongly predissociated, and hence the quantum yield for photodissociation is essentially unity.

Simon et al. (1989) have measured a rate constant value at 300 K of about $3 \times 10^{-12} \text{ cm}^3 \text{ molecule}^{-1} \text{ s}^{-1}$ for the reaction

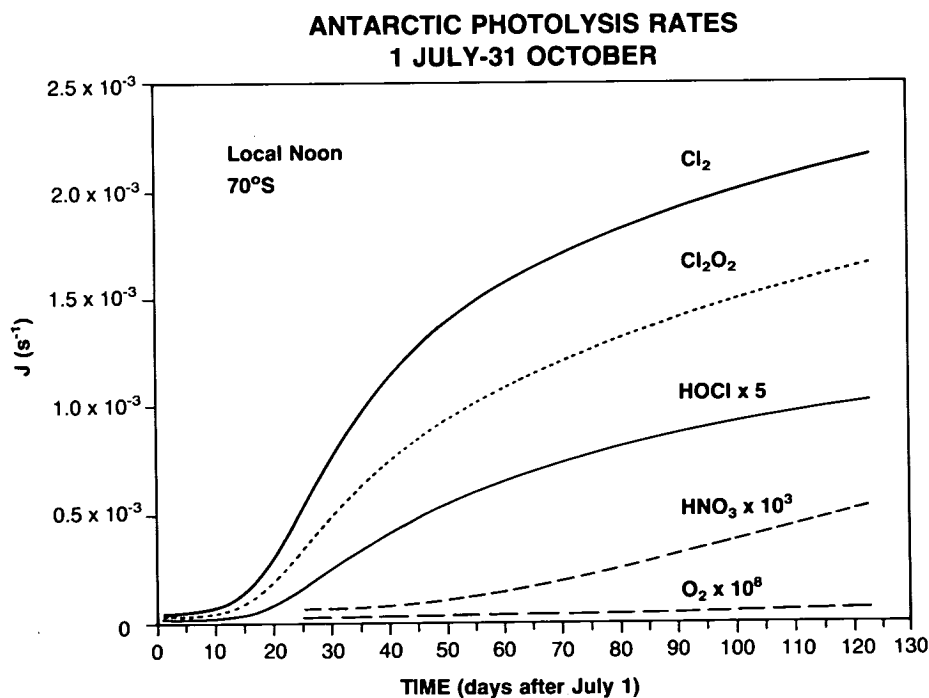


Figure 1.5.2-3. Photolysis rates for Cl₂O₂, HOCl, Cl₂, HNO₃, and O₂ at 70°S at noon as a function of day, at the 50 mb level (approximately 20 km).

POLAR OZONE

The dominant path appears to yield ClOO and CH₃O as products. The authors emphasize that this reaction might lead to enhanced OH levels in the polar stratosphere and hence to ozone depletion through the HO_x/ClO_x catalytic cycle discussed above.

The photolytic properties of many of the molecules considered above are critical to their role in polar ozone depletion. In particular, the products of heterogeneous reactions involving chlorine discussed in Section 1.4 (Cl₂, HOCl, ClONO₂) all have relatively large absorption cross sections in the visible and near-ultraviolet portion of the spectrum. Thus, they photodissociate readily upon exposure to sunlight, even at the exceedingly large solar slant angles typical of polar winter and spring. The photolysis reactions of HNO₃ and O₂ tend to offset the chemical effects of heterogeneous reactions by liberating reactive nitrogen that can reform the ClONO₂ reservoir and by directly producing odd oxygen. These molecules both photolyze at rather short wavelengths in the ultraviolet portion of the spectrum. Hence, their ameliorating influences are likely to be relatively small when solar zenith angles are large and very little ultraviolet penetration is possible. Figure 1.5.2-3 shows the calculated seasonal behavior of the photolysis rates of several of these species, illustrating the fact that chlorine activated by heterogeneous processes can begin to destroy ozone before photochemical processes involving HNO₃ and O₂ can halt or reverse the ozone decline. The points when production of odd oxygen and NO₂ begin to become important will depend not only on the photolysis rates, but also on the HNO₃ abundance.

1.6 PHOTOCHEMISTRY OF THE ANTARCTIC SPRING

Ground-based and aircraft observations, some dating back to the late 1970s, have shown that the chemical composition of the Antarctic spring vortex is highly unusual. The partitioning of both chlorine and nitrogen species has been shown to be dramatically perturbed compared to gas-phase model predictions or measurements at other latitudes, and there is evidence for the removal of substantial quantities of nitrogen oxides and water vapor from the atmosphere. In this section, present understanding of the composition of the lower Antarctic stratosphere will be described. As will be shown, virtually all of the observed perturbations are consistent with the expectation that important heterogeneous reactions take place on the surfaces of polar stratospheric clouds. The implications of these chemical perturbations for ozone depletion are discussed.

The vertical coordinate used for much of the discussion is potential temperature. Approximate equivalent pressures and altitudes for Antarctic spring conditions are given in Table 1.6-1.

1.6.1 Reactive and Reservoir Chlorine

Measurements of ClO coupled with knowledge of the catalytic cycles that destroy ozone (Section 1.5) provide the basis for evaluating the photochemical contribution to Antarctic ozone loss. The primary evidence demonstrating that ClO is responsible for much of the ozone loss in the Antarctic spring is the observation of exceedingly high ClO abundances by two independent techniques. Aircraft and ground-based studies have both shown that the ClO mixing ratios near 18 km inside the Antarctic vortex are on the order of 1 ppbv (deZafra et al., 1987; P. Solomon et al., 1987; Brune et al., 1989a; Anderson et al., 1989). Values expected from measurements at mid-latitudes and from multi-dimensional model studies (neglecting the heterogeneous reactions indicated in Section 1.4) are only about 10 pptv, so that the measured abundances of 1 ppbv are enhanced by a factor of about one hundred. The aircraft studies provide *in-situ* ClO abundances from about 13–20 km using a resonance fluorescence approach, while the ground-based studies employ microwave emission techniques and yield vertical profile information with

Table 1.6-1. Potential temperatures and approximate geometric altitude and pressure equivalents

Potential Temperature (K)	Approximate Geometric Altitude (km)	Approximate Pressure (mb)
428	17.5	55
420	17.0	60
400	16.25	80
380	15.5	100
360	14.25	120
340	12.5	150

about 5 km vertical resolution for the height range from about 15 km to 50 km. Studies using these data (Anderson et al., 1989; Barrett et al., 1988; Ko et al., 1989; Austin et al., 1989; Jones et al., 1989) have shown that such concentrations of ClO can account for much of the observed ozone loss using measured photochemical rates, although there is some debate at present regarding whether the calculated total ozone loss rate is fully consistent with that inferred from observations (see Section 1.6.4).

Proffitt et al. (1989a) have suggested that the latitude at which ClO mixing ratios exceed about 130 pptv is a useful definition of the boundary of the chemically perturbed region (CPR). Figure 1.6.1-1 displays measured ClO abundances as a function of latitude relative to this boundary averaged over the AAOE mission at two different potential temperatures. Within the CPR, ClO mixing ratios are over an order of magnitude greater than outside. The very high ClO mixing ratios observed within the CPR are consistent with calculations employing semi-empirical estimates for the heterogeneous chemistry, likely surface areas, and frequencies of PSCs based on meteorological data, as discussed in greater detail in Section 1.6.4 (Jones et al., 1989). It is also possible that the ClO abundances well outside of the CPR reflect some influence of heterogeneous processes, either through local PSCs that occur occasionally or earlier in the season, or through transport of air out of the polar vortex (see Fahey et al., 1989a; Jones et al., 1989).

Figure 1.6.1-2 displays vertical profiles of ClO mixing ratio obtained over Antarctica in 1987. Data above about 20 km (left) are from ground-based measurements made from McMurdo (Barrett et al. 1988), while those on the right were obtained from aircraft observations (Brune et al. 1989a). The ground-based data show a double-peaked structure, with one mixing ratio maximum near 40 km that is consistent with homogeneous, gas-phase photochemistry, and another near 20 km that is not observed at other latitudes and is thought to be the result of heterogeneous reactions on PSC cloud surfaces in the lower stratosphere. A strong vertical gradient is visible in the aircraft data below 20 km, with rapidly decreasing abundances at lower potential temperatures. This gradient likely reflects in large part the gradient in the abundance of available reactive chlorine as compared to that in organic forms (largely CFCs), as well as altitude variations in the partitioning between the ClO dimer and ClO.

The ground-based data have also provided information on the diurnal variation of ClO. As shown in Figure 1.6.1-3, the ClO observed near 20 km rapidly disappears at night. Such diurnal variation is expected due to formation of nighttime reservoirs such as Cl₂O₂ and OClO (Section 1.5) and supports the identification of ClO. Measurements show that daytime ClO mixing ratios remain high within the vortex for a period of a month or more in the austral spring. Ground-based microwave data (P. Solomon et al., 1987) showed that ClO was greatly elevated in the lower stratosphere throughout September 1986, although little was

POLAR OZONE

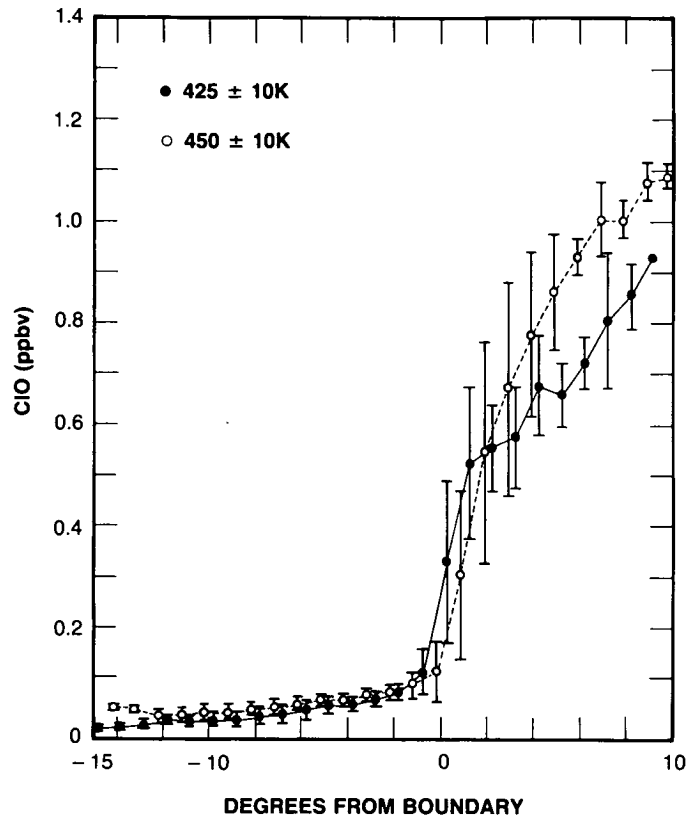


Figure 1.6.1-1. Observed ClO mixing ratio latitude gradients on the 425 and 450 K potential temperature surfaces averaged over the AAOE mission period (Brune et al., 1989a). The latitude averages were performed relative to the boundary of the chemically perturbed region (see Fahey et al., 1989b).

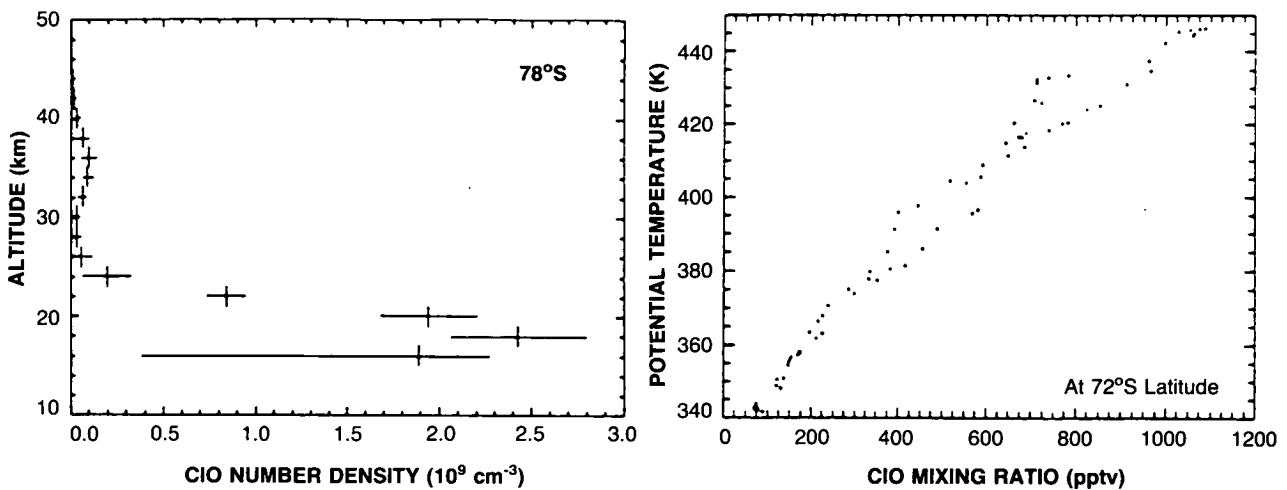


Figure 1.6.1-2. The vertical profile of ClO mixing ratio within the southern polar vortex, from ground-based microwave measurements (left, from Barrett et al., 1988) and from *in situ* measurements at 72°S (right, from Brune et al., 1989a.).

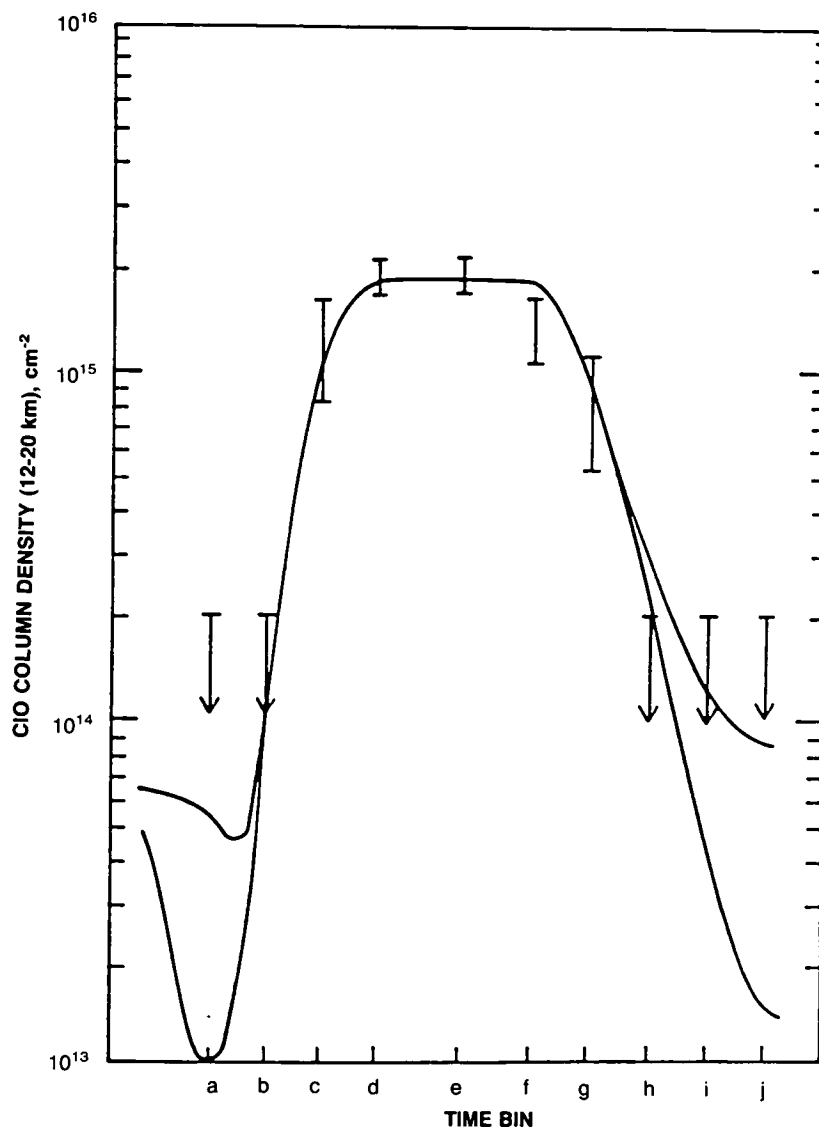


Figure 1.6.1-3. Diurnal variation of the column abundance of CIO below about 25 km at McMurdo Station, Antarctica (from deZafra et al., 1989).

detected in October 1987 (see also, Figure 1.6.1-5). This seasonal trend is broadly consistent with the observed September loss of Antarctic ozone.

Other measurements of chlorine-containing species confirm and support these results. Observations of the column abundance of OCIO have been obtained from ground-based and aircraft-borne spectrometers using many spectral absorption bands in the wavelength range from about 340 to 430 nm (S. Solomon et al., 1987; Wahner et al., 1989b). These have shown that the abundance of OCIO is about 50–100 times greater in the Antarctic polar vortex than can be accounted for without considering heterogeneous chemistry. The enhancement in OCIO is consistent with the observed enhancement in CIO noted above (Solomon

POLAR OZONE

et al., 1989) and provides important, independent confirmation of large perturbations in Antarctic chlorine chemistry.

Figure 1.6.1-4 presents observations of the diurnal variation of OCIO above McMurdo station, showing evidence for rapid formation of OCIO at sunset. Similar diurnal variations were measured by Wahner et al. (1989b). Model calculations predict a pronounced diurnal behavior for OCIO due to rapid formation at sunset, proceeding unhindered by photolysis (Rodriguez et al., 1986; Salawitch et al., 1988). Figure 1.6.1-5 presents observations of the seasonal trend in OCIO in evening twilight from McMurdo Station during 1986

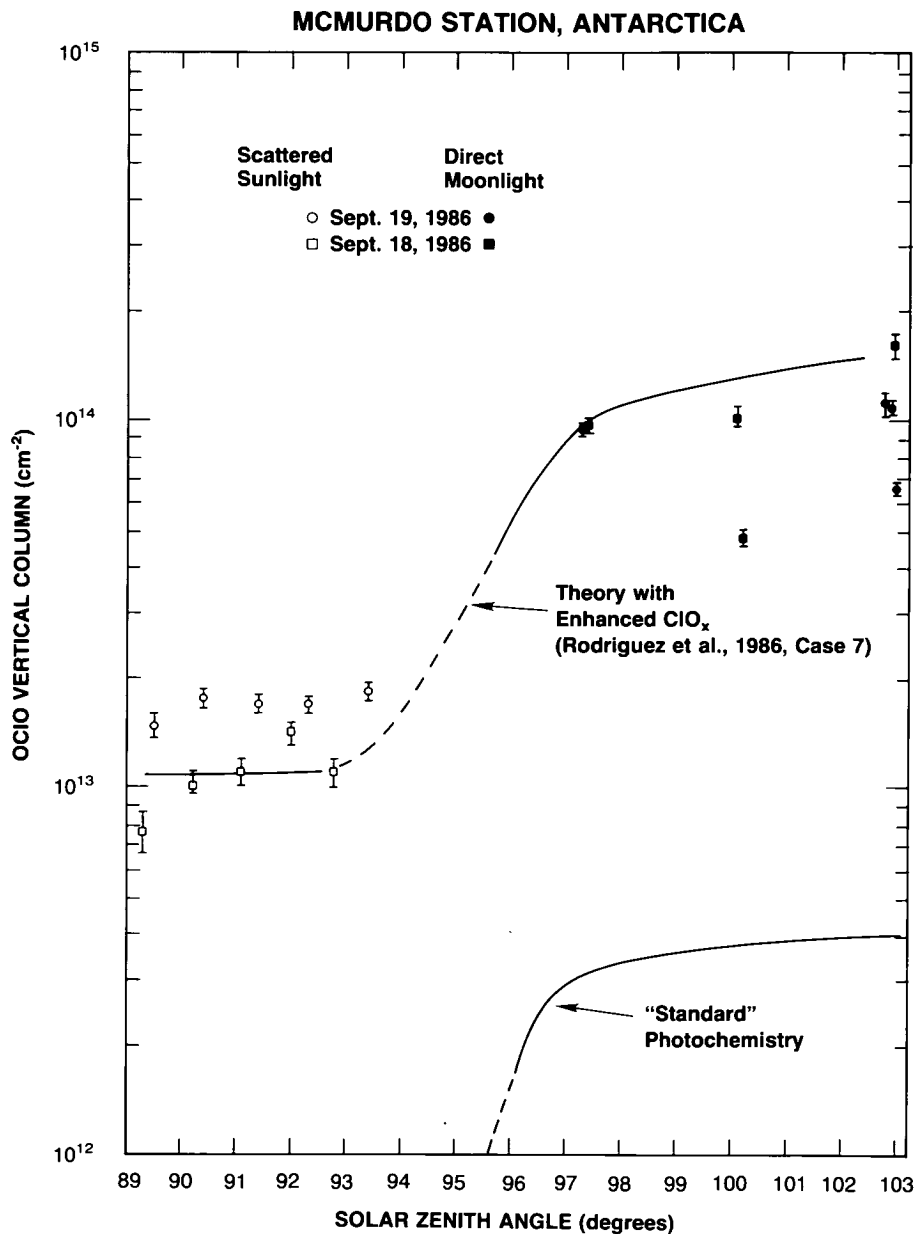


Figure 1.6.1-4. Diurnal variation of the column abundance of OCIO above McMurdo Station, September 18-19, 1986. Twilight and moon measurements are indicated (from S. Solomon et al., 1987).

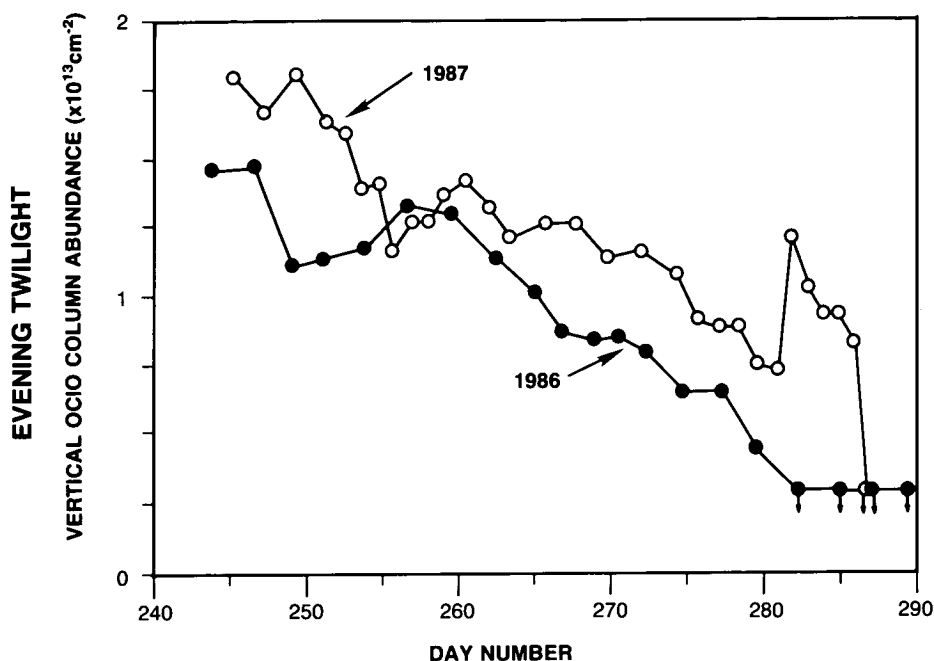


Figure 1.6.1-5. Daily measurements of the sunset OClO column abundances above McMurdo Station in 1986 and 1987 (from Sanders et al., 1989a).

and 1987 (from Sanders et al., 1989). These data show that the abundance of OClO decreases throughout September, falling to zero in early October in both years. This seasonal trend is qualitatively consistent with that in ClO noted above. Poole et al. (1989) have shown a close correspondence between the seasonal evolution of observed OClO abundances and optical depths of PSCs observed in 1986 and 1987. Morning twilight OClO abundances are generally lower than the evening twilight values, and disappear a few weeks earlier (see Section 1.6.4).

Observations of ClONO₂ (Farmer et al., 1987; G. Toon et al., 1989a) and HCl (Farmer et al., 1987; Toon et al., 1989a; Coffey and Mankin, 1989) are also of great importance to understanding the perturbations to chemistry and photochemistry induced by PSCs. Figure 1.6.1-6 presents measurements of the column abundance of ClONO₂ as a function of latitude as indicated by G. Toon et al. (1989a). The abundances of ClONO₂ obtained near the edge of the CPR are a good deal higher than model predictions, and strongly suggest formation of ClONO₂ in those regions where ClO abundances are enhanced by cloud processes or by mixing of processed air, but ClONO₂ is not effectively suppressed by the same cloud chemistry (see Section 1.6.4). As shown for example by Jones et al. (1989), any remaining NO_x will rapidly form ClONO₂ following enhancement of ClO by cloud processing. When stoichiometric considerations limit the amount of NO₂ available for ClONO₂ formation, then the abundance of ClONO₂ drops in clear air after cloud processing.

POLAR OZONE

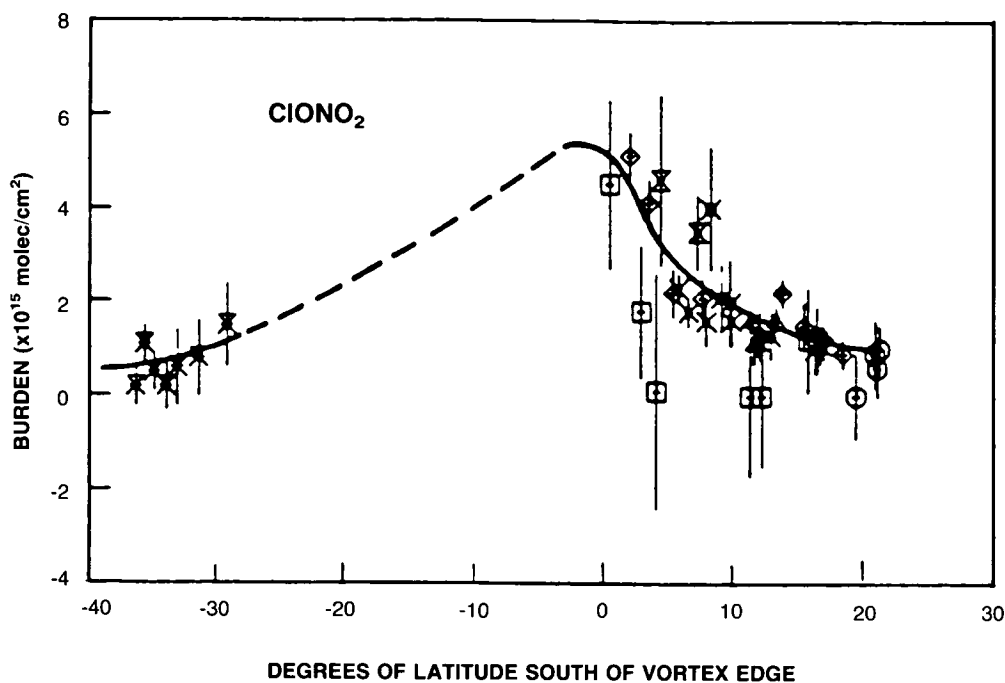


Figure 1.6.1-6. Observed distribution of the ClONO₂ column abundance, plotted as a function of latitude relative to the edge of the vortex in August and September, 1987 (from G. Toon et al., 1989a).

Figure 1.6.1-7 shows observations of the latitude gradients of the HCl and HF column abundances. HF and HCl are both produced by decomposition of chlorofluorocarbons, and are expected to exhibit generally similar latitude gradients, particularly in the winter at high latitudes where chemical loss processes for both are very slow. The ratio between the two quantities provides an important check regarding the contribution of chlorofluorocarbons to the stratospheric chlorine budget, since the relative abundances of fluorine and chlorine released by anthropogenic compounds is well known. The observed mid-latitude column abundances are in agreement with model predictions adopting about 0.6–0.7 ppbv of methyl chloride as the sole significant natural contributor to the stratospheric chlorine budget, with the remainder of stratospheric chlorine and all of the stratospheric fluorine being due to the known release rates of chlorofluorocarbons. In the absence of other processes, one would expect both HCl and HF columns to increase poleward as air with higher concentrations of both compounds moves polewards and downwards. HF exhibits just such a behavior. However, HCl columns decrease sharply with latitude inside the CPR, implying the conversion of virtually all the HCl in the low stratosphere to other forms. This conversion of HCl within the CPR is also clearly evident in the HCl/HF ratio. The observed gradient cannot be explained with homogeneous chemistry, and is consistent with efficient heterogeneous chemistry.

HOCl is of interest since it is believed to be the product of the heterogeneous reaction of ClONO₂ with H₂O. Toon and Farmer (1989) deduced the column abundance of HOCl using about 15 spectral features that occur near 1,227 cm⁻¹. By averaging several spectra, they derived a mid-morning measurement for a latitude near 80°S on September 20 of about 1.5 × 10¹⁴ cm⁻². This value is comparable to estimates from models that include heterogeneous chemistry (see Section 1.6.4).

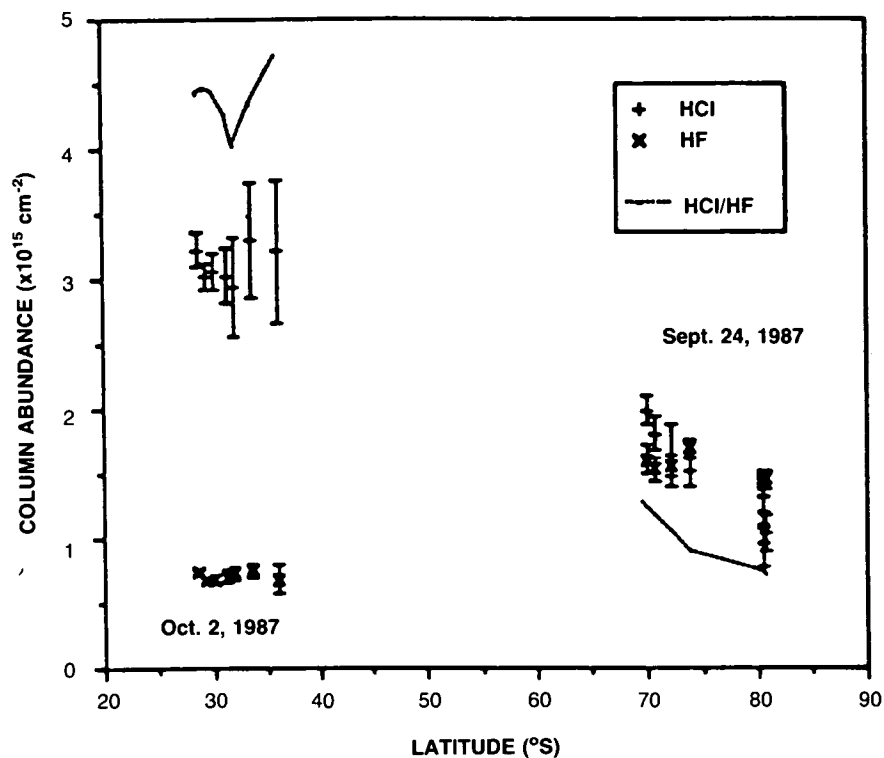


Figure 1.6.1-7. Observed latitude gradients of HCl and HF on the 24th of September and 2nd of October, 1987 (from G. Toon et al., 1989a). The ratio (dashed line) falls from a value of approximately 4 at low latitudes to less than 1 within the polar vortex, indicating conversion of HCl to other forms.

The column measurements of OCIO provide some insight into the photochemical destruction of ozone through the catalytic cycle involving ClO and BrO, while those of HOCl provide indications regarding the column integrated ozone loss rate due to the catalytic cycle involving coupling between HO_x and ClO_x. The photolysis of HOCl is the rate-limiting step in the latter cycle. Assuming a photolysis rate of about $2 \times 10^{-4} \text{ s}^{-1}$ in mid-September throughout much of the sunlit portion of the day, one obtains an ozone loss rate in the sunlit atmosphere of about $3 \times 10^{10} \text{ molec cm}^{-2} \text{ s}^{-1}$, or about $1.3 \times 10^{15} \text{ molec cm}^{-2} \text{ day}^{-1}$ (about 0.02% of the ozone column per day, which is far less than the observed ozone loss rate of roughly 1–2%/day). Neglecting possible ozone loss through OCIO photoisomerization (Vaida et al., 1989), the ozone destruction through bromine/chlorine chemistry occurs through the cycle whose rate-limiting step is $\text{BrO} + \text{ClO} \rightarrow \text{Br} + \text{ClO}_2$. Since the branching ratio for this channel is nearly equal to that for the channel that leads to OCIO production, and since OCIO is very short lived and hence in photochemical equilibrium during the day, we may write:

$$d(\text{O}_3)/dt = -k (\text{ClO}) (\text{BrO}) \approx -J (\text{OCIO})$$

where k is the rate constant for the reaction indicated above and J is the OCIO photolysis rate. The measured twilight OCIO column is about $1 \times 10^{13} \text{ molec cm}^{-2}$ at twilight (90-degree solar zenith angles). Model calculations suggest that the OCIO column abundances present at the smaller solar zenith angles typical of the sunlit period of the day are roughly 0.25–0.5 of these twilight values and that the rate of OCIO photolysis is about $5 \times 10^{-2} \text{ s}^{-1}$ (Solomon et al., 1989). Hence the column integrated loss of ozone

POLAR OZONE

due to the reaction between ClO and BrO is estimated to be about $1.25\text{--}2.5 \times 10^{11}$ molec $\text{cm}^{-2} \text{s}^{-1}$, or about $0.5\text{--}1 \times 10^{16}$ molec $\text{cm}^{-2} \text{day}^{-1}$ (about 0.1–0.2%/day, or about 5–20% of the observed total ozone column loss rate in 1987). The estimates of column ozone loss given here are crude, as they do not include possible effects of atmospheric waves (e.g., zonal asymmetries which influence photolysis processes; see Jones et al., 1989). Seasonal and latitudinal changes in the HOCl and OClO column abundances have also been neglected and the estimates do not include detailed diurnal photochemistry. Nevertheless, such estimates are based directly on observations and, hence, are of use in examining the approximate roles of various photochemical processes. More detailed model calculations based on aircraft and ground-based measurements of ClO suggest that the bulk of the ozone loss rate in Antarctica in 1987 occurred through formation of the ClO dimer (see Section 1.6.4).

1.6.2 Reactive and Reservoir Nitrogen

In retrospect, observations of the column abundance and diurnal cycle of nitrogen dioxide obtained in the late 1970s and early 1980s provided strong indications of perturbed chemistry in the polar winter and spring long before the discovery of the Antarctic ozone hole directed worldwide attention to south polar regions. The NO_2 column abundance in the Arctic winter and spring was found to be significantly lower than theoretical expectations (Noxon, 1979). This phenomenon came to be known as the Noxon “cliff” and was highlighted as a major challenge to our understanding of stratospheric chemistry. Although many of the observations were obtained in the Northern Hemisphere winter, a similar Antarctic “cliff” was found in the only available latitude survey from the Southern Hemisphere (Noxon, 1978). Observations from the New Zealand Antarctic research station (Scott Base at 78°S) published prior to the discovery of the Antarctic ozone hole also displayed remarkably low levels of NO_2 during Antarctic spring (McKenzie and Johnston, 1984), well below those generally found in the Arctic spring. In the high latitude air, both the diurnal variation and absolute abundance of NO_2 were greatly reduced compared to theoretical expectations.

Observations and interpretation of HNO_3 abundances in the Arctic polar night (Wofsy, 1978; Austin et al., 1986b) provided important evidence for an unexplained source of HNO_3 in polar winter, and the possibility of heterogeneous production on atmospheric aerosol was suggested. In particular, the observations showed larger abundances of HNO_3 inside the heart of the polar vortex than found at lower latitudes. These are difficult to reconcile with purely gas-phase production of HNO_3 in the dark polar winter. A few observations of the column abundance of HNO_3 were also available from Antarctica (Williams et al., 1982), confirming that its behavior there was extremely difficult to reconcile with “standard” gas-phase photochemical schemes, and supporting the very low NO_2 column measurements of McKenzie and Johnston (1984). Solomon et al. (1986) compared these observations of the latitude gradient of total HNO_3 column abundance observed in Antarctica to two-dimensional model calculations both including and neglecting heterogeneous production. They suggested that the observed low NO_2 and high HNO_3 column amounts in Antarctica indicated net production of HNO_3 , probably through surface reactions.

Thus, early observations of reactive nitrogen species strongly suggested the possibility that heterogeneous reactions affected the partitioning of nitrogen species in the Antarctic winter and spring. While these observations were very important and strongly suggestive of major gaps in our understanding, it was not until further measurements of reactive nitrogen species were carried out following the discovery of the ozone hole that the mechanisms responsible for them and their significance to ozone chemistry became clearer.

Observations of the NO_2 column abundance in Antarctic spring were obtained with both visible (Keys and Johnston, 1986; Mount et al., 1987; Wahner et al., 1989a) and infrared absorption methods (Farmer et

al., 1987; Coffey and Mankin, 1989; Toon et al., 1989a) from ground-based and aircraft-borne instruments. A detailed comparison between techniques and platforms is beyond the scope of this review, but the measurements are in broad agreement, particularly insofar as the very low column abundances of NO_2 within the Antarctic vortex in the spring are concerned. The ground-based measurements allowed study of the diurnal and seasonal variations at a fixed point, while the aircraft measurements provide important latitude gradient information. Figure 1.6.2-1 shows the observed latitude gradient of NO_2 (from Coffey and Mankin) for two periods before and after 8th September 1987. Also shown are the earlier measurements of Noxon (1979). It is clear that a sharp decrease in NO_2 occurred as the Antarctic polar vortex was approached.

Figure 1.6.2-2 shows observations of the seasonal trend in morning and evening column NO_2 from three different Antarctic sites in 1986 (Keys and Johnston, 1988). Of particular interest is the abrupt onset and end to diurnal variations in NO_2 during the fall season (i.e., on days 53 and 110 at Halley Bay), indicated by the merging of data taken in morning and evening twilight. Farman et al. (1985b) and Keys and Johnston (1986) emphasized the fact that the behavior near day 53 delineates the point in the annual cycle when continuous daytime photolysis of NO_3 ceases, allowing NO_3 to be converted to N_2O_5 during the night and thus introducing NO_2 diurnal variability. These observations also revealed that the spring abundances of NO_2 are far smaller than the autumn levels, and the diurnal variation largely absent in spite of the fact that the diurnal variations apparent in the fall season should be expected to take place in a similar manner during spring. At Arrival Heights, for example, significant NO_2 diurnal variations should be expected from day 240 through day 280, but are nearly absent in the observations. The lower absolute NO_2 abundances and the absence of diurnal variation observed in spring as compared to fall points strongly towards removal of reactive nitrogen or its sequestration in a reservoir whose lifetime exceeds a few days (e.g., HNO_3). Figure 1.6.2-3 presents similar NO_2 observations from the Soviet stations of Molodezhnaya and Mirny (Elokhov and Gruzdev, 1989). The Soviet measurements are taken at a lower latitude (near 67°S) than

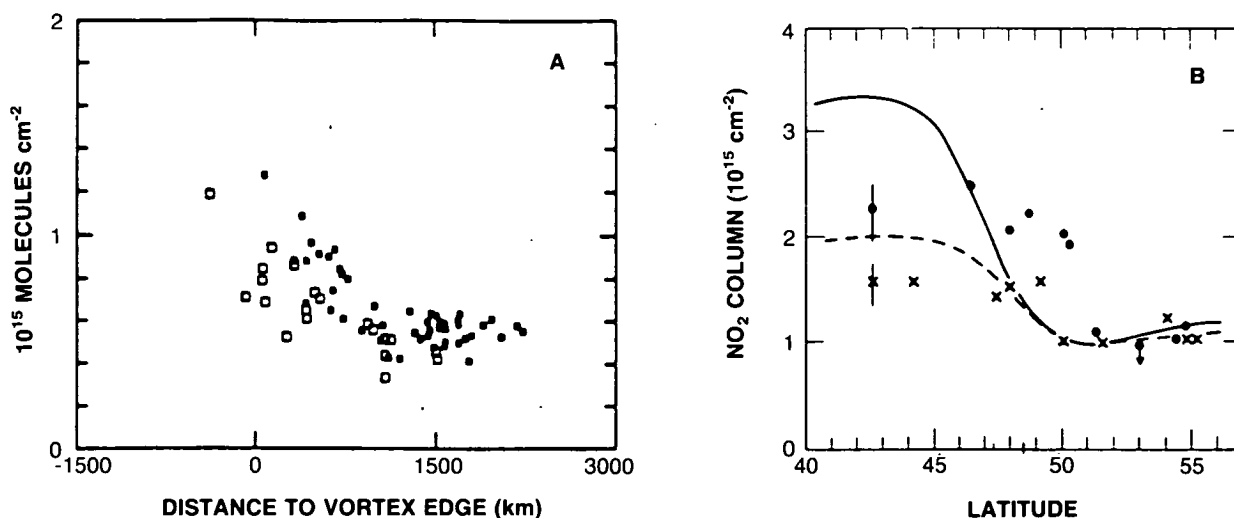


Figure 1.6.2-1. Observations of the latitude gradient of column NO_2 in the Southern Hemisphere. The data from Coffey and Mankin (1989) (A) were obtained with an airborne infrared absorption technique during September 1987, while those of Noxon (1979) (B) were obtained with a shipboard visible spectroscopy instrument.

POLAR OZONE

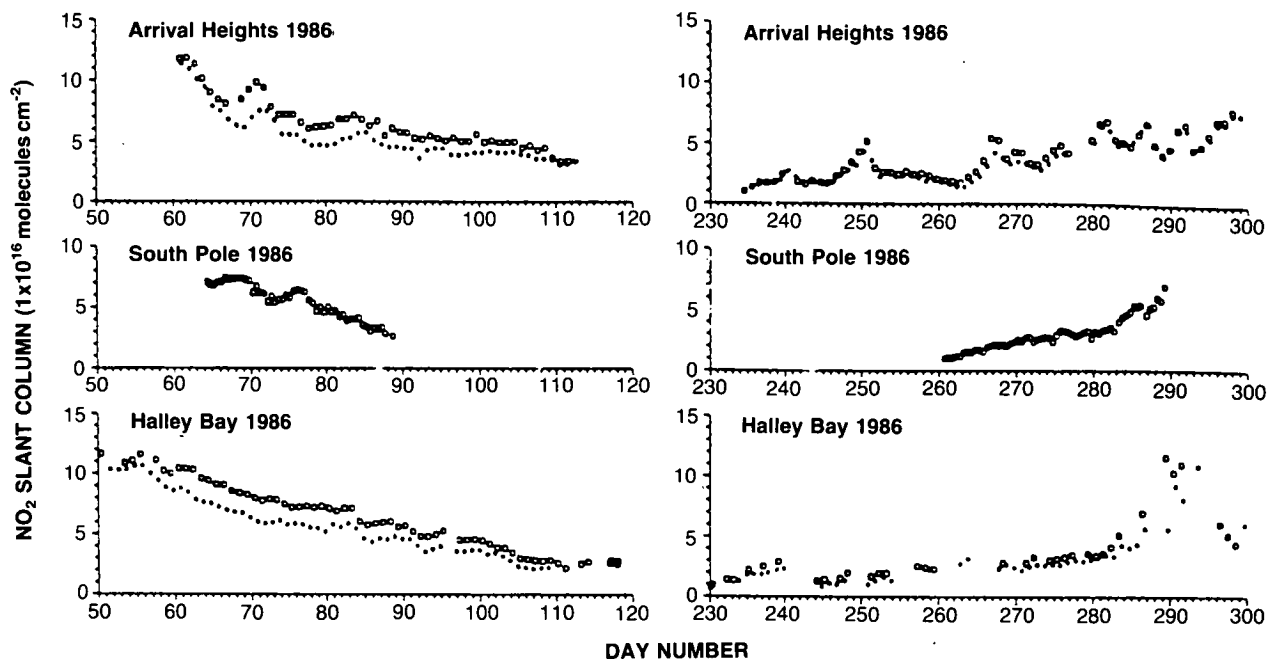


Figure 1.6.2-2. Observations of the seasonal trend in morning and evening twilight slant column NO_2 abundances from three Antarctic sites (from Keys and Johnston, 1988). The vertical column can be deduced by division by about twenty.

those shown in Figure 1.6.2-2, and hence, the diurnal variations of NO_2 persist throughout the fall season there. It is interesting to note that the NO_2 column abundances obtained at Molodezhnaya were very low until late November 1987 (compare Figure 1.6.2-2 for 1986), suggesting limited resupply of nitrogen to the polar vortex until about the time of the stratospheric warming in early December in that particular year (see Section 1.7 for a detailed discussion of the Antarctic vortex dynamics in 1987).

Satellite measurements of NO_2 are also available from the SME, SAGE, and SAGE II experiments. These data reveal sharp reductions in NO_2 in the Antarctic winter, with latitudinal gradients that are qualitatively similar to those obtained from the column measurements discussed above. Thomas et al. (1988) described SME observations of the abundance of NO_2 . The SME observations are restricted to the altitude range above about 28 km. Thomas et al. (1988) compared these data to observations of the total NO_2 column abundance over McMurdo by Mount et al. (1987), and showed that much of the NO_2 normally expected to be located below 28 km was missing. The SAGE and SAGE II satellite observations also provide important information on the altitude profiles of NO_2 within and outside the Antarctic polar vortex. Figure 1.6.2-4 presents a contour plot of NO_2 densities in early October, 1987 from SAGE II, showing evidence for very low average abundances of NO_2 below about 30 mb (approximately the altitude range where polar stratospheric clouds are generally observed, see Section 1.2). The relatively low abundances at higher altitudes in the polar regions as compared to lower latitudes are consistent with other measurements such as LIMS (Russell et al., 1984) and with model calculations. These likely reflect photochemical destruction of reactive nitrogen in the upper stratosphere and mesosphere and subsequent downward transport, and are predicted by multi-dimensional photochemical models employing standard gas-phase photochemistry (see e.g., Garcia and Solomon, 1983).

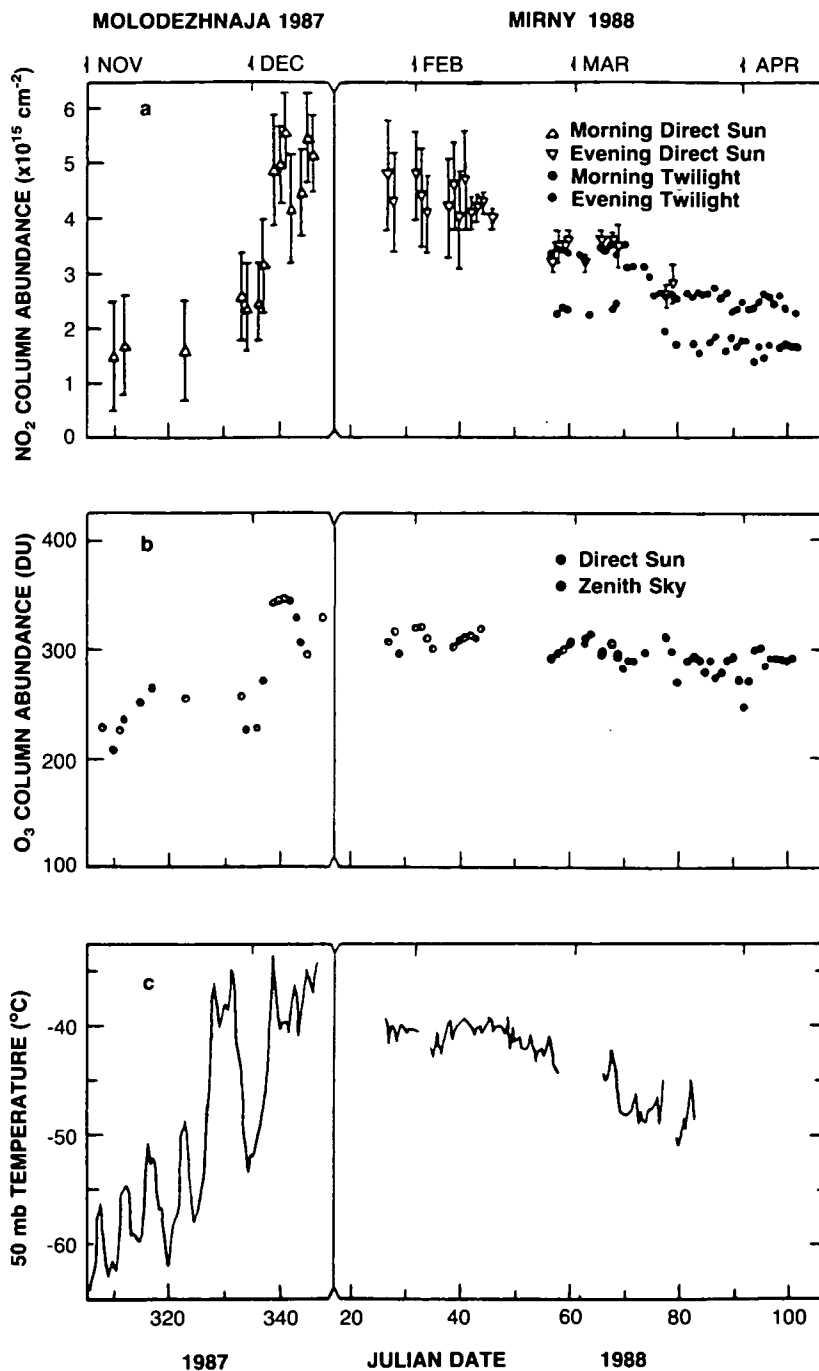


Figure 1.6.2-3 Total NO_2 (a), total O_3 (b), and 50 mb temperature (c) at Molodezhnaya in 1987 and Mirny in 1988 (from Elokhov and Gruzdev, 1989).

HNO_3 column abundances were also measured by infrared absorption methods (Farmer et al., 1987; Coffey and Mankin, 1989; G. Toon et al., 1989a). Figure 1.6.2-5 displays the measured nitric acid column abundance within the Antarctic polar vortex in mid-September. Note the abrupt drop in the HNO_3 column to very low values within the vortex. HNO_3 can be affected by heterogeneous chemistry in several ways.

POLAR OZONE

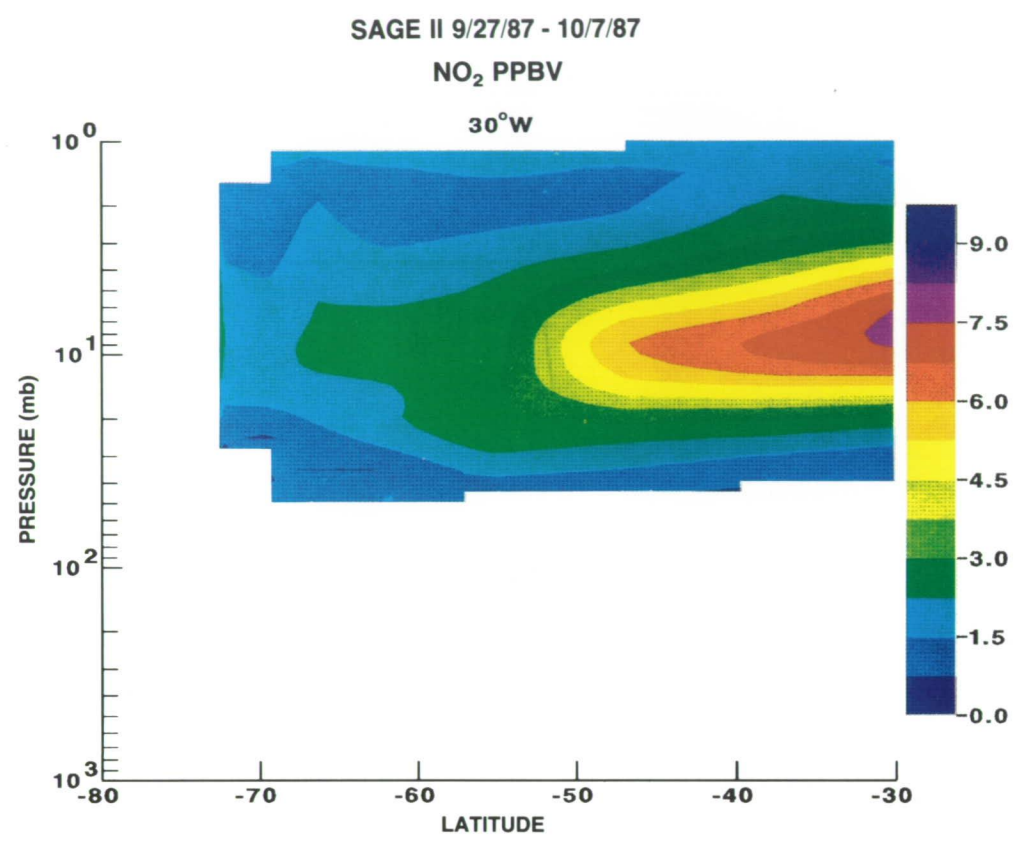


Figure 1.6.2-4. Cross section of NO₂ (ppbv) vs. latitude and pressure for the period from September 27 to October 7, 1987, from SAGE II observations in the Southern Hemisphere (from McCormick, personal communication).

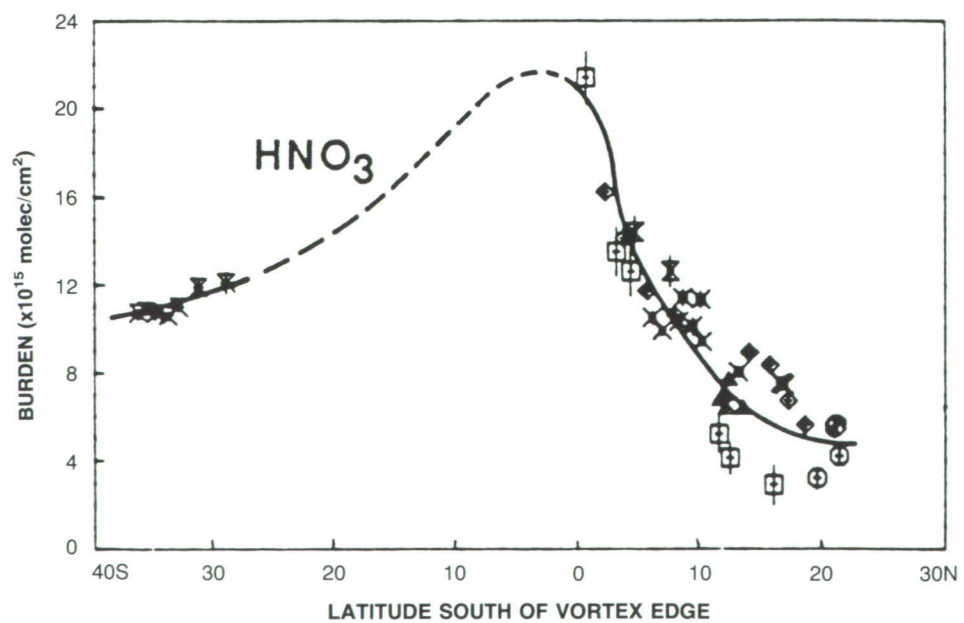


Figure 1.6.2-5. Observed column of HNO₃ plotted as a function of latitude relative to the edge of the polar vortex in August and September, 1987 (from G. Toon et al., 1989a).

If PSC clouds are present, then a substantial amount of the gas-phase HNO_3 can be incorporated into the clouds and abundances of gas-phase HNO_3 will be low. However, the presence of the clouds is believed to lead to conversion of other forms of reactive nitrogen (N_2O_5 , ClONO_2 , see Section 1.4) into particulate HNO_3 . If the cloud particles then evaporate, HNO_3 abundances should be expected to be unusually high. If, on the other hand, the cloud particles sediment out of the stratosphere, then the HNO_3 and NO_y abundances will remain low until transport processes replace or effectively mix with the denitrified air.

In situ measurements of NO_y shown below (Figure 1.6.2-6) demonstrate that substantial, though not complete, denitrification of the Antarctic lower stratosphere (near 18–20 km) occurred in September 1987. The very low column abundances of nitric acid observed in 1987 and the vertical extent of very cold temperatures observed in that particular year indicated that this denitrification extended throughout much of the stratosphere. In contrast, the high values of HNO_3 column observed in November 1978 (Williams et al., 1982) suggest that either a) denitrification was not very extensive in that year (e.g., due to warmer temperatures) or b) that nitric acid was brought in through transport processes, perhaps those associated with the stratospheric warming (but see also, Section 1.7.3). Further observations, particularly of the seasonal trend in HNO_3 throughout the spring season, are needed to understand how transport processes associated with the final stratospheric warming and chemical/microphysical processes associated with formation and evaporation of polar stratospheric clouds influence the abundances of HNO_3 and reactive nitrogen in the Antarctic lower stratosphere.

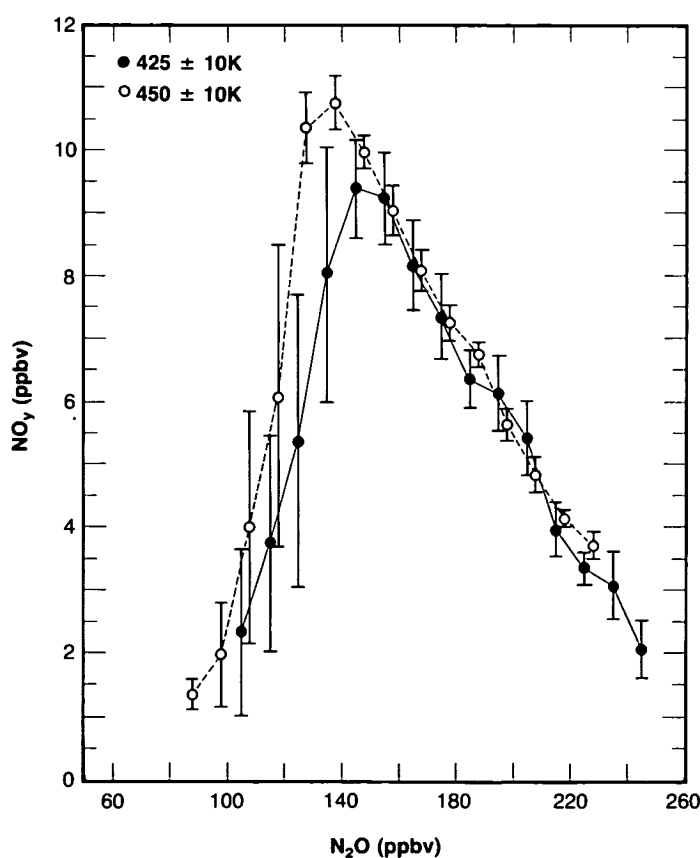


Figure 1.6.2-6. Measurements of total reactive nitrogen (NO_y) versus N_2O obtained from aircraft observations on the 425 and 450 K potential temperature surfaces (from Fahey et al., 1989a).

POLAR OZONE

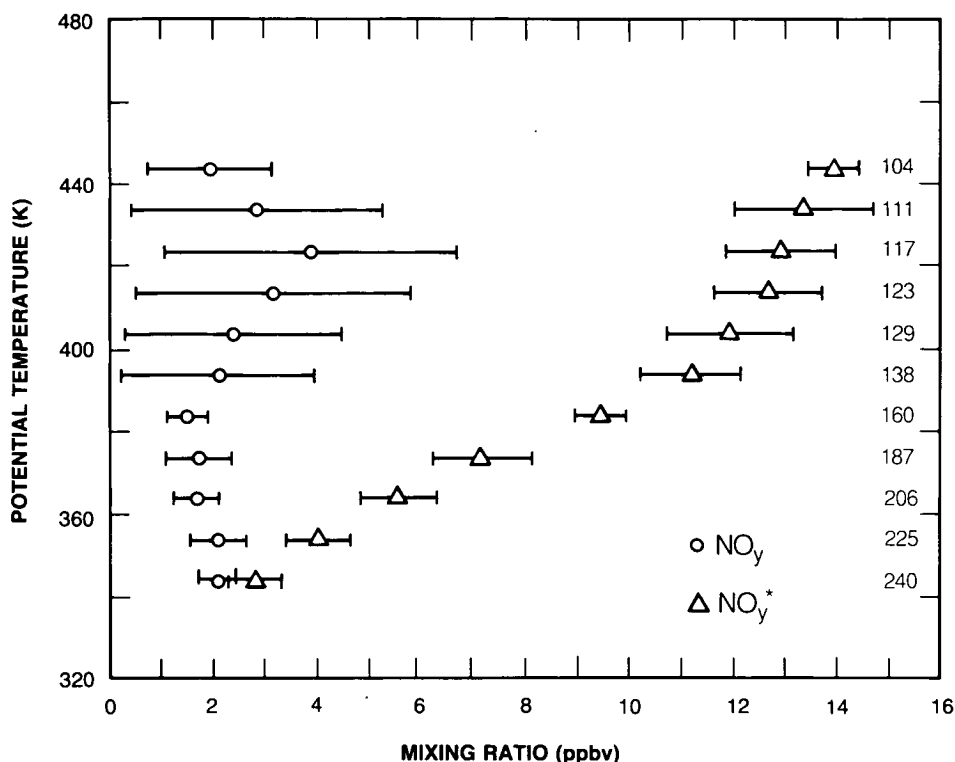


Figure 1.6.2-7. Observed total reactive nitrogen profile (NO_y , circles) and the amount which would be inferred to be present (NO_y^* , triangles) from the N_2O mixing ratios (see right margin), as a function of potential temperature (from Fahey et al., 1989a).

Karcher et al. (1988) report measurements of HNO_3 , NO_2 , HCl , and O_3 column abundances between 64°N and 57°S in June, 1983 and 1984. The latitude gradients obtained and the similarity with measurements from other studies in Antarctic spring led Karcher et al. to conclude that their observations at 57°S revealed significant perturbations due to heterogeneous chemistry. These findings indicate that anomalous chemistry takes place well before springtime and can be evident at latitudes rather far equatorward of the CPR. Such perturbations could have important effects on the seasonal and latitudinal variations in ozone depletion.

In situ measurements of NO and NO_y in the Antarctic vortex were obtained by Fahey et al. (1989a,b). The interpretation of measurements of NO_y can be complicated, since the instrument is more sensitive to the NO_y present in particles than the gas phase. This leads to NO_y "enhancements" when large amounts of NO_y -containing particulate material is present. As discussed in Section 1.3.2, measured NO_y enhancements during PSC events provide strong evidence that Type 1 PSCs contain a substantial fraction of nitrate and begin to form at approximately the temperatures expected for the nitric acid trihydrate (Fahey et al., 1989b).

Fahey et al. (1989a) also studied the behavior of NO_y on occasions when clouds were not present locally (as indicated by the cloud particle counter measurements). Since N_2O is the source of stratospheric NO_y through the reaction $\text{O}(\text{D}) + \text{N}_2\text{O} \rightarrow 2\text{NO}$, the destruction of N_2O is accompanied by a production of NO_y . Thus, one expects increasing concentrations of NO_y as N_2O decreases, and this indeed occurs for N_2O mixing ratios greater than about 140 ppbv at 450 K (about 20 km) as shown in Figure 1.6.2-6. However, for N_2O mixing ratios below about 140 ppbv (in the interior of the Antarctic vortex) this behavior breaks

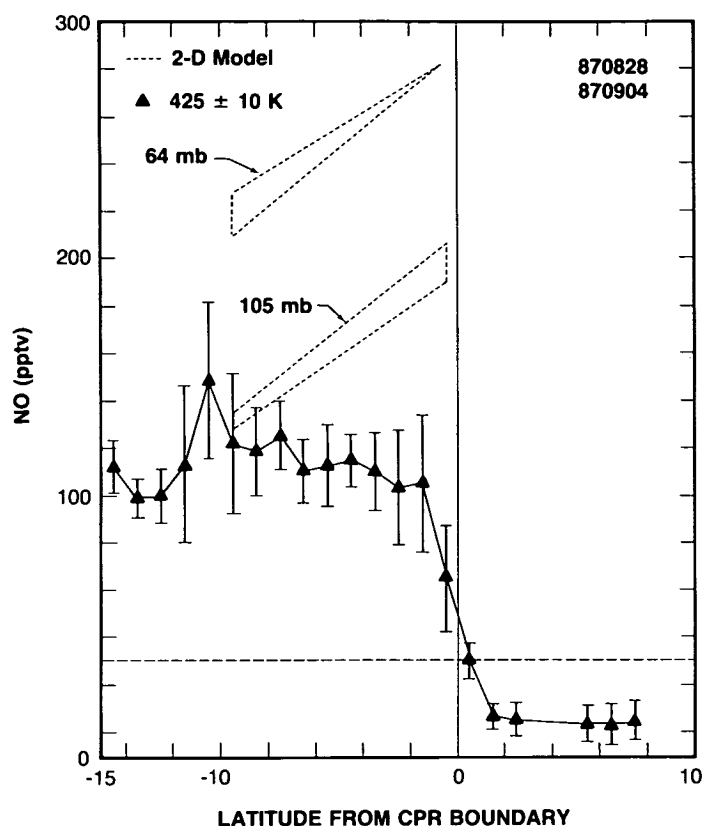


Figure 1.6.2-8. Observed NO mixing ratios versus latitude relative to the chemically perturbed region (from Fahey et al., 1989b).

down, and substantial decreases in NO_y abundances are found. This strongly suggests denitrification processes. Using the correlation between N_2O and NO_y for N_2O mixing ratios above 140 ppbv, a linear expression relating NO_y to N_2O can be derived. From this, the expected NO_y mixing ratio for a given N_2O mixing ratio can be obtained. Figure 1.6.2-7 shows the vertical profile of NO_y^* measured inside the Antarctic vortex and the expected NO_y , referred to here as NO_y^* . The observed N_2O distribution in this region suggests that NO_y values closer to 10 ppbv would be anticipated in the absence of odd nitrogen removal processes. However, NO_y mixing ratios between 1 and 4 ppbv were observed over a wide range of potential temperatures, suggesting that denitrification had occurred over a considerable depth of the low stratosphere. As noted earlier, these results are consistent with the very low HNO_3 columns observed at the same time by G. Toon et al. (1989a) and Coffey and Mankin (1989).

On two Antarctic flights, Fahey et al. (1989a) measured NO rather than NO_y . The results of these observations are summarized in Figure 1.6.2-8. Figure 1.6.2-8 shows that the NO mixing ratios decreased as the polar vortex was approached, in contrast to model calculations that predict increasing abundances in the absence of removal processes (e.g., on PSCs). NO mixing ratios inside the chemically perturbed region were on the order of a few tens of parts per trillion by volume or less. Measurements of the diurnal variations of OCIO and BrO reported by Solomon et al. (1989) suggest similar values of 10–100 pptv of NO_2 (see next section). These measurements show that very little NO_x was available within the polar vortex, which is a prime requirement for elevated levels of ClO and attendant ozone loss as emphasized in Section 1.5.

POLAR OZONE

1.6.3 Other Chemical Species

Water vapor is of particular importance in the Antarctic vortex because it plays an active role in the formation of polar stratospheric clouds. The first reported winter Antarctic measurement of water vapor is that of Iwasaka et al. (1985b), who employed a balloon-borne Lyman-alpha hygrometer from Syowa Station. They reported water vapor mixing ratios of only about 1 ppmv just above the tropopause, and argued that dehydration may have occurred through formation and sedimentation of large ice crystals. Iwasaka (1986) also used lidar observations of particles observed above Syowa Station to show that small, non-depolarizing particles formed prior to and at warmer temperatures than ice saturation. Further, Iwasaka (1986) suggested that large, non-spherical particles formed when temperatures dropped below the frost point based on lidar observations of optical depths and depolarization. As discussed in Section 1.2, these observations are consistent with what is now known as Type 1 particles, believed to be largely composed of nitric acid trihydrate, and Type 2 particles believed to contain largely water-ice (see Poole and McCormick, 1988a). The latter are expected to take up much of the available water vapor, thus dehydrating the stratosphere upon sedimentation. Denitrification could also take place through sedimentation of such particles. In the Antarctic in 1987, the region of denitrification corresponded closely to the dehydration (see e.g., Fahey et al., 1989a). Arctic observations display quite different behavior, as will be discussed in Section 1.10.

Rosen et al. (1988b) conducted a series of three balloon observations of water vapor using frost-point hygrometers at McMurdo Station. They also concluded that the mixing ratios of water vapor displayed a minimum near 15–20 km, suggesting vertically localized dehydration through cloud formation.

These conclusions were confirmed and expanded upon by the observations of Kelly et al. (1989). A Lyman-alpha hygrometer was employed on board the ER-2 aircraft to determine the distribution of stratospheric water vapor. Figure 1.6.3-1 shows measurements of the latitude gradient of water vapor

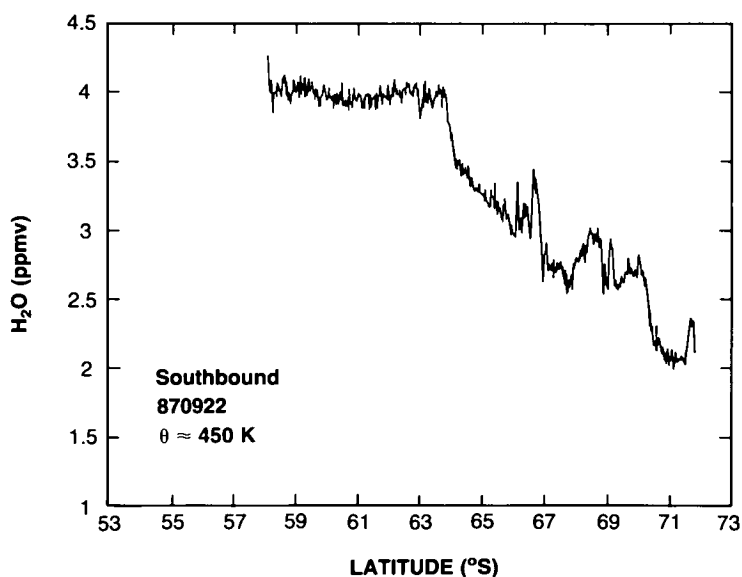


Figure 1.6.3-1. Observed latitude gradient of H₂O on September 22, 1987 near 450 K surface (about 20 km) (from Kelly et al., 1989).

obtained on the 2 September 1987 near 20 km (Kelly et al., 1989). The sharp decreases between 65°S and 67°S provide important evidence of dehydration. Kelly et al. have also argued that the relatively low water vapor abundances obtained at 50–70°S suggest some mixing of air from inside the vortex out to lower latitudes (see Section 1.7).

Figure 1.6.3-2 presents observations of the water vapor distribution in early October 1987 from SAGE II. These data provide a detailed view of the vertical and horizontal structure of the dehydrated region, suggesting that it extends from about 200 to 30 mb (in general agreement with the altitude range where PSCs are observed) and from the polar vortex to perhaps 50°S during the time period of these measurements. This figure was constructed from approximately 10 days of measurements by linear interpolation to an equidistant longitude grid and then to a latitude grid with variable spacing following the density of the measurements for a number of pressure levels. The measurements start at 30°S in late September and finish at 72°S in early October. During this time period the vortex was strongly perturbed along 30°W, allowing SAGE II to obtain a number of observations in the core of the vortex. The water vapor dehydration region overlaps the ozone depletion region to a large extent. Minimum levels of water approach 1 ppmv inside the vortex. Detailed study of such observations is badly needed to determine the extent to which dehydrated air is exported to lower latitudes. Such mixing would also imply transport of denitrified air rich in ClO radicals, and could have important photochemical effects at the lower latitudes (see Fahey et al., 1989a).

Another important chemical species measured in the Antarctic stratosphere is BrO. BrO has been measured both by *in situ* resonance fluorescence on board the ER-2 aircraft (Brune et al., 1989b) and by

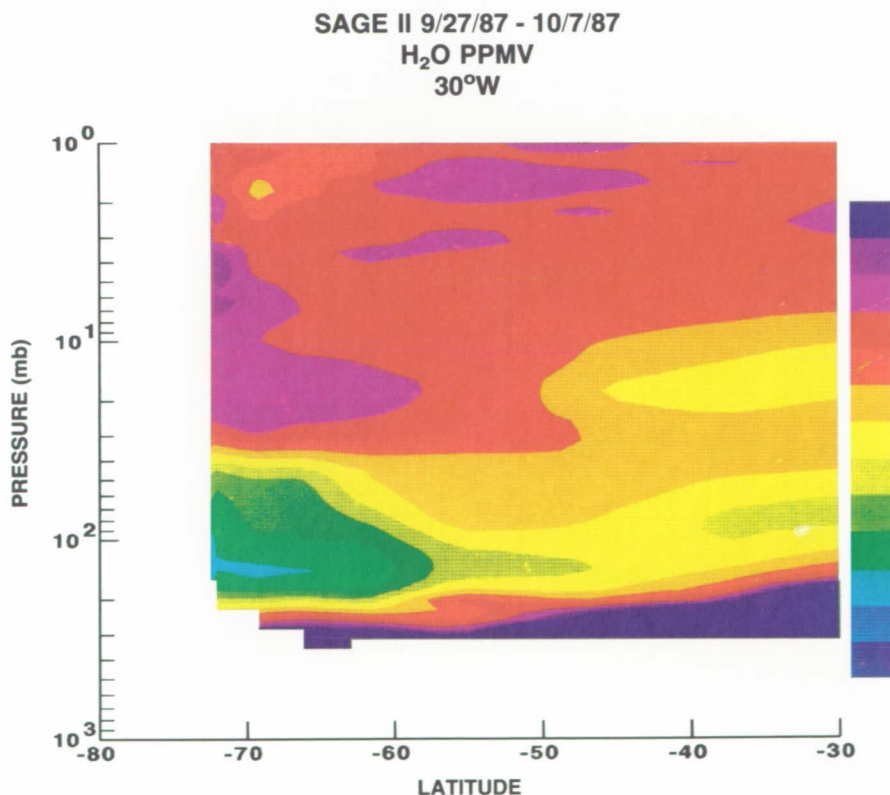


Figure 1.6.3-2. Cross section of H₂O (ppmv) versus latitude and pressure for the period from September 27 to October 7, 1987, measured by the SAGE II instrument (from McCormick, private communication, 1989).

POLAR OZONE

ground-based near-ultraviolet absorption (Carroll et al., 1989). BrO is of particular importance because it participates in a catalytic cycle that can destroy ozone effectively in the lower stratosphere in winter as discussed previously (McElroy et al., 1986a; Rodriguez et al., 1986). The *in situ* measurements of BrO imply mixing ratios of about 2–8 pptv, although it must be noted that the small abundances of BrO lead to greatly reduced signal-to-noise for these measurements as compared, for example, to the resonance fluorescence measurements of ClO. Figure 1.6.3-3 shows the abundances of BrO obtained on several flights as a function of latitude during 1987. As noted in Section 1.5, the balance between ClO and ClONO₂ is critically dependent on the abundance of NO₂, since ClONO₂ photolyzes rather slowly. The sharp gradient in ClO abundances at the edge of the CPR is associated with an inverse behavior for NO and NO₂ believed

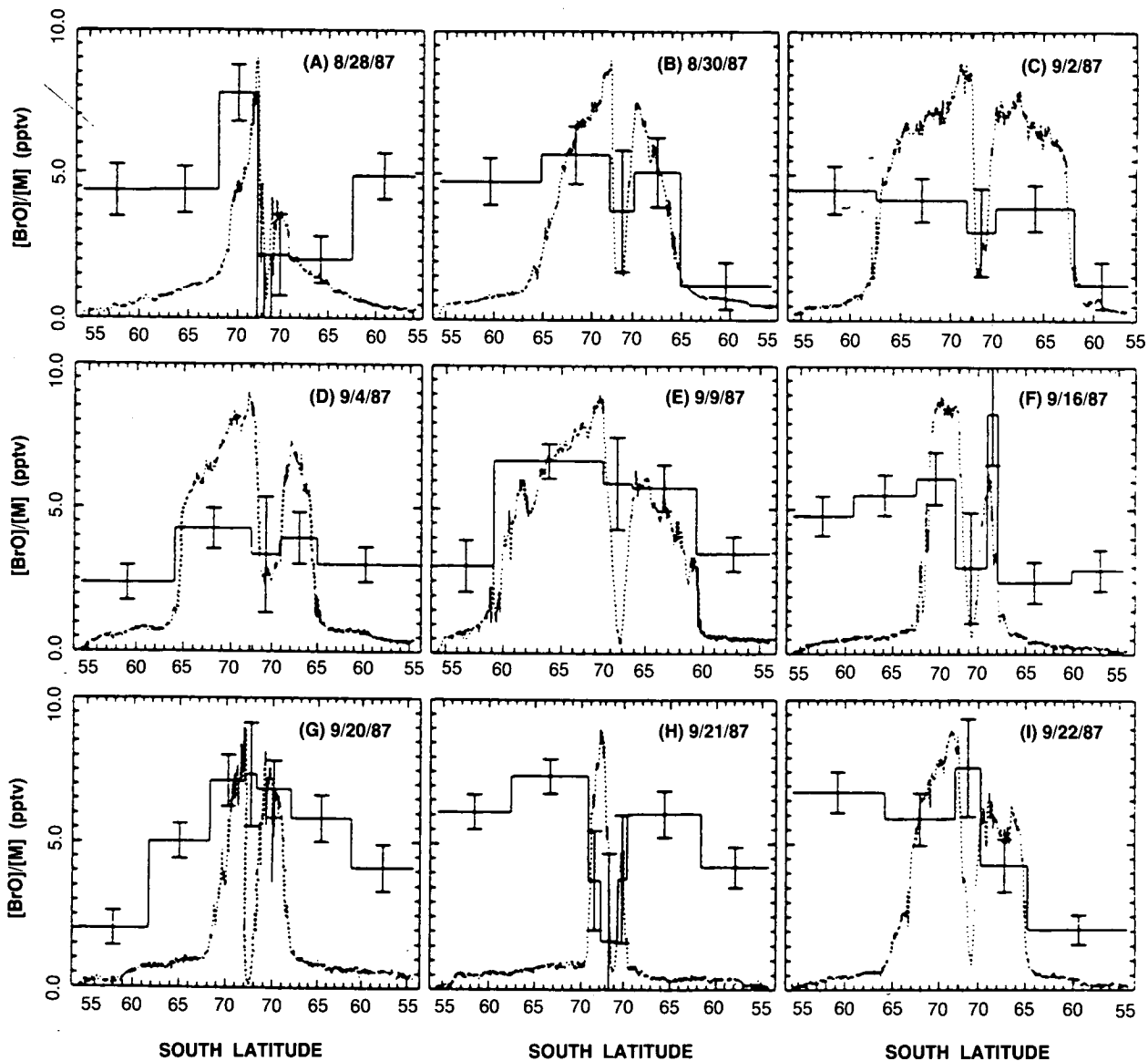


Figure 1.6.3-3. BrO mixing ratios versus latitude for nine flights from about 54 and 72°S, taken between August 28 and September 22, 1987. Horizontal bars represent the distance over which the signals are averaged. ClO mixing ratios are superimposed for comparison, identifying the chemically perturbed region (from Brune et al., 1989b).

to be due to cloud processing (Fahey et al., 1989a). The partitioning between BrO and BrONO₂ is far less sensitive to the abundance of NO₂, since BrONO₂ photolyzes considerably faster than does ClONO₂, and the noontime abundance of BrO is therefore expected to be nearly independent of latitude, consistent with the measurements shown in Figure 1.6.3-3.

Figure 1.6.3-4 depicts the observed vertical profile of BrO at approximately 72°S, showing that it increases with altitude from about 380 to 460 K (about 14 to 20 km). This gradient may reflect the altitude dependence of the bromocarbons and hence the available reactive bromine levels and/or formation of BrONO₂ or other reservoirs at lower altitudes. Figure 1.6.3-5 presents observed diurnal variations of the BrO slant column abundance obtained over McMurdo Station. Carroll et al. (1989) showed that the absolute levels of BrO obtained in the evening twilight measurements were consistent with mixing ratios in the low stratosphere of about 5–15 pptv. Solomon et al. (1989) noted that the much lower morning twilight measurements suggested that BrO levels were reduced at sunrise due to formation of a relatively long-lived reservoir during the night, probably BrONO₂. Both sets of measurements suggest that BrO mixing ratios are large enough to contribute 5–20% of the ozone decline observed in Antarctic spring (see Section 1.6.4).

A broad range of long-lived compounds (e.g., CF₂Cl₂, CFCl₃, CH₃Br) were measured during AAOE by grab sampling and gas chromatographic/mass spectrometric (GC/MS) methods. N₂O was also measured, both by GC/MS and by a tunable diode laser technique (Podolske et al., 1989). The GC/MS technique and an overview of the results are given by Heidt et al. (1989). The implications of these measurements for the chlorine budget and for the dynamics of the polar lower stratosphere are discussed in the next section and in Section 1.7.1.

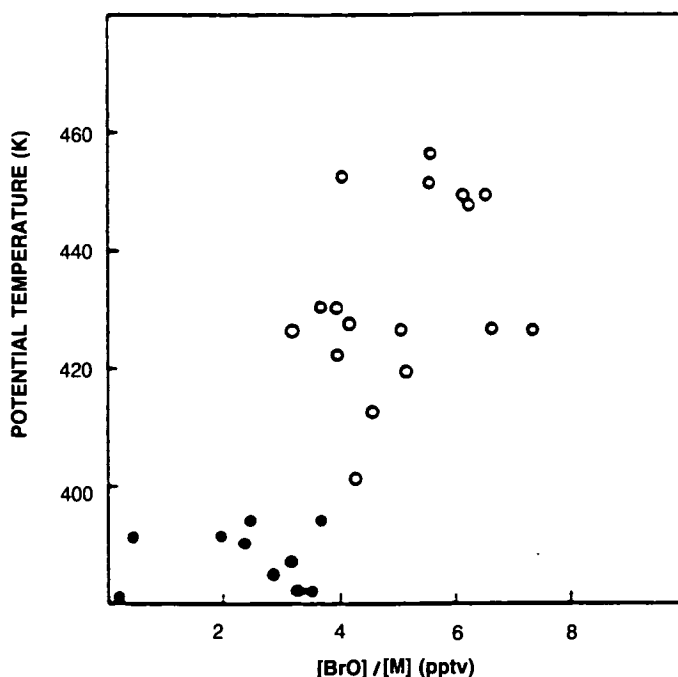


Figure 1.6.3-4. Variation of the BrO mixing ratio with potential temperature. Open circles represent data taken during aircraft flights on constant potential temperature surfaces, closed circles indicate data taken during aircraft ascent and descent at 72°S (from Brune et al., 1989b).

POLAR OZONE

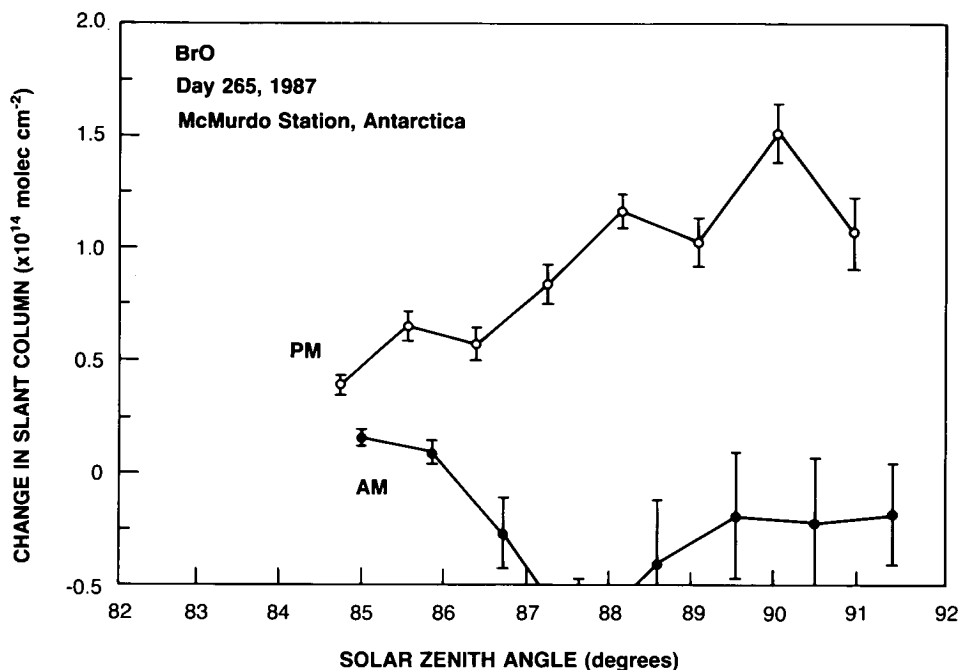


Figure 1.6.3-5. Diurnal variation of the BrO slant column at McMurdo Station (from Solomon et al., 1989).

1.6.4 Modeling Studies of the Composition and Photochemistry

Several of the early chemical modeling studies suggesting mechanisms to understand the Antarctic ozone hole were briefly described in Section 1.1.4. In this section, theoretical studies aimed at interpreting observations of a broad range of chemical species will first be discussed. Specific studies dealing with evaluation of the associated ozone loss rates will then be reviewed.

Rodriguez et al. (1986) and Salawitch et al. (1988) discussed the diurnal chemistry of chlorine compounds such as ClO, OCIO, and Cl_2O_2 under conditions where the chlorine levels are greatly perturbed by the presence of PSCs. Rodriguez et al. (1986) emphasized the important roles of Cl_2O_2 and OCIO as nighttime reservoirs for ClO. Salawitch et al. (1988) emphasized the possible role of BrCl in modulating the diurnal cycle of BrO and thus limiting the nighttime OCIO abundance. Observations of OCIO by S. Solomon et al. (1987), Wahner et al. (1989b) and Solomon et al. (1989) exhibit strong diurnal variations broadly consistent with these predictions. Solomon et al. (1989) also showed that the observed asymmetries in morning and evening twilight OCIO and BrO measurements provided another important element in the diurnal cycle that could be used to infer formation of a relatively long-lived nighttime BrO reservoir, likely BrONO_2 .

McElroy et al. (1988) discussed the ground-based measurements of column abundances of HCl, ClONO_2 , NO, and NO_2 by Farmer et al. (1987). They noted that the low abundance of HCl observed in early September and its subsequent increase during the spring season was qualitatively consistent with the expected recovery of HCl following chemical processing on PSC particles. Their calculations also revealed

general agreement with the observed seasonal trends in HNO₃, NO, and NO₂ abundances and, most important, in the seasonal rate of decline of the ozone column during 1986.

Wofsy et al. (1988) discussed the thermodynamics of mixed HCl/HNO₃/H₂O ices and explored the implications of heterogeneous chemistry for chemical composition and ozone loss. They emphasized that the nonlinear growth in ozone depletion since about 1980 and its rather sudden onset may be related to the titration of reactive chlorine by reactive nitrogen radicals. In particular, they emphasized that dramatic ozone loss might begin when the initial HCl abundance exceeds the sum of 1/2 NO_x (defined as NO + NO₂ + NO₃ + 2 × N₂O₅). The success of such a formulation depends in part on a thorough understanding of the denitrification process, which influences the residual reactive nitrogen available for titration.

Many recent modeling studies have focussed on obtaining a better understanding of observations of the composition of the Antarctic vortex observed in 1987. The broad morphology of the long-lived tracers in the Antarctic spring vortex, in particular the unusually low absolute mixing ratios and the latitude gradients of N₂O and many chlorofluorocarbons is understood in terms of air within the vortex having undergone substantial diabatic descent during the winter months (see, for example Heidt et al., 1989; G. Toon et al., 1989b; Podolske et al., 1989; Parrish et al., 1988; and Section 1.7). These findings have important implications for the understanding of atmospheric dynamics and will be discussed further in Section 1.7.

The appearance of extensive denitrification and dehydration in the Antarctic vortex is understood (at least qualitatively) in terms of the formation of Type 1 nitric acid trihydrate particles that eventually grow to large Type 2 ice crystals and sediment out of the stratosphere. The particle sizes predicted by micro-physical models (e.g., Poole and McCormick, 1988a) are of the order of a few microns, capable of sedimenting at a rate of the order of a few kilometers per week.

Given this basic picture, Heidt et al. (1989) and Jones et al. (1989) have examined the latitude and vertical gradients of chlorofluorocarbons observed within the Antarctic vortex during the 1987 AAOE, and used these data to deduce the abundance of inorganic chlorine available for cloud processing. Such a derivation is dependent upon the measured gradients in chlorofluorocarbons and (to a small extent) upon assumptions regarding the "age of the air" descending within the vortex, since this determines the amount of total chlorine it contains (see Jones et al., 1989 and Section 1.7). Table 1.6.4-1 presents deduced organic

Table 1.6.4-1 Assumed chlorine tracer concentrations and inorganic chlorine content as a function of potential temperature at 72°S. The cases 'A' and 'B' refer to different assumed tropospheric chlorine contents, appropriate to the mid- and late 1980s (see text). The total chlorine contents are 3.15 and 3.5 ppbv

Potential Temperature	420 K	400 K	380 K	360 K	340 K
F11	28.0	53.0	79.0	142.0	200.0
F12	130.0	180.0	220.0	255.0	306.0
F113	9.7	14.0	19.4	27.0	42.0
CH ₃ CCl ₃	6.0	11.5	19.2	30.0	45.7
CCl ₄	7.0	10.0	60.0	90.0	100.0
CH ₃ Cl*	230.0	320.0	390.0	450.0	550.0
net ClO _y (case 'A')	2555.0	2200.0	1750.0	1250.0	750.0
net ClO _y (case 'B')	2970.0	2620.0	2170.0	1670.0	1170.0

*The concentrations of this gas have been inferred using F12 as a proxy (see text).

POLAR OZONE

and likely inorganic chlorine abundances derived from such measurements for one of the studies. The observations suggest that more than 2.5 ppbv of chlorine may be available (i.e., not tied up in chlorofluorocarbons) at the higher altitudes near 420 K (about 18 km) within the vortex. Observations made during the 1986 and 1987 Antarctic springs indicate that a substantial fraction of the available chlorine was present in reactive forms. For models to simulate the latitude and vertical gradients of reactive species within the vortex it was essential to include the effects of heterogeneous reactions taking place primarily on Type 1 nitric acid trihydrate particles (see Section 1.2). In Figure 1.6.4-1 is shown a comparison of observed ClO mixing ratios as a function of latitude with those modeled using an approach that includes a detailed treatment of air flow (Jones et al., 1989). The comparison is for early September on the 428 K potential temperature surface. Poleward of 65°S an abrupt increase in ClO mixing ratio is evident in the observations. In the model, polar stratospheric clouds are predicted to form polewards of 65°S during the relevant period and the modeled ClO mixing ratios increase through the effects of heterogeneous reactions, primarily between HCl and ClONO₂. The same model also simulates well the vertical gradient of ClO within the vortex (see Figure 1.6.4-2), which arises primarily from the vertical gradient in available chlorine. As noted earlier, this and other studies (e.g., Rodriguez, et al., 1989) demonstrate that without heterogeneous reactions on PSCs, modeled ClO mixing ratios in the polar vortex would be about two orders of magnitude lower than observed.

Fahey et al. (1989a) show that chemical processes also play a critical role in establishing the observed NO latitude gradient. NO mixing ratios exhibited a marked fall off for ClO levels above about 70 pptv. Increased ClO due to cloud processing is expected to lead to a faster rate of formation of ClONO₂, higher ClONO₂ levels, and reduced NO and NO₂ abundances. Fahey et al. showed that these considerations are consistent with the observation of a pronounced ClONO₂ "collar" (ring of high ClONO₂ values just inside the chemically perturbed region) by infrared absorption methods (see Section 1.6.1). Clearly, these obser-

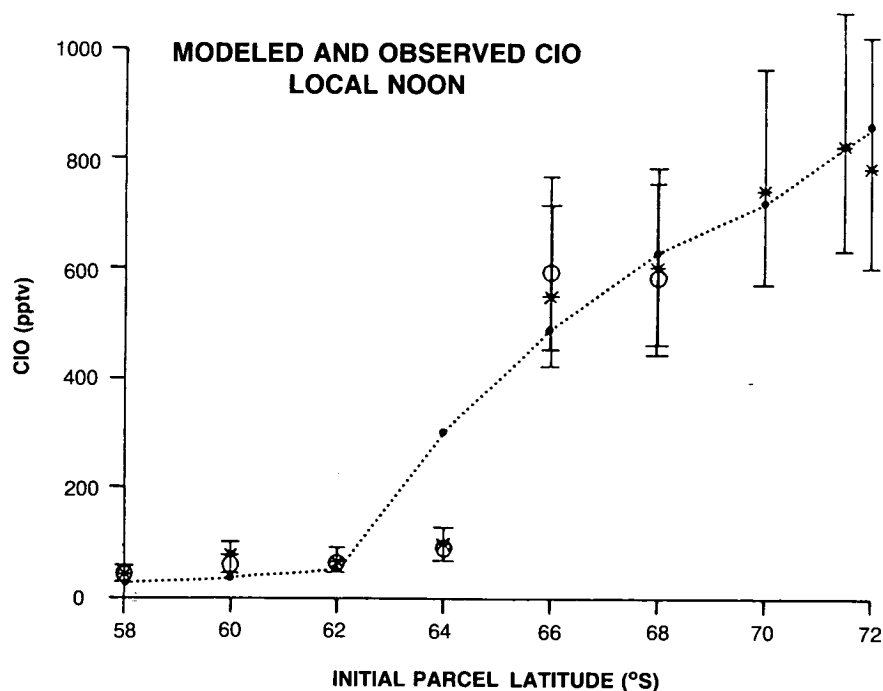


Figure 1.6.4-1. Calculated and observed ClO mixing ratios on the 428 K surface, 4-12 September, 1987 (from Jones et al., 1989).

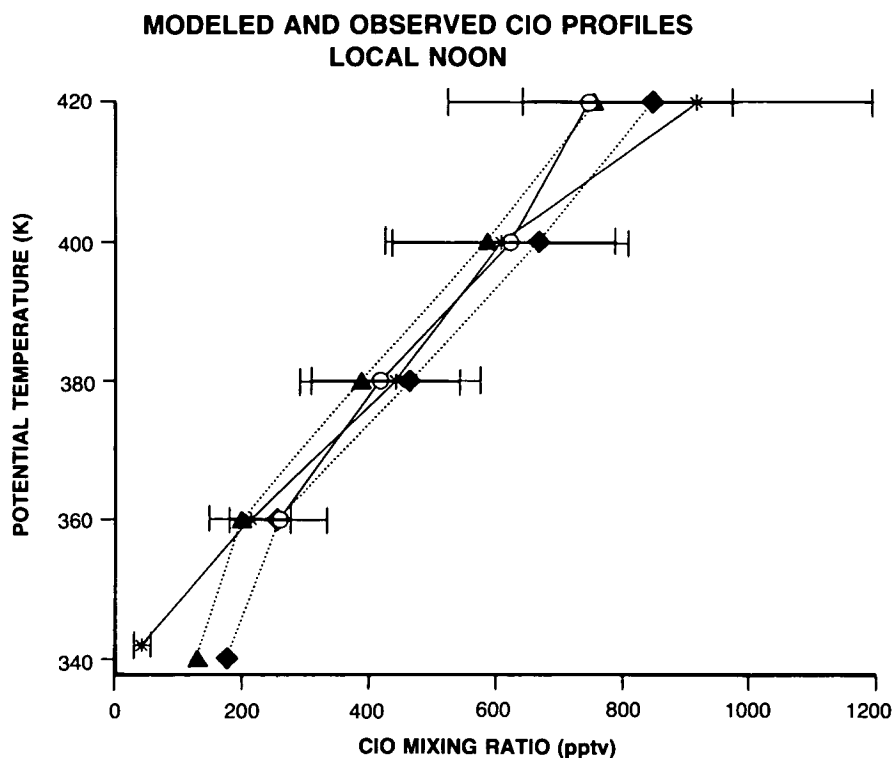


Figure 1.6.4-2. Calculated and observed ClO mixing ratio profiles at 72°S, 4 and 9 September, 1987 (from Jones et al., 1989).

variations and the possibility of rapid formation of ClONO₂ may play an important role in determining the form of the remaining NO_y inside the vortex as shown above.

Jones et al. (1989) noted that the NO abundances and the inferred NO/NO_y ratios observed outside the dehydrated, denitrified region were lower than theoretical predictions, and the ClO mixing ratios higher. They argued that this, and the existence of temperatures outside the denitrified region close to and below the threshold for Type 1 PSC formation, indicate that PSC processes are occurring at latitudes outside of the polar vortex, although mixing of air from within the denitrified region out to lower latitudes may also play an important role in the NO_y and ClO_y partitioning. Airflow through PSC clouds (produced for example, by orographic forcing and/or cyclonic scale weather systems) can process large volumes of stratospheric air, particularly near the edge of the polar vortex where wind speeds are high (see, McKenna et al., 1989a; Cariolle et al., 1989a). Reactions on background sulfate aerosols may also be important. It is worthy of emphasis that perturbations to the NO/NO_y ratio and available chlorine partitioning as far equatorward as 50°S may be of considerable importance to mid-latitude ozone trends.

The observations of high abundances of ClO and OClO throughout September within the vortex, followed by declining values of these reactive species in October are consistent with the picture of heterogeneous release of reactive chlorine on PSCs and the known morphology of the clouds (see Section 1.2). Solomon et al. (1989) have argued that the seasonal cycle of OClO is consistent with an increase in the available NO₂ during September. Using a model including the effects of wind motions but not those of small-scale mixing or diabatic processes, Austin et al. (1989) have suggested that once PSCs vanish, and

POLAR OZONE

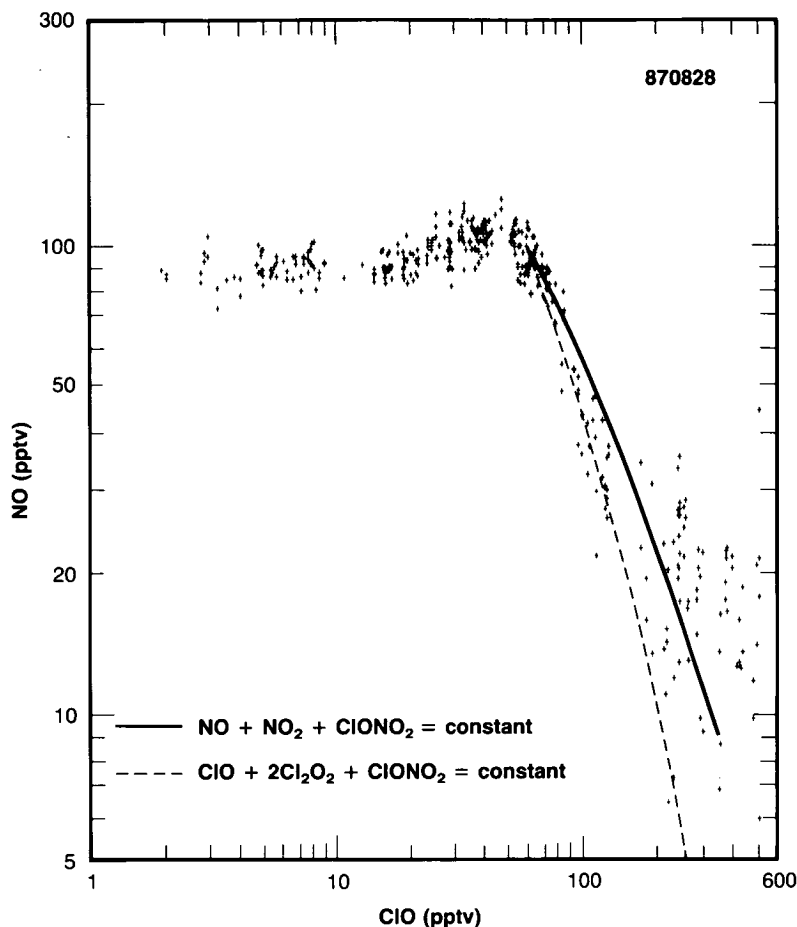


Figure 1.6.4-3. Observed NO and ClO mixing ratios from an aircraft flight on August 28, 1987. The rapid decline of NO at the higher ClO mixing ratios is consistent with $ClONO_2$ formation (from Fahey et al., 1989b).

as sun angles increase, NO and NO_2 abundances begin to rise through increased HNO_3 and $ClONO_2$ destruction (as discussed briefly in Section 1.5). They argue that as a result, atomic Cl abundances rise and HCl begins to be reformed at a significant rate, so tying up reactive chlorine, reducing ClO, and halting further ozone loss. These studies suggest that the onset and termination of photochemical ozone loss (as reflected in ClO and OCIO abundances) is closely tied to the availability of reactive nitrogen.

It has been suggested (Tuck, 1989; McKenna et al., 1989b) that significant mixing between vortex air and that from lower latitudes can occur during September. Mixing in of air containing high NO and NO_2 would accelerate photochemical recovery to normal gas phase ClOy partitioning, as discussed in detail in Section 1.5. Further work is needed to determine whether NO and NO_2 do indeed increase (especially in late September) and, if so, to determine the contribution of mixing to the seasonal cycle of the reactive chlorine species.

Several groups have attempted to model the ozone decline observed in 1987 using a variety of approaches. The studies are in general agreement although there are important differences in detail.

Figure 1.6.4-4 shows measured ozone decreases from AAOE aircraft data and computed rates using the dimer formation rates of Hayman et al. (1986) and Sander et al. (1989), along with observed noontime ClO (Anderson et al., 1989). Diurnal variations were computed assuming a zonally symmetric circulation (i.e., constant temperatures equal to those observed at noon along the aircraft flight track and assuming that air parcels circulate along latitude circles as they undergo their diurnal variations). Broad general agreement with the rate of observed ozone decline is obtained for the Hayman et al. rate, but the observed decline is significantly underestimated (by about 35%) if the Sander's et al. rate is used. Anderson et al. adopted the latter, and postulated the existence of an additional termolecular reaction involving ClO and ozone. Hofmann (1989a) suggested that ozone may be destroyed directly on PSC surfaces, based on an observed spatial correlation between ozone loss and particle surface areas. Other possible mechanisms for polar ozone loss were explored in Section 1.5.

Barrett et al. (1988) examined the observed ozone loss over McMurdo Station from ozonesonde observations in 1987 and compared these to calculated values based on their observed ClO observations using the JPL (1987) reaction rate constant for formation of the ClO dimer. They found good agreement between the observed and calculated loss rates. However, Sander et al. (1989) have re-evaluated the same data set using their revised lower reaction rate constant. They concluded that current photochemical mechanisms can quantitatively account for the observed ozone losses from about September 17 through October 7, but noted that additional losses appeared to be required to explain the observed loss earlier in the spring season (August 28 through September 17). Like the calculations of Anderson et al. (1989), these

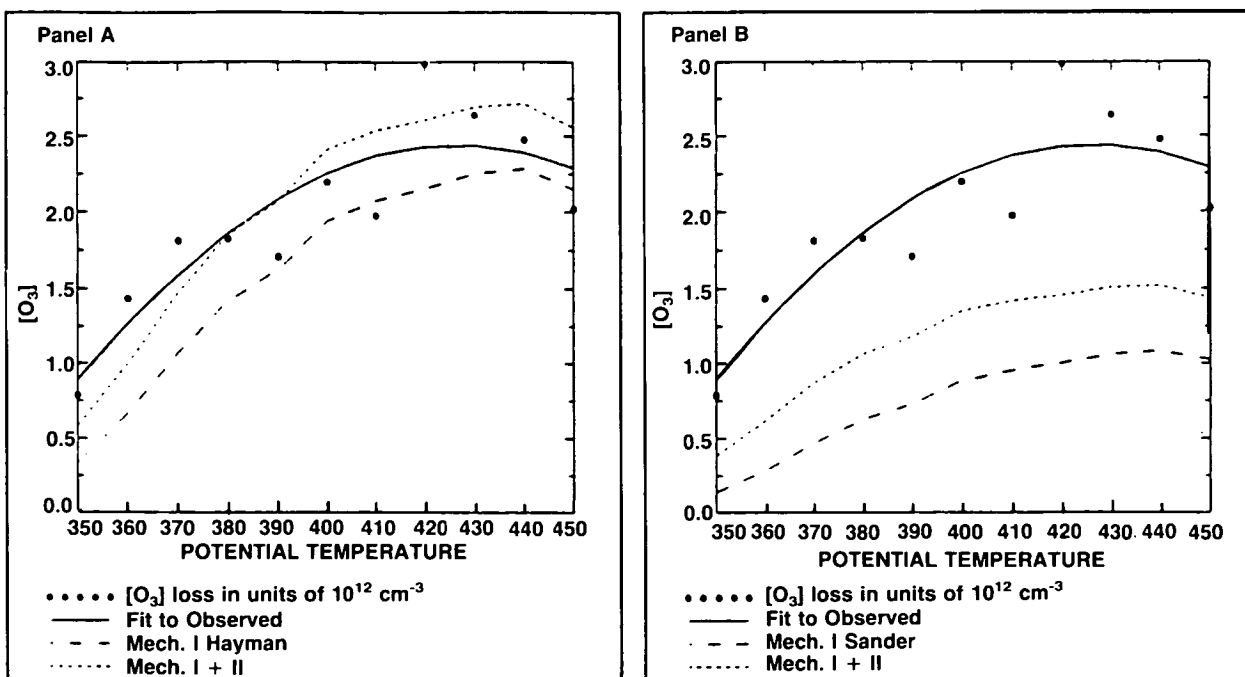


Figure 1.6.4-4. Observed and calculated rates of ozone decline for different ClO dimer formation rates (from Anderson et al., 1989) as a function of potential temperature surface. Panel A displays loss rates for the mechanism involving ClO dimer photolysis (Mechanism I) using the Hayman et al. (1986) rate and for dimer photolysis plus bromine chemistry (Mechanism II). Panel B displays loss rates for the same quantities, employing the Sander et al. (1989) rate for ClO dimer formation.

POLAR OZONE

studies both assumed that observed temperatures and photochemical conditions at a single point were representative of those experienced by air parcels moving around the vortex. A further limitation of these studies was the assumption that ClO measurements obtained during a period of a few days in mid-September applied throughout the month.

The analyses of Jones et al. (1989) included a detailed treatment of airflow along isentropic trajectories appropriate for AAOE observations. Their analysis suggested that the rate of ozone loss in the chemically perturbed region approached 2% per day in early September 1987 using the dimer formation rate of JPL (1987). Of this, about 71% was due to the ClO dimer mechanism, 17% to the reaction of ClO with HO₂, and 12% to the reaction of ClO with BrO. Austin et al. (1989) have shown that when a detailed treatment of air motions is included but mixing is neglected, photochemical ozone losses can exceed 90% at some altitudes by late October, consistent with observations of the vertical profile of the ozone depletion. The calculations by Jones and co-workers suggest that the observed rate of ozone loss remains consistent with model calculations even when the updated rate constants of Sander et al. are considered. This suggests that the effects of zonal asymmetries on the ozone loss rate may be quite significant. Given the sharp gradients in photolysis rates prevalent in the Antarctic spring stratosphere, it is plausible that latitudinal excursions of air parcels may greatly influence photochemical loss rates.

The study of Ko et al. (1989) suggested that while the ozone loss in 1987 could be reproduced, there were some difficulties in simulating the development of the springtime ozone decrease since the 1970s (that is, the seasonal trend in 1987 was found to be consistent with the observed ClO levels, but the decadal trend since the late 1970s could not be entirely resolved solely through consideration of the known increases in chlorofluorocarbon abundances). Measurements of PSCs described in Section 1.2 suggest a trend in PSC abundances during the October months of recent years of westerly QBO phase. Section 1.8 demonstrates that the observed decreases in ozone have caused a trend in October temperatures, which is probably responsible for at least a portion of the observed PSC trend. This suggests that as ozone depletion becomes more pronounced, temperatures may remain unusually low, which in turn can enhance and/or prolong the PSC activity. This is likely to lead to greater ozone depletion and may represent an important mechanism for acceleration of the decadal ozone trend beyond that anticipated solely on the basis of the known increases in chlorofluorocarbon abundances.

In addition to trends in chlorine (and bromine) abundances, non-linear chemical depletion processes, and PSC frequency or intensity, the decadal trend in total ozone should be expected to be influenced by any trends in planetary wave activity, denitrification, the persistence or strength of the polar vortex, and synoptic-scale systems. All of these factors can influence the dynamics, temperatures, and chemical balance of the polar lower stratosphere. Further work is needed to understand the roles played by each.

While there are differences between the individual studies, the observations of sustained high concentrations of ClO throughout the polar spring, coupled with laboratory studies of key reactions (see Section 1.4 and 1.5) provide conclusive evidence that substantial ozone loss is occurring in Antarctica as a result of halogen chemistry, primarily through the formation and destruction of the ClO dimer.

Quantitative uncertainties exist in the absolute rate of the chlorine catalyzed ozone loss. Also, it is not certain whether dynamical mechanisms can contribute a small ozone loss, nor can it be stated that all chemical mechanisms are fully understood. However, it is clear that the available measurements coupled with laboratory rate measurements prove that chlorine chemistry is capable of accounting for at least the major fraction of the total ozone destruction in Antarctic spring in 1987 and can thus account, at least in large part, for the development of the Antarctic spring depletion first noted by Farman et al. (1985a).

Given that chlorine and coupled chlorine/bromine chemistry is responsible for the bulk of the Antarctic ozone reduction observed currently, it is possible to estimate how large a reduction in stratospheric chlorine loading is needed to eliminate the ozone hole. It is assumed that there will be no significant changes in Antarctic meteorology or in PSC frequency due to external processes. Figure 1.6.4-5 displays the October average total ozone abundances at Halley Bay since the late-1950s along with the total tropospheric chlorine content (which is well known, based on worldwide measurements of the CFCs and industrial releases). It is reasonable to expect that the chlorine content of the Antarctic lower stratosphere lags that of the troposphere by a few years due to the time scale for transport to that region. Preliminary analyses of CO_2 measured simultaneously with the CFCs in the Arctic vortex (Heidt, personal communication, 1989) suggest that the average age of air within the polar vortex at about 20 km is 5 years. Figure 1.6.4-5 and measurements at the South Pole and Syowa (see Section 1.1) indicate that ozone abundances were detectably reduced in the late 1970s. Those observations coupled with the above estimate of the age of vortex air imply that it is necessary to return to the CFC levels of the early to mid-1970s in order to eliminate the Antarctic ozone hole. Figure 1.6.4-5 shows that this was a period when atmospheric CFC abundances were rising rapidly. The total tropospheric chlorine abundances then were in the range of 1.4 to 2.0 ppbv, including 0.6–0.7 ppbv of methyl chloride believed to be of natural origin. It would therefore be necessary to achieve a man-made abundance of organic chlorine of about 0.7 to 1.4 ppbv. This analysis assumes no decadal increases in bromine abundances; any long-term trends in the bromine loading of the stratosphere due to halon releases will make this requirement even stricter. It must be emphasized that this is a crude estimate, and that the determination of the average age of air within the polar vortex is a subject of ongoing research.

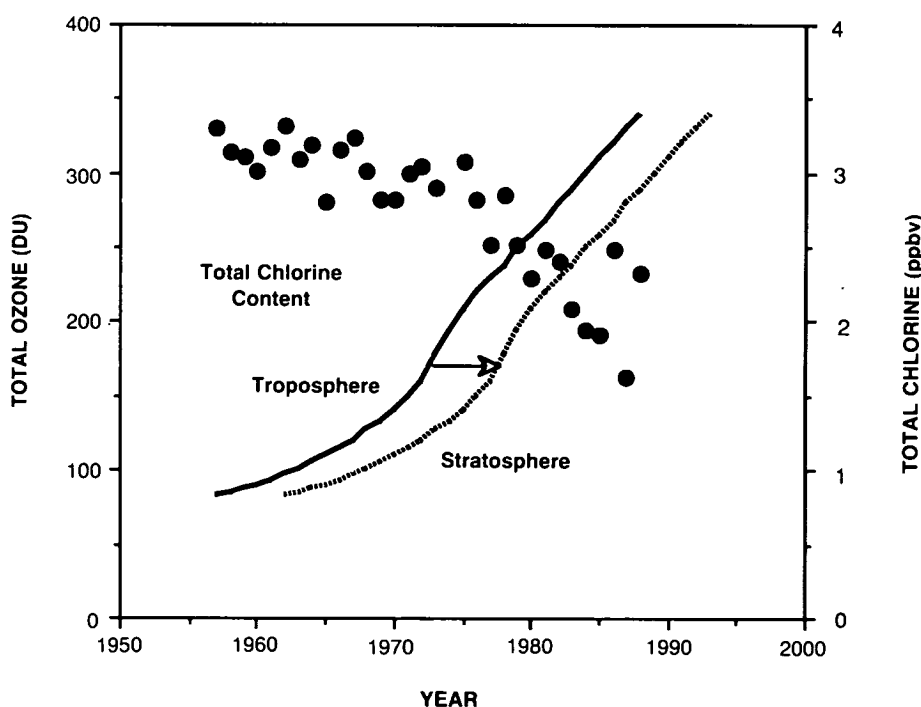


Figure 1.6.4-5. Observed October mean total ozone abundance over Halley Bay, Antarctica, along with the tropospheric total chlorine content, versus year over about the past three decades (from Farman, personal communication, 1989).

POLAR OZONE

1.7 DYNAMICAL PROCESSES

In this section, dynamical processes influencing the ozone distribution and its depletion are summarized. The climatologies of the two hemispheres are compared and contrasted in Section 1.7.1, where particular attention is paid to the observed conditions during recent observational campaigns (Antarctica in 1987 and the Arctic in 1989) as well as to the contrast between the Antarctic springs of 1987 and 1988, in which dramatically different ozone depletions were observed. The inter-annual variations in polar dynamics that appear to be related to the QBO and to the solar cycle are also described, with a view towards gaining a better understanding of their influence on measurements of trends and their cause. Synoptic scale disturbances, known to influence total ozone distributions, particularly the occurrence of mini-holes, are the subject of Section 1.7.2. In Section 1.7.3, different descriptions of the dynamics of the Antarctic vortex are presented and the notion that the vortex may behave as a processor for ozone depletion is described. Finally, Section 1.7.4 is a summary of modeling studies aimed at evaluating the possible ozone depletion effects associated with dilution of the ozone hole.

1.7.1 Differences in Climatology Between the Two Hemispheres and Their Relationship to Observed Ozone Amounts

Measurements of the seasonal and latitudinal variability of total ozone were discussed in Section 1.1, where the large differences between ozone observations made in the Northern and Southern Hemispheres were presented. Some of the chemical and meteorological factors influencing the total ozone distribution were also briefly summarized in Section 1.1. In the following section, factors influencing the transport of ozone are described in more detail, with a particular view towards understanding interannual and inter-hemispheric differences.

The rate of transport of chemical species in the stratosphere (where ozone mixing ratios are largest) is governed mainly by the intensity of planetary-scale disturbances which, in winter, propagate upward from the troposphere, where they are generated by variations in continentality and orography. In the height-latitude plane, such disturbances lead to a poleward and downward overturning of mass in the stratosphere, together with a lateral dispersion of air parcels (see Andrews et al. 1987 for an outline of basic concepts). The result is a poleward and downward transport of ozone during winter, and hence a maximum in the total column in spring.

Interhemispheric differences in total ozone (displayed in Figure 1.1.2-3) stem largely from differences in planetary-wave activity. In winter, disturbances are generally stronger and more persistent in the Northern Hemisphere than in the Southern Hemisphere so transport of ozone is more vigorous and higher values of the total column are reached at polar latitudes. In early spring, however, strong disturbances develop in the Southern Hemisphere during the so-called final warming, transporting ozone and "filling in" the polar ozone hole to some extent.

Planetary-wave activity also displays interannual variability, to which may be attributed at least some of the interannual variability found in the distribution of ozone: the stronger the wave activity, the more rapid the poleward ozone transport, and hence the higher the polar ozone amounts in spring. Such dynamical variations influence temperatures as well as ozone. The variability is especially marked in the Northern Hemisphere. Figure 1.7.1-1 gives an indication of the interannual and interhemispheric differences in lower stratospheric temperatures. For each hemisphere and for the years 1980-88, it shows the envelope of the minimum (brightness) temperatures measured around 90 mb by channel 24 of the Multiwave Sounding Unit (MSU) instrument (see Pick and Brownscombe, 1981, for details of the instrument). Horizontal lines mark

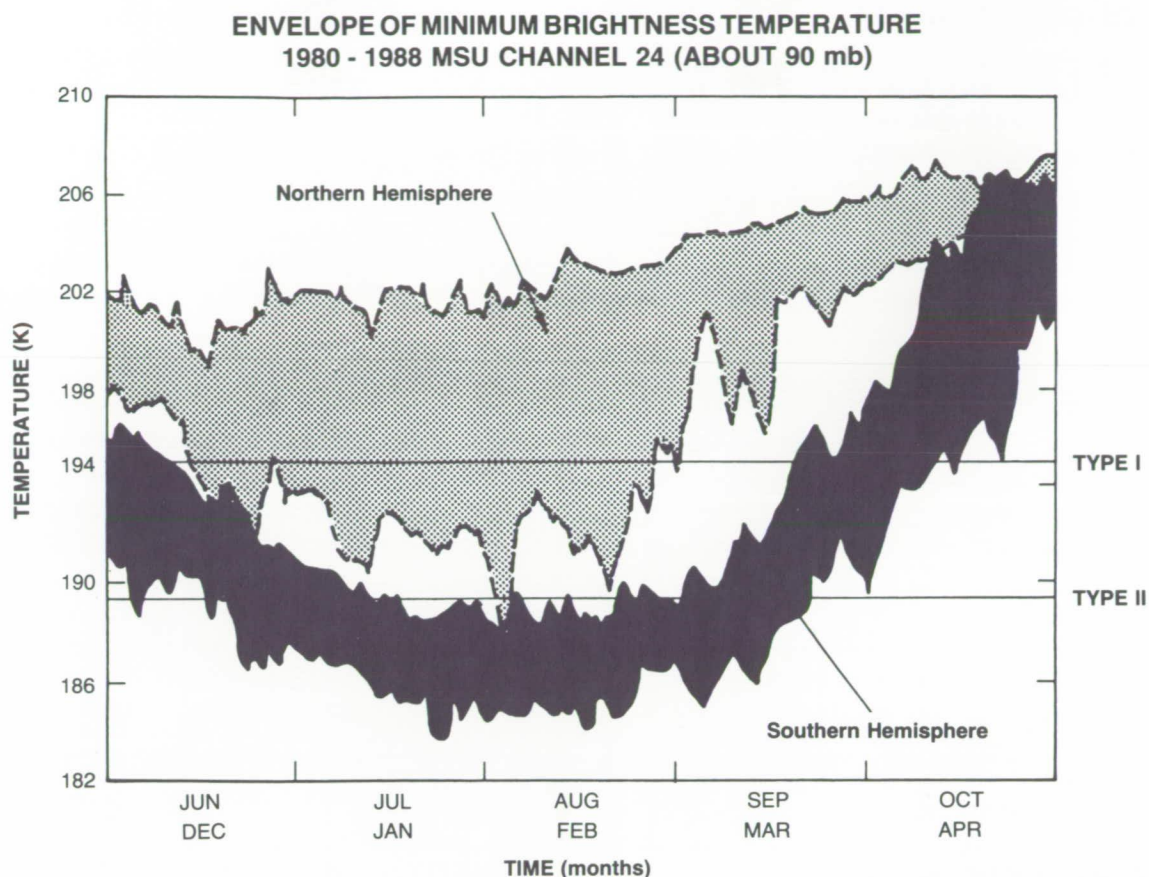


Figure 1.7.1-1 The range, near 90 mb, of minimum brightness temperatures poleward of 20° latitude (deduced from channel 24 of the MSU), computed daily for winter and spring from 1980 to 1988. The location of the minimum temperature is near the pole in winter, but moves to low latitudes during spring. Solid lines and heavy shading correspond to the Southern Hemisphere from June to October (upper labels in the time axis). Dashed lines correspond to the Northern Hemisphere from December to April (lower labels on the time axis). The horizontal lines across the figure represent the temperatures below which type I and type II PSCs can form (from Mechoso et al., 1989).

approximate threshold temperatures for the occurrence of Type 1 and Type 2 PSCs (assuming 5 ppmv H_2O and 7 ppbv HNO_3). Note that the MSU channel 24 measurements represent a weighting over the pressure range from about 200 to 30 mb, so that local temperatures may be considerably colder at some levels if sharp vertical temperature gradients prevail. Several general features can be noted in spite of the averaging. Minimum temperatures are typically 10 K or so warmer in the Northern Hemisphere than in the Southern Hemisphere, seldom falling below the required temperature for Type 2 PSCs. In the Northern Hemisphere in mid-winter, there is a 20-K spread in the minimum temperature. By contrast, in the Southern Hemisphere the minimum temperature is cold enough for Type 2 PSCs for 2 to 3 months, and there is only about a 4-K spread in the mid-winter temperature. Interannual variability is most pronounced in the Southern Hemisphere in October during the transition from winter westerlies to summer easterlies—the final warming. At the corresponding time of year in the Northern Hemisphere (April), there is less variability; the final warming has generally already happened and planetary-waves cannot propagate in the easterly winds.

POLAR OZONE

Measurements of nitrous oxide have provided important insights into the dynamics and transport in the polar regions (Heidt et al., 1989; Podolske et al., 1989). Figure 1.7.1-2 displays observations of the vertical profiles of N_2O observed in the Antarctic vortex during winter (Podolske et al., 1989; note that these values should be scaled upwards by about 9.6% due to recalibration). Summer data are also shown (Schmeltekopf et al., 1977), along with calculations from the GFDL general circulation model. The observed values in winter are far lower than the summer observations, but even the summer data lie well below the winter model predictions. Similar comparisons are found with other three-dimensional models such as the GISS model (Podolske, private communication, 1989). The greatly suppressed wintertime nitrous oxide profile is believed to result from strong downward motion within the Antarctic vortex which is not currently simulated in the model. Such downward motion clearly has important implications for ozone and nitrous oxide abundances. The data suggest that upward motion does not contribute significantly to the observed ozone decline (see Section 1.1.4). Another important finding from measurements of long-lived tracers obtained in both polar regions is the fact that the net effect of diabatic descent coupled with planetary wave disturbances leads to comparable quantities of inorganic chlorine present in the winter vortices of both hemispheres. Figure 1.7.1-3 shows the vertical distributions of the total amount of chlorine bonded in the five most abundant anthropogenic halocarbons obtained from measurements over mid- and high latitudes of both hemispheres during August and September 1987 (Heidt et al., 1989) and February 1988 (Schmidt et al., 1989). The difference between the stratospheric value and the tropospheric value is related to the amount of organic chlorine released to more reactive forms. Note the large differences in inferred available reactive chlorine between polar regions and mid-latitudes, presumably a result of descent within the vortex. The figure suggests that the amount of reactive chlorine available for chemical reactions in the lower stratospheres of both polar vortices is comparable.

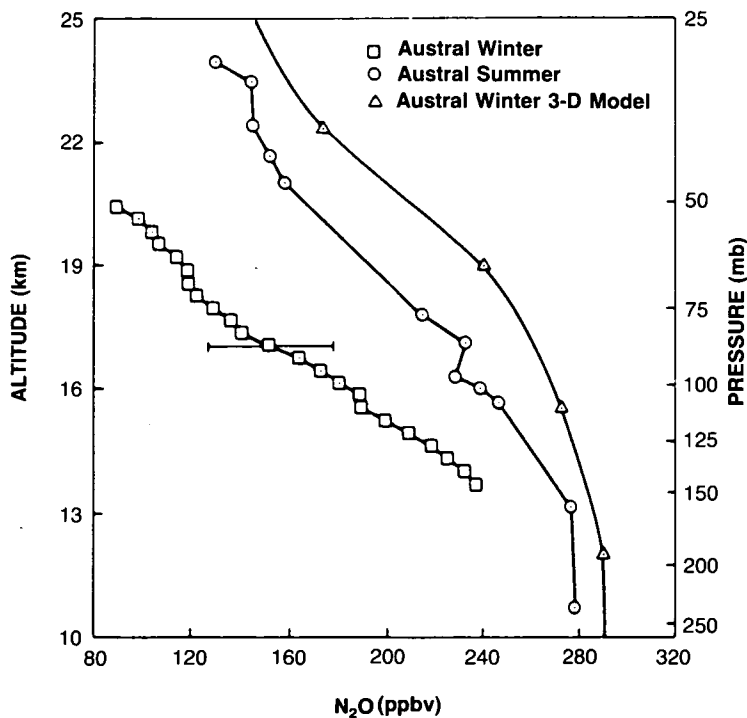


Figure 1.7.1-2. Comparison of N_2O vertical profiles during austral winter-spring from $72^\circ S$, austral summer data from $78^\circ S$ and $90^\circ S$ obtained from the NOAA data set and austral winter three-dimensional model result. Horizontal bars represent range of observed data (2-sigma) (from Podolske et al., 1989).

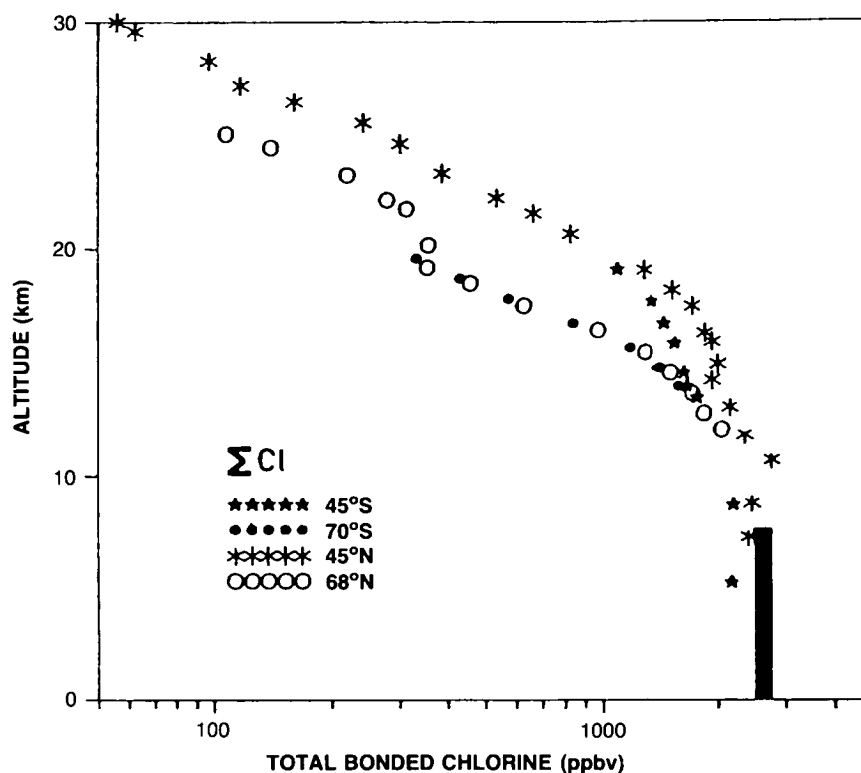


Figure 1.7.1-3. Vertical distributions of the total amount of chlorine bonded in the five most abundant anthropogenic halocarbons. The data are derived from measurements over mid- and high latitudes of both hemispheres during AAOE (Heidt et al., 1989) and CHEOPS (Schmidt et al., 1989). The corresponding tropospheric amount, calculated from the global mean mixing ratios of these species, is given by the vertical bar.

Strong downward motion within the polar vortex may also affect the time scale for exchange of stratospheric air with the troposphere and hence influence the lifetimes for all chemical species within the stratosphere. This may have important implications for calculations of the residence time of chlorofluorocarbons in the stratosphere and thus for ozone depletion potentials (see Chapter 4 of this document).

The stratosphere exhibits substantial variability on time scales longer than 1 year. A quasi-biennial oscillation is found in tropical winds, and in both tropical and extra-tropical ozone amounts (see Section 1.7.3). Longer trends, with a variety of potential causes, have also been identified (see e.g., the summary in OTP, 1989). A long-term trend in planetary-wave activity in the winter troposphere is likely to lead to a trend in the stratosphere of, say, springtime polar temperature and ozone amounts (see Mahlman and Fels, 1986, for a discussion). A putative trend in October temperatures between 1979 and 1985 over Antarctica led Newman and Schoeberl (1986) to suggest that there had been a change in circulation during the period, which may have accounted for all or part of the secular trend in total ozone over Antarctica discovered by Farman et al. (1985a). Even in the Southern Hemisphere, however, there is too much interannual variability to identify dynamical trends clearly in such a short data record (see discussion below of the year 1988). Much longer records of three-dimensional meteorological and chemical fields are needed. Newman and Randel (1988) analyzed a more extensive data set and deduced a much smaller temporal trend in October

POLAR OZONE

temperatures than that presented in Newman and Schoeberl (1986). Section 1.8 describes the observed temperature trends and their causes in much more detail.

1.7.1.1 Outline of the Climatology of the Southern Hemisphere

During the Southern Hemisphere winter, the coldest temperatures occur in the lower stratosphere over the polar region. A strong westerly vortex covers a large fraction of the Southern Hemisphere, extending through the stratosphere (Figure 1.7.1-4[i]). The vortex is nearly axisymmetric about the South Pole; planetary-scale disturbances are weak. After mid-winter, the vortex begins to weaken, at first slowly, because of the evolving field of solar radiative heating. In spring, the weakening is accelerated when planetary-scale disturbances develop. Warm air extends towards middle and high latitudes, and the vortex shrinks (Figure 1.7.1-4[ii]). Typically toward the end of September and during October, the vortex becomes highly distorted as a strong, persistent (though fluctuating) planetary-scale anticyclone develops in a preferred geographical region, 90° E–90° W (Mechoso et al., 1988, give a more detailed description). Warm air extends towards middle and high latitudes, and the vortex shrinks quickly. Finally, it breaks down, first in the upper stratosphere, and then later (and more slowly) in the middle stratosphere (Figure 1.7.1-4[iii]). As the vortex breaks down during this so-called final warming, warm, ozone-rich air spreads from low latitudes over the polar cap. Notice, however, that in the lower stratosphere a remnant of the cold core of the vortex lasts throughout October and generally through November. The maximum in the total column of ozone is held off the pole (Figure 1.1.2-3).

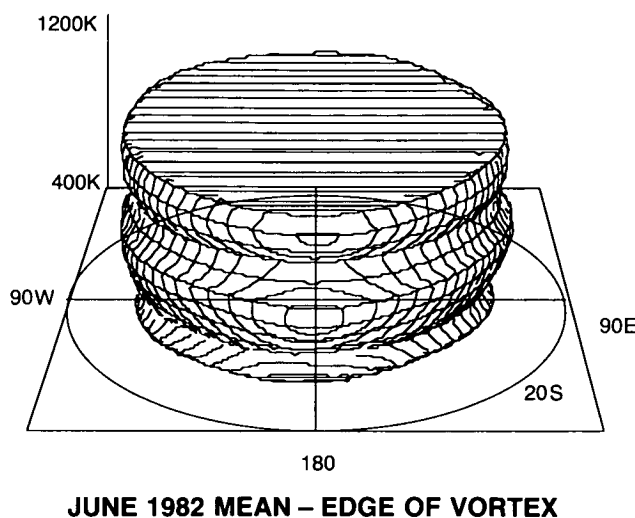


Figure 1.7.1-4(i). Monthly mean perspectives during June 1982 of the three-dimensional structure of the westerly vortex in the Southern Hemisphere from the lower stratosphere (potential temperature surface of 400 K) to the upper stratosphere (potential temperature surface of 1200 K). The edge of the vortex marks the transition from large meridional gradients of potential vorticity at high latitudes to weak gradients at low latitudes, and lies in the transition zone from strong westerly winds at high latitudes to weak westerly or easterly winds at low latitudes. The evolution shown for 1982 is typical of final warmings in the period 1979-1986 (see Mechoso et al., 1988, Figure 13), though the strength of planetary-scale disturbances does vary from year to year.

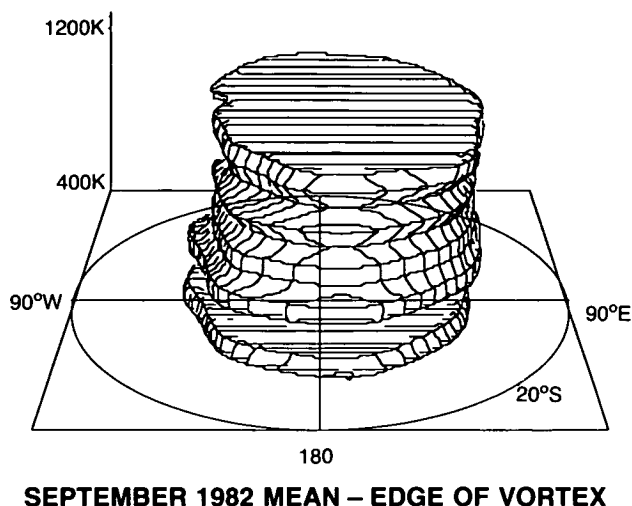


Figure 1.7.1-4(ii). As in Figure 1.7.1-4(i), but for September.

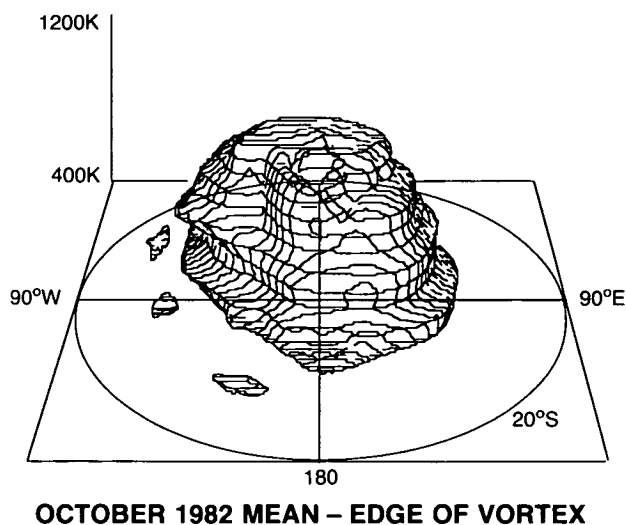


Figure 1.7.1-4(iii). As in Figure 1.7.1-4(i), but for October.

1.7.1.2 Outline of the Climatology of the Northern Hemisphere

The mid-winter circulation of the stratosphere of the Northern Hemisphere is seldom quiescent. Frequent minor warmings occur as planetary-scale disturbances grow and decay. Synoptically, these warmings generally involve (1) an intensification of a climatological anticyclone in the stratosphere (called the Aleutian High), (2) a displacement of the polar vortex over Europe, and (3) a rapid warming of air at polar latitudes where air sinks (and warms adiabatically) at the jet entrance between the anticyclone and the westerly vortex. During some winters, there are major stratospheric warmings: the disturbances are so strong that the normal circumpolar westerly flow is completely broken down, to be replaced by easterlies (in the zonal mean) through a large depth of the stratosphere. Synoptically, the warmings involve the development of either one anticyclone (usually the Aleutian High), when the westerly vortex is displaced

POLAR OZONE

from the pole (see O'Neill and Taylor, 1979), or of a pair of anticyclones, when the vortex splits (see Fairlie and O'Neill, 1988). Air from low latitudes spreads over the polar cap. Polar temperatures rise sharply, often by more than 50 K in a few days. Although rapid radiative cooling in the upper stratosphere can re-establish the westerly flow in a week or two, the longer radiative relaxation times for the lower stratosphere and the persistence of strong disturbances in the upper troposphere may mean that the westerly flow remains weak and polar temperatures high for the rest of the winter and spring. This vertical structure is in marked contrast to the top-down weakening of the westerly vortex in the Southern Hemisphere.

Final warmings in the Northern Hemisphere show much more interannual variability than in the Southern Hemisphere (Yamazaki, 1987), both in the structure of the flow and in the timing of the final breakdown of the westerly vortex (See Figure 1.7.1-5). During some examples, the circulation is highly distorted in the presence of a persistent Aleutian High. The breakdown of the westerlies may happen first in the upper stratosphere, as it does in the Southern Hemisphere, or in the lower stratosphere (in Figure 1.7.1-5, the temperature gradient reversal may precede or succeed the wind reversal). Generally, the breakdown of the westerly vortex is almost complete in the stratosphere; ozone-rich air can spread to higher latitudes in spring than in the Southern Hemisphere (Figure 1.1.2-3). Curiously, some final warmings in the Northern Hemisphere (e.g., that of 1981) are quiescent. The weakening of the westerly vortex proceeds slowly, on a radiative time scale, leading to a late final warming. This may happen after the vortex

TIMING OF FINAL WARMING

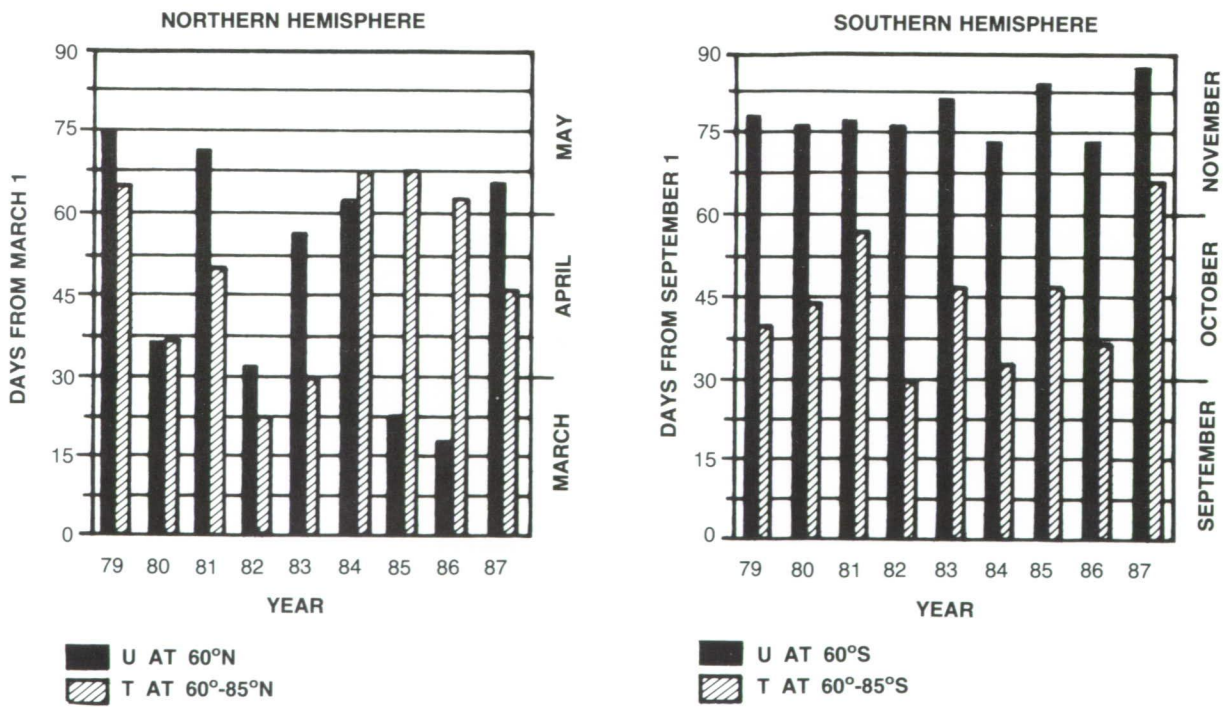


Figure 1.7.1-5. Time of the reversal, at 10 mb, of the zonal wind at latitude 60°, and of the temperature difference between 60° and 85° for the Northern and Southern Hemispheres. Zonal wind is solid; temperature difference is hatched.

has been largely broken down during an earlier major warming (as in 1981). Planetary-scale disturbances of tropospheric origin cannot then penetrate into the stratosphere.

The Southern Hemisphere stratosphere during 1987 and 1988

Total ozone amounts

Knowledge of the circulation in the Southern Hemisphere during 1987 is necessary for a full interpretation of the observations made during an international scientific campaign (the Antarctic Airborne Ozone Experiment) to study the springtime ozone depletion over Antarctica. That year, the ozone hole was the deepest yet recorded (Krueger et al., 1988). The year 1988 is of particular interest because springtime ozone depletion was markedly less pronounced than during the previous several years, and it is important to know whether this presages a long-term recovery of springtime ozone values, or whether 1988 was an unusual year because of natural interannual variability.

Figure 1.7.1-6 shows that there were large differences between 1987 and 1988 in the evolution of total ozone in the Southern Hemisphere, particularly at high latitudes. In 1987, the polar ozone hole was deep, with total ozone amounts falling below 150 DU in October. Polar ozone was eventually replenished, but not until late in the year; the ozone column did not reach 300 DU near the pole until late November. In contrast, in 1988 the ozone hole was not as deep (the ozone column remained above about 200 DU), and the ozone column reached 300 DU near the pole by the end of October. By November, the polar ozone column exceeded that in 1987 by over 200 DU.

As discussed below, the elevated ozone amounts in 1988 are unlikely to signify a long-term recovery of springtime polar ozone in the Southern Hemisphere. It appears that differences in ozone amounts between 1987 and 1988 can be attributed qualitatively to natural variability in the atmospheric circulation, which happens to have mitigated the destruction of ozone to some extent in 1988. In brief, the stratospheric polar vortex was warmer and more disrupted by strong disturbances in 1988 than in 1987. PSCs, and hence heterogeneous chemistry, presumably operated on a smaller volume of air, leading to less ozone depletion. Greater transport into polar latitudes replenished faster the already shallower ozone hole. The following discussion will focus on the lower stratosphere, since processes there have the most effect on the total column of ozone.

Figure 1.7.1-7 shows, for winter and spring 1987 in the Southern Hemisphere, the variation of minimum temperature near 90 mb, as determined from channel 24 of the MSU instrument. Figure 1.7.1-8 shows the fraction of the area of the Southern Hemisphere where temperatures were less than 193 K, a representative value for PSCs to form (ignoring, for simplicity, the distinction between Type 1 and Type 2 PSCs). Solid curves mark the envelope of such curves in the 9-year set, 1980–1988; the vertical separation of these bounding curves represents the inter-annual variability of minimum temperature or area. These figures show that, for most of winter and spring, minimum temperatures in 1987 were low, and that the area where lower stratospheric temperatures were below 193 K was the greatest in the 9-year set. The low temperatures probably result, at least in part, from the decreased solar heating associated with the record minimum in ozone amounts (Shine, 1986; Kiehl et al., 1988) as discussed in Section 1.8. Minimum temperatures rose above 193 K in early October, when PSCs should have mostly disappeared.

Figures 1.7.1-9 and 1.7.1-10 show the corresponding figures for 1988. At the end of August, minimum temperatures rose to their highest values in the 9-year set, and the area below 193 K to its lowest value. By the time sunlight returned to polar regions in September, the chemical make-up of polar air was

POLAR OZONE

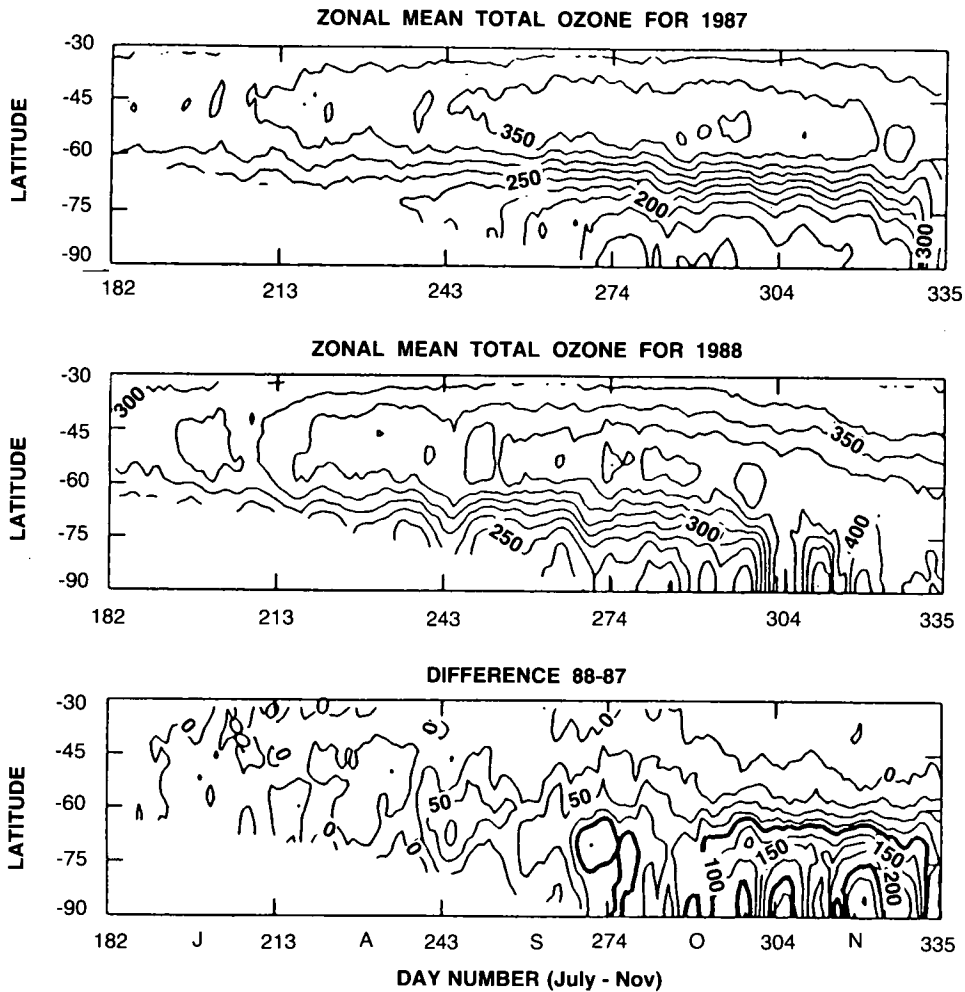


Figure 1.7.1-6. Evolution of zonal-mean total ozone (Dobson units) derived from the TOMS instruments during 1987 and 1988, and of the difference between these two years. Courtesy of M.R. Schoeberl and P.A. Newman.

presumably less anomalous in 1988 than in 1987. Consequently, the decline rate of the total column of ozone was less in 1988.

A slower rate of decline of ozone in 1988 compared with 1987 was followed by an earlier rise in ozone amounts. An explanation for this requires a detailed comparison of the circulations and photochemistry during the 2 years.

The circulation

Figure 1.7.1-11 is the map of Ertel's potential vorticity P and winds on the 500-K isentropic surface near 40 mb in the lower stratosphere for 1 August 1987 (the absolute value of P is plotted). (See Hoskins et al., 1985 for a discussion of the dynamical significance of the quantity P and of its use in interpreting meteorological phenomena.) A strong cyclone coincides with the high values of P over the polar cap. The strong gradients of P marked by the shaded ring resist displacements of air parcels by planetary-scale

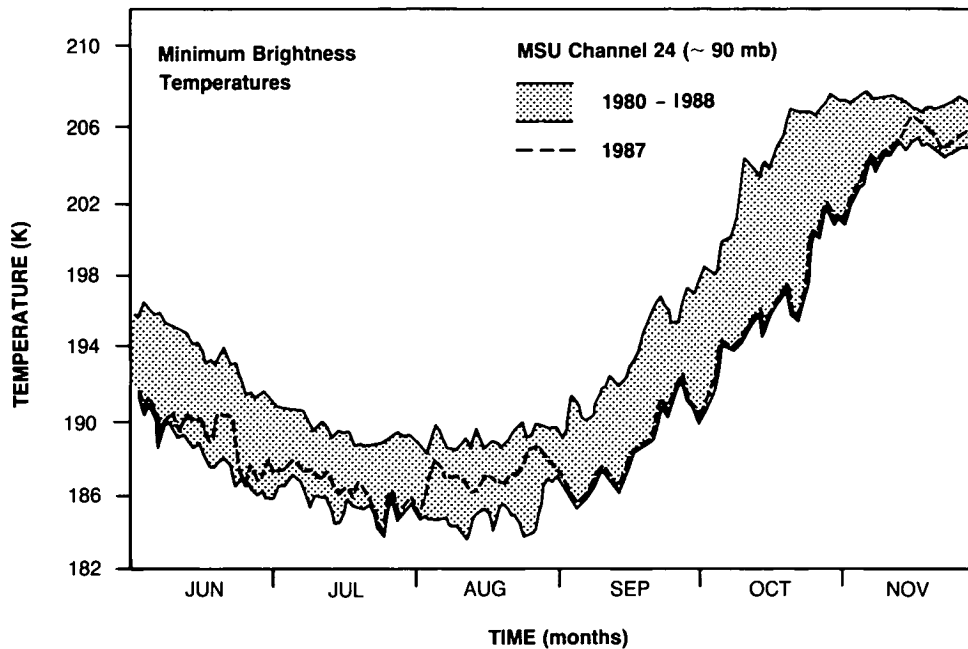


Figure 1.7.1-7. Minimum brightness temperature near 90 mb (derived from channel 24 of the MSU instrument) in the Southern Hemisphere during 1987 (dashed).

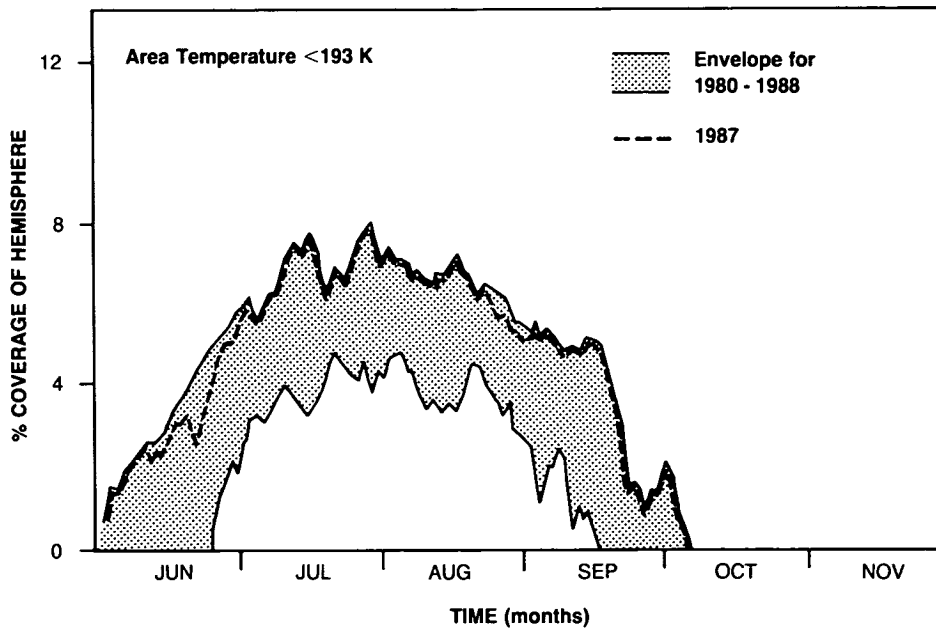


Figure 1.7.1-8. The fractional area (expressed as a percentage) of the Southern Hemisphere over which minimum temperatures near 90 mb in 1987 fell below 193 K, roughly the threshold temperature for formation of polar stratospheric clouds (neglecting the distinction between types of PSC). Solid curves show the envelopes of temperature and area curves for the years 1980-1988.

POLAR OZONE

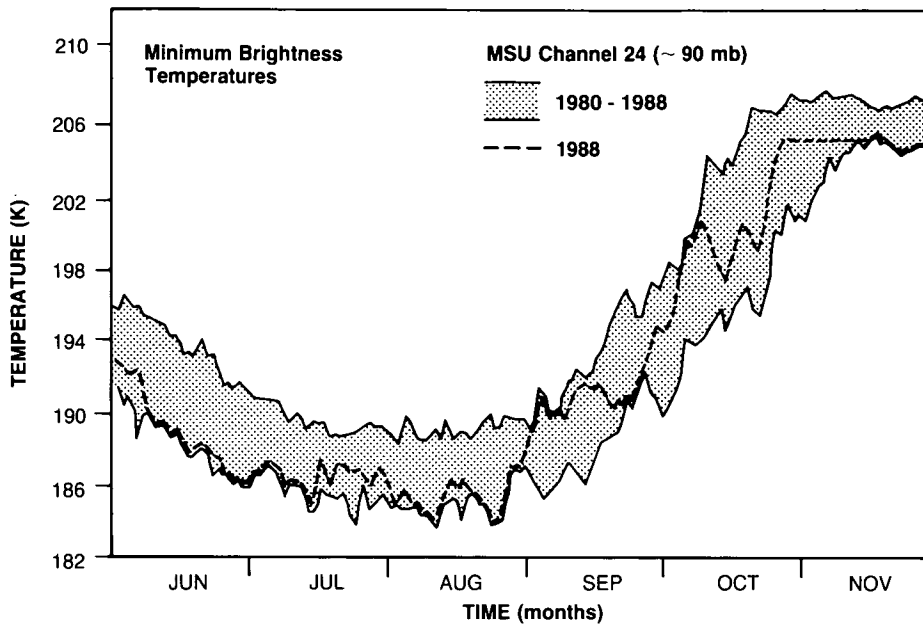


Figure 1.7.1-9. As for Figure 1.7.1-7 but for 1988.

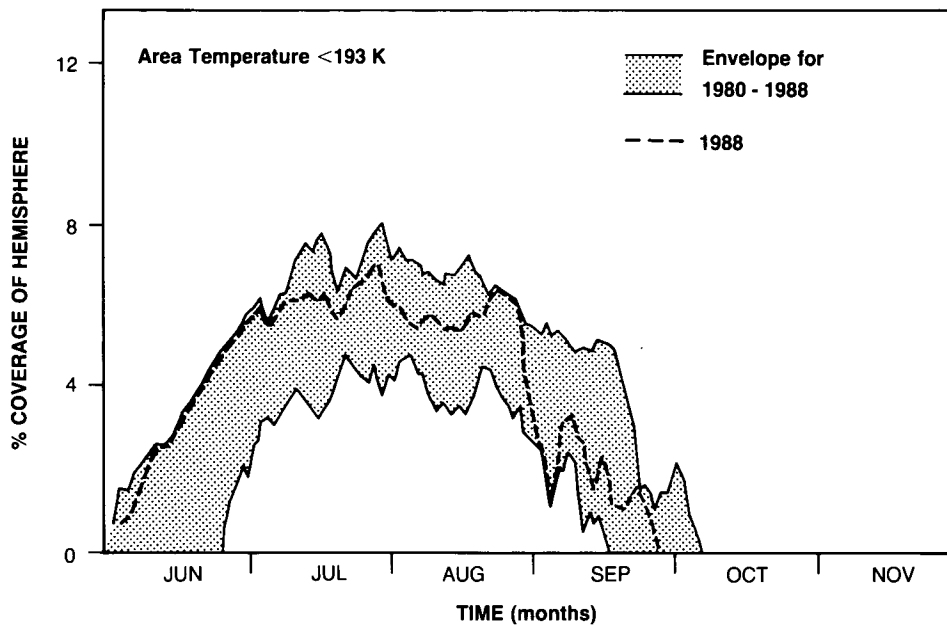


Figure 1.7.1-10. As for Figure 1.7.1-8 but for 1988.

disturbances, and little meridional transport of ozone or other trace chemicals into polar latitudes can occur while strong gradients in the vortex persist. Apart from any slow drift of air parcels due to radiative cooling, air well within the vortex forms an isolated air mass (Jukes and McIntyre, 1987; see also the discussion in Section 1.7.3).

As noted above, planetary-scale disturbances in the stratosphere can accelerate the weakening of the westerly vortex, especially in spring. In terms of the distribution of P , the vortex is broken down as its high- P air is drawn away to lower latitudes around developing anticyclones (see McIntyre and Palmer, 1983). As the vortex shrinks, air can migrate poleward. In addition, disturbances raise the temperature of the air in the vortex, especially near its outside edge. Here, air sinks and warms adiabatically at the entrances to localized jet streams between the westerly vortex and regions of anticyclonic circulation. One would infer that radiative cooling causes air parcels to spiral into the vortex and downward, effecting a corresponding transport of ozone and other trace chemicals. (Note that this picture lacks reliable quantitative details; see Section 1.7.3.)

In winter and spring 1987, however, disturbances to the stratospheric flow were comparatively weak and vortex erosion slow (see also Randel, 1988). Figure 1.7.1-12 shows that by the end of October a strong vortex, associated with strong gradients of P , remained in the lower stratosphere. The maps suggest that, apart from the slow transport due to radiation, the large area of the vortex inside the shaded ring was isolated during winter. In this cold region, heterogeneous reactions in the large volume of air occupied by PSCs could chemically precondition the air for rapid ozone destruction when sunlight returned to polar latitudes.

Figure 1.7.1-13 shows that in early August 1988 the westerly vortex in the lower stratosphere was as strong as in early August 1987. Thereafter, and unlike 1987, the circulation throughout the stratosphere in the Southern Hemisphere was strongly disrupted by planetary-scale disturbances (Kanzawa and

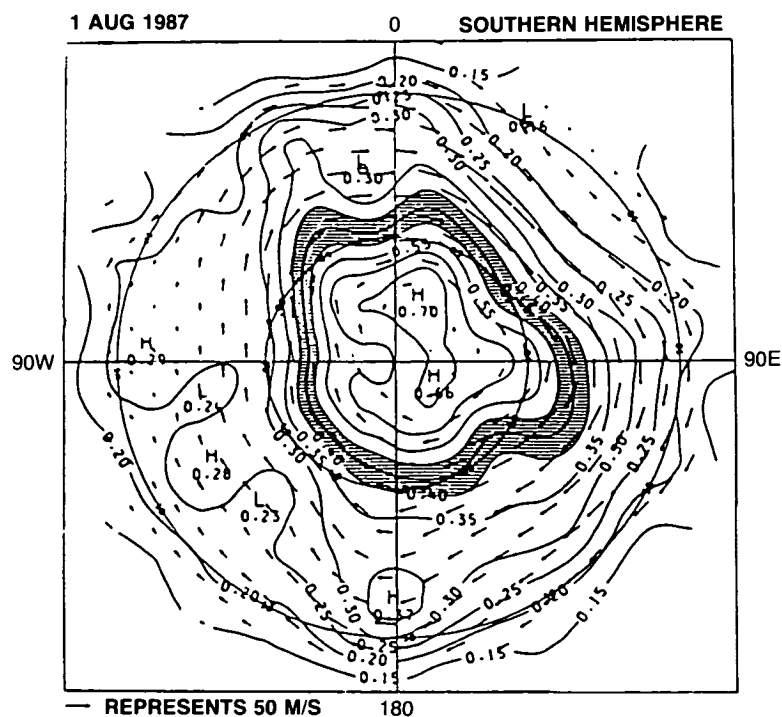


Figure 1.7.1-11. Isentropic maps of Ertel's potential vorticity (units: $10^{-4} \text{ Km}^2 \text{ kg}^{-1}$) and winds on the 500 K isentropic surface in the Southern Hemisphere on 1 August 1987. The wind speed may be deduced by using the scaling arrow at the bottom left.

Kawaguchi, 1989). The vortex was displaced from the pole and broken down as it was progressively stripped of its high-P air. In the process, air from lower latitudes migrated polewards. Radiative cooling in the vortex would have contributed to the migration of air parcels into it. By the end of October 1988, only a small remnant of the vortex remained in the lower stratosphere, as shown in Figure 1.7.1-14.

In summary, the following seems the likely explanation for elevated polar ozone amounts in the Southern Hemisphere during spring 1988. There was a comparatively early breakdown of the westerly vortex in the stratosphere of the Southern Hemisphere and an early rise in temperature of most of the air in the vortex above threshold values for the occurrence of PSCs. As the vortex broke down, the ozone-destroying chain of chemical reactions was presumably quenched (1) as PSCs evaporated, bringing heterogeneous reactions to a stop, and (2) as NO_x was transported into polar regions, locking up chlorine radicals in less reactive "reservoir" compounds. The early breakdown of the vortex was also clearly accompanied by poleward transport of ozone-rich air and an early recovery of the total ozone column.

In 1988, natural processes happened to ameliorate, to some extent, the destruction of ozone by man-made pollutants. In view of the importance of heterogeneous chemistry in perturbing chlorine abundances (see Sections 1.3 and 1.6), and the strong dependence of PSC formation on temperature (Section 1.2), it would be surprising if years such as 1987 and 1988 did not exhibit dramatically different ozone depletions.

The Northern Hemisphere winter of 1988/89

During the Northern Hemisphere winter of 1988/89, several measurement campaigns were conducted in Arctic regions (see Section 1.10.2). The goal of those studies was to determine whether the anomalous chemical and meteorological conditions found to favor ozone destruction over Antarctica were also present

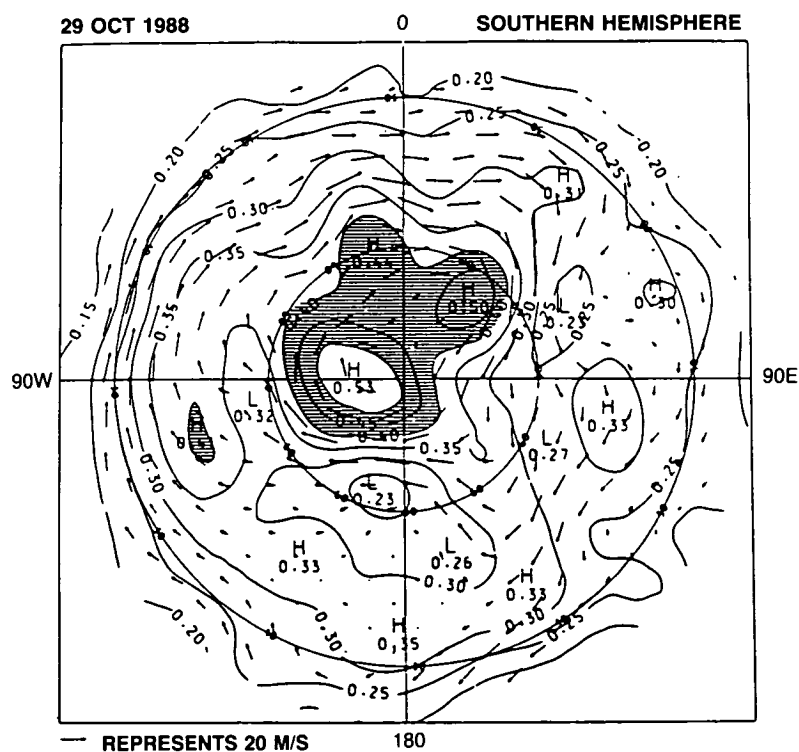


Figure 1.7.1-14. As in Figure 1.7.1-11, but on 29 October 1988.

POLAR OZONE

over the Arctic. In the following, we discuss briefly the dynamical conditions that prevailed in the 1988/89 Northern Hemisphere winter.

The meteorological conditions found during 1988/89 cannot be taken as fully representative of the winter stratosphere in the Northern Hemisphere (indeed, there is so much interannual variability that no one year can be taken as truly representative). January 1989 was the coldest January, at 30 mb in 25 years. Kuhlbarsch and Naujokat (1989) found temperatures as low as 181 K at 30 mb. Associated with these record low temperatures was a strong westerly vortex over the polar cap, as shown in Figure 1.7.1-15.

There followed a dramatic major warming. In the first half of February, temperatures rose sharply through the whole depth of the stratosphere at polar latitudes as a strong planetary-scale disturbance developed (see Fairlie et al., 1989, for details). The westerly vortex elongated as two anticyclones developed, first one over the Pacific and then one over the Atlantic. By mid-February, the vortex was split into two distinct centers of cyclonic circulation (Figure 1.7.1-16). This split extended through most of the stratosphere (the split was incomplete near 100 mb). In the lower stratosphere, the two cyclonic vortices continued to weaken during March. Gradients of potential vorticity were weak at middle and high latitudes; large meanders in the weak flow brought air from subtropical to polar latitudes.

Figure 1.7.1-17 shows the evolution during 1988/89 of the minimum temperature in the lower stratosphere (dashed curve), as derived from channel 24 of an MSU. The shaded region defines an envelope of such curves for the years 1980 through winter 1989. At the end of January, the minimum temperature fell

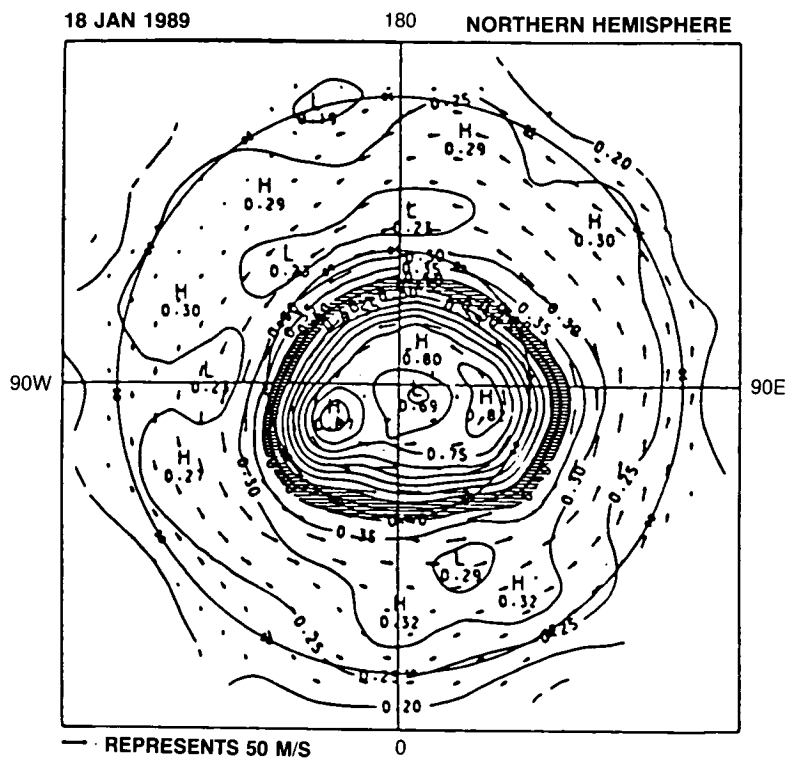


Figure 1.7.1-15. As for Figure 1.7.1-11, but for the Northern Hemisphere on 18 January 1989.

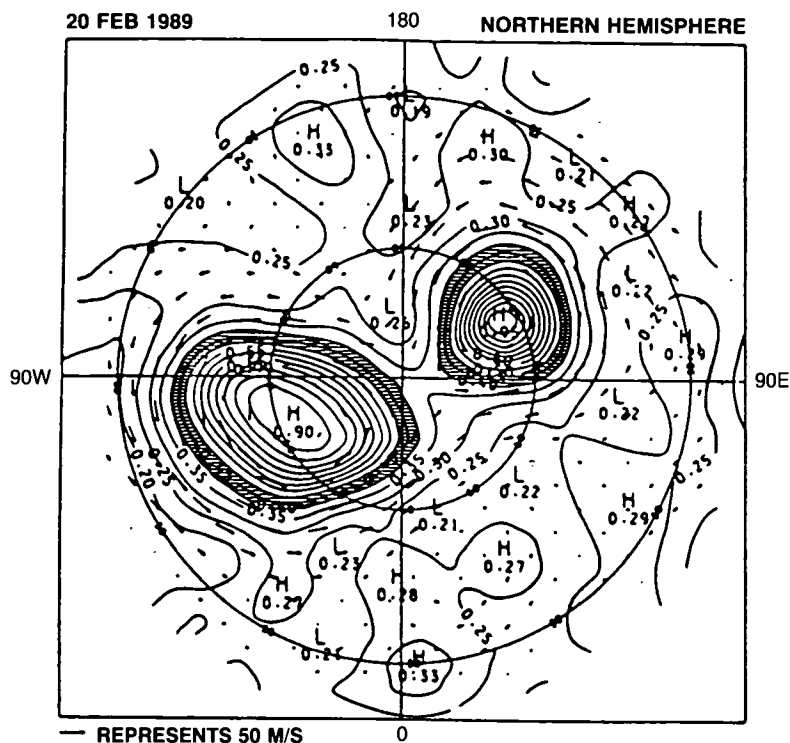


Figure 1.7.1-16. As for Figure 1.7.1-11, but for the Northern Hemisphere on 20 February 1989.

to 190 K, cold enough (less than about 195 K) for Type 1 PSCs to form at these levels, and even for Type 2 PSCs (according to calculations based on the laboratory measurements of Hanson and Mauersberger 1988a,b). MSU temperatures imply that PSCs have covered the polar cap north of about 75° N for about 10 days in mid-January (the presence of local pockets of PSCs farther south is not excluded by the measurements, owing to their limited resolution). Using measurements from the SAM II instrument on board the satellite Nimbus-7 (see McCormick et al., 1979 for details of the instrument), McCormick and Poole (personal communication) inferred the presence of large quantities of PSCs, including Type 2 PSCs, as far south as 50° N in January and early February. Figure 1.7.1-17 shows that, in early February, minimum temperatures rose rapidly above 195 K; SAM II measurements indicate that PSCs disappeared almost everywhere (McCormick and Poole, personal communication).

The MSU temperatures indicate that the area affected by PSCs over the Arctic in winter 1989 was much smaller than over the Antarctic. Taking 193 K as a representative temperature for PSC occurrence (ignoring the distinction between Type 1 and Type 2 PSCs), one infers that the areal coverage is at most one third of that over the Antarctic (although we note that the Antarctic coverage will be overestimated if denitrification or dehydration takes place, altering the abundance of condensables and hence the threshold temperature for PSCs). The duration of PSC activity is much shorter in the Northern as compared with the Southern Hemisphere—the figure of one third applies to a few weeks at most. So far, there have been no reports of dramatic ozone reduction during spring in the Northern Hemisphere (see Section 1.1.6). Note, however, that the MSU measurements span only about 10 years.

POLAR OZONE

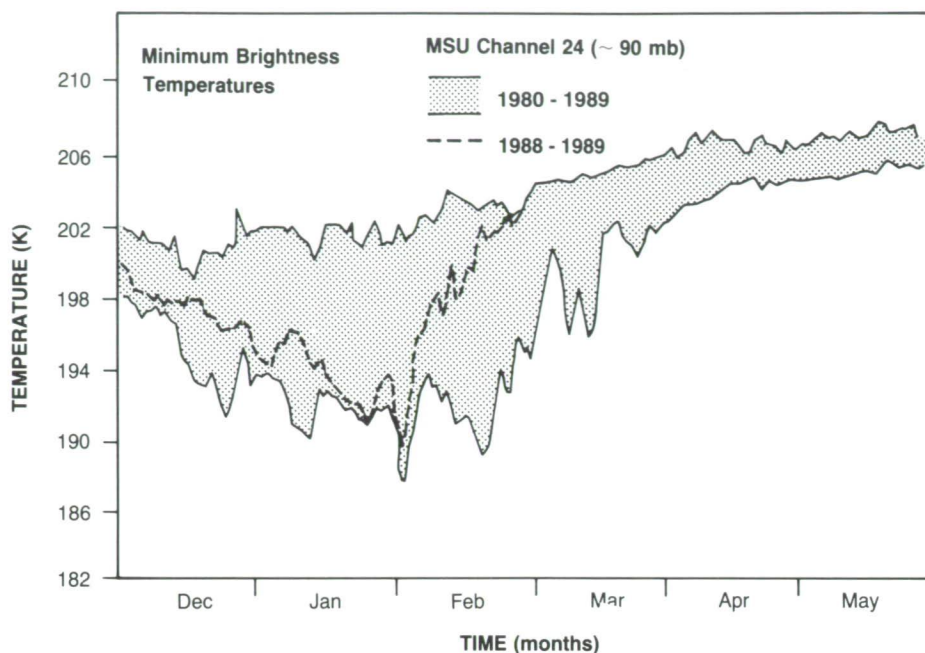


Figure 1.7.1-17. Minimum brightness temperature derived from channel 24 of the MSU (centered near 90 mb) in the Northern Hemisphere for December through May. The dashed curve is for 1988-1989; the full lines form the envelope of such curves for the years 1980 through winter 1989.

1.7.1.3 Effects of the Quasi-Biennial Oscillation and the Solar Cycle

The quasi-biennial oscillation (QBO)

As discussed briefly in Section 1.1, there is evidence that the quasi-biennial oscillation (QBO) in stratospheric tropical winds is linked with QBO oscillations in temperatures, geopotential heights, and total ozone abundances not only in the tropics but at extra-tropical latitudes as well. Observed QBO signals in total ozone and the dynamical factors that influence it will be discussed in more detail in this section. Angell and Korshover (1962, 1964, 1967) detected a quasi-biennial oscillation in temperature at middle and high latitudes of both hemispheres, while Holton and Tan (1980, 1982) and van Loon and Labitzke (1987) found that the winter westerly vortex in the lower stratosphere was weaker during the easterly phase of the QBO. The QBO variability of extra-tropical ozone was recorded by Angell and Korshover (1964, 1967, 1973, 1978), who found that (1) total ozone amounts tended to be low (high) during the westerly (easterly) phase of the QBO; (2) this variation was out of phase with that in the tropics, where ozone amounts vary in phase with the wind; and (3) total ozone changed by about 4% (about 12 Dobson units) between extremes of the QBO. Oltmans and London (1982) and Hasebe (1983) confirmed these findings, as do the recent results derived from the TOMS instrument by Lait et al. (1989), which are shown in Figures 1.7.1-18 and 1.7.1-19. The QBO in total ozone at high latitudes must be allowed for in an explanation of the increasing depletion of ozone in the southern polar spring in the 1980s (Bojkov, 1986; Garcia and Solomon, 1987).

The means by which the tropical QBO is communicated to extra-tropical latitudes is not fully understood. The tropical zonal wind QBO is believed to be driven by the interaction of upward-propagating,

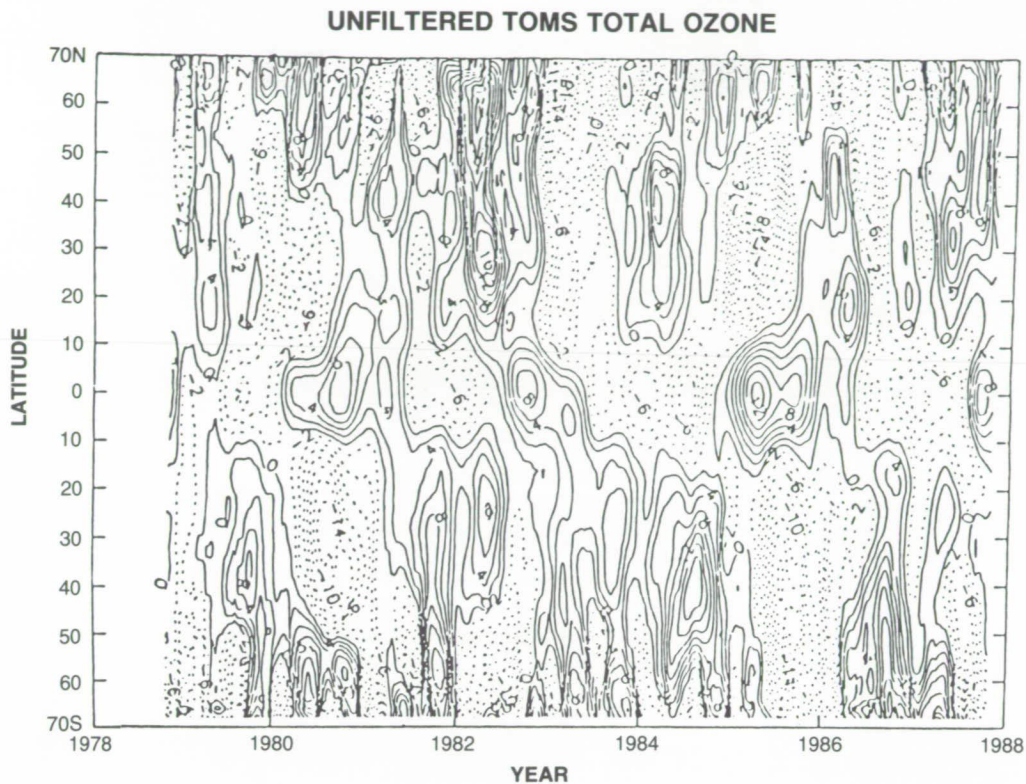


Figure 1.7.1-18. The total ozone fields (in Dobson units) from November 1978 to October 1987 with annual cycle removed.

large-scale tropical waves with the zonal-mean flow. Associated with this forcing is a secondary circulation, which gives rise to a QBO in total ozone and temperature in the tropics, and an oscillation of opposite phase in the subtropics (Plumb and Bell, 1982; Plumb, 1984; Gray and Pyle, 1989). Calculations suggest that this circulation can extend only up to about 15° of latitude from the center of the wave forcing. However, the interaction of this circulation with the global mean circulation may further extend its influence (Gray and Pyle, 1989). Further poleward influence of the QBO may result from a modulation of extratropical planetary-wave activity during winter (Holton and Tan, 1982). These waves can propagate upwards from the troposphere only when winds are westerly. During the easterly phase of the QBO wave activity would be more confined than during the westerly phase, and greater polar warming and poleward transport of ozone would be expected. Evidence for such effects has been given by Labitzke (1982). However, in the first two-dimensional modeling study of the ozone QBO, Gray and Pyle (1989) achieved a realistic latitudinal distribution of the ozone QBO signal without the latter effect, suggesting that it may not represent the dominant mechanism for the ozone QBO.

Concerning the Antarctic ozone hole, Bojkov (1986) first noted an apparent correspondence of the QBO with year-to-year changes in minimum total ozone amounts. Garcia and Solomon (1987) studied variations in total ozone and temperature minima for the October months of 1979–1986, and found that low (high) ozone and temperature were apparently associated with the westerly (easterly) phase of the tropical QBO at 50 mb. Recently, however, Lait et al. (1989) have pointed out that this simple correlation becomes seriously degraded when observations for 1986 are examined carefully and when an extra year, 1987, is included in the series.

POLAR OZONE

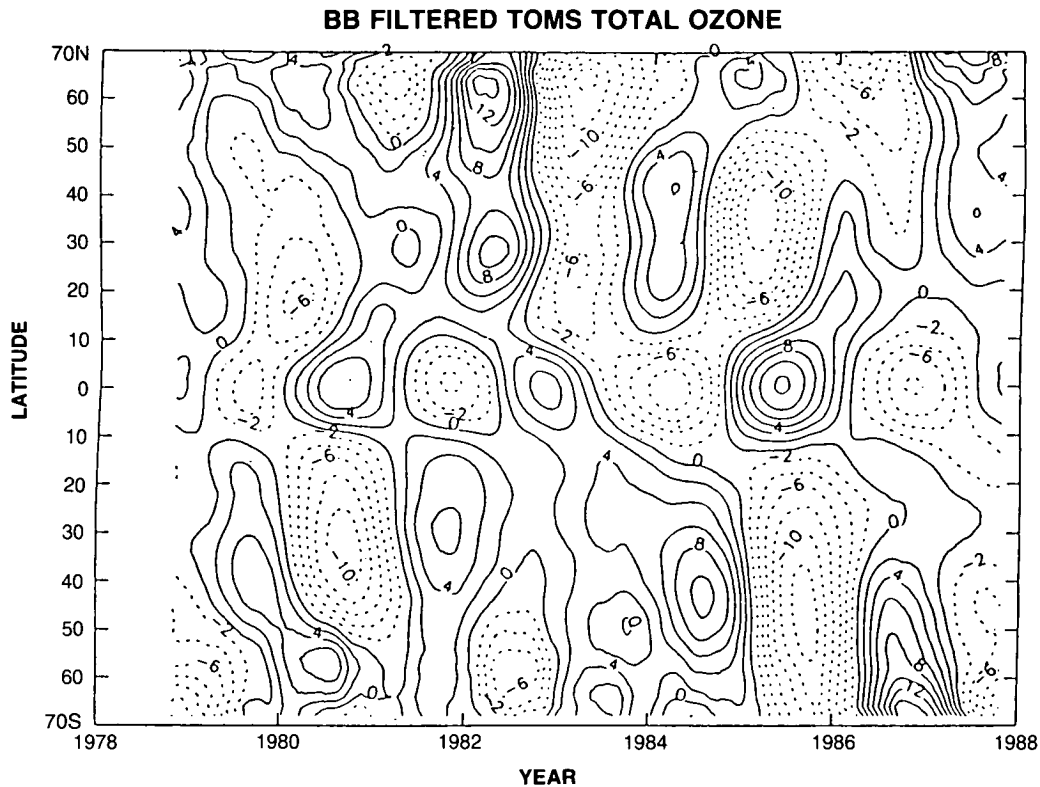


Figure 1.7.1-19. As in Figure 1.7.1-18, but after application of a broad-band filter (taken from Lait et al., 1989).

Figures 1.7.1-20 and 1.7.1-21 show the year-to-year variations over the South and North Poles in October-mean and (correspondingly) April-mean total ozone amounts and 70-mb temperatures for 1979–1988 (note the scale change for ozone between the two hemispheres). Also indicated is the phase of the tropical QBO in 50-mb winds over Singapore for the appropriate month. In the Northern Hemisphere, there is no clear evidence of a correlation between the tropical winds and parameter values at the pole. In the Southern Hemisphere, on the other hand, there appears to be a quasi-biennial modulation of the time series of temperatures and ozone amounts from 1979 through 1985, with minor peaks in temperature and ozone amounts coinciding with the easterly phase of the tropical QBO, and troughs with the westerly phase. In 1986, however, this apparent correlation breaks down if only 50-mb winds are considered: peaks in temperature and ozone coincide with a westerly rather than easterly phase at the 50-mb level. The lowest values of temperature and total ozone occur in 1987. These minima do coincide with the (monthly-mean) westerly phase of the tropical QBO, but winds reversed from easterly to westerly only in October; throughout the austral winter of 1987 tropical winds at 50 mb were easterly. Therefore, it may be fortuitous that the apparent correlation holds up in 1987. In 1988, ozone amounts are about 100 DU higher and 70-mb temperatures almost 20 K warmer in October 1988 than in October 1987, whereas QBO-related increases of no more than about 20 DU and 5 K might have been anticipated from previous years. This discrepancy might be attributable to interannual variability not directly related to the tropical QBO, or it might indicate that different parameters from those used in the figure should be used to establish a more robust correlation.

According to Lait et al. (1989), a much better QBO correlation between tropical winds and polar ozone can be exposed for the Southern Hemisphere by using as a variable the decline rate in September of the minimum value of total ozone (they use the map minimum value of total ozone south of 30°S on daily

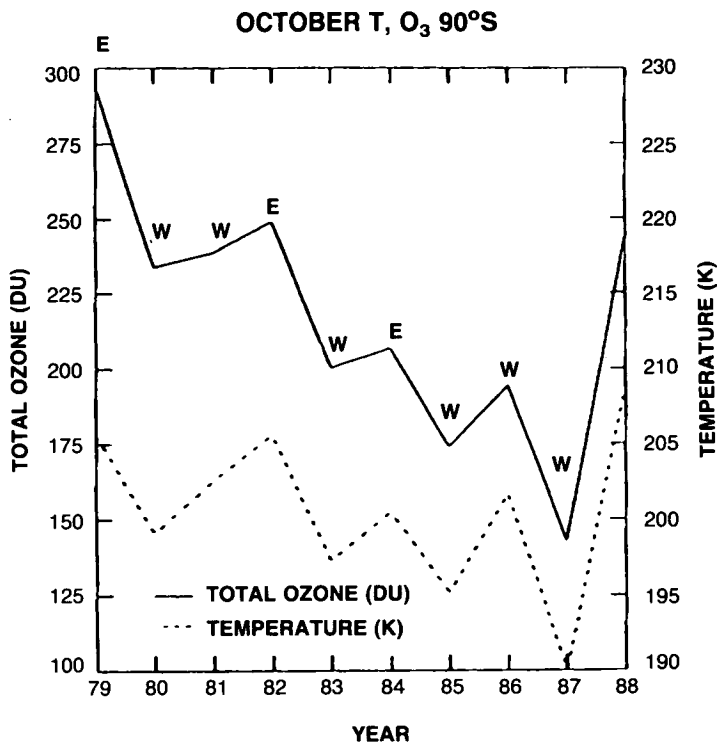


Figure 1.7.1-20. Variation in October mean total ozone and 70 mb temperature over the South Pole. Letters W and E denote the west and east phases of equatorial winds at 50 mb over Singapore.

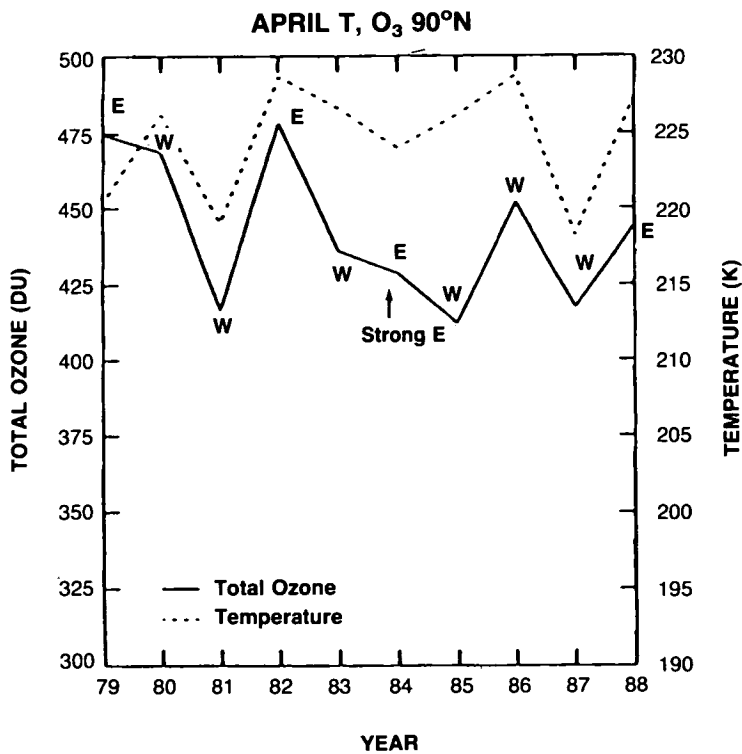


Figure 1.7.1-21. As in Figure 1.7.1-20, but for the April mean in the Northern Hemisphere.

POLAR OZONE

fields derived from the TOMS instrument). This seems reasonable in that any extra-tropical effect of the tropical QBO would presumably modulate the chemical and dynamical processes controlling ozone amounts, and hence the time rate of change of ozone. They found that the correlation is better when tropical winds at 30 mb instead of 50 mb are used. (Why this should be so is not known.) Their results are shown in Figure 1.7.1-22. There appears to be a high degree of correlation between 30-mb tropical winds and the September decline rate of the polar minimum in total ozone (and also between the winds and equatorial total ozone).

It is worthy of note that the QBO oscillation in tropical winds is not coherent at all levels; rather, tropical winds reverse direction first at higher altitudes and progress downwards. In some QBO cycles, the progression below 30 mb can lag considerably that of higher levels (as shown, for example, in Naujokat, 1986). This suggests that a fuller understanding of the correlation between tropical winds and the extra-tropical response may be rather sensitive to the altitude chosen for the correlation, and requires a better understanding of the causal mechanism (especially any relevant time lags) before the appropriate parameters for correlation can be identified. It is particularly important for causal mechanisms to explain the observed discrepancy between the period of the ozone QBO at the Equator (approximately 27 months, corresponding to the period of the zonal wind QBO there) and at higher latitudes, where the period is closer to 2 years. These observations have suggested a strong interaction of the polar ozone QBO with the annual cycle (Gray and Pyle, 1989).

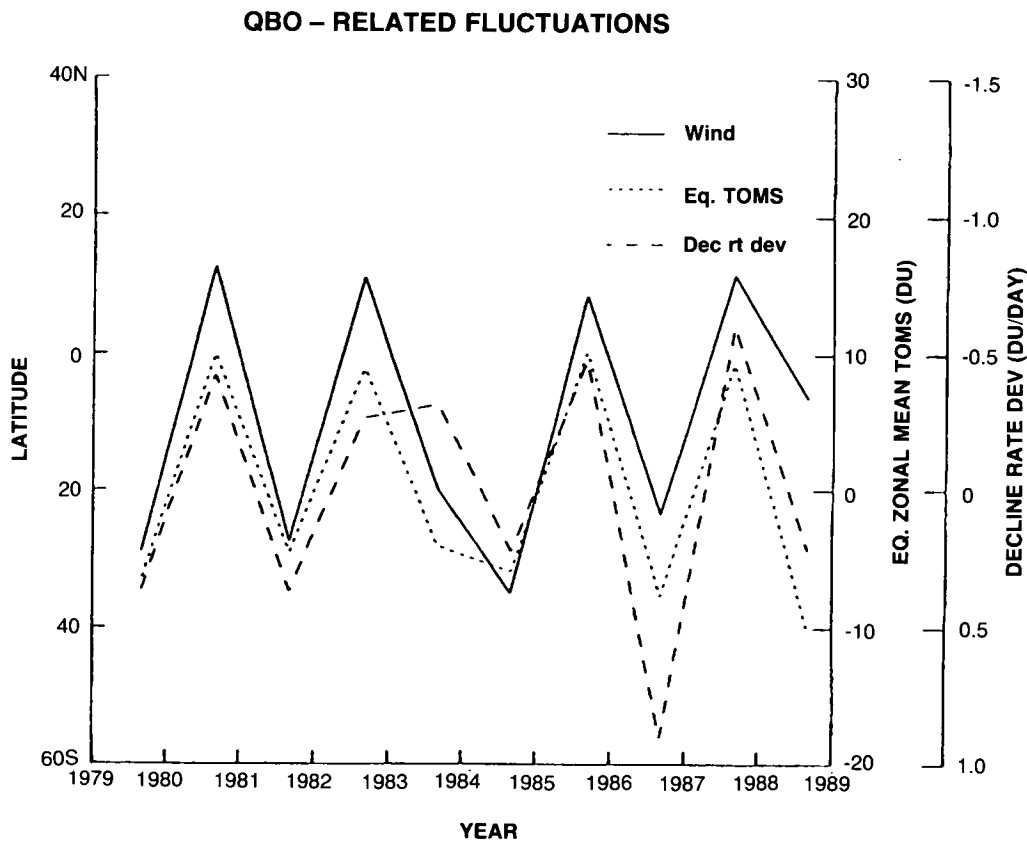


Figure 1.7.1-22. Correlation of August-September winds over Singapore at 30 mb (solid line) with the total ozone decline rate in September (large dashes). A linear trend has been removed from the decline rates. The September-mean values of equatorial total ozone are also shown (short dashes).

POLAR OZONE

NO_x at the low altitudes where the bulk of the total ozone column resides. Calculations by Brasseur et al. (1987) indicate that a 10% increase in UV radiation at 205 nm would be accompanied at 5 mb by globally averaged increases of about 3.5% in ozone and 1.5 K in temperature. Calculations of the expected ozone response to solar activity as a function of latitude and season were discussed in OTP (1989).

Recent observational analyses of the possible response of ozone to 11-year solar variations include the works of the OTP (1989), Keating et al. (1981), Chandra (1984), Oehlert (1986), and Reinsel et al. (1987, 1988). Using Umkehr data, Reinsel et al. (1987) detected a 3% variation in ozone at 36 km over the solar cycle. The amplitude of the cycle in total ozone was estimated to be about 2% by Keating et al. (1981), who used data from the Nimbus 4 BUUV instrument. Various investigators have detected a possible relation between stratospheric temperature and the 11-year solar cycle (Schwentek 1971; Angell and Korshover 1978; Quiroz 1979, Nash and Forrester 1987; Labitzke 1987a; Chanin et al. 1987). Using summertime rocketsonde temperatures, Quiroz (1979) found a high correlation between the temperature deviations and sunspot number in the middle and upper stratosphere. Nash and Forrester (1987) found evidence in SSU data of a drop in upper stratospheric temperatures of about 1.5 K from 1980 to 1986, which they attributed to a drop in solar activity.

Recently Labitzke and van Loon (1988a) reported some intriguing results. Linear correlations between three solar cycles in the period 1956–1987 and high-latitude stratospheric temperatures and geopotential heights showed no associations. But when the data were grouped according to the phase of the equatorial quasi-biennial oscillation (QBO), statistically significant correlations resulted: when the QBO is in its west phase, the polar data are positively correlated with the solar cycle, while those in middle and low latitudes are negatively correlated; the converse holds for the east phase. They also found that no major mid-winter warming occurred in the west phase of the QBO during minima in the three solar cycles, though major warmings were found at the minima during the east phase. Because greater poleward transport of ozone occurs during major warmings, one would expect the QBO signal in extra-tropical ozone amounts to be strengthened in solar minima and weakened in solar maxima. Provided the data are divided according to the phase of the QBO, statistically meaningful relationships are also found throughout the troposphere (Labitzke and van Loon, 1988a, b) and in the mesosphere (Labitzke and Chanin, 1988).

As yet no plausible mechanisms have been advanced to explain the correlations in the lower atmosphere; they could be flukes. For example, one could argue that low-frequency variations associated with the dynamics of the coupled ocean/atmosphere system would have, over a limited data sample, apparently significant projections onto a broad range of frequencies, including the 11-year solar cycle. The findings remain a source of debate and speculation.

A major difficulty in assessing atmospheric response to the 11-year solar cycle is the lack of a long-term (many cycles) data base from which statistically significant inferences can be drawn. There may be drifts in instrument sensitivity over extended periods of time, and individual instruments have a limited lifetime (especially those on satellites). One approach has been to investigate the response to short-term variations related to the 27-day solar rotation (Gille et al., 1984a; Hood, 1987; Keating et al., 1987). Results of such studies should be applicable to the 11-year cycle if the main processes controlling ozone amounts respond to solar UV variations on time scales much less than 27 days. Calculations by Brasseur et al. (1987) indicate that ozone changes induced by the 11-year and 27-day cycles are similar in the mesosphere and upper stratosphere, but that there may be appreciable differences in the lower stratosphere.

The analysis of total ozone measurements reported in OTP (1989) and summarized in Section 1.1.6 suggested solar-induced changes in Arctic total ozone of as much as 1.8%. Further, the solar-induced

changes in stratospheric temperatures outlined by Labitzke and Van Loon (1988a,b, 1989) may have appreciable effects on the formation of PSCs and hence on polar ozone depletion. Clearly, such fluctuations must be considered in attempts to deduce ozone and temperature trends, particularly in the Northern Hemisphere where current trends appear to be small (Sections 1.1.6 and 1.7).

1.7.2 Role of Synoptic-Scale Disturbances

It has been known for many years that tropospheric weather systems can have a substantial impact on total ozone amounts by changing the height of the tropopause between the ozone-poor air of the troposphere and the ozone-rich air of the stratosphere, and through horizontal mixing and advection (Dobson et al., 1928). Cyclonic weather systems are usually associated with low tropopause heights and high values of total ozone; anticyclonic systems with high tropopause heights and low values of total ozone.

During the course of the 1987 Airborne Antarctic Ozone Experiment (AAOE), column ozone amounts at southern high latitudes were observed to decline from values near 250 DU to below 150 DU. Particularly rapid reductions in ozone were found to occur on a synoptic scale in so-called mini-holes (Krueger et al., 1988), which last for several days and move slowly from west to east. On several occasions, the total ozone amount measured by the Total Ozone Mapping Spectrometer (TOMS) decreased over a period of 24-48 hours by several tens of DUs. Recently, Newman et al. (1988) noted correlations between low total ozone amounts, low temperatures, and low values of potential vorticity. They concluded that the Antarctic Peninsula is a preferred site for mini-hole intensification. Figure 1.7.2-1 shows an example of a mini-hole

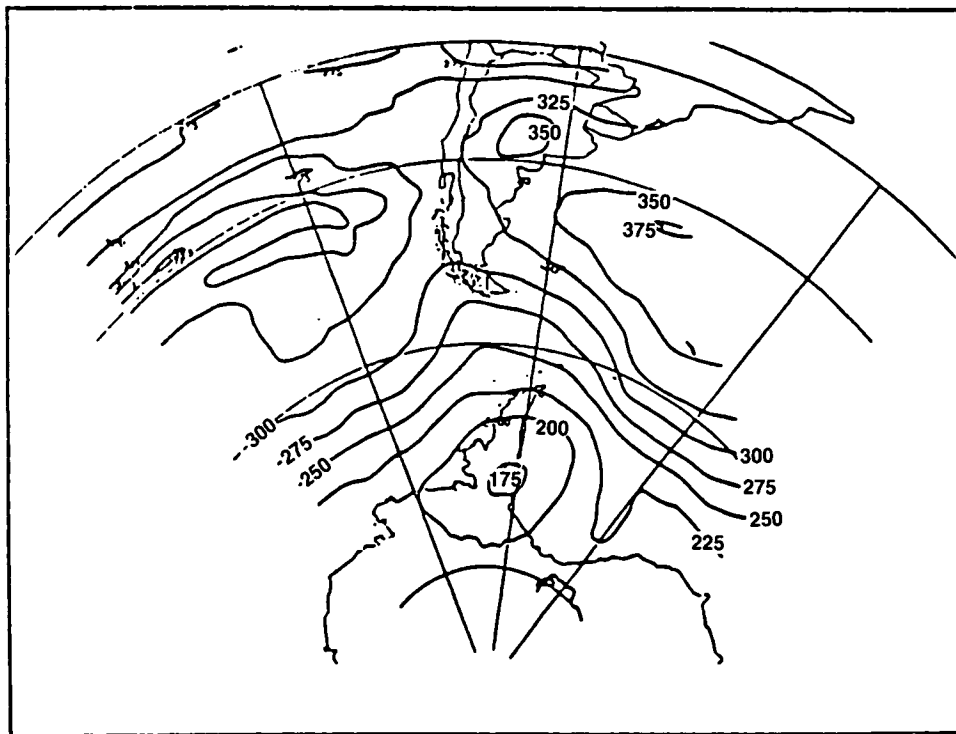


Figure 1.7.2-1. An example of mini-hole over the Antarctic Peninsula on 5 September 1987 (denoted by the bull's eye pattern near the Palmer Peninsula). Data derived from the TOMS instrument (contours labeled in Dobson units). Courtesy of P.A. Newman and M.R. Schoeberl.

POLAR OZONE

over the Antarctic Peninsula on 5 September 1987. Mini-holes are also found in the Northern Hemisphere. A particularly intense mini-hole was observed during the recent Airborne Arctic Stratospheric Expedition (AASE). Total ozone amounts measured by TOMS over Scandinavia fell as low as 125 DU.

Mini-holes are found to be associated with stratospheric clouds (Tuck, 1989). Krueger et al. (1987) pointed out that, as a result of this, total ozone amounts deduced from TOMS measurements could be underestimated in mini-holes because of the effects of high clouds on the ultraviolet radiation measured by the satellite (the problem is particularly acute at high solar zenith angle).

Two possible explanations for the observed rapid reductions in ozone amounts are (1) fast chemical processes and (2) atmospheric motions. On the basis of current photochemical theory, Jones et al. (1989) and Anderson et al. (1989) argued that it is not possible to destroy ozone fast enough to account for the observed transient mini-hole reductions. That atmospheric motions could lead to mini-holes was demonstrated by McKenna et al. (1989a). By calculating air parcel trajectories, they showed that the mini-hole in Figure 1.7.2-1 formed in association with a synoptic-scale anticyclone in the troposphere and lower stratosphere, which concentrated ozone-poor air below the level of the stratospheric polar vortex, thus reducing the column amount. The mini-hole is thus a manifestation of localized dynamical effects rather than irreversible transport of ozone-poor air.

Though of dynamical origin, mini-holes may be associated with important chemical effects, perhaps on spatial scales larger than the holes themselves. The formation of PSCs above synoptic-scale anticyclones provides the mechanism. Isentropic surfaces tend to rise above tropospheric anticyclones, and air cools as it glides upward along these surfaces. If it cools enough to saturate, clouds will form. Figure 1.7.2-2(i) shows cross sections of temperature, and Figure 1.7.2-2(ii) cross sections of potential temperature and saturated mixing ratio of water vapour taken through the mini-hole shown in Figure 1.7.2-1. There is an

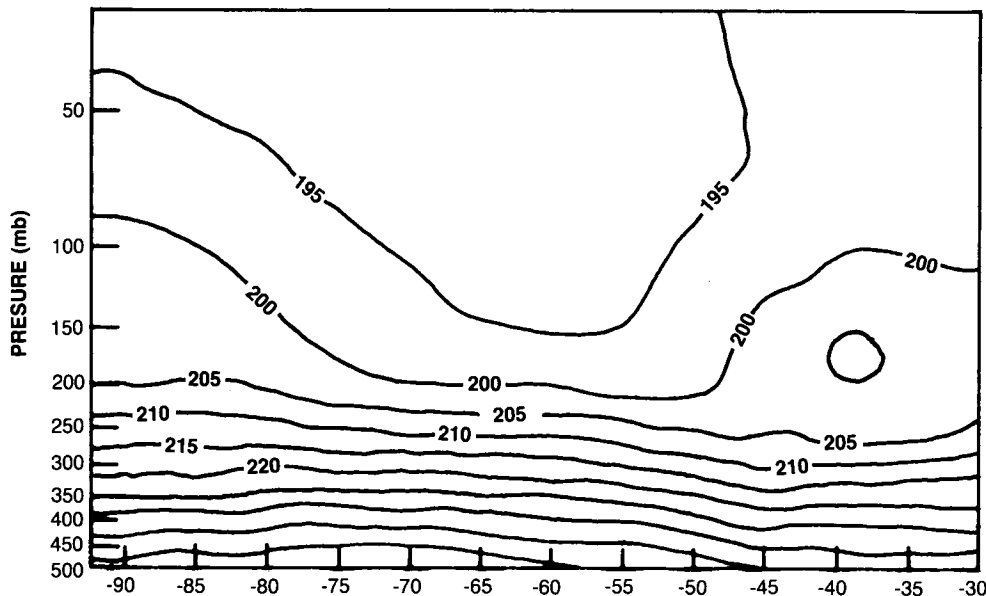


Figure 1.7.2-2(i). Longitude/pressure cross sections on 5 September 1987 at latitude 65°S from 90°W to 30°W, and from 250 to 30 mb (derived from U.K. Meteorological global analysis). (i) Temperature (5 K contour interval).

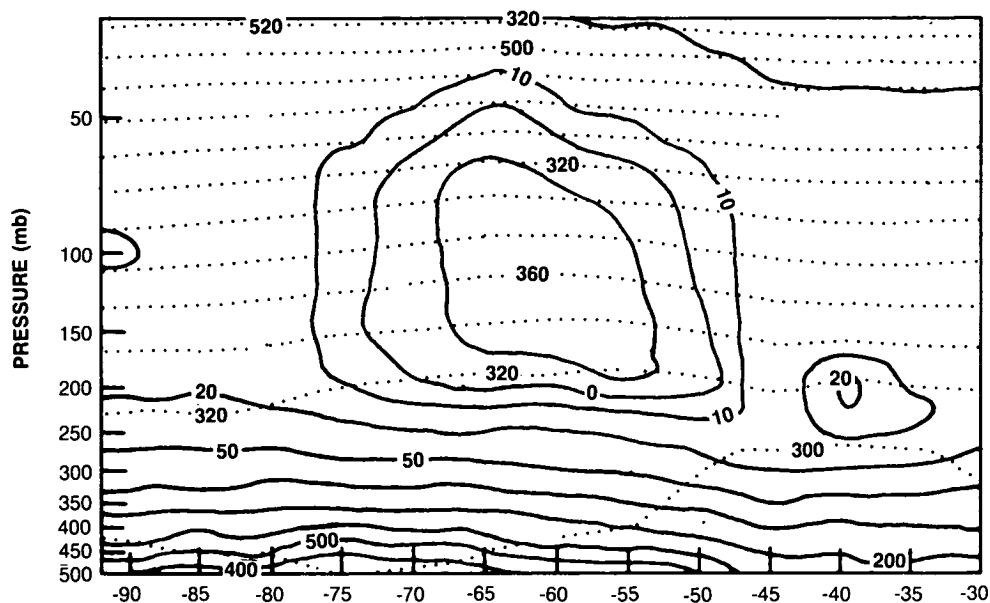


Figure 1.7.2-2(ii). As in Figure 1.7.2-2(i). Saturation water vapor mixing ratios (solid; at 6, 8, 10, and 20 ppmv) and isopleths of potential temperature (broken; contour interval 20 K).

area above 90 mb where temperatures were below 192 K. This local temperature minimum was associated with gently bowed up contours of potential temperature, indicating that air had ascended. The potential for saturation was greatest in the temperature minimum, where saturation mixing ratios were lowest. Type 1 or Type 2 PSCs would form preferentially in such a region.

A cloud deck so formed will remain linked to its generating anticyclone, and will tend to move with the anticyclone. Note, however, that in the lower stratosphere strong winds blow through the localized temperature minimum. Although an air parcel's exposure to PSCs will be short in any one encounter, it may be long enough for heterogeneous chemical reactions to occur to some extent, and thus to perturb the parcel's chemical composition. Tuck (1989) has also postulated that strong radiative cooling above cold polar stratospheric cloud decks causes air to sink, leading to further exposure of air to heterogeneous reactions.

Synoptic-scale disturbances also promote some meridional transport of air in the lower stratosphere (below about 70 mb). The disturbances cannot penetrate much higher because they are trapped by the strong westerly winds in the stratosphere (Charney and Drazin, 1961). Figure 1.7.2-3 shows a sequence of isentropic maps of Ertel's potential vorticity P for the lower stratosphere in late September 1987. Shading marks the edge of the region that was found to be chemically perturbed (Tuck, 1989). Near longitude 180 it appears that air is being peeled off the chemically perturbed region to form an isolated blob of P , which slowly disappears (either because of dissipation or because of inadequate resolution in the synoptic analyses). Murphy et al. (1989) also found evidence for some interchange of air at the edge of the chemically perturbed region.

In summary, synoptic-scale disturbances can increase the amount of air that is subject to heterogeneous chemistry (1) by generating PSCs on a synoptic scale, through which air may flow to give chemical

POLAR OZONE

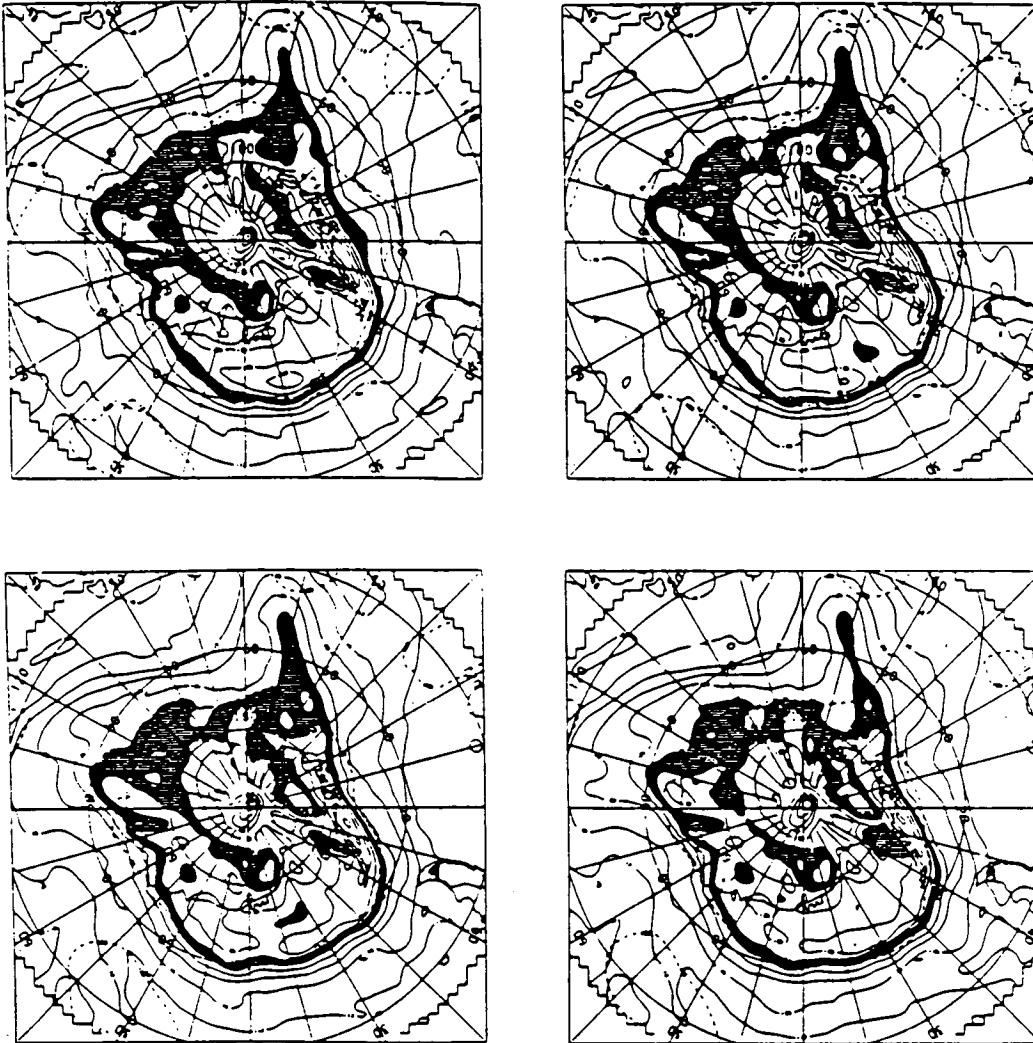


Figure 1.7.2-3. A sequence of potential vorticity distributions on the 428 K surface of potential temperature (from Tuck, 1989).

effects on a larger scale, and (2) by transporting air in and out of large-scale cloud decks (formed by large-scale cooling in the polar night). Quantitative details are uncertain, however.

1.7.3 Processing of Antarctic Air

The heterogeneous chemical reactions that eventually lead to ozone destruction require PSCs, which are found at temperatures below about 193 K within the stratospheric polar vortex. To quantify the amount of ozone that will be destroyed in a given year, one might begin by assuming that the PSC-containing volume is a fixed slug of air. Then the maximum amount of ozone that could be destroyed is the amount in the largest volume of air ever to contain PSCs. Such a calculation would seriously underestimate the amount of ozone destruction if a large amount of air flowed through the PSC-containing volume—that is,

if the PSCs and atmospheric circulation could be viewed as components of a giant “chemical processor.” If that were so, ozone amounts could be affected hemispherically, or even globally, by a sink confined to southern polar latitudes. Some findings relevant to this issue are now outlined.

The PSCs are contained within an intense westerly vortex that is characterized by strong gradients of potential vorticity (see Figure 1.7.1-13). Such gradients resist lateral displacements of air parcels (McIntyre and Palmer, 1983), inhibiting to some extent the mixing of chemically perturbed vortical air with unperturbed extra-vortical air. The term “containment vessel” has been used to describe this situation. There is, of course, no impermeable seal around polar air. Air is stripped from the outer portion of the vortex by planetary-scale waves (Juckes and McIntyre, 1987; Mechoso et al., 1988) and, in the lower stratosphere, by synoptic-scale disturbances (Tuck, 1989; see Figure 1.7.2-3). This air may then mix with extra-vortical air. Moreover, disturbances warm some of the air in the vortex. Increased radiative cooling brings air poleward, downward, and then equatorward in a slow meridional circulation. Thus, air may encounter PSCs, become chemically perturbed, and then move to regions that have remained free from PSCs.

Possible constraints on the putative Antarctic chemical processor have been given by Hartmann et al. (1989a), who used a simplified two-dimensional model, together with data derived from the ER-2 flights during the Airborne Antarctic Ozone Experiment (AAOE) in 1987. By assuming a cooling rate of 0.2 K per day (in agreement with the estimate of Rosenfield and Schoeberl, 1986), they found that the flux of ozone into the region of ozone depletion was only about 20% of the observed decline rate for ozone—that is, the transport effects are much smaller than depletion caused by the local photochemical sink.

Hartmann et al. further argued that a rapid increase in ozone mixing with distance from the center of the ozone hole implies relatively weak meridional dispersion of air parcels. They estimated an upper bound for the effective meridional “diffusion coefficient” in their model, and found it to be rather small: it would take about 125 days to change the ozone mixing ratio by a factor of e . They concluded that only about 20% more ozone could be processed than was in the chemically perturbed region at the beginning of September 1987.

Profitt et al. (1989b) concurred with Hartmann’s et al. estimate of weak lateral dispersion, but argued for much larger subsidence rates. These two views could be reconciled if there were substantial gravity-wave drag, and much more rapid radiative cooling than was used by Hartmann et al. Significant gravity-wave activity has been detected at the altitude of the ozone depletion over Antarctica, but the strength of the associated momentum source is not known (Hartmann et al., 1989b). The required strong cooling could result from the presence of PSCs and cirrus cloud decks, as has been suggested by Kinne and Toon (1989) and Tuck (1989), but cooling rates are uncertain (see Section 1.2). Some evidence that could be viewed as favoring the notion of a chemical processor has been reported.

Tuck used the F11/N₂O ratio at constant potential temperature and potential vorticity to infer a diabatic cooling rate of 4-6 K per day in potential temperature, much larger than the 0.4 K per day used by Hartmann et al. He concluded that the diabatic subsidence was substantial, in broad agreement with the analysis of possible cloud radiative effects presented by Kinne and Toon (1989), as discussed in Section 1.2.4. Murphy et al. (1989) found a positive, small-scale horizontal correlation between N₂O and H₂O in the chemically perturbed region, even though they have oppositely directed vertical gradients. They argued that this was the result of patchy diabatic sinking in regions where air had been dehydrated (i.e., where PSCs had formed), but did not estimate the rate of descent.

POLAR OZONE

Evidence that the containment vessel is not impermeable to lateral air movement comes from several sources.

The distribution of PSCs, as deduced from SAM II data, shows a pronounced longitudinal asymmetry, despite there being no such asymmetry in coldest temperatures. Clouds are found most frequently near the edge of the vortex in the 0-90°W sector; as early as July, the interior of the polar vortex has low incidences of clouds. An interpretation of these observations was given by Watterson and Tuck (1989), who argued that there must be a resupply of condensable material near the edge of the vortex for clouds to persist despite gravitational settling of particulates. They proposed that the clouds recur by adiabatic expansion and cooling of warm, moist air that is injected poleward by upper tropospheric weather systems. Murphy et al. (1989) found evidence for isentropic (quasi-horizontal) mixing at the edge of the polar vortex, while Tuck (1989) suggested that efficient mixing, perhaps by interstitial instability, could account for "flat" regions in N₂O mixing ratios. Kelly et al. (1989) recorded a decrease in the mixing ratio of water vapor on an aircraft flight from Puerto Montt (41°S) to Punta Arenas (53°S) in August 1987. They suggested that this finding was consistent with air being dehydrated over Antarctica and then spreading to mid-latitudes. A tropical origin for the dry air was inconsistent with the measured mixing ratios of other trace chemicals.

On the basis of current modeling and observational studies, no firm judgment can be offered on the degree to which the polar stratosphere may be viewed as a chemical processor. Hartmann's et al. (1989a) model is a considerable idealization of atmospheric transport. It is a co-ordinate based model, and does not recognize explicitly the polar vortex as a physical entity which may move and deform over the polar cap (perhaps not a serious shortcoming for the year 1987, when planetary waves were comparatively weak). Moreover, heating rates used in the model are uncertain, and radiative effects of PSCs (also uncertain) are neglected. On the other hand, the above-cited observational studies do not supply enough quantitative information to estimate the through-put of air in the imagined chemical processor. Local observations (taken from aircraft, say) may lead to erroneous conclusions about large-scale processes. To resolve the issue, simulations with high-resolution general circulation models are called for, backed by parallel studies of both ground-based and satellite data. (Data from the Upper Atmosphere Research Satellite, scheduled for launch in 1990 or 1991, should be of great value.) Some questions requiring attention are:

1. If substantial mass is circulated through the polar region, can temperatures remain below the threshold for PSCs despite dynamical warming?
2. Would the accompanying transport of chemical species limit or enhance the chemical processor?
3. If the notion of a chemical processor is useful, should we expect more ozone to be destroyed in a year with strong dynamical activity and mass circulation (e.g. 1988), or are there complicating factors?
4. Could significant ozone depletion take place in the Northern Hemisphere despite the limited coverage of PSCs?

1.7.4 The Dilution Effect

Initial concern over the observed springtime Antarctic ozone depletion (Farman et al., 1985a) was focused largely upon the high latitude region over the Antarctic continent. As discussed in Section 1.1 and in the above, examination of a number of years of ozone data revealed that a very rapid decline in ozone occurred in the lower stratosphere during the month of September as sunlight returned to the polar region. Reductions in the ozone column of as much as 50% were observed (e.g., references in Solomon, 1988). After reaching a minimum in late September to early October, the ozone column recovered within a few weeks with onset of the final warming and breakup of the polar vortex. Replenishment of the polar ozone

column occurred as the ozone-poor air was exchanged with air masses with relatively higher ozone content from lower latitudes by large-scale, quasi-horizontal transport. This large-scale latitudinal mass exchange apparently occurs throughout austral spring as evidenced by the potential vorticity analyses of Newman (1986) shown on Figure 1.7.4-1. Typically, amplifying anticyclones erode the vortex edge, and air from this region is transported to lower latitudes. Later in spring (usually in November), the vortex breaks up and more extensive lateral mixing takes place.

Export of ozone-poor air from polar regions to middle latitudes produces a deficit in ozone (a "dilution effect," Sze et al., 1989) which might persist for a long period because of the relatively slow chemical replacement time (on order of a month to a year, depending upon latitude) for ozone in the lower stratosphere. Further chemical effects might result from the accompanying export of denitrified and dehydrated

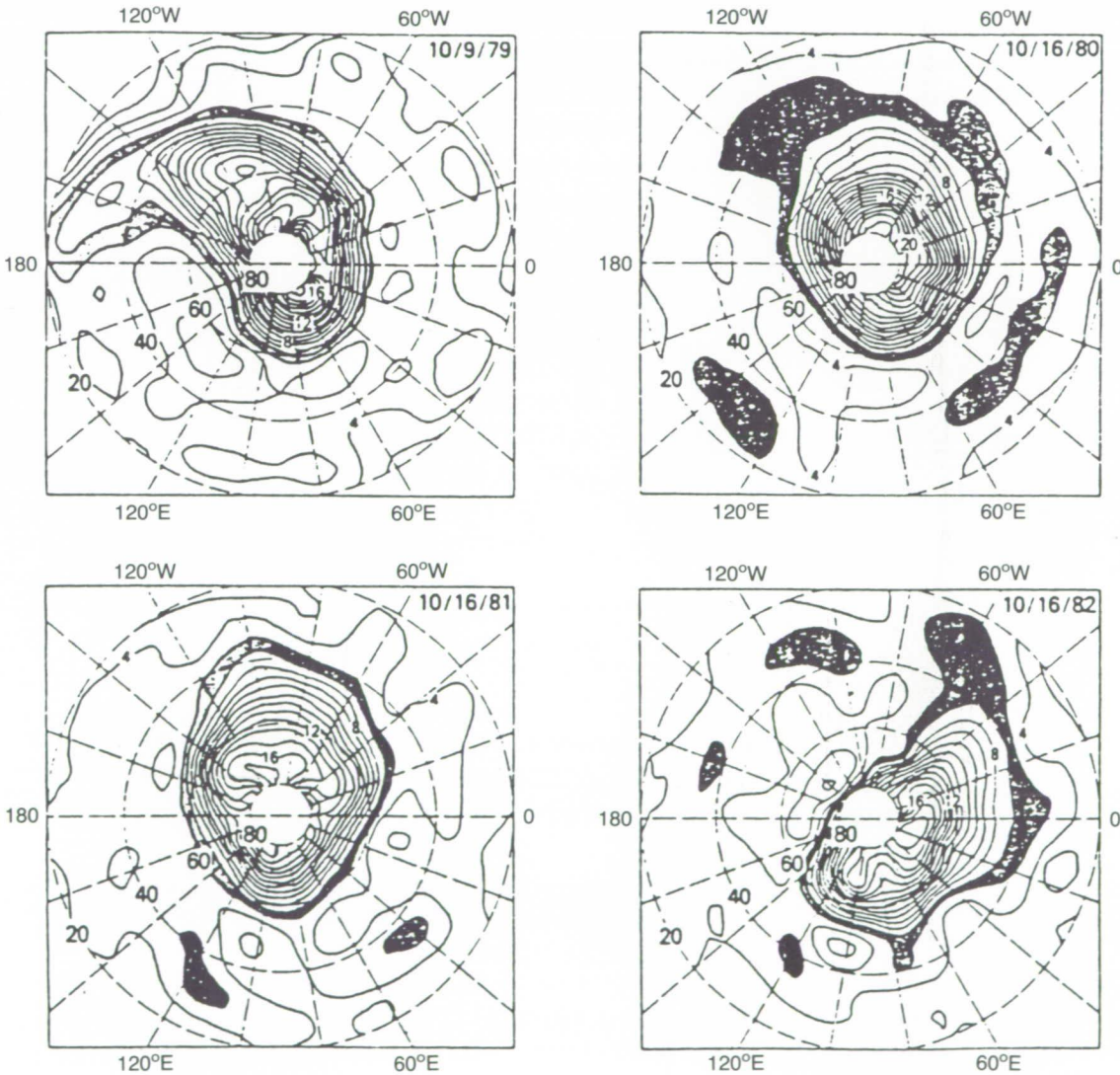


Figure 1.7.4-1. Ertel's potential vorticity on the 600 K isentropic surface. Units $\text{Km}^2/\text{kg s}$. (from Newman, 1986).

POLAR OZONE

air. If the ozone deficit lasts until the next springtime depletion episode at polar latitudes, the effect may be cumulative with a permanent reduction in the global ozone budget. The data from the Total Ozone Mapping Spectrometer (TOMS) instrument is not inconsistent with such a scenario. Displayed in Figure 1.7.4-2 is the monthly variation of the difference between the 1987-88 TOMS data and that for 1979-80. The 2-year averages for 1987-88 and 1979-80 have been used to reduce the effect of the quasi-biennial oscillation (e.g., Garcia and Solomon, 1987; Lait et al., 1989). Noticeable reductions (4% or greater) for this time period are apparent throughout the year at 50–60°S. The outward bulge toward mid-latitudes is particularly marked in late spring/early summer (November/December) at a time when dynamical considerations suggest that dilution would occur. Moreover, a second bulge toward midlatitudes is seen in April/May coincident with the autumnal peak in wave activity in the Southern Hemisphere noted by Hirota et al. (1983) and Randel (1988). Although the data are supportive of the dilution concept, it should be noted that changes arising from the influence of volcanic aerosols, the 11-year solar cycle, the quasi-biennial oscillation, or other factors cannot be unambiguously separated from changes which might arise from dilution.

Several model simulations have been conducted to study the consequences of dilution. Sze et al. (1989) used a 2-D model (Ko et al., 1985) with an extensive representation of the gas phase chemistry to perform a number of dilution studies. In their simulations, the region from 63°S to the pole was assumed to be an isolated vortex from April to October with no exchange of air permitted across the vortex boundary. An ozone hole was empirically imposed (no heterogeneous chemistry was included) and exchange of extra-vortical air with that from within the vortex was allowed beginning the first of November. In one experiment, the ozone hole (80% reduction from 63°S to the pole from 14 to 22 km) was imposed only in the first year

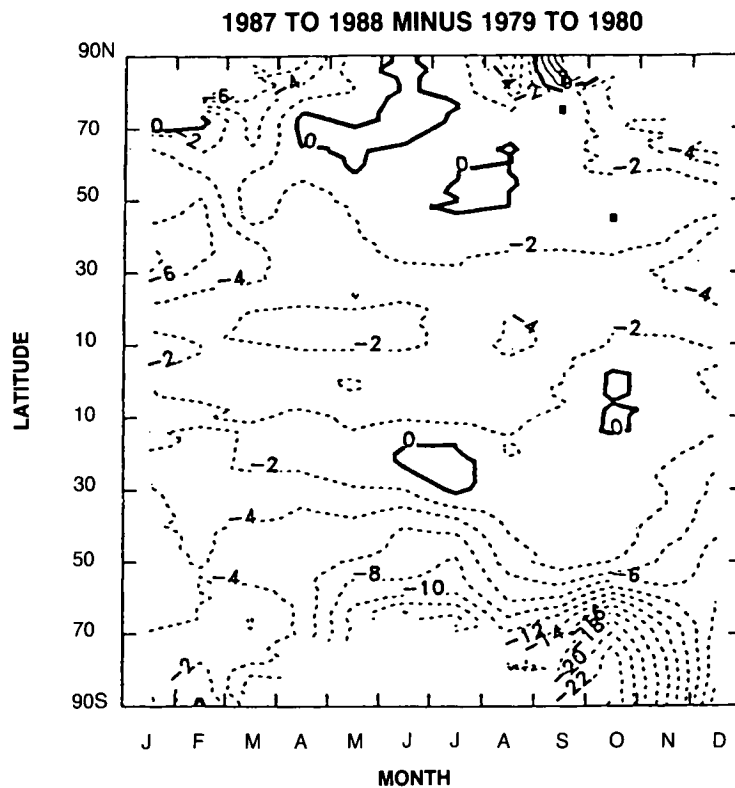


Figure 1.7.4-2. TOMS total ozone. Monthly variation of difference between 1987-1988 average and 1979-1980 average as a function of latitude. Courtesy of R. Stolarski.

with the simulation continued for 3 years. Column ozone reductions of 2 to 6% between 45°–60°S persisted throughout most of the second year with full recovery occurring in the third year. A second experiment was conducted with the simulation lasting 12 years with a prescribed ozone hole occurring each year. The results of that experiment are shown in Figure 1.7.4-3. Steady-state reductions of 3% or larger are evident between 50–60°S throughout the year. Broadly speaking, the results exhibit latitudinal and seasonal variations similar to those seen in the TOMS data (Figure 1.7.4-2). Chipperfield and Pyle (1988) have performed similar studies with their 2-D model. Their results are similar, but smaller in magnitude. The differences in the two studies are most probably a result of differences in the model transport: Sze et al. use the diabatic circulation formulation, while Chipperfield and Pyle use an Eulerian formulation requiring that eddy heat and momentum fluxes be included explicitly.

Prather et al. (1989) have also modeled the dilution effect. Their study differs from that of Sze et al. by using a 3-D off-line tracer model and adopting a simplified, linearized ozone photochemistry. In this study, the ozone hole was imposed instantaneously on October 1 in the region 70.5°S to the pole between 22 and 200 mb. The simulation was then carried out for 2 years (again imposing the ozone hole on October 1). One year later, column reductions of 2% exist as far equatorward at 40°S (see Figure 1.7.4-4). At the end of the second year, the average ozone depletion is about 20% larger than at the end of the first year. These results indicate that most of the ozone deficit existing 1 year after imposition of the hole is in the upper troposphere, south of 40°S. Additional 3-D model studies of the dilution effect have been carried out by Grose et al. (1989), Mahlman (1989) and Cariolle et al. (1989b). The study by Grose et al. used an off-

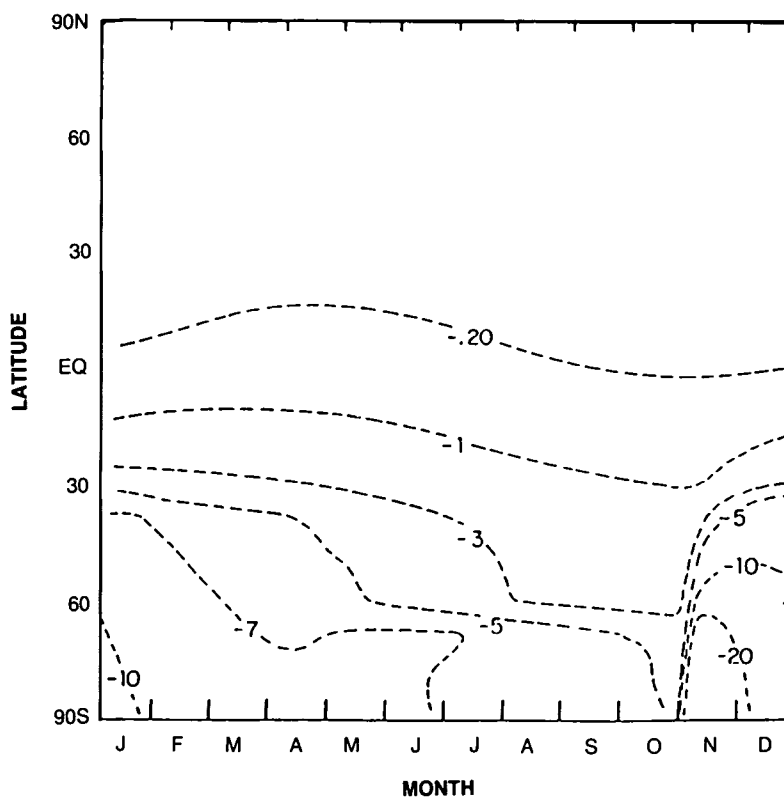


Figure 1.7.4-3. Percent change in the simulated steady-state seasonal and latitudinal distribution of zonal-mean column ozone (from Sze et al. 1989).

POLAR OZONE

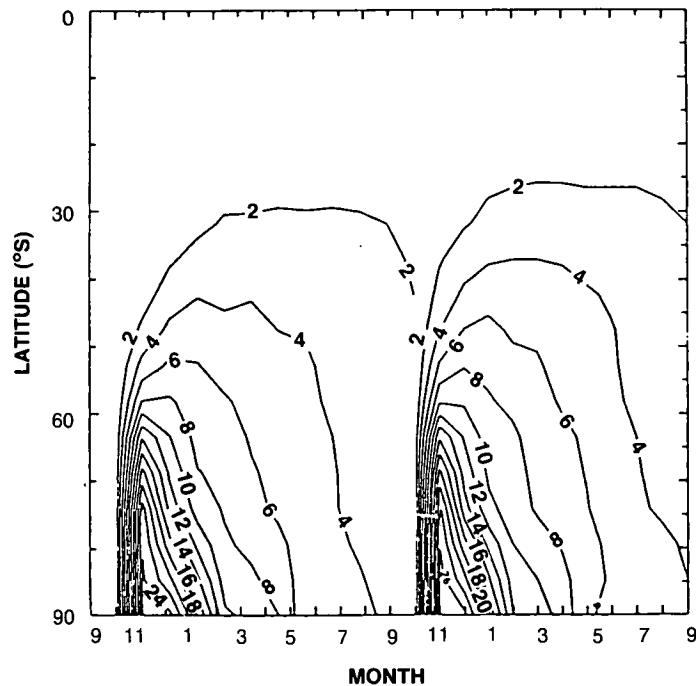


Figure 1.7.4-4. Percent difference in zonal-mean column ozone for Antarctic ozone hole simulation relative to control simulation as a function of season and latitude (from Prather et al., 1989).

line tracer model including comprehensive gas phase chemistry. An ozone hole was imposed in the simulation by specifying a linear loss rate for ozone such that 90% of the ozone in the region from 69°S to the pole between 27 to 112 mb was removed during the month of September (5.75% of the total ozone in the Southern Hemisphere). One year later, a residual deficit of approximately 1.3% persists in the total ozone in the Southern Hemisphere (see Figure 1.7.4-5). Most of the deficit in the ozone exists below the 100-mb level and between 30°S and the pole (approximately 1% of the column at 30°S, 2% of the column from 60°S to the pole). Mahlman (1989) used the GFDL SKYHI model to evaluate the dilution effect (without explicit ozone chemistry but allowing for dynamical feedbacks). Perturbations to an ozone climatology were parameterized as a function of the desiccation of water vapor. The results of this study are similar to those obtained by Prather et al. and by Grose et al. However, an important feature of this study is that the temperature and hence the circulation could change in response to the changing ozone distribution, a feature not possible in the studies with the off-line models. A robust feature of the Mahlman results is a significant temperature decrease (order of 10 K, compared with a simulation with no ozone hole) at polar latitudes in the lower stratosphere which persists approximately 6 months after formation of the ozone hole. Accompanying the decrease in the lower stratosphere is an increase in the middle stratosphere. A similar response was seen both in the study by Kiehl et al. (1988) who studied the response of a general circulation model to reduced polar ozone and in the study by Chipperfield and Pyle (1988) with their 2-D model. These results suggest that a model in which radiative, chemical, and dynamical processes are fully coupled may be required to understand possible feedbacks and their implications over long periods.

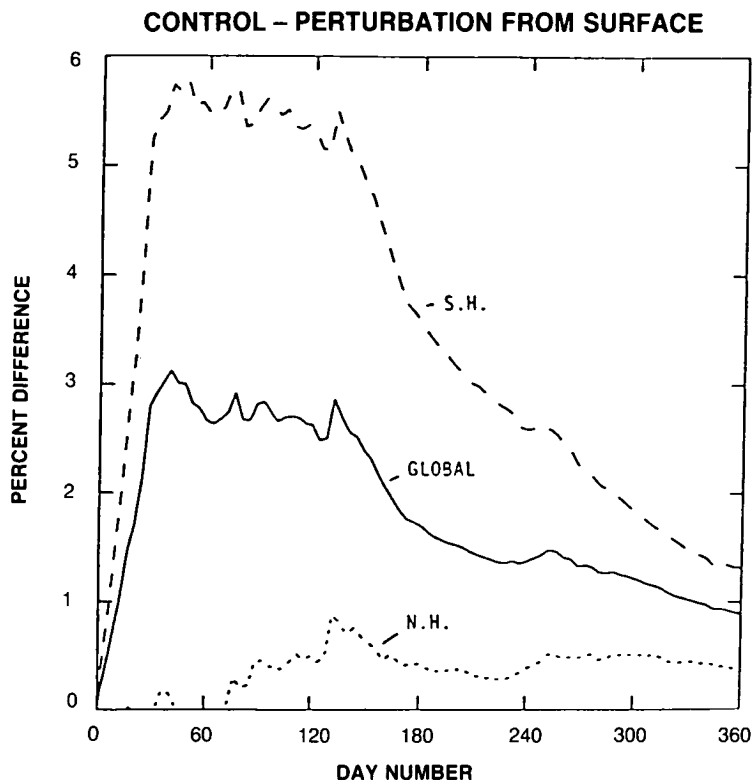


Figure 1.7.4-5. Percent difference in the integrated global and hemispheric column ozone for Antarctic ozone hole simulation relative to control simulation as a function of time (Day 0 is 1 September) (from Grose et al., 1989).

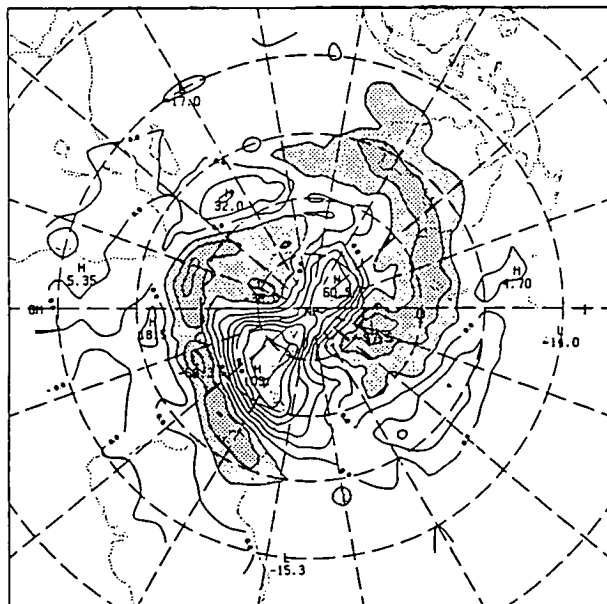


Figure 1.7.4-6. TOMS total ozone for the Southern Hemisphere. Difference (Dobson units) between 8 December and 14 December, 1987. Difference is between three-day means centered about those dates. Shading represents reductions exceeding 15 DU.

POLAR OZONE

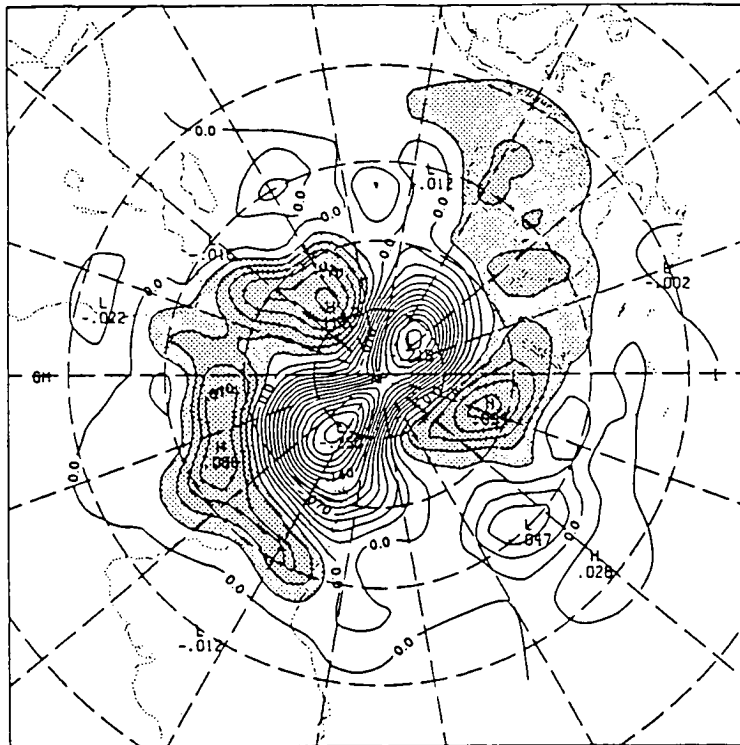


Figure 1.7.4-7. Difference between Ertel's potential vorticity (500 K isentropic surface) for 8 December and 14 December, 1987. Difference is between three-day means centered about those dates. Contour interval of $7.5 \times 10^{-8} \text{ K s}^{-1} \text{ Pa}^{-1}$. Shading represents increases greater than $7.5 \times 10^{-8} \text{ K s}^{-1} \text{ Pa}^{-1}$. (Cyclonic potential vorticity is positive.)

Cariolle et al. (1989b) have also run a comprehensive simulation of the springtime Antarctic ozone depletion with a GCM which allows for an interaction between radiation and ozone mixing ratio. In this study, the ozone loss due to chlorine was represented in a simplified way. Significant ozone decreases were found at Southern Hemisphere mid-latitudes before and after the final warming. In addition, a temperature decrease of about 7 K was found inside the polar vortex in October at 50 mb, and the final warming in November was delayed by about two weeks.

The most remarkable aspect of the model studies cited herein is the degree to which they agree with one another and with the TOMS observations of Figure 1.7.4-2. There are substantial differences among the various models, each model having its own particular shortcomings. Nevertheless, although differences in detail exist, a general conclusion is common to all of these studies. The conclusion is that dilution of mid-latitude ozone by export of ozone-poor air from polar latitudes after breakup of the depleted Antarctic vortex might produce a small residual deficit in ozone which is cumulative from year-to-year. These simulated results should be further qualified by noting that those factors that may also be influencing the ozone data (e.g., volcanic aerosols, solar cycle, QBO) have not been taken into account in the model simulations.

Determining the actual latitudinal extent of the dilution effect is of crucial importance. Inferring the northward limit of the effect from the TOMS data (Figure 1.7.4-2) is difficult for reasons of the limited statistics. Certainly, one cannot categorically deduce the existence of a trend northward of about 50°S from the TOMS data alone. Atkinson and Easson (1988) reported evidence of a significant year-to-year downward trend in ozone at Melbourne (38°S). However, data from a single station is informative, but not definitive. There is some direct evidence that transport of ozone-poor air reached 32°S in the Australia - New Zealand area in December 1987 (Atkinson et al., 1989) following the lowest springtime ozone values ever observed over Antarctica. The Dobson data record exhibited a sudden drop in mid-December across southern Australia and New Zealand to about 10% below normal December values, which lasted for the rest of the month. In fact, the December mean ozone in 1987 was the lowest ever recorded at Melbourne. The timing of this sudden drop coincided with the final breakdown of the polar vortex in the lower stratosphere. Figure 1.7.4-6 depicts the difference in total ozone before and after this event. A corresponding plot of Ertel potential vorticity on the 500 K isentropic surface is shown in Figure 1.7.4-7. The high degree of correlation between these two figures (supported by independent trajectory analyses) suggests that the observed sudden drop in ozone values was a result of the transport of ozone-poor air from the fragmenting vortex. It will require studies from further years to determine whether this was an extraordinary event or a typical example of the dilution effect.

1.8 TEMPERATURE TRENDS—CAUSES AND EFFECTS

The significance of observed changes in temperature in the Antarctic lower stratosphere during springtime remained unclear for some time after the discovery of the ozone hole. Some attributed the changes to dynamical mechanisms that could also be responsible for the ozone hole itself. Other workers believed the temperature changes were an effect of the depletion of ozone rather than related to its cause. It now seems clear that most, if not all, of the year-to-year springtime temperature trend is a result of the diabatic effects of ozone loss; such an effect has been simulated in simple 1-D models (Shine 1986; OTP 1989), 2-D models (Chipperfield and Pyle 1988) and 3-D general circulation models (Kiehl et al. 1988; personal communication Rowntree and Lean, UK Met. Office, 1989). This implies that the radiative effects associated with the near-absence of ozone at some altitudes within the ozone hole have led to a significant change in the climatology of the stratosphere.

Changes in Antarctic lower stratosphere temperatures have assumed particular significance given the central role now thought to be played by polar stratospheric clouds in the chemical mechanisms causing the depletion of ozone. Any long-term trend in temperature, particularly in winter and early spring, might be expected to impact the extent and duration of polar stratospheric clouds.

In the following, measurements of temperature trends and their interpretation will be described. In Section 1.8.1, observations included in the summary of temperature trends measurements in OTP (1989) will be summarized. In Section 1.8.2, more recent studies of temperature trends are described. Section 1.8.3 presents theoretical studies aimed at interpreting the observed trends in temperature and describes their implications for the interpretation of the Antarctic ozone hole.

1.8.1 Resume of Work Discussed by OTP (1989)

Chapter 11 of the Ozone Trends Panel Report (OTP, 1989) contains much detail on observations and modeling of lower stratospheric temperatures in the Antarctic springtime; it is only necessary to give a

POLAR OZONE

brief resume of this report before progressing to more recent studies. The overriding difficulty for trend detection in this region and season is the strong interannual variability in temperature, as discussed in some detail in Section 1.7. Labitzke (1987b) reports October mean temperatures at 50 mbar ranging from -46°C to -69°C at Syowa station (from a sample of 18 years' data) with a standard deviation of 6.2°C . For November a range of -32°C to -50°C is found with a standard deviation of 4.2°C . A similar spread is found at the South Pole, although the variability is slightly greater in November than in October. As discussed in Section 1.7, much of this variability is due to variations in planetary wave activity, perhaps related in part to the QBO, while some is also attributed to the solar cycle by a number of authors.

Sekiguchi (1986) and Chubachi (1986) used radiosonde data from Syowa to deduce temperature trends. Chubachi's analysis showed that the biggest changes in temperature at both 100 and 50 mbar occur during November; over the period from 1974 to 1985 the cooling was found to be about $1.2^{\circ}\text{C}/\text{year}$. Temperature decreases were found in all months except July and September, although the statistical significance of the trends was not discussed. Sekiguchi found strong correlations between interannual variations in ozone and temperature for the period October-December. These were particularly marked in October and November between about 150 and 50 mbar. Angell (1986) used data from 16 radiosonde stations between 60° and 90°S to show strong long-term coolings at 30, 50, and 100 mbar in the austral spring (Sept-Oct-Nov). Angell also showed that the trend varies greatly across the Antarctic continent, with the largest trends occurring along the coast from 30°W to 60°E (including Halley Bay and Syowa).

Other work reported in OTP (1989) concentrates on the more recent NMC data set. From 1,000 to 100 mbar these data are a mixture of radiosonde and satellite data, while from 70 to 0.5 mbar they are based primarily on satellite data. The satellite retrievals are based on a regression with a number of colocated radiosonde and rocketsonde observations; for the layer 70 - 10 mbar the regression coefficients are updated, on average, every 2.5 weeks, while at lower pressures the coefficients are constant. The most complete analysis of these data was performed by Newman and Randel (1988). Their study showed that while there was some offset between radiosonde temperatures and colocated satellite observations, the interannual variation and trends were generally in agreement. A linear trend analysis of satellite observations from 1979 to 1986 (Figure 1.8.1-1) provided support for the radiosonde studies. Of particular importance were the observations showing little or no trend during September. A strong trend exceeding $0.9^{\circ}\text{C}/\text{year}$ was found in the lower stratosphere in October. In order to show the consistency of trends in both radiosonde and NMC data sets, Newman and Randel presented differences in October monthly mean temperatures at 100 and 70 mbar for both sets. The changes are generally in good agreement, although individual radiosonde stations can be as much as 30-40% different. There is certainly no systematic difference in the temperature changes obtained using the two data sets.

Thus, the studies are generally in agreement that a marked downward trend in the springtime temperatures in the Antarctic lower stratosphere has occurred. The trend appears to be restricted to October and November, unlike the change in ozone that occurs predominantly in September. This represents crucial evidence against dynamical theories, as it lags rather than leads the ozone change. Indeed, the change in temperature at pressures greater than 50 mbar, and as importantly its timing, appears to be modeled adequately as a response to reduced diabatic heating resulting from ozone reductions as shown in Section 1.8.3. OTP (1989) presents results from radiatively-determined model calculations, using three different radiation schemes. Calculations with one of the models showed that 80% of the temperature change was due to decreased absorption of solar radiation, while the rest was due to less thermal infrared radiation being absorbed from the warmer troposphere. Hence, most of the cooling would be expected to be observed after the Sun rises.

POLAR OZONE

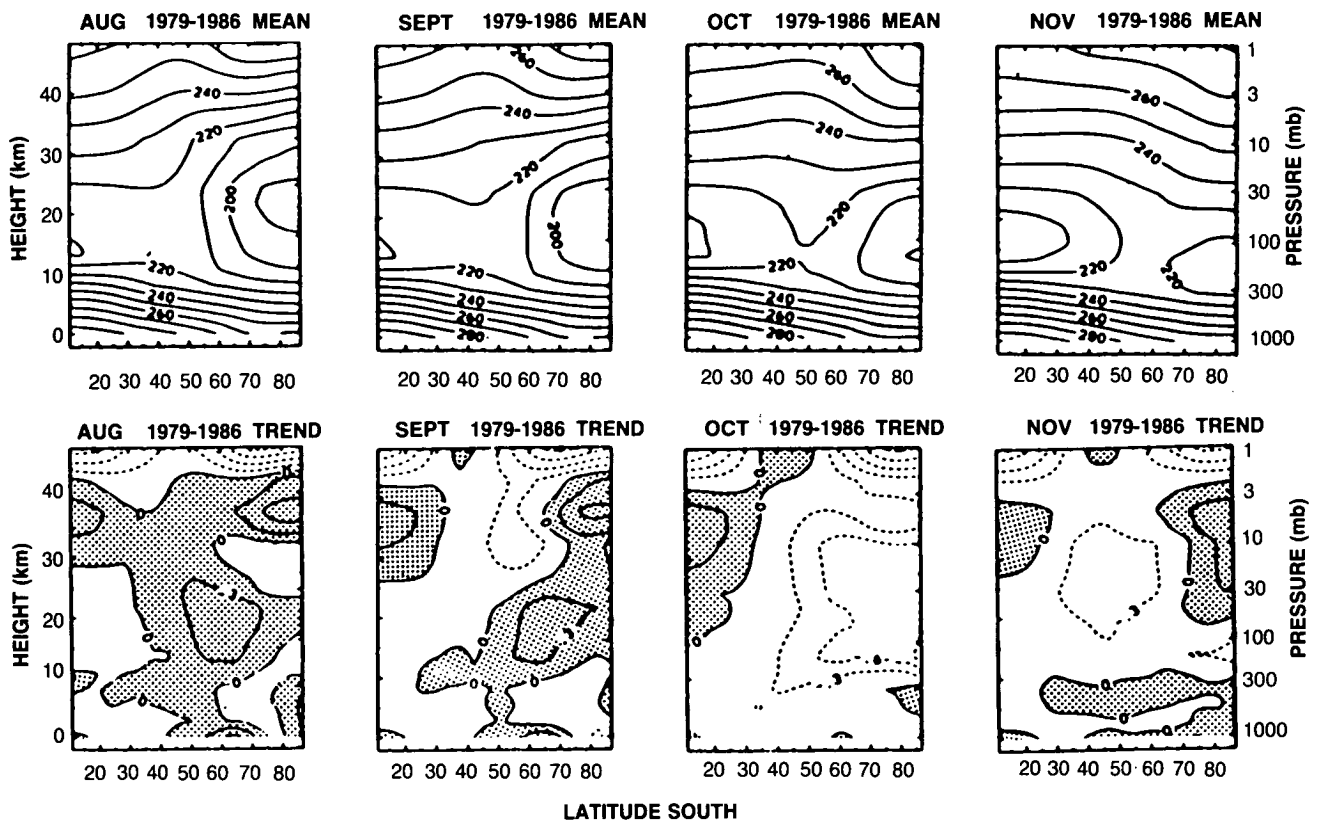


Figure 1.8.1-1. Linear trends calculated from NMC data (in °C/year) for the period 1979-1986, for August, September, November, and December (from Newman and Randel, 1988).

The work reviewed by OTP (1989) leaves a number of unresolved questions. For example, the radiosonde observations indicate that the largest cooling is found in November, whereas the satellite observations indicate that the biggest cooling is in October. Another question stems from the results of the radiatively-determined calculations. All model calculations show an increase in temperature in the upper stratosphere that is related to an increased penetration of thermal infrared radiation from the troposphere due to the decreased ozone amounts in the lower stratosphere. A smaller contribution comes from an increased heating due to solar radiation reflected from the troposphere penetrating to greater heights, for a similar reason. The only slight evidence for such a heating can be seen in the November plots of Newman and Randel (1988) (our Figure 1.8.1-1). More recent developments in this area will be discussed below.

1.8.2 Other Recent Work

The problem of interannual variability has been highlighted by the two most recent austral springs; 1987 and 1988 have been very cold and relatively warm, respectively. This can be seen in temperature data during springtime for the layer 100-50 mbar, shown in Figure 1.8.2-1, which uses data collected from six Antarctic stations as described in Angell (1988b) updated to include 1988 (Angell, personal communication).

POLAR OZONE

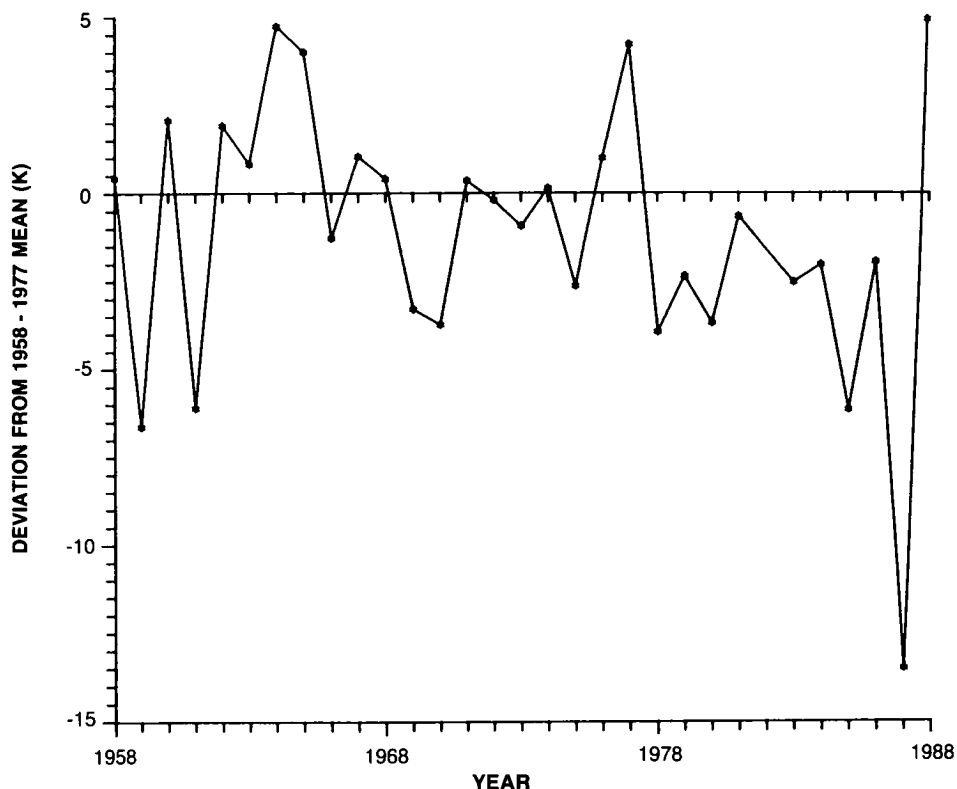


Figure 1.8.2-1. Deviations of temperatures 1958-1988 ($^{\circ}\text{C}$) from the 1958-1977 mean for September to November for Angell's (1988b) six polar stations.

From this figure it can be seen that 1987, in the context of the last 30 years, was exceptionally cold, while 1988 was (narrowly) the warmest on record (see Section 1.7). The difference in measured temperatures between the two springs exceeds 18°C . These data are, however, collected over a broad geographical region (with stations ranging over 24 degrees of latitude) and averaged over the three spring months. The temporal and spatial averaging may disguise, to some extent, the changes in the ozone depleted region, which was far smaller in 1988 than in 1987 (Schoeberl et al., 1989). This view is supported to some extent by other data (see also, the discussion of 1987 and 1988 temperatures and dynamics in Section 1.7). Gardiner (1989) shows that at Halley Bay (this station is one of the six used by Angell for his composite analysis) at 100 mbar, 1987 was indeed the coldest on record in October, November, and December; however 1988, while warm, does not rank as anything like the warmest in the 30-year record (Figure 1.8.2-2). The October mean temperature is about 9°C warmer in 1988 than in 1987, the corresponding figure being 20°C in November. Schoeberl et al. (1989) report that 70-mbar temperatures (from NMC analyses) in late September and October were 5°C warmer in the vortex in 1988 compared to 1987.

Strong evidence of a change in the behavior of the annual cycle of temperature as a result of the ozone depletion can be seen in Figure 1.8.2-3 (Farman, private communication). This figure shows the annual cycle of 100-mbar temperatures at Halley Bay for 1987, together with the mean and extreme values for the period 1957-1975. The severe depletion of ozone within the polar vortex in 1987 was followed by exceedingly low temperatures in October and November, and a delay in the spring warming. Differences

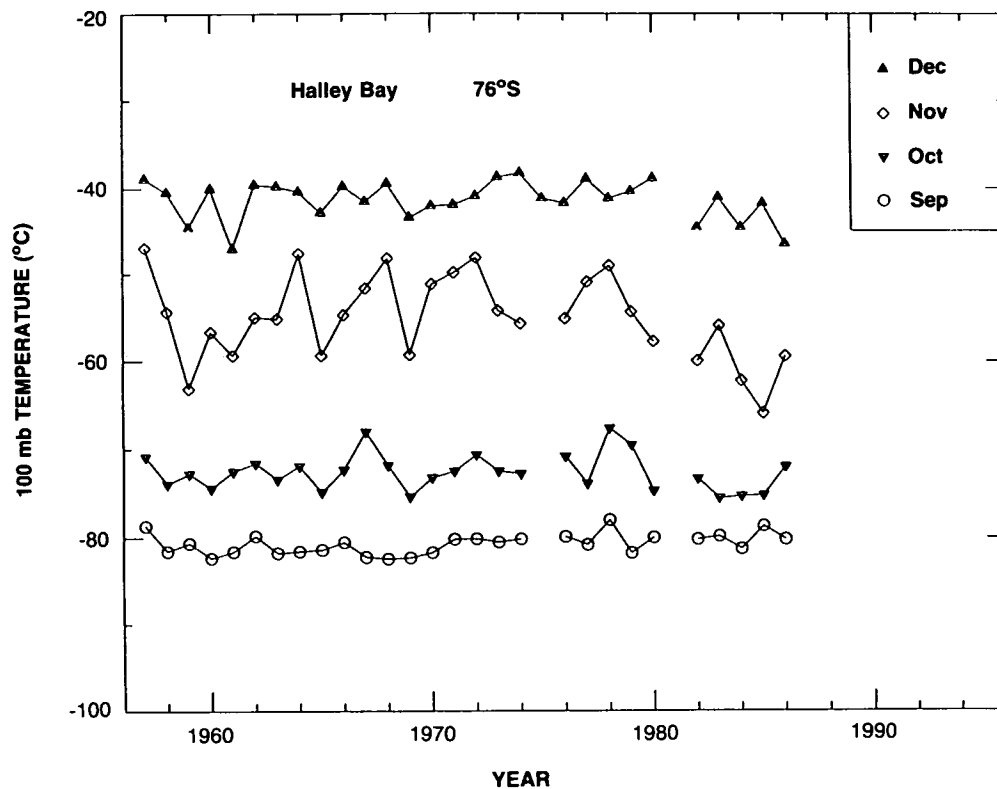


Figure 1.8.2-2. Monthly mean temperatures at 100 mbar for Halley Bay, 1958-1988 (from Gardiner, 1989).

between 1987 and the 1957-1975 extreme minimum exceed 10 K in early November. In 1988, with the less marked ozone depletion, temperatures were found to lie within the envelope of the 1957-1975 extremes.

Randel (1988) has extended the study of Newman and Randel (1988) to look specifically at spring 1987 using NMC data. Figure 1.8.2-4 shows the deviation of temperatures for September to December 1987 from the average for the period 1979 to 1986. The lower stratospheric cooling reached 6°C in October and 14°C in November, a value four standard deviations from the 1979-1986 mean. As with the earlier study, there is little evidence for changes during September. Of some interest is the warming observed in the upper stratosphere; this is qualitatively consistent with the modeling studies mentioned earlier (although Randel cautions that the temperature data at these levels should be considered a qualitative indication only, due to simplifications in the NMC analysis procedure at these levels).

Randel and Newman (1988) rederived linear temperature trends for the period 1979-1987 (compared with 1979 to 1986 in Newman and Randel [1988]). The addition of the single year's data has a substantial impact on the trends; for example, at 50 mbar at the South Pole the trend for 1979 to 1986 is close to zero for November, while including the 1987 data generates a cooling trend in excess of 0.5°C per year. This illustrates the problem of deducing trends from short-period data sets in regions with so much interannual variability.

Angell (1988a) presents temperature trends for four seasons from standard radiosonde observations. His "South Polar" region is the latitude band 60–90°S, and uses data from six stations. Of all the trends

POLAR OZONE

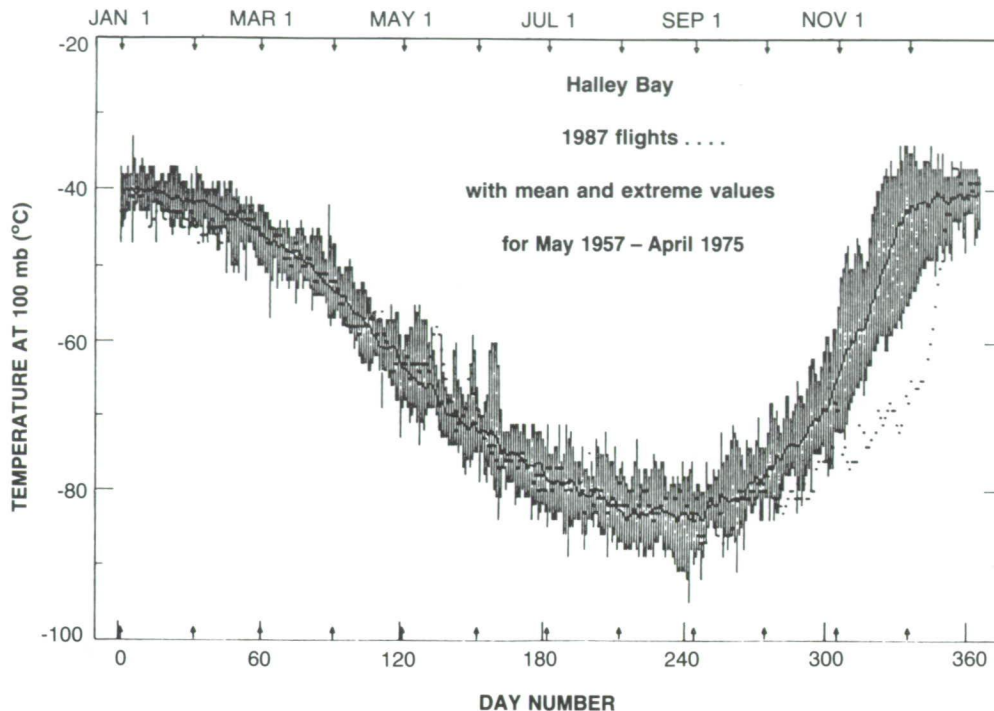


Figure 1.8.2-3. Temperatures at 100 mbar as a function of month from Halley Bay. The dots indicate measurements from 1987. The solid line shows the 1957-1975 mean, with the extremes during this period indicated by the vertical bars.

measured at any altitude or latitude region, the September-October-November trend at 100-50 mbar for the South Polar region is by far the most striking. For the period 1973-1987 the cooling amounts to 5°C per decade and is significant at the 1% level. Some evidence exists for coolings of 2°C per decade for the austral winter, but because of large interannual variations, Angell does not deem them to be statistically significant. For the remaining two seasons, the trends at these levels were found to be small and non-significant.

Temperature trends at the 100-mb level in the Southern Hemisphere were also evaluated by Koshelkov (1989), using data from 1964 to 1985 (two solar cycles). Koshelkov (1989) reported a small trend in the zonal mean temperature at 70°S during September of -0.03 K/yr from 1975 to 1985, while the trends obtained in October and November were considerably larger during this period, -0.25 K/yr and -0.46 K/yr, respectively. Essentially no trend was obtained during the winter months of July and August during the 1975-1985 period, while a slight cooling (-0.22 K/yr) was deduced for the earlier 1964-1974 period.

A different view is presented by Iwasaka et al. (1989) who used radiosonde data from Syowa from 1966 to 1987. Comparing means for the period 1981 to 1987 with means for 1966-1980, it was found that for pressure levels 50 to 100 mbar cooling occurred in all months, except for a short period in mid-winter. The most prominent changes were found in October/November when the later period was found to be up to 9°C cooler than the mean for 1966-1980, with 2°C coolings extending into January. When these changes were scaled by the standard deviations calculated using the 1966-1980 data, the trend was found to be most clear from mid-October to late February; the 1981-1987 temperatures were found to be more than 2 standard deviations from the 1966-1980 mean. From March to October the temperature changes were found to be less than 1 standard deviation from the mean.

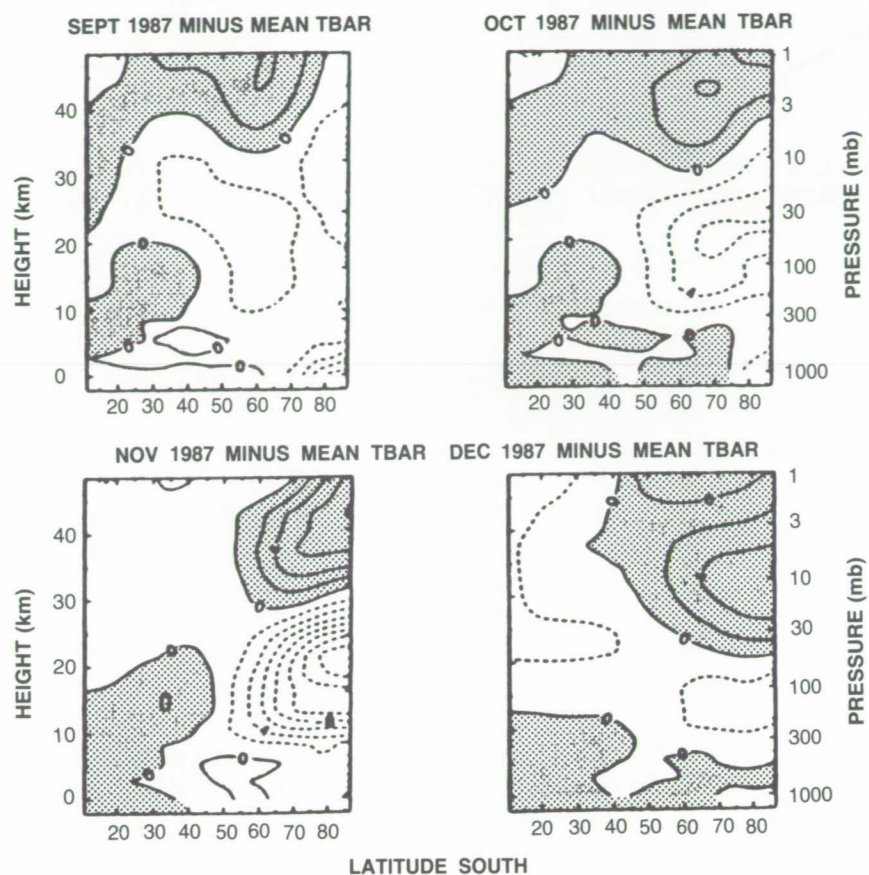


Figure 1.8.2-4. Deviation of NMC zonal mean temperatures for 1987 from the 1979-1986 mean for the period September to December (from Randel, 1988).

Trenberth and Olson (1989) have performed a detailed study of temperature changes at McMurdo and South Pole stations and warn against the dangers of forming monthly average temperatures in regions with irregular observations and large annual cycles. The conventional method of forming monthly-means is to simply average all available observations. Such a procedure is adequate provided that observations are made regularly or there is little change in mean temperature during the month. However, the difference in mean temperature between the first and last day of October at 70 mbar at South Pole is 27°C; a monthly mean formed from a few observations at either the beginning or the end of the month could lead to a biased mean. This is a very real problem, particularly at high altitudes. Trenberth and Olson show that the total number of observations at 100 mbar at McMurdo during October has varied between 2 and 42 over the past decade. Differences between monthly means calculated from a mean of all observations and the average of daily means were found to exceed 2°C on some occasions.

In order to examine recent temperature trends, Trenberth and Olson defined a mean annual cycle at each level at each station, using least squares harmonic fits to daily mean temperatures. Deviations of daily values from this annual cycle were then computed; these deviations were then averaged to produce a monthly anomaly.

POLAR OZONE

At South Pole station, little change of note was found in September, consistent with other studies. In October trends were most evident at 50-100 mbar, and since 1985, temperatures have gone outside the range of observed interannual variability since 1961. The trend is also visible in November, but this month is found more subject to large interannual variation. A significant cooling is also found in Dec-Jan-Feb, and is consistent with changes reported by Iwasaka et al. (1989) from an analysis of observations from Syowa Station. The years 1985-1987 were found to be about 2°C cooler than the long-term mean.

Trenberth and Olson compare their analysis with the NMC analysis. At the South Pole, at 70 mbar, the two analyses display a root-mean square difference of 2.4°C between 1979 and 1987 for October. At McMurdo, the average difference at 100 mbar is 5.8°C and reaches 11.7°C in 1982; they comment that there is little resemblance between the trends and interannual variability from the NMC data and the actual observations from McMurdo.

The question of whether temperature trends are greatest in October or November appears unresolved. Data from Halley Bay show the most noticeable changes in November, in agreement with the Syowa analysis of Chubachi (1986). While the 8-year data set of Newman and Randel (1988) indicates that most the trend is in October, the addition of 1987 to this data set markedly reduces the difference in trends between October and November (Randel and Newman, 1988).

1.8.3 Causes of Temperature Trends

Calculation of the diabatic response of the lower stratosphere to a depletion of ozone is relatively straightforward. As discussed in Section 1.8.2, one-dimensional radiatively determined calculations of the effect of ozone depletion are in relatively good agreement, and can certainly account for a substantial part of observed changes in the lower stratosphere temperatures. Since OTP (1989) a number of studies have performed similar calculations, but using models that allowed for a dynamical response to the temperature changes.

Chipperfield and Pyle (1988) used a 2-D model and imposed a depletion of about 120 DU on a model's predicted Antarctic springtime ozone column of 270 DU. They found temperature decreases exceeding 9 K at 70 mbar by the end of October and, like the 1-D calculations, found substantial warming (reaching 6°C) in the upper stratosphere. Figure 1.8.3-1 shows their predicted temperature change at 39 mbar between the runs with and without the ozone hole. Clear differences in temperature can be seen to persist until late March. These exceed 4°C during January. This indicates that temperature changes outside the springtime may also be due to the after effects of the spring time ozone depletion. This may account for the observations at Syowa (Iwasaka et al. 1989) of a temperature trend in January, given the small decreases in summertime ozone reported in Section 1.1.3. Chipperfield and Pyle's coupled model allows study of the seasonal cycle of ozone as well as temperature following the ozone hole. Although the calculated ozone abundances recovered substantially after the end of October, ozone decreases as large as 15% persisted in January, and remained greater than 5% into early February (Pyle, personal communication, 1989). Chipperfield and Pyle's calculation does not allow us to distinguish between whether the January cooling is due to the lingering ozone depletion or to the long radiative relaxation times delaying the recovery of the temperature. Given radiative relaxation times of the order of 100 days in this region, a 9 K perturbation to temperatures in late October might cause a cooling of 3 K in January.

Two sets of 3-D general circulation calculations have been performed. Kiehl et al. (1988) used the NCAR Community Climate Model. Their imposed ozone hole (which reached a minimum of 160 DU in early October, compared with a control calculation of about 320 DU during springtime) caused coolings of

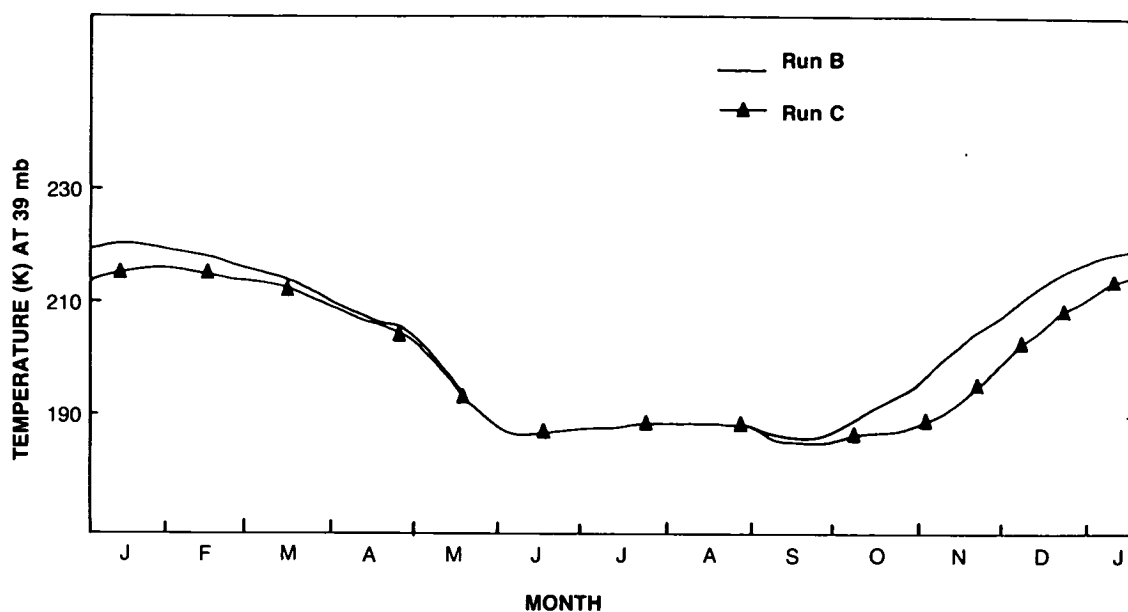


Figure 1.8.3-1. 2-D model temperatures at 39 mb and 76°S with (Run C) and without (Run B) an imposed ozone hole (from Chipperfield and Pyle, 1988).

6°C by the end of October (Figure 1.8.3-2). These authors also found a heating above 10 mbar that exceeded 4°C for some periods. Unlike the simpler model studies, they attributed little of this warming to changes in diabatic forcing. They attributed the difference to the particular vertical profile of the ozone depletion used. The behavior appeared to be closely tied to the model dynamics; in a second experiment with different initial conditions, they found the upper stratospheric temperature changes differed by a factor of two from those found in the first calculation. Rowntree and Lean (personal communication) used the UK Meteorological Office GCM; they imposed a depletion similar to that found in 1987 and, at 90 mbar, obtained coolings of 16 K by the end of November.

A difficult problem concerns the possibility that changes in temperature have altered the dynamical heating in the polar vortex. Some evidence of changes is presented by Kiehl et al. (1988). In their calculations with the imposed ozone hole they found increased downward motion during September and October, which results in a dynamical heating. Further, by the end of November, no final warming had occurred, in contrast to the control simulation. Further work by the same group (Boville, personal communication 1988) shows that an imposed ozone hole can delay the transition to easterlies by 10 to 14 days. Newman and Schoeberl (1988) have presented some observational evidence that years with low ozone are associated with late vortex breakdowns, at least at 100 mbar.

Thus, modeling work performed so far has provided strong evidence that the ozone depletion is likely to lead to a marked temperature trend in the lower stratosphere in October and November, and a smaller warming of the upper stratosphere. The role of dynamics in altering the temperature structure has not yet been studied in great detail, but there is now some evidence that the changes in temperature structure can delay the breakdown of the vortex.

It is important to recognize that these studies do not include a number of potentially important processes. The direct radiative effects of PSCs are ignored and the effects of dehydration (e.g., Ramaswamy

POLAR OZONE

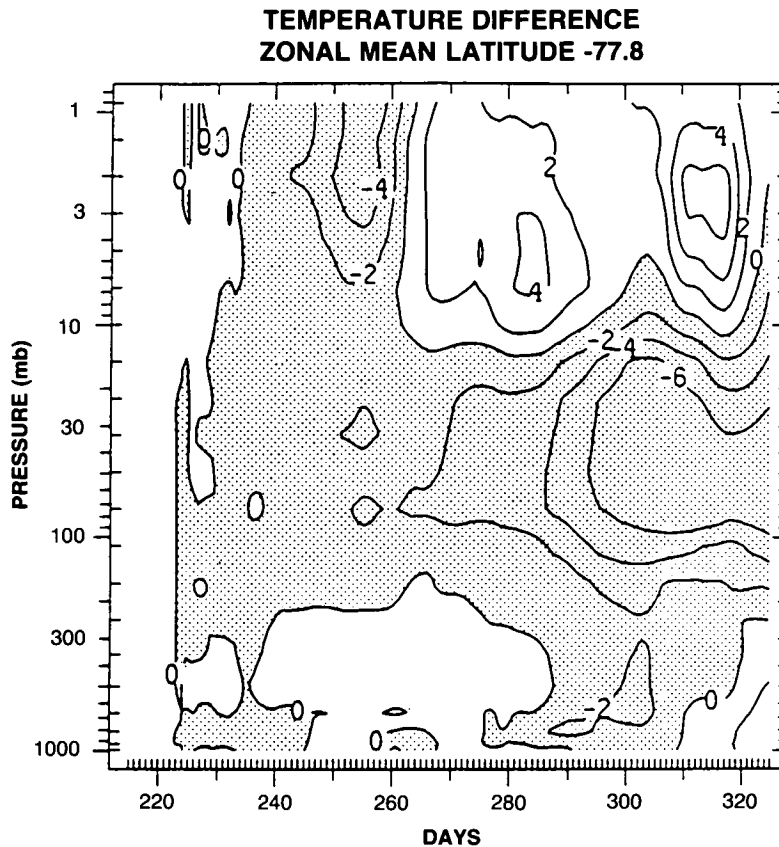


Figure 1.8.3-2. Deviation of zonal mean temperature for a calculation with an imposed ozone hole from a control run without the hole, using the NCAR Community Climate Model (from Kiehl et al., 1988).

1988; O. B. Toon et al. 1988; Kelly et al., 1989) are not considered. The loss of water vapor leads to an effective heating of the Antarctic stratosphere that may amount to several tenths of a K/day (Pollack and McKay, 1985; Shine, 1986); this is a significant perturbation to the radiative budget of the region. Such processes would be important in the prediction of temperature changes if there had been a significant change in dehydration or PSC formation over the period in which the ozone hole had developed; the PSC observations shown in Section 1.2 suggest that a long-term trend in PSC frequency has occurred on average in the month of October, but the likely radiative effects of these trends have not been studied in detail.

A number of workers have suggested mechanisms that may, over the long term, affect the thermal balance of the lower stratosphere. For example, it is well known that increased concentrations of greenhouse gases will lead to a cooling of the stratosphere which may affect the duration and extent of PSCs (Blanchet, 1989; Shine, 1988). Further, Blake and Rowland (1988) have pointed out that likely increases in stratospheric water vapor resulting from increased emissions of methane lead to an increase in the temperature at which PSCs can form (especially Type 1 clouds, which are believed to be particularly sensitive to water content; see Section 1.3 and Hanson and Mauersberger, 1988a,b). However, these effects are unlikely to be as important as changes in temperature, since the formation of PSCs is more sensitive to temperature decreases than to changes in the water vapor mixing ratio. Indeed, the water vapor on its own will lead to a cooling of the lower stratosphere, increasing the probability of PSC formation. The possible coolings could be

balanced by a number of mechanisms. These include the possibility that PSCs warm the lower stratosphere (see Section 1.2.4), the effective warming induced by dehydration and altered dynamics. In the absence of detailed modeling, it is not yet possible to assess the size and importance of the above mechanisms.

1.9 CALCULATED AND OBSERVED CHANGES IN ULTRAVIOLET RADIATION AT THE GROUND

The prime reason for concern about stratospheric ozone depletion is the threat of biological damage due to increased solar ultraviolet radiation reaching the surface. Studies considering the effect of Antarctic ozone depletion on surface ultraviolet irradiances have been performed by Frederick and his colleagues (Frederick and Snell 1988; Frederick et al., 1989; Lubin et al., 1989a, b). The spectral region of most relevance here is the UV-B (280-320 nm). Shorter wavelength radiation (UV-C) is unable to penetrate to the surface, while UV-A (320-400 nm) occupies a region of relatively low absorption by ozone.

Frederick and Snell (1988) presented calculations of the downward solar irradiance at the surface at Miami (chosen as a typical low- to mid-latitude station) and McMurdo Station for both depleted and non-depleted springtime ozone amounts. For all realistic ozone amounts, the UV exposure in the Antarctic spring is lower than typical values at Miami, indicating that visitors to the Antarctic are unlikely to be in danger of excessive doses at this time of year. However, life indigenous to the Antarctic is likely to receive increased doses. To elucidate the danger, Frederick and Snell weight the calculated fluxes by an action spectrum which indicates the relative sensitivity of organisms to UV exposure. One such action spectrum is for erythema, which is believed to be a precursor to skin cancer development. Figure 1.9-1 shows this

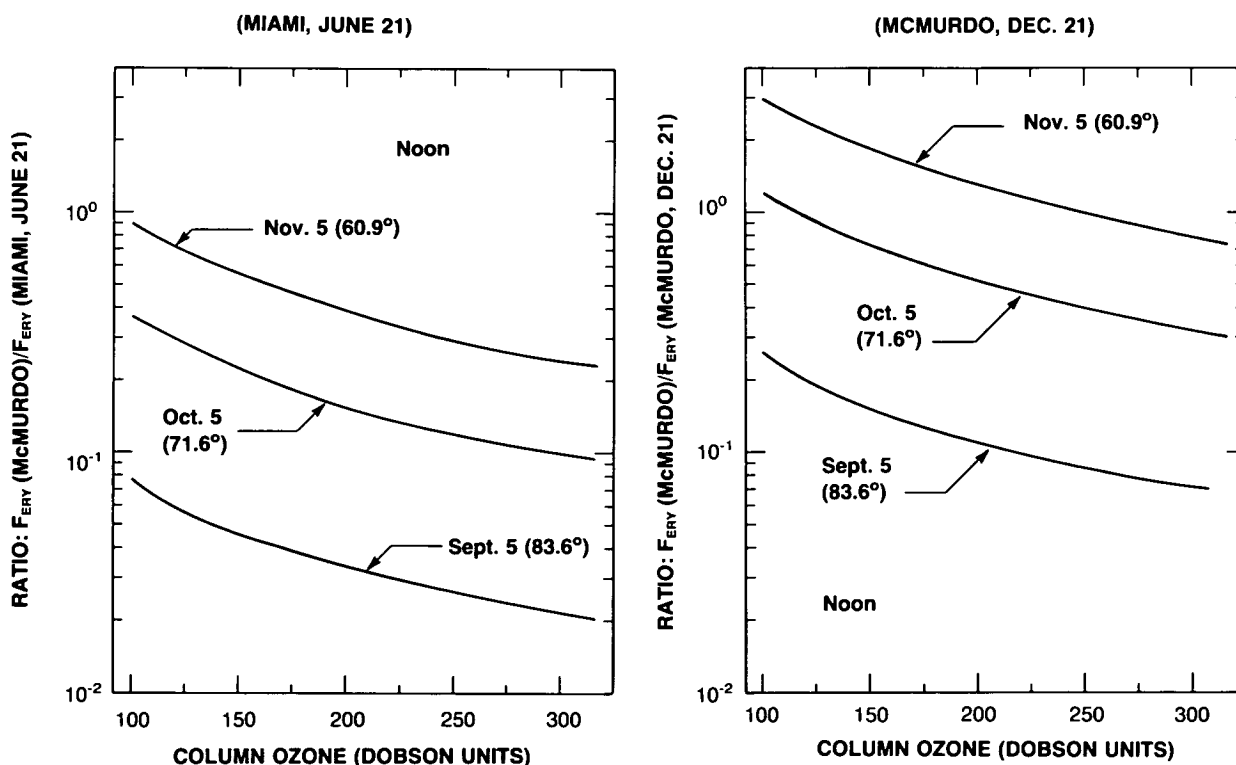


Figure 1.9-1. Ratio of biologically effective downward radiation computed for a range of ozone values at McMurdo during the austral spring to that for McMurdo on 21 December for an ozone column of 350 D.U. All values refer to local noon; solar zenith angles appear in parentheses (from Frederick and Snell, 1988).

POLAR OZONE

Table 1.9-1. Comparison of noontime irradiances computed for McMurdo during October with values for the summer solstice

Spectral Region	Irradiance ratio ^a	
	Day 276/Day 355	Day 300/Day 355
317.5–322.5 nm	0.38	0.83
303.0–307.7 nm	0.96	2.7
298.5–303.0 nm	2.1	8.5
DNA effective	0.85	2.5
R-B effective	0.54	1.1

^aDay 276 is October 3, with a column ozone value equal to 141 DU; day 300 is October 27, with a column ozone equal to 150 DU and Day 355 is December 21 with column ozone equal to 350 DU.

biologically effective downward irradiance at McMurdo for local noon in early October, November, and December as a function of ozone column, expressed as a fraction of the irradiance calculated for McMurdo at the summer solstice with a total ozone column of 350 DU. From this figure it is clear that biologically active irradiances in the springtime can exceed those experienced at the unperturbed Antarctic summer solstice. When averaged over a day, it is found that a 5 November value of 150 DU (as observed in 1987) gives an irradiance 50% greater than the solstice value.

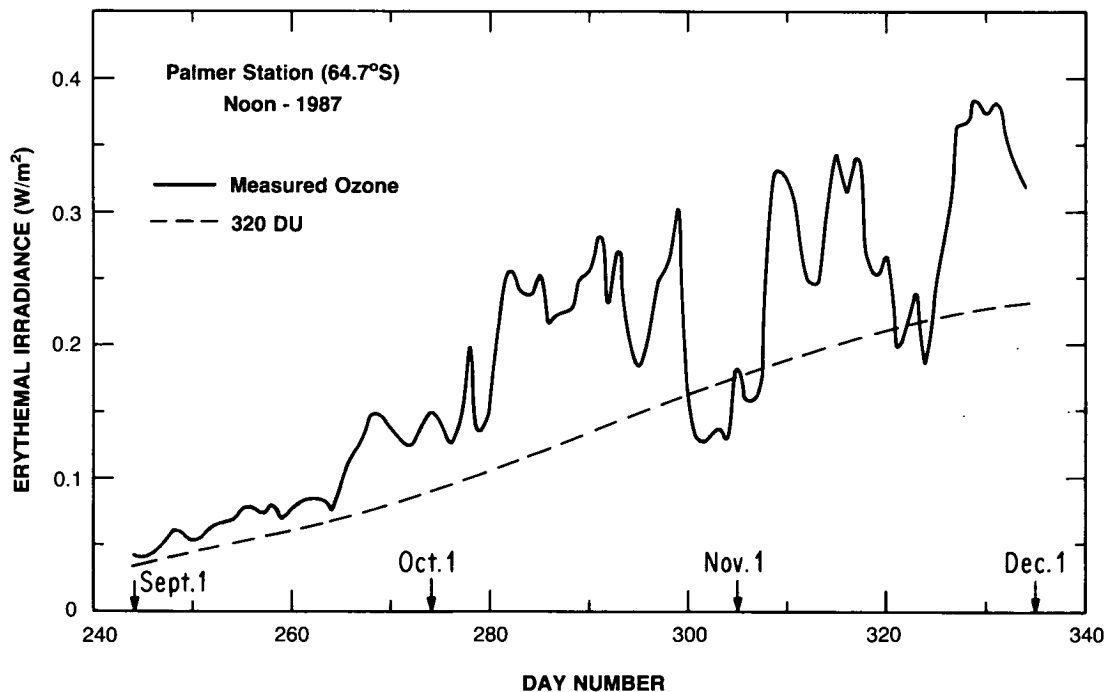


Figure 1.9-2. Computed time history of erythemal irradiance for local noon and clear skies over Palmer Station for September 1 to November 30, 1987 (from Frederick et al., 1989).

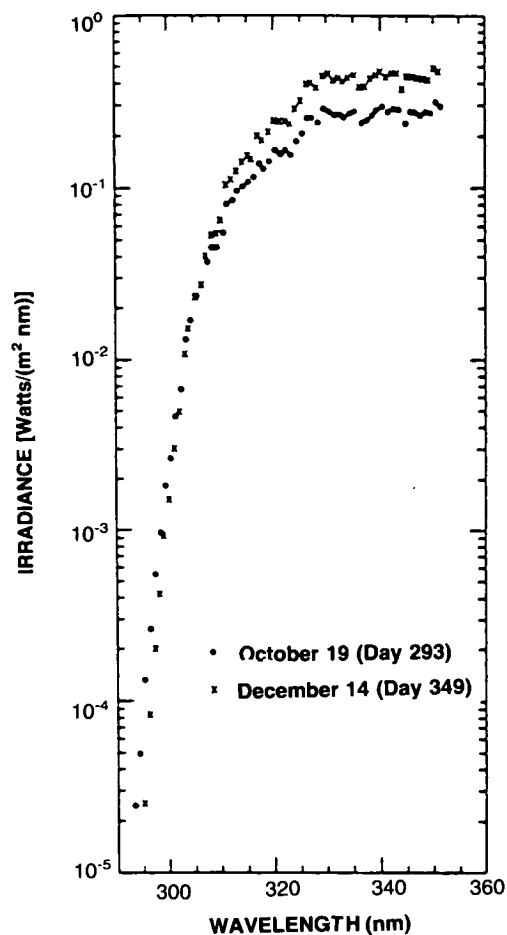


Figure 1.9-3. Spectra of UV solar irradiance measured from Palmer Station at local noon on 19 October and 14 December. The solar zenith angles were 53-54 degrees and 41-42 degrees respectively (from Lubin et al., 1989b).

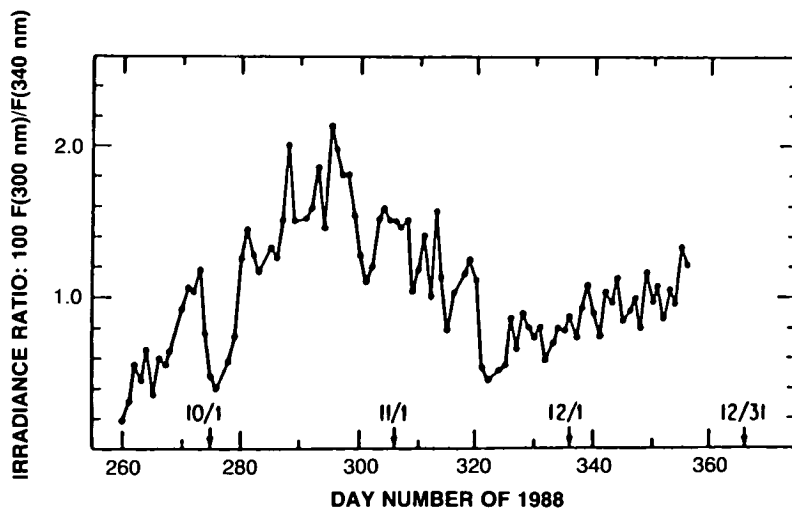


Figure 1.9-4. Ratio of noontime irradiance for 295-305 nm to that for 335-345 nm, for the period 19 September (day 260) and 21 December, 1988 (day 356). The plotted ratios have been multiplied by 100 (from Lubin et al., 1989b).

POLAR OZONE

Lubin et al. (1989a) and Frederick et al. (1989) present calculations of UV radiation in the austral spring for McMurdo Station and Palmer Station, respectively; column ozone amounts are taken from TOMS observations. Table 1.9-1 presents results from Lubin et al. (1989a) for various wavelengths and two alternative action spectra (DNA effective and Robertson-Berger effective). Again the irradiances are expressed as a fraction of the summer solstice values. These model calculations predict a significant perturbation to the UV dose by late October. Frederick et al. (1989) extend the calculation to late November, and choose the latitude of Palmer Station (64.7°S). UV irradiances are compared with those calculated for an ozone column of 320 DU, a typical pre-depletion value. Figure 1.9-2 shows the irradiances, weighted by the erythemal action spectrum for local noon. The increased irradiance is striking, exceeding the reference values by a factor of 2.3 on 5 October and 1.7 on 15 November.

As is pointed out in these studies, the increased day length and decreased solar zenith angle experienced as the summer solstice approaches means that any extension of the depletion into December could cause UV levels to well exceed those normally received.

Observational support for these calculations has been presented by Lubin et al. (1989b). While observations from the unperturbed Antarctic stratosphere are lacking, current observations present strong evidence that ozone depletion (even in the relatively unperturbed austral spring of 1988), caused marked perturbations in surface irradiance in the UV. Lubin et al. measured surface irradiance between 295 and 350 nm using a scanning spectroradiometer at Palmer Station. Figure 1.9-3 shows spectra for 19 October, an ozone-depleted period, and 14 December. Given the increased solar zenith angle at local noon at the later date, it would be expected that the irradiances would be higher in December. While this is true at the longer wavelengths (of which ozone absorbs little), at shorter wavelengths subject to stronger ozone absorption the October value exceeds that observed in December. Figure 1.9-4 shows the ratio of the irradiance at 300 nm and 340 nm for the period 19 September to 21 December. The 340-nm value is little affected by ozone. The purpose of using a ratio is to eliminate changes in irradiance resulting from changes in cloudiness. As can be seen from Figure 1.9-4, the ratio peaks during October, in contrast to the steady rise from solstice to equinox that would be expected in the absence of an ozone depletion.

A discussion of the biological consequences of the ozone depletion is beyond the scope of this report. Nevertheless, the above calculations and observations indicate that the Antarctic ozone depletion has caused a significant perturbation to the biologically effective UV irradiances reaching the surface. Several biological studies are currently examining the possible sensitivity of the spring bloom of phytoplankton to changes in UV radiation incident upon the surface waters surrounding Antarctica. Trodahl and Buckley (1989) emphasized that the radiation dose for organisms in the surface waters beneath Antarctic ice is greatest in spring, when the ice is relatively transparent. Ice turbidity significantly decreases the radiation dose in summer. Further studies of Antarctic biological systems are badly needed to assess possible impacts.

1.10 ARCTIC PHOTOCHEMISTRY

The foregoing discussion has illustrated the important chemical effects induced by polar stratospheric clouds and their relationship to ozone depletion. As shown in Section 1.2, such clouds are far more prevalent in Antarctica than in the Arctic (as first pointed out by McCormick et al., 1982). Further, Section 1.7 illustrated the pronounced differences in dynamical structure and temperature between the two hemispheres. These considerations suggest that the photochemistry of the Arctic winter and spring may be rather different from that of the Antarctic, and is likely to exhibit a greater degree of interannual variability.

In the following, observations of chemical constituents in the Arctic stratosphere will be summarized, with a view towards gaining insight to the possibility of Arctic ozone depletion.

1.10.1 Observations Prior to the 1988-1989 Arctic Winter

As emphasized in Section 1.6, observations of photochemical species in the Arctic polar regions have long provided cause to question purely gas-phase photochemical schemes. Most prominent among these data were the total NO_2 column abundance measurements by Noxon and co-workers. Noxon (1979) emphasized the puzzling occurrence of exceedingly steep latitudinal gradients in NO_2 column amounts in winter. He noted that the steep gradients were associated with stratospheric flow from polar regions. One such Noxon cliff is depicted in Figure 1.10.1-1. Because of the prominent role played by NO_2 and its interaction with chlorine species in ozone depletion (as discussed in Sections 1.3 through 1.6), the characteristics of the Arctic Noxon cliff will next be discussed in some detail.

Noxon noted that not only the absolute amount but also the diurnal variation in NO_2 was unusually small on the poleward side of the cliff, and suggested that this implied conversion of NO_x into a form whose photochemical lifetime exceeds a few days, such as HNO_3 . Noxon et al. (1979) presented observations of the NO_2 column abundance during a wave number 2 sudden warming event in 1979, wherein the arctic polar vortex split in two and one of the low centers moved over western Canada. Observations made near the center of the low indicated NO_2 column abundances of only about $0.5 \times 10^{15} \text{ cm}^{-2}$ in late February,

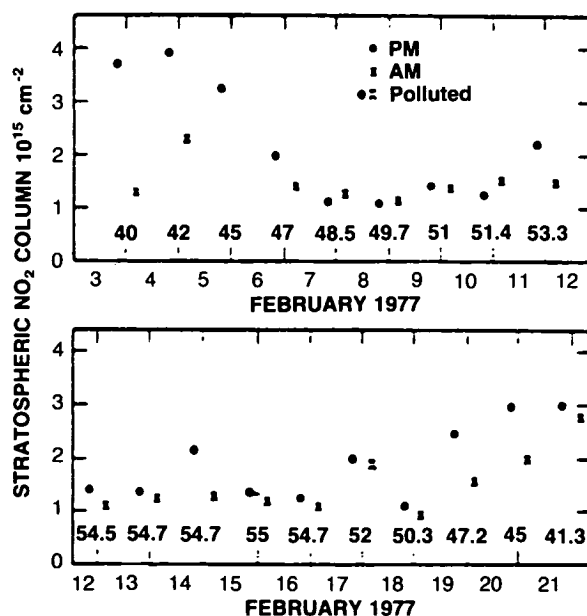


Figure 1.10.1-1. Observation of the Noxon 'cliff' from Noxon (1978). The variation of the column NO_2 is shown as a function of latitude, observed near 110°W longitude. North latitude is shown above the bottom line and the date is shown below it.

POLAR OZONE

lasting for nearly one week. These observations also pointed towards HNO_3 as a likely reservoir for NO_x in high-latitude winter, and, in retrospect, suggest that similar chemical processes to those that lead to ozone depletion in Antarctica could be active in the Arctic.

Noxon et al. (1983) presented a series of observations from various latitudes and emphasized the variable behavior of NO_2 depending upon temperature and flow regime. Figure 1.10.1-2 presents the mean annual cycle of stratospheric NO_2 observed by Noxon et al. (1983) from Point Barrow, Alaska (71°N), while Figure 1.10.1-3 presents the seasonal cycle obtained in three winter-spring observing sequences. These may be compared to observations from 78°S by McKenzie and Johnston (1984), Mount et al. (1987), and Keys and Johnston (1988, see Section 1.6.2). On some occasions in January and February, the NO_2 abundances observed in the Arctic were as low as those obtained in Antarctica, even at latitudes as far equatorward as 50°N (e.g., Noxon et al., 1979). On the other hand, it is evident that the averaged spring NO_2 values over Antarctica are considerably lower than those observed by Noxon et al. (1983) even when account is taken for the differences in the locations of the two sets of measurements relative to the polar vortices. Note that the lowest values obtained in March of the 3 years studied are of the order of $3.5 \times 10^{15} \text{ cm}^{-2}$ even within the polar vortex, while those obtained at McMurdo in the conjugate month of September are often well below $1.0 \times 10^{15} \text{ cm}^{-2}$. This interhemispheric difference in NO_2 is likely to be closely related to the interhemispheric differences in circulation and temperatures noted in Section 1.1 and 1.7. Like ozone, NO_2 is produced in the middle and upper stratosphere at subpolar latitudes; indeed, NO_y and ozone are expected to have similar distributions. This implies that NO_2 column abundances are strongly dependent on downward, poleward transport processes as well as on chemical processes that control the partitioning of NO_y species. The important differences in NO_2 abundances obtained in the Arctic in March as compared to Antarctica in September are likely to reflect at least in part the generally much earlier stratospheric warmings of the Northern Hemisphere and the resulting downward transport of NO_y . Clearly,

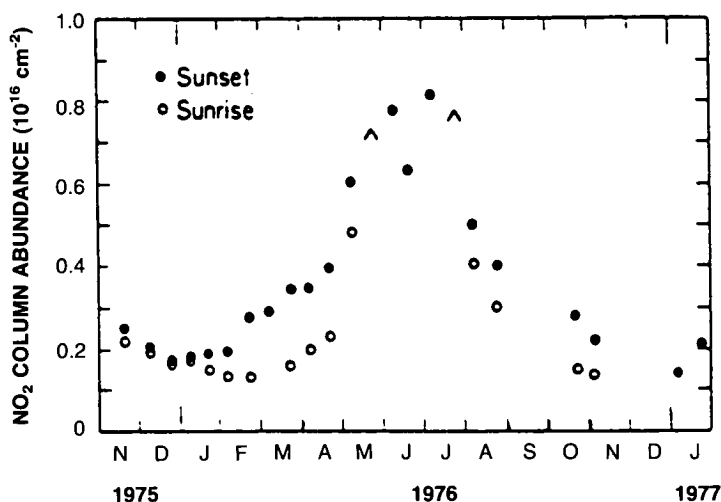


Figure 1.10.1-2. The mean annual cycle of NO_2 at 71°N (Point Barrow, Alaska) from Noxon et al. (1979). Solid circles are sunset measurements, while open circles are measurements taken at sunrise. The arrowheads denote upper limits.

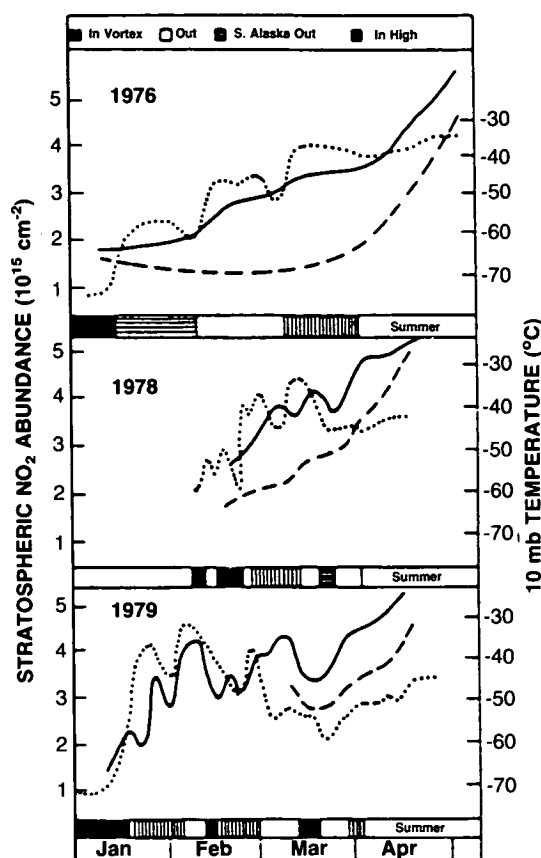


Figure 1.10.1-3. Variation of total NO_2 column abundance over Point Barrow, Alaska (71°N) in three different winter-spring seasons (from Noxon et al., 1983). The solid and dashed lines give the evening and morning NO_2 column abundances, respectively. The dotted line is the 10-mbar temperature over Barrow. The coding at the bottom indicates the position of Barrow relative to the polar vortex at 10 mbar.

this difference suggests that the time period in the spring when NO_2 abundances are suppressed sufficiently to allow effective ozone destruction through chlorine chemistry may be rather more limited in the Arctic than in the Antarctic.

A few measurements of the vertical profiles of reactive nitrogen species are also available from balloon observations. Ridley et al. (1987) presented measurements of NO and NO_2 near 50°N in summer and winter. Those authors emphasized the fact that the sum of NO and NO_2 was apparently reduced by a factor of 10 in winter as compared to summer, as shown in Figure 1.10.1-4. Since NO and NO_2 interchange rapidly with one another in the sunlit atmosphere, it is their sum that is important in considering, for example, the amount of nitrogen oxide available to form ClONO_2 . Thus, the observation of a substantial reduction in nitrogen oxides has important implications for chlorine chemistry. Ridley et al. concluded that the reduction of NO_x was consistent with formation of the N_2O_5 reservoir, based in part on trajectory analyses and observations of the diurnal variation of the total column (which was considerably greater than many of Noxon's observations).

POLAR OZONE

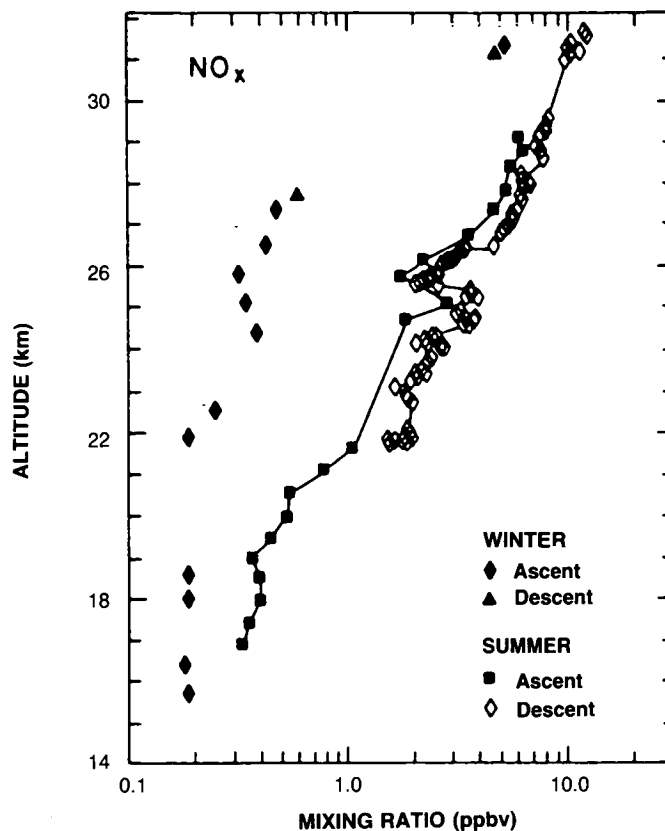


Figure 1.10.1-4. NO_x ($\text{NO} + \text{NO}_2$) mixing ratio profiles observed on balloon flights using a chemiluminescent detector launched from Gimli, Canada (50.6°N) on August 10, 1982 and December 15, 1982 (from Ridley et al., 1987).

More recent observations of the NO_2 column abundance in the Arctic winter include those of McCormick and Larsen (1986), Coffey et al. (1981), Mount et al. (1984), Russell et al. (1984), Pommereau and Goutail (1988) and Mount et al. (1988). Pommereau and Goutail examined the diurnal variability of NO_x chemistry and concluded that their data could not be understood without considering conversion into a longer lived storage species (e.g., HNO_3 , or removal from the gas phase via particles), and suggested that the observations imply that the removal must be active at temperatures as warm as -45°C . This temperature is far warmer than that appropriate to polar stratospheric cloud formation, suggesting that reactions on background sulfuric acid aerosols may play a role. While these later data have certainly improved the details of our knowledge of Arctic NO_2 abundances and variability, they have not led to major modifications to the general picture delineated by Noxon a decade ago. Indeed, it is worthy of note that while some improvements in our understanding have emerged from recent work, especially insofar as the interplay between NO_2 and N_2O_5 in disturbed conditions is concerned, it is nonetheless the case that recent studies of the importance of heterogeneous chemistry have shown that Noxon's conclusions regarding the origin of the cliff held a great deal of merit.

Solomon and Garcia (1983) pointed out that the relatively long photochemical lifetime of N_2O_5 under cold conditions and the rapid meridional flow induced by displacement and elongation of the Arctic polar

vortex could also make N_2O_5 an important reservoir for NO_2 under some conditions. They emphasized the need to consider the photochemical history of the air parcels, particularly when mid-latitudes receive air from dark polar regions, where NO_x is rapidly converted to N_2O_5 via gas-phase chemistry. Callis et al. (1983) and Zawodny (1986) showed that such processes were likely to be important in understanding satellite observations of NO_2 in polar latitudes. In particular, Zawodny (1986) showed several case studies illustrating that low NO_2 values were associated with flow of air parcels from the polar vortex, but that much higher values were observed when similar air parcels continued their trajectories and were subjected to a day or two of exposure to sunlight at lower latitudes. This observation pointed strongly towards N_2O_5 as an important NO_2 reservoir in those cases.

Observations of the total HNO_3 column abundance in the Arctic include those of Murcray et al. (1975), Coffey et al. (1981), Girard et al. (1982) and Arnold and Knop (1989). A more detailed view of the vertical and seasonal variations of HNO_3 is provided by the LIMS observations (Gille et al., 1984b; Austin et al., 1986b). Figure 1.10.1-5 presents observations of the zonally and monthly averaged HNO_3 distributions from LIMS.

As Austin et al. (1986b) and others have emphasized, the very large abundances of HNO_3 observed in high-latitude winter are difficult to reconcile with gas-phase photochemical schemes. Austin et al. (1986b) noted that the HNO_3 abundances and their temporal variations required a source of HNO_3 in the Arctic polar night. They suggested that the reaction $N_2O_5 + H_2O \rightarrow 2HNO_3$ might explain the observed trends if the reaction probability for N_2O_5 on background aerosol distributions were as little as 1.0×10^{-3} . Recent measurements of reaction probabilities for N_2O_5 on sulfuric acid/ H_2O aerosol by Tolbert et al. (1988a) and Mozurkewich and Calvert (1988) suggest that this process is likely to proceed at least as fast as this requirement; the recent study by Mozurkewich and Calvert suggests that the effective reaction probability may be as large as 0.05-0.09. Hofmann and Solomon (1989) discussed the possible photochemical effects of heterogeneous reactions on background sulfuric acid aerosol, and emphasized the particularly important role of such reactions in middle and high latitudes during winter and spring.

Although N_2O_5 formation and photolysis is likely to play an important role in determining some of the variability of NO_2 in the north polar regions so long as appreciable NO_x is present, insights gained from the understanding of Antarctic ozone photochemistry suggest that the Noxon cliff phenomenon is also certain to be related to the formation of HNO_3 via heterogeneous processes. The relative roles of the two reservoirs probably depend on temperature, flow patterns, and time. It is well known that polar stratospheric clouds are often present in the Arctic winter, if not as persistently as in Antarctica (as discussed by McCormick et al., 1982 and illustrated in Section 1.2). Heterogeneous conversion of N_2O_5 to HNO_3 on any nitric acid trihydrate particles present will augment, and in the winter months is likely to dominate, that due to conversion on background aerosol. Further, the incorporation of HNO_3 into PSC particles, their capacity to perturb the partitioning of ClO_x , and the possibility of denitrification through particle sedimentation are all likely to contribute to the low abundances of NO_2 observed at high latitudes.

In summary, observations of both NO_2 and HNO_3 point towards the importance of heterogeneous reactions in suppressing the abundance of NO_2 in Arctic winter and producing HNO_3 at rates considerably faster than those expected from gas-phase chemistry. These characteristics are clearly similar to those found in Antarctica, and imply that enhanced chlorine radical abundances should be expected in Arctic regions in the late winter and early spring.

Observations of chlorine-containing species were both more limited and more recent than those of the nitrogen species prior to the 1988-1989 Arctic winter. Girard et al. (1982) and Mankin and Coffey (1983)

POLAR OZONE

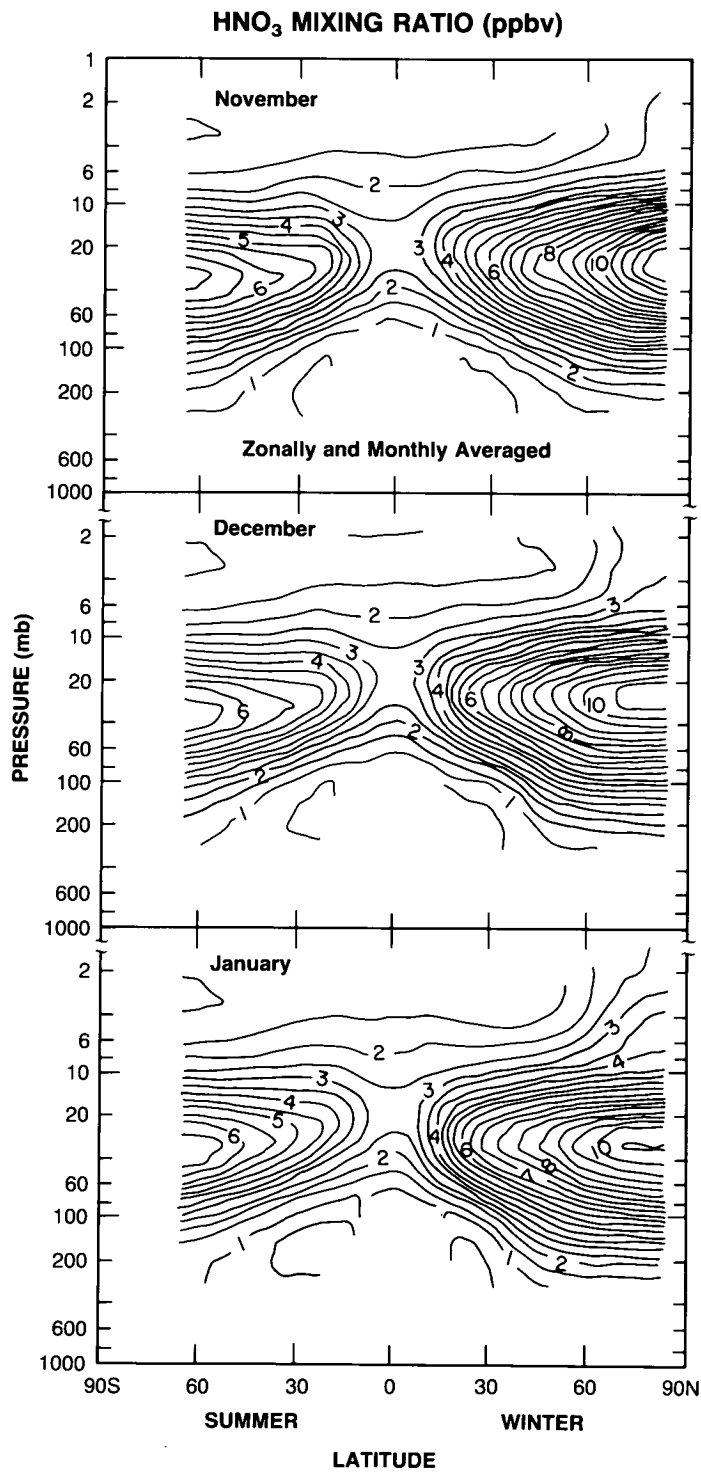


Figure 1.10.1-5. Zonally and monthly averaged HNO₃ mixing ratio distributions for November, December, and January from LIMS observations (from Austin et al., 1986b).

presented latitude surveys of HCl and HF abundances as shown, for example, in Figure 1.10.1-6, but the data were sparse above 50°N and were largely not obtained in winter. It is nevertheless interesting to note in the context of Section 1.6.1 that the HCl and HF abundances observed in the Arctic increase with increasing latitude, and often mirror one another, in contrast to the dramatic depletion of HCl obtained in the Antarctic winter vortex. This suggests that little conversion of HCl to more reactive forms of chlorine had occurred when those particular observations were obtained. Observations of HCl and HF obtained in the Arctic winter vortex in 1989 will be summarized in the next section .

During the winter of 1987-1988, ClO and OClO were both observed in the Arctic. The ClO measurements were carried out in aircraft flights up to about 61°N in western Canada (Brune et al., 1988). Although the ClO observations were obtained rather far from the center of the polar vortex, they were nonetheless of great importance because they revealed ClO mixing ratios of about 60 pptv, in contrast with most photochemical models whose predictions lie around 10-20 pptv for that latitude and time of year. The OClO observations were obtained by visible absorption using the moon as a light source from a latitude of 76.5°N at Thule, Greenland (Solomon et al., 1988). The Arctic polar vortex was centered very near the observing site during this period. Figure 1.10.1-7 presents a comparison of nighttime OClO observations in Antarctica in late August, in Greenland in early February, and at 40°N in Colorado in January. The Arctic measurements of ClO and OClO during the winter of 1987-1988 were thus considerably smaller than those of Antarctica, but were still substantially greater than gas-phase model predictions, suggesting that heterogeneous chemistry had perturbed the chlorine chemistry of the Arctic polar region in winter.

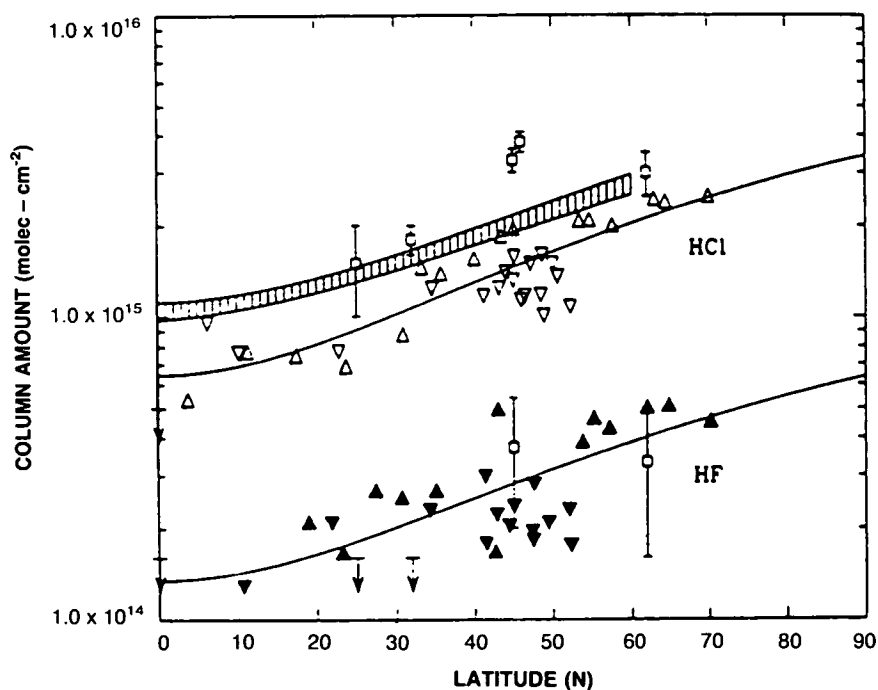


Figure 1.10.1-6. Latitude gradients HCl and HF in the Northern Hemisphere (from Mankin and Coffey, 1983). Upward pointing triangles are summer measurements; downward pointing triangles are winter measurements. The solid curves are least-squares fits to the data. Observations by Girard et al. (1982) are shown as squares with error bars. The hatched band represents model calculations.

POLAR OZONE

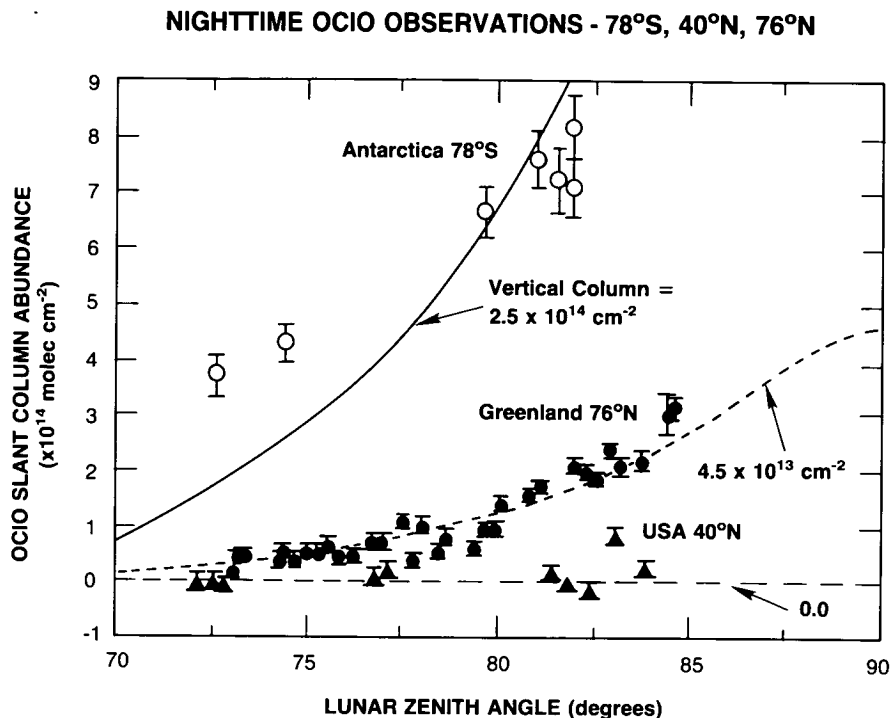


Figure 1.10.1-7. Observations of the nighttime abundance of OCIO versus lunar zenith angle at various locations (from Solomon et al., 1988)

1.10.2 Conclusions from 1989 Research

During January and early February, 1989, several extensive campaigns to probe the composition of the Arctic stratosphere were conducted. The NASA ER-2 and DC-8 aircraft were deployed from Stavanger, Norway, and observations were obtained as far north as the Pole and as far west as western Greenland. *In situ* and long-path instruments probed the composition of the polar stratosphere from these airborne platforms. Other groups of scientists conducted balloon experiments from Kiruna, Sweden and Alert, Canada. Further, measurements were conducted at Heiss Island, USSR, to document the changes in the ozone layer and understand the formation of PSCs. Some of the results from these experiments are currently being analyzed and all will ultimately be presented in peer-reviewed, scientific publications. In the following, we seek only to summarize the major points of these new studies insofar as they are currently available.

In many ways the Arctic Airborne Stratosphere Experiment (AASE) was similar to the Airborne Antarctic Ozone Experiment (AAOE). The major differences between the two campaigns (apart from some differences in instrumentation) were in the timing of the two experiments in relation to the different climatologies of the Arctic and Antarctic (Section 1.7), and their implications for photochemistry and microphysics. In particular, the AAOE experiment was carried out in Antarctica during August and September 1987. The results from that work provided evidence for ozone destruction and allowed measurement of the remarkable perturbations to photochemistry caused by polar stratospheric clouds (summarized in Section 1.6). However, it is quite likely that substantial processing by PSCs had occurred before the AAOE campaign began; thus the end results of PSC activity were clearly observed, but the process was largely not captured in action. The AASE experiment was carried out much earlier in the conjugate

Northern Hemisphere season (January and February). This was the period when widespread PSCs were just beginning to form, allowing study of the conversion of unprocessed to processed air and its subsequent photochemistry. However, substantial ozone loss was not expected during the AASE mission due to the much reduced solar illumination in polar regions at that point in the winter/spring season, and no unambiguous identification of photochemical ozone loss was made.

The observations of PSCs themselves during AASE were carried out by LIDAR, particle spectrometers, satellites, and via the NO_y instrument's enhancement in the presence of clouds. These observations confirmed the presence of both Type 1 and Type 2 clouds and showed that they occur at approximately the expected temperatures based on laboratory studies.

The observed abundance of ClO was far greater than that predicted by gas-phase photochemical models, reaching levels as high as 1100 pptv (enhanced by about a factor of 50 above gas-phase model predictions). Similar enhancements in OClO were also obtained, providing excellent cross-corroboration. ClONO₂ column abundances were elevated near the edge of the vortex, often reaching 3×10^{15} cm⁻², but decreased towards the interior of the vortex. These observations are consistent with the observations and interpretation of the ClONO₂ "collar" in Antarctica discussed by G.C. Toon et al. (1989a) and the observed relationship between NO and ClO noted by Fahey et al. (1989b).

The ratio between HCl and HF column abundances was about 3-4 outside the vortex (consistent with the above discussion) but decreased to values ranging between 2.5 and 1 inside the polar vortex (as compared to minimum values of 0.7 found in Antarctica). These observations strongly indicate chemical conversion of HCl to more reactive forms of chlorine. However, since the observed perturbation to the total column was smaller, the data suggest that chemical conversion was either less complete or occurred over a more restricted height range as compared to Antarctica. The combination of the above chemical observations points strongly towards the importance of PSC chemistry. A more direct link was found on some occasions when, in relatively homogeneous air masses (as indicated by atmospheric tracers such as N₂O), abrupt increases in ClO were observed. Those 'edges' in ClO could not be attributed to solar zenith angle effects and were associated in a number of cases with predicted edges in PSCs and hence in cloud processing.

Extremely low column abundances of NO₂ were found inside the vortex, dropping to values as low as 0.3×10^{15} cm⁻². As discussed above, these observations are consistent with those obtained by Noxon et al. (1979) and suggest that cloud processing had influenced the abundance of atmospheric NO₂. The observed abundance of NO_y reached a maximum of about 15 ppbv, and little evidence was found for denitrification prior to late January. Flights on January 30 and February 7 and 8 showed extensive denitrification similar to that found in Antarctica near 20 km altitude. *In situ* measurements of NO_y near 12 km suggested enhancements of the local NO_y abundances, very possibly through evaporation of particles sedimented from higher levels. On the other hand, measurements of the column abundance of HNO₃ were as large as 30×10^{15} cm⁻², much larger than those found in Antarctica. This suggests that although denitrification had clearly occurred at some altitudes, the PSC particles may have evaporated in the low stratosphere, limiting the column reduction of HNO₃. This view is consistent with the enhanced NO_y levels found at 12 km.

Perhaps the most important issue highlighted by the AASE campaign is the mechanism for denitrification. In contrast to the Antarctic measurements, the Arctic denitrification was associated with modest, if any, dehydration. The detailed mechanism for denitrification is not presently understood. The observation suggests that denitrification and the attendant important effects on chlorine chemistry (as discussed in Section 1.5) may take place at warmer temperatures than previously believed.

POLAR OZONE

The AASE investigators concluded that further studies were required to establish the extent of any ozone loss in 1989 given the highly perturbed photochemistry seen until mid-February. The winter of 1988/89 was somewhat unusual in that temperatures were exceedingly cold until the sudden warming in mid-February, when PSCs disappeared. In other years, the low stratosphere may remain sufficiently cold for PSCs to be present from early December and in some cases (e.g., 1979) from late November until at least the beginning of March (see Section 1.2), extending the period over which significant ozone loss may occur. Such interannual differences likely have a large effect on the net ozone depletion in the northern vortex.

Hofmann et al. (1989a) described some preliminary results from the Kiruna measurements. Particle counter measurements revealed PSCs near 20-25 km on both available flights. Further, as noted in Section 1.2, thin layers of very large particles were sometimes observed. Hofmann et al. emphasized observations of "notches" in the ozone mixing ratio profiles, as shown in Figure 1.10.2-1. The observed notches are qualitatively similar to those identified by Hofmann et al. (1987a) in association with the development of the Antarctic ozone layer, and Hofmann et al. suggest that the same mechanism may be responsible. The implied ozone depletion is about 10-25% near 20-25 km, and only about 3% of the total column. Hofmann et al. emphasize that their study is consistent with but not proof of ozone depletion, since transport processes could conceivably produce similar notches.

Rosen et al. (1989) report preliminary findings from the measurements carried out at Alert, Canada. The optical backscatter instrument clearly detected PSCs on several occasions, and study of the scattering color ratio suggested that the particles fell both into the 0.1-2 μm and 2 μm size ranges. No clear observations of Type 2 PSCs were obtained. The observed altitude range of the PSCs was in fair agreement with

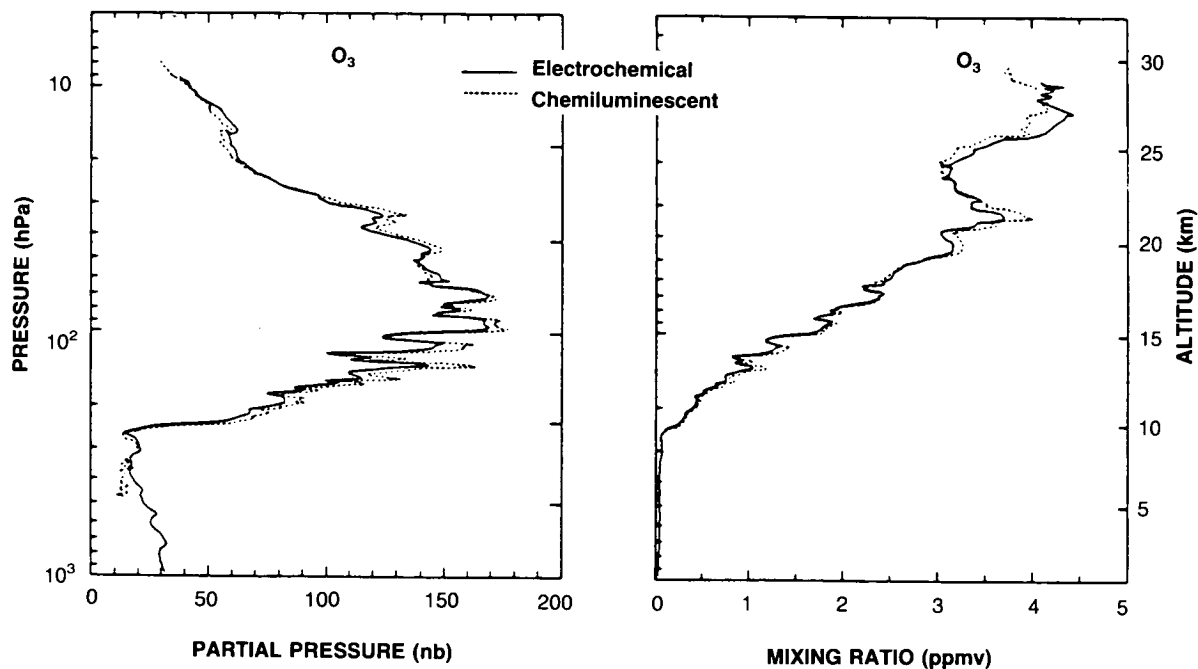


Figure 1.10.2-1. Ozone partial pressure and mixing ratio profiles measured at Kiruna, Sweden, on 23 January, 1989 (from Hofmann et al., 1989b).

predictions based on nitric acid trihydrate thermodynamics. Measurements of HNO_3 suggested that perhaps half of the available HNO_3 had been incorporated into the clouds. On one occasion, nitric acid vapor was almost completely removed near 23.5 km, although no clouds were observed at that level, suggesting possible denitrification.

The Heiss Island study showed that PSCs occurred at temperatures below about -80°C and found no apparent correlation between PSCs and ozone. This important finding suggests that direct removal of ozone on PSCs is unlikely. They also observed a considerable displacement between the temperature minimum and the occurrence of PSCs (by about 5 km altitude). They therefore conclude that denitrification may have occurred, reducing the amount of condensate (HNO_3) available for cloud formation near the temperature minimum. Finally, they noted that there was no convincing evidence for an anomalous ozone decrease similar to that over Antarctica (Khattatov et al., 1989).

Thus, it is clear that a wide range of observational studies conducted in the 1988-1989 boreal winter established perturbations to Arctic photochemistry quite similar to those obtained in Antarctica. However, it was difficult to identify a photochemical ozone loss in association with the observed chemical perturbations. Figure 1.10.2-2 presents the 30-mb temperatures observed during this season. Zonal mean values at 80°N and 60°N are shown, along with the minimum temperature within the polar vortex from NMC analyses (R. Nagatani, personal communication, 1989). As discussed in Section 1.7, a strong major warming occurred around day 65 (mid-February). Therefore, the ozone changes anticipated during this year are considerably smaller than those obtained in Antarctica, in part because air sufficiently cold for rapid ozone loss through ClO dimer photolysis (see Figure 1.5.1-1) was not subject to much solar illumination. Further, mixing of

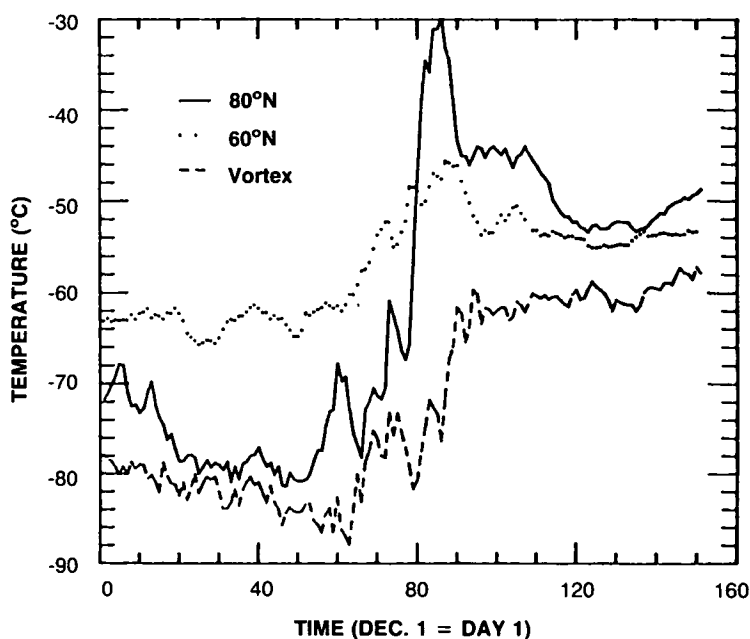


Figure 1.10.2-2. NMC temperatures at 30 mb for the 1988-1989 Northern Hemisphere winter-spring season. Zonal means for 60°N and 80°N are shown, along with the minimum temperatures within the polar vortex (from Nagatani, personal communication, 1989).

POLAR OZONE

air containing high levels of reactive nitrogen in association with the warming may have returned the chlorine partitioning to nearly normal status by about the end of February. Thus, because of warm temperatures or because of mixing associated with the warming (or perhaps both factors) little ozone loss would be expected after about February 15, 1989.

The Antarctic ozone decline occurs largely in September, when the polar cap becomes illuminated and temperatures remain cold. By analogy, one might expect an Arctic ozone depletion in the contemporary atmosphere if temperatures remained cold and the polar vortex relatively isolated as late as the conjugate Northern Hemisphere month of March. Although these conditions were not met during the 1988-1989 Northern Hemisphere winter, other years in the climatological record display different behavior. Figure 1.10.2-3 presents observations of temperatures at 30 mb in the zonal mean for 60°N, 80°N, and the vortex minimum from the NMC analyses for the winter of 1975–1976, one of the coldest Northern Hemisphere spring seasons on record. In that year, the temperatures remained below -70°C until about mid-March. No ozone loss would be expected in 1975–1976, since the chlorine content of the stratosphere was much lower than contemporary levels (Figure 1.6.4-5). However, the studies described in this Section suggest that it is likely that significant Northern Hemisphere ozone loss would occur if a winter-spring season like that of 1975-1976 were to occur in the near future.

1.11 PRINCIPAL CONCLUSIONS AND OUTSTANDING ISSUES

There is now very strong evidence that the ozone depletions observed over Antarctica in spring since the late 1970s are largely the result of chemical reactions with chlorine and bromine compounds, introduced

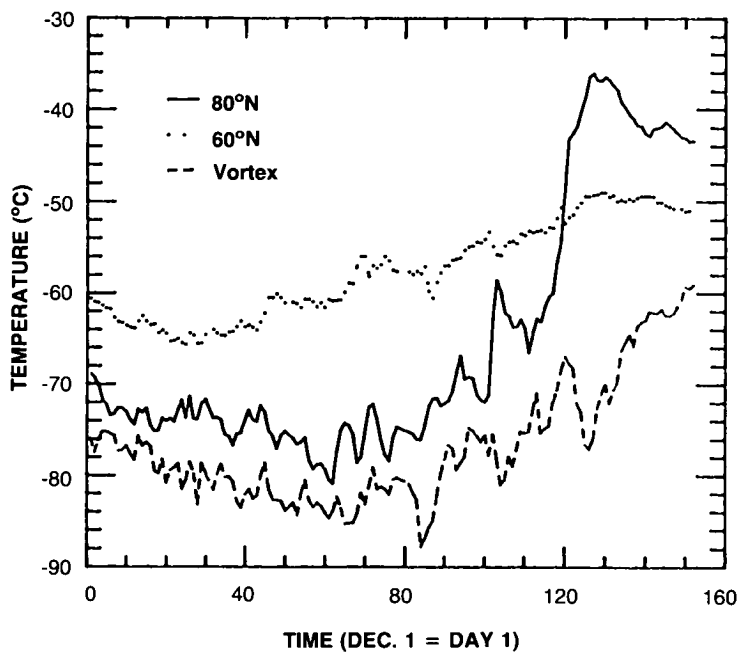


Figure 1.10.2-3. NMC temperatures at 30 mb for the 1975–1976 Northern Hemisphere winter-spring season. Zonal means for 60°N and 80°N are shown, along with the minimum temperatures within the polar vortex (from Nagatani, personal communication, 1989).

into the atmosphere mainly in the form of man-made chlorofluorocarbons and halons. Although some uncertainties remain, in semi-quantitative terms the processes that lead to ozone destruction are well understood. Air containing chlorofluorocarbons (CFCs) and halons enters the stratosphere primarily at equatorial latitudes. In the middle and upper stratosphere the CFCs are broken down by sunlight, releasing chlorine. Much of the available chlorine forms the relatively inert reservoirs, HCl and ClONO₂, particularly as the air descends to low altitudes. The air then moves poleward and downward on seasonal timescales, with some lateral dispersion. In the absence of solar heating, the polar regions cool during the winter months, eventually reaching temperatures at which nitric acid trihydrate and then water ice clouds can form in the low polar stratosphere. On the cloud particles, the HCl and ClONO₂ undergo heterogeneous conversion to highly reactive forms. In sunlight, chemical reactions then release reactive chlorine radicals produced by the heterogeneous chemistry. Chlorine (and bromine) monoxide are observed at levels sufficient to destroy ozone at rates of up to a few percent per day, consistent with observations, leading to a springtime ozone decline.

The effectiveness of this chlorine/bromine catalyzed ozone destruction is enhanced by the heterogeneous conversion of NO_x to nitric acid, which decreases (or even essentially eliminates) the possibility of reformation of the ClONO₂ and HCl reservoirs. Further, sedimentation of cloud particles can remove a substantial fraction of the available NO_x, leading to an even greater and long-lasting suppression of NO_x, ClONO₂ and HCl, and a corresponding enhancement in reactive chlorine. These processes allow high chlorine abundances to be sustained long enough to yield local ozone depletions of over 90% at some levels, and height-integrated depletions on the order of 50%. This picture is based on strong direct evidence from airborne and ground-based measurements made in Antarctica during 1986 and 1987, along with a range of laboratory kinetics and theoretical studies.

The interannual variability of the Antarctic ozone hole, and in particular the correlation between the depth of the ozone hole with the QBO, is not fully understood. However, the magnitude of the ozone depletion observed in 1988 compared to the exceedingly low ozone values of 1987 is qualitatively consistent with the above picture and may be at least partially attributed to the less extensive cold temperatures, fewer PSCs, and more vigorous vortex dynamics and transport in 1988 compared to 1987. It is anticipated that the QBO will likely be in the easterly phase during austral spring, 1989, and return to the westerly phase in 1990. Thus, the 1989 ozone depletion may be expected to be relatively modest, while that in 1990 may be considerably greater if the correlation with the QBO persists. The next few years are therefore likely to provide an excellent test of the QBO-ozone hole correlation. The heterogeneous conversion from reservoir to reactive chlorine on nitric acid trihydrate particles can only occur in the cold winter stratosphere, broadly restricting the geographical extent of the severe ozone depletion to Antarctica and to spring time. There is strong evidence, however, of the impact of the ozone hole at lower latitudes, most notably in the observation of reduced ozone concentrations year round at latitudes well equatorward of the polar vortex. This is attributable in part to the dilution of ozone depleted air as the vortex breaks down in late spring, although the vortex may also act to process a larger volume of air, priming the chemistry for ozone destruction during winter and spring.

In the Northern Hemisphere, while PSCs are frequently observed, they are far less ubiquitous than over Antarctica. Temperatures are generally warmer than in the corresponding season over Antarctica, and frequently temperatures rise dramatically during sudden warmings. The temperature increases can prevent further PSC formation, often well before sunlight returns to the polar cap. Thus, while conditions are in many respects similar to those over Antarctica, in certain important respects they differ, likely resulting in less efficient ozone depletion.

POLAR OZONE

While no comparable Arctic ozone hole has yet been observed, there is evidence of perturbed chemistry in the northern polar vortex. Observations obtained in both 1987/88 and 1988/89 showed that the chemical composition of the polar vortex was perturbed in a way similar to that over Antarctica. At the end of the 1988/89 airborne mission, the vortex was found to be primed to destroy ozone, with ClO mixing ratios exceeding 1 ppbv. However, no unequivocal evidence for ozone depletion was observed by the end of the airborne mission in mid-February. Noting the expected time scale for ozone depletion and the observed evolution of elevated ClO abundances and temperatures, no substantial ozone loss would have been expected in that year. However, years exhibiting colder temperatures later in the season would likely exhibit larger ozone decreases.

An important new finding of the Northern Hemisphere aircraft study was the observation of denitrification with far less evident dehydration than that obtained in Antarctica, implying that removal of substantial amounts of reactive nitrogen (a necessary prerequisite for sustaining high chlorine concentrations) may occur at temperatures above the frost point, and may thus be spatially more extensive than implied by the Antarctic results. This finding is not yet fully understood.

The studies in the Arctic in 1988/89 showed that while exposure to nitric acid trihydrate cloud particles (PSCs) could substantially perturb the partitioning of the chlorine species, an underlying, longer term contribution due to background aerosol could not be ruled out.

There are a number of very specific outstanding issues which significantly limit our ability to understand and predict reliably trends in ozone over both polar regions:

- It is not known whether the ozone trends in the Northern Hemisphere noted in the OTP (1989) are the result of the anomalous chemistry known to be present in the Arctic vortex.
- The detailed mechanism for denitrification, and in particular, the process of denitrification with less severe dehydration than observed in Antarctica, is not adequately understood.
- The rapid appearance of the Antarctic ozone hole, on the time scale of a decade, has not yet been successfully modeled. It is not clear whether the trend can be reproduced by existing models incorporating known changes in reactive chlorine abundances and perhaps in PSC frequency and duration, or whether changes in dynamics and transport also play a role.
- While there is evidence suggesting that heterogeneous reactions on sulfate aerosols can influence ozone concentrations (e.g., immediately after the El Chichon eruption), the importance of normal background aerosol concentrations on gas-phase chemical species is not known.
- The understanding of the role of HO_x species in polar chemistry is constrained only indirectly by HOCl measurements.
- The abundances, partitioning, and stratospheric sources of bromine are uncertain.
- The partitioning of the residual NO_y in the Antarctic vortex is not known.
- The absolute amount of total reactive chlorine and its partitioning among chlorine species (including higher oxides) are uncertain.
- There are significant uncertainties surrounding a number of key reaction rate constants, in particular the rate of the ClO dimer formation at warmer temperatures. It has also been suggested that Cl₂ may be formed during thermal decomposition of the dimer. There are also uncertainties regarding the absolute absorption cross section of Cl₂O₂, particularly at the long wavelengths

that control its photolysis rate at large solar angles. The significance of several suggested additional mechanisms (e.g., $\text{ClO} + \text{O}_3 + \text{M}$) is unclear.

- Additional heterogeneous reactions may be found to influence photochemistry (e.g., $\text{ClO} + \text{ice}$; $\text{HOCl} + \text{ice}$).
- It is possible that Type I PSCs may cause ozone loss at the edge of the Antarctic vortex throughout the winter season from May to August. The detailed observations necessary to test this possibility are not presently available.
- The extent to which the polar vortex can process air, destroying ozone prior to breakdown is uncertain. The possible impact of rising chlorine concentrations on the extent of processing is similarly unknown. Other processes (e.g., natural climatic cycles) may also influence the climatology of the stratosphere and hence vortex processing. The implications of these processes for mid-latitude ozone decreases are unknown.
- The effect on the stratospheric circulation of reduced solar heating in spring arising from reduced ozone concentrations is not known.
- The mechanisms causing strong descent in the polar vortex have not been properly explained. The importance of synoptically forced clouds for diabatic processes is not adequately understood.
- The implications of strong descent for the lifetimes of N_2O , CFCl_3 , etc., have not been evaluated quantitatively.
- The “age” and degree of turnover of air within the vortex is of critical importance in determining the availability of reactive chlorine and is a subject of ongoing research.
- The longitudinal variations in PSC formation are not understood quantitatively.
- While marked correlations between polar temperatures and the depth of the Antarctic ozone hole have been observed with the phase of winds in the low equatorial stratosphere (QBO), the detailed mechanism communicating the two regions is not understood.
- The implications of stratospheric cooling associated with greenhouse warming and increases in H_2O due to atmospheric CH_4 increases for the spatial extent and effect of PSCs are unknown. These and other climatic effects that could increase the latitudinal extent of polar ozone depletion are currently under study.
- The origin and significance of summertime temperature trends in Antarctica is not clear. It is as yet unresolved whether these are a result of incomplete radiative or chemical recovery, or reflect dynamical changes.

REFERENCES AND BIBLIOGRAPHY

- Akiyoshi, H., M. Fujiwara, and M. Uryu, Radiative aspects of Antarctic ozone hole in 1985, *Geophys. Res., Lett.*, 15, 919, 1988.
- Alekseev, A. P., V. M. Davidov, V. N. Dosov, S. N. Skuratov, A. E. Tyabotov, and V. U. Khattatov, Airborne lidar sounding of lower stratosphere aerosol in the Arctic, 1988, *Atmospheric Optics*, 1, 8, 1988.

POLAR OZONE

- Anderson, J. G., W. H. Brune, S. A. Lloyd, W. L. Starr, M. Loewenstein, and J. R. Podolske, Kinetics of ozone destruction by ClO and BrO within the Antarctic vortex: an analysis based on in-situ ER-2 data, *J. Geophys. Res.*, *94*, 11480, 1989.
- Andrews, D. G., J. R. Holton, and C.B. Leovy, *Middle Atmosphere Dynamics*, Academic Press, New York, pp. 489, 1987.
- Angell, J. K., The close relation between Antarctic total ozone depletion and cooling of the Antarctic low stratosphere, *Geophys. Res. Lett.*, *13*, 1240, 1986.
- Angell, J. K., Relation of Antarctic 100 mb temperature and total ozone to equatorial QBO, equatorial SST, and sunspot number, 1958–87, *Geophys. Res. Lett.*, *15*, 915–918, 1988a.
- Angell, J. K., Variations and trends in tropospheric and stratospheric temperatures: 1958–87, *J. Climate*, *1*, 1296, 1988b.
- Angell, J. K., and J. Korshover, The biennial wind and temperature oscillations in the equatorial stratosphere and their possible extension to higher latitudes, *Mon. Wea. Rev.*, *90*, 127, 1962.
- Angell, J. K., and J. Korshover, Quasi-biennial variations in temperature, total ozone, and tropopause height, *J. Atmos. Sci.*, *21*, 479, 1964.
- Angell, J. K., and J. Korshover, Biennial variation in springtime temperature and total ozone in extratropical latitudes, *Mon. Wea. Rev.*, *95*, 757, 1967.
- Angell, J. K., and J. Korshover, Quasi-biennial and long-term fluctuations in total ozone, *Mon. Wea. Rev.*, *101*, 426, 1973.
- Angell, J. K., and J. Korshover, Comparison of stratospheric trends in temperature, ozone and water vapor in north temperate latitudes, *J. Appl. Meteorol.*, *17*, 1397, 1978.
- Arnold, F., and G. Knop, Stratospheric nitric acid vapor measurements in the cold arctic vortex - implications for nitric acid condensation, *Nature*, *338*, 746, 1989.
- Atkinson, R. J., and J. Easson, A re-evaluation of the Australian total ozone record, *Proceedings of the International Ozone Symposium*, Eds. R.D. Bojkov and P. Fabian, 1988.
- Atkinson, R. J., W. A. Matthews, P. A. Newman, and R. A. Plumb, Evidence of the mid-latitude impact of Antarctic ozone depletion, *Nature*, *340*, 290, 1989.
- Austin, J., E. E. Remsberg, R. L. Jones, and A. F. Tuck, Polar stratospheric clouds inferred from satellite data, *Geophys. Res. Lett.*, *13*, 1256, 1986a.
- Austin, J., R. R. Garcia, J. M. Russell, S. Solomon, and A. F. Tuck, On the atmospheric photochemistry of nitric acid, *J. Geophys. Res.*, *91*, 5477–5485, 1986b.
- Austin, J., R. C. Pallister, J. A. Pyle, A. F. Tuck, and A. M. Zavody, Photochemical model comparisons with LIMS observations in a stratospheric trajectory coordinate system, *Quart J. Roy Met. Soc.*, *113*, 361–392, 1987.
- Austin, J., R. L. Jones, D. S. McKenna, A. T. Buckland, J. G. Anderson, D. W. Fahey, C. B. Farmer, L. E. Heidt, M. H. Proffitt, A. F. Tuck, and J. F. Vedder, Lagrangian photochemical modelling studies of the 1987 Antarctic spring vortex, Part 2: Seasonal trends in ozone, *J. Geophys. Res.*, *94*, 16717, 1989.
- Barnett, J. J., and M. Corney, Middle atmosphere reference model derived from satellite data, *Handbook for MAP*, vol. 16, SCOSTEP, 1985.
- Barrett, J. W., P. M. Solomon, R. L. DeZafra, M. Jaramillo, L. Emmons, and A. Parrish, Formation of the Antarctic ozone hole by the ClO dimer mechanism, *Nature*, *336*, 455, 1988.
- Birk, M., R. R. Friedl, E. A. Cohen, H. M. Pickett, and S. P. Sander, The rotational spectrum and structure of chlorine peroxide, submitted to *J. Chem. Phys.*, 1989.
- Blake, D. R., and F. S. Rowland, Continuing worldwide increases in tropospheric methane, 1978–1987, *Science*, *239*, 1129–1131, 1988.
- Blanchet, J. P., On radiative heating due to polar stratospheric clouds, *Tellus*, *37B*, 197, 1985.

- Blanchet, J. P., The response of polar stratospheric clouds to increasing carbon dioxide. *Proceedings of the International Radiation Symposium*, Lille, France, August 1988. Deepak Publishing, 1989.
- Bojkov, R. D., The 1979–1985 ozone decline in the Antarctic as reflected in ground-based observations, *Geophys. Res. Lett.*, *13*, 1236, 1986.
- Bowman, K. P., Interannual variability of total ozone during the breakdown of the Antarctic circumpolar vortex, *Geophys. Res. Lett.*, *13*, 1193, 1986.
- Bowman, K. P., and A. J. Krueger, A global climatology of total ozone from the Nimbus-7 Total Ozone Mapping Spectrometer, *J. Geophys. Res.*, *90*, 7967–7976, 1985.
- Brasseur, G., A. De Rudder, G.M. Keating, and M.C. Pitts, Response of the middle atmosphere to short-term solar ultraviolet variations: 2. Theory, *J. Geophys. Res.*, *92*, 903–914, 1987.
- Brasseur, G., and S. Solomon, *Aeronomy of the Middle Atmosphere*, D. Reidel, Dordrecht, 1984.
- Brune, W. H., and J. G. Anderson, In-situ observations of midlatitude stratospheric ClO and BrO, *Geophys. Res. Lett.*, *13*, 1391, 1986.
- Brune, W. H., E. W. Toohy, J. G. Anderson, W. L. Starr, J. F. Vedder, and E. F. Danielsen, In-situ northern mid-latitude observations of ClO, O₃ and BrO in the wintertime lower stratosphere, *Science*, *242*, 558, 1988.
- Brune, W. H., J. G. Anderson, and K. R. Chan, In situ observations of ClO in the Antarctic: ER-2 aircraft results from 54S to 72S latitude, *J. Geophys. Res.*, *94*, 16649, 1989a.
- Brune, W. H., J. G. Anderson, and K. R. Chan, In situ observations of BrO in the Antarctic: ER-2 aircraft results from 54S to 72S latitude, *J. Geophys. Res.*, *94*, 16639, 1989b.
- Burkholder, J. V., J. J. Orlando, and C. J. Howard, Ultraviolet absorption cross sections of Cl₂O₂ between 210 and 410 nm, *J. Phys. Chem.*, in press, 1989.
- Callis, L. B., J. M. Russell III, M. Natarajan, and K. V. Haggard, Examination of wintertime latitudinal gradients in stratospheric NO₂ using theory and LIMS observations, *Geophys. Res. Lett.*, *10*, 945, 1983.
- Callis, L. B., J. C. Alpert, and M. A. Geller, An assessment of thermal, wind and planetary wave changes in the middle and lower atmosphere due to the 11-year UV-flux variation. *J. Geophys. Res.*, *89*, 1373–1379, 1985.
- Callis, L. B., and M. Natarajan, The Antarctic ozone minimum: relationship to odd nitrogen, odd chlorine, the final warming, and the 11-year solar cycle, *J. Geophys. Res.*, *91*, 10771, 1986.
- Cariolle, D., M. Deque, and J. J. Morcrette, A GCM simulation of the ozone seasonal variations at high latitudes in the southern hemisphere, *Geophys. Res. Lett.*, *13*, 1304, 1986.
- Cariolle, D., S. Muller, F. Cayla, and M. P. McCormick, Mountain waves, polar stratospheric clouds, and the ozone depletion over Antarctica, *J. Geophys. Res.*, *94*, 11233, 1989a.
- Cariolle, D., A. Lasserre-Bigorrry, J. F. Royer, and J. F. Geleyn, A GCM simulation of the springtime Antarctic ozone decrease and its impact on midlatitudes, submitted to *J. Geophys. Res.*, 1989b.
- Carroll, M. A., S. Solomon, R. W. Sanders, and A. L. Schmeltekopf, Visible and near-ultraviolet spectroscopy at McMurdo Station, Antarctica, 6, Observations of BrO, *J. Geophys. Res.*, *94*, 16633, 1989.
- Chandra, S. An assessment of possible ozone-solar cycle relationship inferred from NIMBUS 4 BUV data. *J. Geophys. Res.*, *89*, 1373–1379, 1984.
- Chandra, S., and R. D. McPeters, Some observations on the role of planetary waves in determining the spring time ozone distribution in the Antarctic, *Geophys. Res. Lett.*, *13*, 1224, 1986.
- Chanin, M. L. N. Spires, and A. Hauchecorne, Long-term variation of the temperature of the middle atmosphere at mid latitude: dynamical and radiative causes, *J. Geophys. Res.*, *92*, 4201, 1987.
- Charney, J. G., and P. G. Drazin, Propagation of planetary scale disturbances from the lower into the upper atmosphere, *J. Geophys. Res.*, *66*, 83, 1961.

POLAR OZONE

- Cheng, B. M., and Y. P. Lee, Production and trapping of gaseous ClO: The infrared spectrum of chlorine peroxide (ClOOCl) in solid argon, *J. Chem. Phys.*, **90**, 5930, 1989.
- Chipperfield, M. P., and J. A. Pyle, Two-dimensional modelling of the Antarctic lower stratosphere, *Geophys. Res. Lett.*, **15**, 875, 1988.
- Chu, W. P., M. P. McCormick, J. Lenoble, C. Brogniez, and P. Pruvost, SAGE II inversion algorithm, *J. Geophys. Res.*, **94**, 8353, 1989.
- Chubachi, S., Preliminary result of ozone observations at Syowa Station from February, 1982 to January, 1983, *Mem. Natl. Inst. Polar Res.*, spec. issue no. 34, 13, 1984.
- Chubachi, S., On the cooling of stratospheric temperature at Syowa, Antarctica, *Geophys. Res. Lett.*, **13**, 1221, 1986.
- Cicerone, R. J., L. E. Heidt, and W. H. Pollack, Measurements of atmospheric methyl bromide and bromoform, *J. Geophys. Res.*, **93**, 3745, 1988.
- Clyne, M. A. A., and R. T. Waston, Kinetic studies of diatomic free radicals using mass spectrometry, Part 4, The BrO + OCID and BrO + ClO reactions, *J. Chem. Soc. Faraday Trans.*, **1**, **73**, 1169, 1977.
- Coffey, M. T., W. G. Mankin, and A. Goldman, Simultaneous spectroscopic determination of the latitudinal, seasonal, and diurnal variability of stratospheric N₂O, NO, NO₂, and HNO₃, *J. Geophys. Res.*, **86**, 7331, 1981.
- Coffey, M. T., On the temporal change of stratospheric NO₂, *Geophys. Res. Lett.*, **15**, 331, 1988.
- Coffey, M. T., and W. G. Mankin, Airborne measurements of stratospheric constituents over Antarctica in the austral spring 1987, 2, Halogen and nitrogen trace gases, *J. Geophys. Res.*, **94**, 16597, 1989.
- Connor, B. J., J. W. Barrett, A. Parrish, P. M. Solomon, R. L. DeZafra, and M. Jaramillo, Ozone over McMurdo Station, Antarctica, austral spring, 1986: Altitude profiles for the middle and upper stratosphere, *J. Geophys. Res.*, **92**, 13221, 1987.
- Cox, R. A., and G. D. Hayman, The stability and photochemistry of dimers of the ClO radical and implications of Antarctic ozone depletion, *Nature*, **322**, 796–800, 1988.
- Cox, R. A., D. W. Sheppard, and M. P. Stevens, Absorption coefficients and kinetics of the BrO radical using molecular modulation, *J. Photochem.*, **19**, 201, 1982.
- Crutzen, P. J., and F. Arnold, Nitric acid cloud formation in the cold Antarctic stratosphere: a major cause for the springtime "ozone hole," *Nature*, **324**, 651–655, 1986.
- DeMore, W. B., M. J. Molina, S. P. Sander, D. M. Golden, R. F. Hampson, M. J. Kurylo, C. J. Howard, and A. R. Ravishankara, Chemical kinetics and photochemical data for use in stratospheric modeling, evaluation number 8, JPL Publ. 87-41, 1987.
- Deutsch, H. U., Ozone distribution in the atmosphere, *Can. J. Chem.*, **52**, 1491, 1974.
- DeZafra, R. L., M. Jaramillo, A. Parrish, P. Solomon, B. Connor, and J. Barnett, Observation of abnormally high concentrations of chlorine monoxide at low altitudes in the Antarctic spring stratosphere, I. Diurnal variation, *Nature*, **328**, 408, 1987.
- DeZafra, R. L., M. Jaramillo, J. Barrett, L. K. Emmons, P. M. Solomon, and A. Parrish, New observations of a large concentration of ClO in the springtime lower stratosphere over Antarctica and its implications for ozone-depleting chemistry, *J. Geophys. Res.*, **94**, 11423, 1989.
- Dobson, G. M. B., D. N. Harrison, and J. Lawrence, Measurements of the amount of ozone in the earth's atmosphere and its relation to other geophysical conditions. *Proc. Roy. Soc. London, A*, **122**, 456–486, 1928.
- Dobson, G. M. B., Forty year's research on atmospheric ozone at Oxford: A history, *Applied Optics*, **7**, 401, 1968.
- Dobson, G. M. B., The laminated structure of ozone in the atmosphere, *Quart. J. Roy. Met. Soc.*, **99**, 599, 1973.
- Dunkerton, T. J., Body force circulation and the Antarctic ozone minimum, *J. Atmos. Sci.*, **45**, 427, 1988.

- Eckman, R. S., Response of ozone to short-term variations in the solar ultraviolet irradiance. 1. A theoretical model, *J. Geophys. Res.*, *91*, 6695–6704, 1986.
- Elokhov, A. S., and A. N. Gruzdev, Total ozone and NO₂ observations at Molodeznaja and Mirny stations, Antarctica, in spring 1987 and in summer and fall, 1988, Middle Atmosphere Symposium, Dushanbe, USSR, 1989.
- Fahey, D. W., D. M. Murphy, C. S. Eubank, K. K. Kelly, M. H. Proffit, G. V. Ferry, M. K. W. Ko, M. Loewenstein, and K. R. Chan, Measurements of nitric oxide and total reactive nitrogen in the Antarctic stratosphere: observations and chemical implications, *J. Geophys. Res.*, *94*, 16437, 1989a.
- Fahey, D. W., K. K. Kelly, G. V. Ferry, L. R. Poole, J. C. Wilson, D. M. Murphy, and K. R. Chan, In situ measurements of total reactive nitrogen, total water and aerosols in polar stratospheric clouds in the Antarctic stratosphere, *J. Geophys. Res.*, *94*, 11299, 1989b.
- Fairlie, T. D. A., and A. O'Neill, The stratospheric major warming of winter 1984/85: observations and dynamical inferences, *Quart. J. Roy. Met. Soc.*, *114*, 557–578, 1988.
- Fairlie, T. D. A., A. O'Neill, and V. D. Pope, The sudden breakdown of an unusually strong cyclone in the stratosphere during winter 1988/89, submitted to *Nature*, 1989.
- Farman, J. C., B. G. Gardiner, and J. D. Shanklin, Large losses of total ozone in Antarctica reveal seasonal ClO_x/NO_x interaction, *Nature*, *315*, 207, 1985a.
- Farman, J. C., R. J. Murgatroyd, A. M. Sinnickas, and B. A. Thrush, Ozone photochemistry in the Antarctic stratosphere in summer, *Quart. J. Roy. Met. Soc.*, *111*, 1013, 1985b.
- Farmer, C. B., G. C. Toon, P. W. Shaper, J. F. Blavier, and L. L. Lowes, Ground-based measurements of the composition of the Antarctic atmosphere during the 1986 spring season, I. Stratospheric trace gases, *Nature*, *329*, 126, 1987.
- Farrara, J. D., and C. R. Mechoso, An observational study of the final warming in the Southern Hemisphere stratosphere, *Geophys. Res. Lett.*, *13*, 1232, 1986.
- Frederick J. E., and H. E. Snell, Ultraviolet radiation levels during Antarctic spring. *Science*, *241*, 438–440, 1988.
- Frederick, J. E., H. E. Snell, and E. K. Haywood, Solar ultraviolet radiation at the Earth's surface, *J. Photochem. Photobiol.*, in press, 1989.
- Friedl, R. R., and S. P. Sander, Studies of ClO and BrO reactions important in the polar stratosphere; kinetics and mechanism of the ClO + BrO and ClO + ClO reactions, Paper presented at the Polar Ozone Workshop, Snowmass, Colorado, May 9–13, 1988.
- Friedl, R. R., and S. P. Sander, Kinetics and product studies of the reaction ClO + BrO using discharge flow-mass spectrometry, *J. Phys. Chem.*, *4756*, 1989.
- Gandrud, B. W., P. D. Sperry, L. Sanford, K. K. Kelly, G. V. Ferry, and K. R. Chan, Filter measurement results from the Airborne Antarctic Ozone Experiment, *J. Geophys. Res.*, *94*, 11285, 1989.
- Garcia, R. R. and S. Solomon, A numerical model of the zonally averaged dynamical and chemical structure of the middle atmosphere, *J. Geophys. Res.*, *88*, 1379, 1983.
- Garcia, R. R., and S. Solomon, The effect of breaking gravity wave on the dynamics and chemical structure of the middle atmosphere, *J. Geophys. Res.*, *90*, 3850, 1985.
- Garcia, R. R., and S. Solomon, Interannual variability in Antarctic ozone and the Quasi-Biennial Oscillation, *Geophys. Res. Lett.*, *14*, 848, 1987.
- Garcia, R., S. Solomon, R. G. Roble, and D. W. Rusch, A numerical study of the response of the middle atmosphere to the 11-year solar cycle, *Planet. Space Sci.*, *32*, 411–421, 1984.
- Gardiner, B. G., and J. D. Shanklin, Recent measurements of Antarctic ozone depletion, *Geophys. Res. Lett.*, *13*, 1199, 1986.
- Gardiner, B. G., Comparative morphology of the vertical ozone profile in the Antarctic spring, *Geophys. Res. Lett.*, *15*, 901, 1988.

POLAR OZONE

- Gardiner, B. G., The Antarctic ozone hole, *Weather*, *44*, 291–298, 1989.
- Gernandt, H., The vertical ozone distribution above the GDR research base, Antarctica in 1985, *Geophys. Res. Lett.*, *14*, 84, 1987.
- Gille, J. C., C. M. Smythe, and D. F. Heath, Observed ozone response to variations in solar ultraviolet radiation, *Science*, *225*, 315–317, 1984a.
- Gille, J. C., J. M. Russell, P. L. Barley, E. E. Remsberg, L. L. Gordley, W. F. J. Evans, H. Fischer, B. W. Gandrud, A. Girard, J. E. Harries, and S. A. Beck, Accuracy and precision of the nitric acid concentrations determined by the limb infrared monitor of the stratosphere experiment on Nimbus 7, *J. Geophys. Res.*, *89*, 5179, 1984b.
- Girard, A., L. Gramont, N. Louisnard, S. LeBoiteux, and G. Fergant, Latitudinal variation of HNO₃, HCl and HF vertical column density above 11.5 km, *Geophys. Res. Lett.*, *9*, 135, 1982.
- Gray, L. J., and J. A. Pyle, A two-dimensional model of the quasi-biennial oscillation of ozone, *J. Atmos. Sci.*, *46*, 203–220, 1989.
- Grose, W. L., R. S. Eckman, R. E. Turner, and W. T. Blackshear, Potential effects of Antarctic ozone depletion upon the global ozone budget, MASH Workshop on Dynamics, Transport and Photochemistry in the Middle Atmosphere of the Southern Hemisphere, San Francisco, CA, April 1989 (to appear in a volume of the NATO Advanced Research Workshop series, 1989).
- Hamill, P., O. B. Toon, and R. P. Turco, Characteristics of polar stratospheric clouds during the formation of the Antarctic ozone hole, *Geophys. Res. Lett.*, *13*, 1288, 1986.
- Hamill, P., R. P. Turco, and O. B. Toon, On the growth of nitric and sulfuric acid aerosol particles under stratospheric conditions, *J. Atmos. Chem.*, *7*, 287–315, 1988.
- Hanson, D. R., and K. Mauersberger, Laboratory studies of the nitric acid trihydrate: Implications for the South Polar stratosphere, *Geophys. Res. Lett.*, *15*, 855–858, 1988a.
- Hanson, D. R., and K. Mauersberger, Vapor Pressures of HNO₃/H₂O solutions at low temperatures, *J. Phys. Chem.*, *92*, 6167–6170, 1988b.
- Hanson, D. R., and K. Mauersberger, Solubility and equilibrium vapor pressures of HCl dissolved in polar stratospheric cloud materials: Ice and the trihydrate of nitric acid, *Geophys. Res. Lett.*, in press, 1989a.
- Hanson, D. R., and K. Mauersberger, HCl/H₂O solid phase vapor pressures and HCl solubility in ice, submitted to *J. Phys. Chem.*, 1989b.
- Hartmann, D. L., L. E. Heidt, M. Loewenstein, J. R. Podolske, J. Vedder, W. L. Starr, and S. E. Strahan, Transport into the south polar vortex in early spring, *J. Geophys. Res.*, *94*, 16779, 1989a.
- Hartmann, D. L., M. R. Schoeberl, P. A. Newman, R. L. Martin, B. L. Gary, K. R. Chan, M. Loewenstein, J. R. Podolske, and S. E. Strahan, Potential vorticity and mixing in the south polar vortex during spring, *J. Geophys. Res.*, *94*, 11625, 1989b.
- Hasebe, F., Interannual variation of global total ozone revealed from Nimbus 4 BUUV and ground-based observations, *J. Geophys. Res.*, *88*, 6819, 1983.
- Hayman, G. D., J. M. Davies, and R. A. Cox, Kinetics of the reaction ClO + ClO → products and its potential relevance to Antarctic ozone, *Geophys. Res. Lett.*, *13*, 1347, 1986.
- Heidt, L. E., J. F. Vedder, W. H. Pollock, B. E. Henry, and R. A. Lueb, Trace gases in the Antarctic atmosphere, *J. Geophys. Res.*, *94*, 11599, 1989.
- Heysfield, A. J., Ice particles observed in a cirriform cloud at -83C and implications for polar stratospheric clouds, *J. Atmos. Sci.*, *43*, 851, 1986.
- Hills, A. J., R. J. Cicerone, J. G. Calvert, and J. W. Birks, Kinetics of the BrO + ClO reaction: implications for stratospheric ozone, *Nature*, *328*, 405, 1987.
- Hills, A. J., R. J. Cicerone, J. G. Calvert, and J. W. Birks, Temperature dependence of the rate constant and product channels for the BrO + ClO reaction, *J. Phys. Chem.*, *92*, 1853–1858, 1988.

- Hirota, I., T. Hirooka, and M. Shiotani, Upper stratosphere circulation in the two hemispheres, *Quart. J. Roy. Met. Soc.*, 109, 443, 1983.
- Hofmann, D. J., Direct ozone depletion in springtime Antarctic lower stratospheric clouds, *Nature*, 337, 447, 1989a.
- Hofmann, D. J., Comparison of stratospheric clouds in the Antarctic and in the Arctic, submitted to *Geophys. Res. Lett.*, 1989b.
- Hofmann, D. J., J. M. Rosen, J. W. Harder, and S. R. Rolf, Ozone and aerosol measurements in the springtime Antarctic stratosphere in 1986, *Geophys. Res. Lett.*, 13, 1252, 1986.
- Hofmann, D. J., J. W. Harder, S. R. Rolf, and J. M. Rosen, Balloonborne observations of the temporal development and vertical structure of the Antarctic ozone hole in 1986, *Nature*, 326, 59, 1987a.
- Hofmann, D. J., J. M. Rosen, J. W. Harder, and S. R. Rolf, Observations of the decay of the El Chichon stratospheric aerosol cloud in Antarctica, *Geophys. Res. Lett.*, 14, 614, 1987b.
- Hofmann, D. J., J. M. Rosen, and J. W. Harder, Aerosol measurements in the winter/spring Antarctic stratosphere: I. Correlative measurements with ozone, *J. Geophys. Res.*, 93, 655, 1988.
- Hofmann, D. J., J. M. Rosen, J. W. Harder, and J. V. Hereford, Balloonborne measurements of aerosol, condensation nuclei, and cloud particles in the stratosphere at McMurdo Station, Antarctica during the spring of 1987, *J. Geophys. Res.*, 94, 11253, 1989a.
- Hofmann, D. J., P. Amedieu, W. A. Matthews, P. V. Johnston, Y. Kondo, W. R. Sheldon, and G. J. Byrne, Stratospheric clouds and ozone depletion in the Arctic during January 1989, *Nature*, 340, 117, 1989b.
- Hofmann, D. J., J. W. Harder, J. M. Rosen, J. V. Hereford, and J. R. Carpenter, Ozone profile measurements at McMurdo Station, Antarctica during the spring of 1987, *J. Geophys. Res.*, 94, 16527, 1989c.
- Hofmann, D. J., and S. Solomon, Ozone destruction through heterogeneous chemistry following the eruption of El Chichon, *J. Geophys. Res.*, 94, 5029, 1989.
- Holton, J. R., and H.-C. Tan, The influence of the equatorial quasi-biennial oscillation on the global circulation at 50 mb, *J. Atmos. Sci.*, 37, 2200, 1980.
- Holton, J. R., and H.-C. Tan, The quasi-biennial oscillation in the Northern Hemisphere lower stratosphere, *J. Meteor. Soc. Japan*, 60, 140, 1982.
- Hood, L. L., Solar ultraviolet induced variations in the stratosphere and mesosphere, *J. Geophys. Res.*, 92, 876-888, 1987.
- Hoskins, B. J., M. E. McIntyre, and A. W. Robertson, On the use and significance of potential vorticity maps, *Quart. J. Roy. Met. Soc.*, 111, 877, 1985.
- Isaksen, I. S. A., and F. Stordal, Antarctic ozone depletion: 2-D model studies, *Geophys. Res. Lett.*, 13, 1327, 1986.
- Iwasaka, Y., Non-spherical particles in the Antarctic polar stratosphere - Increase in particulate content and stratospheric water vapor budget, *Tellus*, 38B, 364, 1986.
- Iwasaka, Y., T. Hirasawa, and H. Fukunishi, Lidar measurement on the Antarctic stratospheric aerosol layer: [I] Winter enhancement, *J. Geomag. Geoelectr.*, 37, 1087, 1985a.
- Iwasaka, Y., A. Ono, and S. Saitoh, Measurement of water vapor content in the polar stratosphere: Syowa station, spring 1983, *Mem. Pol. Res. (Tokyo)*, 39, 51, 1985b.
- Iwasaka, Y., and K. Kondoh, Depletion of antarctic ozone: Height of ozone loss region and its temporal changes, *Geophys. Res. Lett.*, 14, 87, 1987.
- Iwasaka, Y., K. Kondoh, and K. Kawahira, Long term trend in ozone content and temperature in the Antarctic stratosphere - Cooling and ozone decrease tendency, submitted to *Geophys. Res. Lett.*, 1989.
- Jones, R. L., J. Austin, D. S. McKenna, J. G. Anderson, D. W. Fahey, C. B. Farmer, L. E. Heidt, K. K. Kelly, D. M. Murphy, M. H. Proffit, and A. F. Tuck, Lagrangian photochemical modelling studies of the 1987 Antarctic spring vortex: comparison with observations, *J. Geophys. Res.*, 94, 11529, 1989.

POLAR OZONE

- Juckes, M. N., and M. E. McIntyre, A high resolution, one-layer model of breaking planetary waves in the stratosphere, *Nature*, 328, 590, 1987.
- Kanzawa, H., and S. Kawaguchi, Large stratospheric sudden warming in Antarctic late winter and shallow ozone hole in 1988, submitted to *Nature*, 1989.
- Karcher, F., M. Amodei, G. Armand, C. Besson, B. DuFour, G. Froment, and J. P. Meyer, Simultaneous measurements of HNO₃, NO₂, HCl, O₃, N₂O, CH₄, H₂O and CO, and their latitudinal variations as deduced from airborne infrared spectrometry, *Ann. Geophysicae*, 4, 425, 1988.
- Kawahira, K., and T. Hirooka, Interannual temperature changes in the Antarctic lower stratosphere - A relation to the ozone hole, *Geophys. Res. Lett.*, 16, 41-44, 1989.
- Keating G. M., and D. F. Young, Interim reference ozone models for the middle atmosphere, *Handbook for MAP*, vol. 16, SCOSTEP, 1985.
- Keating, G. M., L. R. Lake, J. Y. Nicholson III, and M. Natarajan, Global ozone long-term trends from satellite measurements and the response to solar activity variations, *J. Geophys. Res.*, 86, 9873-9880, 1981.
- Keating, G. M., G. P. Brasseur, J. Y. Nicholson III, and A. DeRudder, Detection of the response of ozone in the middle atmosphere to short-term solar ultraviolet variations, *Geophys. Res. Lett.*, 12, 449, 1985.
- Keating, G. M., M. C. Pitts, G. Brasseur, and A. DeRudder, Response of middle atmosphere to short-term solar ultraviolet variations: 1. Observations, *J. Geophys. Res.*, 92, 889-902; 2. Theory. 903-914, 1987.
- Kelly, K. K., A. F. Tuck, D. M. Murphy, M. H. Proffitt, D. W. Fahey, R. L. Jones, D. S. McKenna, M. Loewenstein, J. R. Podolske, S. E. Strahan, G. V. Ferry, K. R. Chan, J. F. Vedder, G. L. Gregory, W. D. Hypes, M. P. McCormick, E. V. Browell, and L. E. Heidt, Dehydration in the lower Antarctic stratosphere during late winter and early spring, 1987, *J. Geophys. Res.*, 94, 11317, 1989.
- Kent, G. S., C. R. Trepte, U. O. Farruckh, and M. P. McCormick, Variation in the stratospheric aerosol associated with the north cyclonic polar vortex as measured by the SAM II satellite sensor, *J. Atmos. Sci.*, 42, 1536, 1985.
- Keys, J. G., and P. V. Johnston, Stratospheric NO₂ and O₃ in Antarctica: Dynamic and chemically controlled variations, *Geophys. Res. Lett.*, 13, 1260, 1986.
- Keys, J. G., and P. V. Johnston, Stratospheric NO₂ column measurements from three Antarctic sites, *Geophys. Res. Lett.*, 15, 898, 1988.
- Khattatov, V. U., V. U. Rudakov, V. A. Yushkov, and J. M. Rosen, Observations of ozone and polar stratospheric clouds from Heiss Island, 1989, in press, *Meteorologia i Gidrologia*, 1989.
- Kiehl, J. T., B. A. Boville, and B. P. Briegleb, Response of a general circulation model to a prescribed Antarctic ozone hole, *Nature*, 332, 501-504, 1988.
- Kinne, S., and O. B. Toon, Studies of the radiative effects of polar stratospheric clouds, *Proceedings of AMS Conference on Atmospheric Radiation*, in press, 1989.
- Ko, M. K. W., K. K. Tung, D. K. Wenstein, and N. D. Sze, A zonal-mean model of stratospheric tracer transport in isentropic co-ordinates: numerical simulations for nitrous oxide and nitric acid, *J. Geophys. Res.*, 90, 2013, 1985.
- Ko, M. K. W., J. M. Rodriguez, N. D. Sze, M. H. Proffitt, W. L. Starr, A. Krueger, E. V. Browell, and M. P. McCormick, Implications of AAOE observations for proposed chemical explanations of the seasonal and interannual behavior of Antarctic ozone, *J. Geophys. Res.*, 94, 16705, 1989.
- Kokin, G. A., S. P. Perov, D. A. Tarasenko, and A. F. Chizhov, A study of Antarctic ozone anomaly in spring by rocket and ground-based ozonometers, *Meteorologia i Gidrologia*, in press, 1989.
- Komhyr, W. D., R. D. Grass, and R. K. Leonard, Total ozone decrease at South Pole Antarctica, 1964-1985, *Geophys. Res. Lett.*, 13, 1248, 1986.

- Komhyr, W. D., S. J. Oltmans, and R. D. Grass, Atmospheric ozone at South Pole, Antarctica, in 1986, *J. Geophys. Res.*, *93*, 5167, 1988.
- Komhyr, W. D., Oltmans, S. J., Grass, R. D., Franchois, P. R., and R. K. Leonard, Changes in total ozone and ozone vertical distribution at South Pole, Antarctica, 1962–1987, *Proceedings of Quadrennial Ozone Symposium*, Gottingen, FRG, 1989a.
- Komhyr, W. D., R. D. Grass, P. J. Reitelbach, S. E. Kuester, P. R. Franchois, and M. L. Fanning, Total ozone, ozone vertical distributions, and stratospheric temperatures at South Pole, Antarctica, in 1986 and 1987, *J. Geophys. Res.*, *94*, 11429, 1989b.
- Kondoh, K., Y. Iwasaka, T. Suzuki, and S. Kaneto, Ozonesonde measurements at Syowa Station, Proc. NIPR Symp., *Polar Meteorol. Glaciol.*, *1*, 10, 1987.
- Koshelkov, Yu. P., Southern hemisphere reference middle atmosphere, *Adv. Space Res.*, *7*, 83, 1987.
- Koshelkov, Yu. P., Kovshova, E. N., and Fedorov, V. V., Day-to-day variability of temperature and wind speed in the stratosphere of the Southern and Northern Hemisphere, *Antarctica*, *26*, 37, 1987.
- Koshelkov, Yu. P., Temperature trends in the lower stratosphere of the Antarctic and environs, in press, *Meteorologia i Hidrologia*, 1989.
- Krueger, A. J., M. R. Schoeberl, and R. S. Stolarski, TOMS observations of total ozone in the 1986 Antarctic spring, *Geophys. Res. Lett.*, *14*, 527, 1987.
- Krueger, A. J., M. R. Schoeberl, R. S. Stolarski, and F. S. Sechrist, The 1987 ozone hole: A new record low, *Geophys. Res. Lett.*, *15*, 1365, 1988.
- Kruger, B. C., G. Q. Wang, and P. Fabian, The Antarctic ozone depletion caused by heterogeneous photolysis of halogenated hydrocarbons, *Geophys. Res. Lett.*, *14*, 523, 1987.
- Kuhlsbarsch, T., and Naujokat, B., Nordhemispharischer Klimabericht zum Januar 1989, Beilage zur Berliner Wetterkarte, Amsblatt des Instituts für Meteorol., Free University of Berlin, 1989.
- Labitzke, K., On the interannual variability of the middle stratosphere during the northern winters, *J. Met. Soc. Japan*, *60*, 124, 1982.
- Labitzke, K., Sunspots, the QBO and the stratospheric temperature in the north polar region, *Geophys. Res. Lett.*, *14*, 535, 1987a.
- Labitzke, K., The lower stratosphere over the polar regions in winter and spring: relation between meteorological parameters and total ozone, *Annal. Geophys.*, *5A*, 95–102, 1987b.
- Labitzke, K., and M.-L. Chanin, Changes in the middle atmosphere in winter related to the 11-year solar cycle, *Annal. Geophys.*, *6*, 643, 1988.
- Labitzke, K., and H. van Loon, Associations between the 11-year solar cycle, the QBO and the atmosphere, Part I: the troposphere and stratosphere in the Northern Hemisphere in winter, *J. Atmos. Terr. Phys.*, *50*, 197, 1988a.
- Labitzke, K., and H. van Loon, Association between the 11-year solar cycle, the QBO and the atmosphere, Part II: surface and 700 mb in the Northern Hemisphere in winter, *J. Climate*, *1*, 905, 1988b.
- Labitzke, K., and H. van Loon, Association between the 11-year solar cycle, the QBO and the atmosphere, Part III: aspects of the association, *J. Climate*, *2*, 554, 1989.
- Lait, L. R., M. R. Schoeberl, and P. A. Newman, Quasi-biennial modulation of the Antarctic ozone depletion, *J. Geophys. Res.*, in press, 1989.
- Leu, M. T., Laboratory studies of sticking coefficients and heterogeneous reactions important in the Antarctic stratosphere, *Geophys. Res. Lett.*, *15*, 17–20, 1988a.
- Leu, M. T., Heterogeneous reactions of N₂O₅ with H₂O and HCl on ice surfaces: implications for Antarctic ozone depletion, *Geophys. Res. Lett.*, *15*, 855–858, 1988b.
- London, J., R. D. Bojkov, S. Oltmans, and J. I. Kelley, Atlas of the global distribution of total ozone, July 1957–June 1967, National Center for Atmospheric Research, Boulder, CO, 1967.
- London J., Radiative energy sources and sinks in the stratosphere and mesosphere, in Nicolet M., and Aikin, A. C. (eds), *Proceedings of the NATO Advanced Study Institute on Stratospheric Ozone: Its*

POLAR OZONE

- Variation and Human Influences*, pp. 703–721 U. S. Dept. of Transportation, Washington, D. C., 1980.
- Lubin, D., J. E. Frederick, and A. J. Krueger, The ultraviolet radiation environment of Antarctica: McMurdo Station during September-October 1987, *J. Geophys. Res.*, *94*, 8491, 1989a.
- Lubin, D., F. E. Frederick, C. R. Booth, T. Lucas, and D. Neuschuler, Measurements of enhanced springtime ultraviolet radiation at Palmer Station, Antarctica, *Geophys. Res. Lett.*, *16*, 783, 1989b.
- Mahlman, J. D., and S. B. Fels, Antarctic ozone decreases: a dynamical cause, *Geophys. Res. Lett.*, *13*, 1316, 1986.
- Mahlman, J. D., Dynamical effects of the Antarctic ozone hole: A 3-D model experiment, MASH workshop on Dynamics, Transport and Photochemistry in the Middle Atmosphere of the Southern Hemisphere, San Francisco, CA, April 1989, to appear in a volume of the NATO Advanced Research Workshop series, 1989.
- Mankin, W. G., and M. T. Coffey, Latitudinal distributions and temporal changes of stratospheric HCl and HF, *J. Geophys. Res.*, *88*, 10776, 1983.
- Mankin, W. G., and M. T. Coffey, Airborne measurements of stratospheric constituents over Antarctica in the austral spring 1987, 1, Method and ozone observations, *J. Geophys. Res.*, *94*, 11413, 1989.
- Margitan, J. J., Chlorine nitrate: The sole product of the $\text{ClO} + \text{NO}_2 + \text{M}$ recombination, *J. Geophys. Res.*, *88*, 5415–5420, 1983.
- McCormick, M. P., Hamill, T. J. Pepin, W. P. Chu, T. J. Swissler, and L. R. McMaster, Satellite studies of the stratospheric aerosol, *Bull. Am. Met. Soc.*, *60*, 1038, 1979.
- McCormick, M. P., H. M. Steele, P. Hamill, W. P. Chu, and T. J. Swissler, Polar stratospheric cloud sightings by SAM II, *J. Atmos. Sci.*, *39*, 1387, 1982.
- McCormick, M. P., P. Hamill, and U. O. Farrukh, Characteristics of polar stratospheric clouds as observed by SAM II, SAGE, and Lidar, *J. Met. Soc. Japan.*, *63*, 267, 1985.
- McCormick, M. P., and J. C. Larsen, Antarctic springtime measurements of ozone, nitrogen dioxide, and aerosol extinction by SAM II, SAGE, and SAGE II, *Geophys. Res. Lett.*, *13*, 1280, 1986.
- McCormick, M. P., and C. R. Trepte, SAM II measurements of Antarctic PSC's and aerosols, *Geophys. Res. Lett.*, *13*, 1276, 1986.
- McCormick, M. P., and C. R. Trepte, Polar stratospheric optical depth observed between 1978 and 1985, *J. Geophys. Res.*, *92*, 4297, 1987.
- McCormick, M. P., and J. C. Larsen, Antarctic measurements of ozone by SAGE II in the spring of 1985, 1986, 1987, *Geophys. Res. Lett.*, *15*, 907, 1988.
- McCormick, M. P., and C. R. Trepte, Persistence of Antarctic polar stratospheric clouds, *J. Geophys. Res.*, *94*, 11241, 1989.
- McElroy, M. B., R. J. Salawitch, S. C. Wofsy, and J. A. Logan, Antarctic ozone: reductions due to synergistic interactions of chlorine and bromine, *Nature*, *321*, 759, 1986a.
- McElroy, M. B., R. J. Salawitch, and S. C. Wofsy, Antarctic O_3 : Chemical mechanisms for the spring decrease, *Geophys. Res. Lett.*, *13*, 1296, 1986b.
- McElroy, M. B., R. J. Salawitch, and S. C. Wofsy, Chemistry of the Antarctic stratosphere, *Planet. Space Sci.*, *36*, 73, 1988.
- McGrath, M. P., K. C. Clemetshaw, F. S. Rowland, and W. J. Hehre, Thermochemical stabilities and vibrational spectra of isomers of the chlorine oxide dimer, *Geophys. Res. Lett.*, *15*, 883–886, 1988.
- McIntyre, M. E., and T. N. Palmer, Breaking planetary waves in the stratosphere, *Nature*, *305*, 593–600, 1983.
- McKenna, D. S., R. L. Jones, J. Austin, E. Browell, M. P. McCormick, A. J. Krueger, and A. F. Tuck, Diagnostic studies of the Antarctic vortex during the 1987 Airborne Antarctic Ozone Experiment: Ozone mini-holes, *J. Geophys. Res.*, *94*, 11641, 1989a.

- McKenna, D. S., R. L. Jones, A. T. Buckland, J. Austin, A. F. Tuck, R. H. Winkler, and R. Chan, The Southern Hemisphere lower stratosphere during August and September 1987: Analyses based on the United Kingdom Meteorological Office global model, *J. Geophys. Res.*, *94*, 16847, 1989b.
- McKenzie, R. L., and P. V. Johnston, Springtime stratospheric NO₂ in Antarctica, *Geophys. Res. Lett.*, *11*, 73, 1984.
- McPeters, R. D., R. D. Hudson, P. K. Bhartia, and S. L. Taylor, The vertical ozone distribution in the Antarctic ozone minimum measured by SBUV, *Geophys. Res. Lett.*, *13*, 1213, 1986.
- Mechoso, C. R., A. O'Neill, V. D. Pope, and J. D. Farrara, A study of the stratospheric warming of 1982 in the Southern Hemisphere, *Quart. J. Roy. Met. Soc.*, *114*, 1365, 1988.
- Mechoso, C. R., A. O'Neill, J. D. Farrara, M. Fisher, V. D. Pope, and B. Kingston, On the breakdown of the Southern Hemisphere stratospheric polar vortex, submitted to *Nature*, 1989.
- Molina, M. J., The chemistry of some reactions believed to be important in ozone depletion over Antarctica, *Proceedings of the International Ozone Symposium 1988*, R. Bojkov and P. Fabian, Eds., Deepak Pub. Co., Hampton, Virginia, 1989.
- Molina, M. J., and F. S. Rowland, Stratospheric sink for chlorofluoromethanes: Chlorine-atom catalyzed destruction of ozone, *Nature*, *249*, 810, 1974.
- Molina, L. T., M. J. Molina, R. A. Stachnik, and R. D. Tom, An upper limit to the rate of the HCl + ClONO₂ reaction, *J. Phys. Chem.*, *89*, 3779, 1985.
- Molina, L. T., and M. J. Molina, Production of Cl₂O₂ from the self-reaction of the ClO radical, *J. Phys. Chem.*, *91*, 433-436, 1987.
- Molina, M. J., T. L. Tso, L. T. Molina, and F. C. Y. Wang, Antarctic stratospheric chemistry of chlorine nitrate, hydrogen chloride, and ice: Release of active chlorine, *Science*, *238*, 1253-1257, 1987.
- Molina, M. J., A. Fucaloro, L. T. Molina, and K. Zahir, Solubility of HCl vapor in various ice substrates, manuscript in preparation, 1989.
- Mount, G. H., D. W. Rusch, J. F. Noxon, J. M. Zawodny, and C. A. Barth, Measurements of stratospheric NO₂ from the Solar Mesosphere Explorer satellite, 1. An overview of the results, *J. Geophys. Res.*, *89*, 1327, 1984.
- Mount, G. H., R. W. Sanders, A. L. Schmeltekopf, and S. Solomon, Visible spectroscopy at McMurdo Station, Antarctica, 1. Overview and daily variations of NO₂ and O₃ during austral spring, 1986, *J. Geophys. Res.*, *92*, 8320, 1987.
- Mount, G. H., S. Solomon, R. W. Sanders, R. O. Jakoubek, and A. L. Schmeltekopf, Observations of stratospheric NO₂ and O₃ at Thule, Greenland, *Science*, *242*, 555, 1988.
- Mozurkewich, M., and J. G. Calvert, Reaction probability on N₂O₅ on aqueous aerosols, *J. Geophys. Res.*, *93*, 15889, 1988.
- Murcray, D. G., D. B. Barker, J. N. Brooks, A. Goldman, and W. J. Williams, Seasonal and latitudinal variation of the stratospheric concentration of HNO₃, *Geophys. Res. Lett.*, *2*, 223, 1975.
- Murcray, F. J., F. H. Murcray, C. P. Rinsland, A. Goldman, and D. G. Murcray, Infrared measurements of several nitrogen species above the South Pole in December, 1980 and November-December, 1986, submitted to *J. Geophys. Res.*, 1987.
- Murphy, D. M., A. F. Tuck, K. K. Kelly, K. R. Chan, M. Loewenstein, J. R. Podolske, M. H. Proffitt, and S. E. Strahan, 1989: Indicators of transport and vertical motion from correlations between in situ measurements in the Airborne Antarctic Ozone Experiment, *J. Geophys. Res.*, *94*, 11669, 1989.
- Nagatani, R. M., and A. J. Miller, The influence of lower stratospheric forcing on the October Antarctic ozone decrease, *Geophys. Res. Lett.*, *14*, 202, 1987.
- Nash, J., and G. F. Forrester, Long-term monitoring of stratospheric temperature trends using radiance measurements obtained by the Tiros-N series of NOAA spacecraft, *Adv. Space Res.*, *6*, 37, 1987.
- Naujokat, B., An update of the observed quasi-biennial oscillation of the stratospheric winds over the tropics, *J. Atmos. Sci.*, *43*, 1873, 1986.

POLAR OZONE

- Newman, P. A., The final warming and polar vortex disappearance during the southern hemisphere spring, *Geophys. Res. Lett.*, 13, 1228, 1986.
- Newman, P. A., and M. R. Schoeberl, October Antarctic temperature and total ozone trends from 1979 to 1985, *Geophys. Res. Lett.*, 13, 1207, 1986.
- Newman, P. A., and W. J. Randel, Coherent ozone-dynamical changes during the Southern Hemisphere spring, 1979–1986, *J. Geophys. Res.*, 93, 12585-12606, 1988.
- Newman, P. A., and M. R. Schoeberl, The break-up of the Southern Hemisphere spring polar ozone and temperature minimum from 1979 to 1987, *Polar Ozone Workshop Abstracts*, NASA Conference Publication 10014, 7, 1988.
- Newman, P. A., L. R. Lait, and M. R. Schoeberl, The morphology and meteorology of Southern Hemisphere spring total ozone mini-holes, *Geophys. Res. Lett.*, 15, 923, 1988.
- Noxon, J. F., Stratospheric NO₂ in the Antarctic winter, *Geophys. Res. Lett.*, 5, 1021, 1978.
- Noxon, J. F., Stratospheric NO₂: 2, Global behavior, *J. Geophys. Res.*, 84, 5067, 1979.
- Noxon, J. F., E. Marovich, and R. B. Norton, Effect of a major warming upon stratospheric NO₂, *J. Geophys. Res.*, 84, 7883, 1979.
- Noxon, J. F., W. R. Henderson, and R. B. Norton, Stratospheric NO₂: 3, The effects of large-scale horizontal transport, *J. Geophys. Res.*, 88, 5240, 1983.
- Oehlert, G.W., Trends in Dobson total ozone: an update through 1983, *J. Geophys. Res.*, 91, 2675, 1986.
- Oltmans, S. J., and J. London, The quasi-biennial oscillation in atmospheric ozone, *J. Geophys. Res.*, 87, 8981, 1982.
- O'Neill, A., and B. F. Taylor, A study of the major stratospheric warming of 1976/77, *Quart. J. Roy. Met. Soc.*, 105, 71, 1979.
- Ozone Trends Panel (R.T. Watson, M.J. Prather, and M.J. Kurylo et al.), *Present State of Knowledge of The Upper Atmosphere 1988: An Assessment Report*. NASA reference publ. 1208, available from the National Technical Information Service, Springfield, VA 22161, 1989.
- Parrish, A., R. L. de Zafra, M. Jaramillo, B. Connor, P.M. Solomon, and J. Barrett, Extremely low N₂O concentrations in the springtime stratosphere at McMurdo Station, Antarctica, *Nature*, 322, 53–55, 1988.
- Pick, D. R., and J. L. Brownscombe, Early results based on the stratospheric channel of TOVS on the TIROS-N series of operational satellites. International Council of Scientific Unions, Comm. Space Res., *Adv. Space Res.*, 1, 247, 1981.
- Plumb, R. A., *The Quasi-Biennial Oscillation, Dynamics of the Middle Atmosphere*, J.R. Holton and T. Matsuno, Eds., Reidel, Dordrecht, 1984.
- Plumb, R. A., and R. C. Bell, A model of the quasi-biennial oscillation on an equatorial beta plane, *Quart. J. Roy. Met. Soc.*, 108, 335, 1982.
- Podolske, J. R., M. Loewenstein, S. E. Strahan, and K. R. Chan, Stratospheric nitrous oxide distribution in the southern hemisphere, *J. Geophys. Res.*, 94, 16767, 1989.
- Pollack, J. B., and C. P. McKay, The impact of polar stratospheric clouds on the heating rates of the winter polar stratosphere, *J. Atmos. Sci.*, 42, 245, 1985.
- Pommereau, J. P., and F. Goutail, O₃ and NO₂ ground-based measurements by visible spectrometry during Arctic winter and spring, 1988, *Geophys. Res. Lett.*, 15, 891, 1988.
- Poole, L. R., Airborne lidar studies of Arctic polar stratospheric clouds, Ph.D. dissertation, University of Arizona, 1987.
- Poole, L. R., and M. P. McCormick, Airborne lidar observations of Arctic polar stratospheric clouds, Indications of two distinct growth stages, *Geophys. Res. Lett.*, 15, 21–23, 1988a.
- Poole, L. R., and M. P. McCormick, Polar stratospheric clouds and the Antarctic ozone hole, *J. Geophys. Res.*, 93, 8423–8430, 1988b.

- Poole, L. R., M. T. Osborn, and W. H. Hunt, Lidar observations of Arctic polar stratospheric clouds: Signature of small, solid particles above the frost point, *Geophys. Res. Lett.*, *15*, 867–870, 1988a.
- Poole, L. R., M. P. McCormick, E. V. Browell, C. T. Trepte, D. W. Fahey, K. K. Kelly, G. V. Ferry, R. Pueschel, and R. L. Jones, Extinction and backscatter measurements of Antarctic PSCs, 1987: Implications for particle and vapor removal, NASA CP-10014, 77–79, 1988b.
- Poole, L. R., S. Solomon, M. P. McCormick, and M. C. Pitts, Interannual variability of polar stratospheric clouds and related parameters in Antarctic during September and October, *Geophys. Res. Lett.*, *16*, 1157, 1989.
- Prather, M., M. M. Garcia, R. Suozzo, and D. Rind, Global impact of the Antarctic ozone hole: dynamical dilution with a 3-D chemical transport model, submitted to *J. Geophys. Res.*, 1989.
- Proffitt, M. H., J. A. Powell, A. F. Tuck, D. W. Fahey, K. K. Kelly, A. J. Krueger, M. R. Schoeberl, B. L. Gary, J. J. Margitan, K. R. Chan, M. Loewenstein, and J. R. Podolske, A chemical definition of the boundary of the Antarctic ozone hole, *J. Geophys. Res.*, *94*, 11437, 1989a.
- Proffitt, M. H., K. K. Kelly, J. A. Powell, M. R. Schoeberl, B. L. Gary, M. Loewenstein, J. R. Podolske, S. E. Strahan, and K. R. Chan, Evidence for diabatic cooling and poleward transport within and around the 1987 Antarctic ozone hole, *J. Geophys. Res.*, *94*, 16797, 1989b.
- Proffitt, M. H., M. J. Steinkamp, J. A. Powell, R. J. McLaughlin, O. A. Mills, A. L. Schmeltekopf, T. L. Thompson, A. F. Tuck, T. Tyler, R. H. Winkler, and K. R. Chan, In-situ ozone measurements within the 1987 Antarctic ozone hole from a high-altitude ER-2 aircraft, *J. Geophys. Res.*, *94*, 16547, 1989c.
- Pueschel, R. F., K. G. Snetsinger, J. K. Goodman, O. B. Toon, G. V. Ferry, V. R. Oberbeck, J. M. Livingston, S. Verma, W. Fong, W. L. Starr, and K. R. Chan, Condensed nitrate, sulfate and chloride in Antarctic stratospheric aerosols, *J. Geophys. Res.*, *94*, 11271, 1989.
- Quiroz, R. S., Stratospheric temperatures during solar cycle 20, *J. Geophys. Res.*, *84*, 2415, 1979.
- Ramaswamy, V., Dehydration mechanism in the Antarctic stratosphere during winter, *Geophys. Res. Lett.*, *15*, 863, 1988.
- Randel, W. J., The anomalous circulation in the Southern Hemisphere stratosphere during spring 1987, *Geophys. Res. Lett.*, *15*, 911–914, 1988.
- Randel, W. J., and P. Newman, Observations of stratospheric temperature changes coincident with the recent Antarctic ozone depletions, *Polar Ozone Workshop Abstracts*, NASA Conference Publications 10014, 10–12, 1988.
- Reinsel, G. C., G. C. Tiao, A. J. Miller, D. J. Wuebbles, P. S. Connell, C. L. Mateer, and J. L. DeLuisi, Statistical analysis of total ozone and stratospheric Umkehr data from trends and solar cycle relationship, *J. Geophys. Res.*, *92*, 2201, 1987.
- Reinsel, G. C., G. C. Tiao, S. K. Ahn, M. Pugh, S. Basu, J. L. DeLuisi, C. L. Mateer, A. J. Miller, P. S. Connell, and D. J. Wuebbles, An analysis of the 7-year record of SBUV satellite ozone data: Global profile features and trends in total ozone, *J. Geophys. Res.*, *93*, 1689, 1988.
- Ridley, B. A., M. McFarland, A. L. Schmeltekopf, M. H. Proffitt, D. L. Albritton, R. H. Winkler, and T. L. Thompson, Seasonal differences in the vertical distributions of NO, NO₂ and O₃ in the stratosphere near 50°N, *J. Geophys. Res.*, *92*, 11919, 1987.
- Rodriguez, J. M., M. K. W. Ko, and N. D. Sze, Chlorine chemistry in the Antarctic stratosphere: Impact of OClO and Cl₂O₂ and implications for observations, *Geophys. Res. Lett.*, *13*, 1292, 1986.
- Rodriguez, J. M., M. K. W. Ko, and N. D. Sze, Antarctic chlorine chemistry: possible global implications, *Geophys. Res. Lett.*, *15*, 257–260, 1988.
- Rodriguez, J. M., M. K. W. Ko, N. D. Sze, S. D. Pierce, J. G. Anderson, D. W. Fahey, K. K. Kelly, C. B. Farmer, G. C. Toon, M. T. Coffey, L. E. Heidt, W. L. Mankin, K. R. Chan, W. L. Starr, J. F. Vedder, and M. P. McCormick, Nitrogen and chlorine species in the spring Antarctic stratosphere: comparison of models with AAOE observations, *J. Geophys. Res.*, *94*, 16683, 1989.
- Rood, R. B., Global ozone minima in the historical record, *Geophys. Res. Lett.*, *13*, 1244, 1986.

POLAR OZONE

- Rosen, J. M., Simultaneous dust and ozone soundings over North and Central America, *J. Geophys. Res.*, **73**, 479, 1968.
- Rosen, J. M., D. J. Hofmann, and J. W. Harder, Aerosol measurements in the winter/spring Antarctic stratosphere, 2, Impact on polar stratospheric cloud theories, *J. Geophys. Res.*, **93**, 677-686, 1988a.
- Rosen, J. M., D. J. Hofmann, J. R. Carpenter, J. W. Harder, and S. J. Oltmans, Balloon-borne Antarctic frost point measurements and their impact on polar stratospheric cloud theories, *Geophys. Res. Lett.*, **15**, 859, 1988b.
- Rosen, J. M., S. J. Oltmans, and W. F. Evans, Balloon-borne observations of PSCs, frost point, ozone and nitric acid in the north polar vortex, *Geophys. Res. Lett.*, **16**, 791, 1989.
- Rosenfield, J. E., and M. R. Schoeberl, A computation of stratospheric heating rates and the diabatic circulation for the Antarctic spring, *Geophys. Res. Lett.*, **13**, 1339, 1986.
- Rossi, M. J., R. Malhotra, and D. M. Golden, Heterogeneous chemical reaction of chlorine nitrate and water on sulfuric acid surfaces at room temperature, *Geophys. Res. Lett.*, **14**, 127, 1987.
- Rowland, F. S., H. Sato, H. Khwaja, and S. M. Elliott, The hydrolysis of chlorine nitrate and its possible atmospheric significance, *J. Phys. Chem.*, **90**, 1985, 1986.
- Russell, J. M., S. Solomon, L. L. Gordley, E. E. Remsberg, and L. B. Callis, The variability of stratospheric and mesospheric NO₂ in the polar winter night observed by LIMS, *J. Geophys. Res.*, **89**, 7267, 1984.
- Salawitch, R. J., S. C. Wofsy, and M. B. McElroy, Chemistry of OClO in the Antarctic stratosphere: implications for bromine, *Planet. Space Sci.*, **36**, 213, 1988.
- Salawitch, R. J., G. P. Gobbi, S. C. Wofsy, and M. B. McElroy, Dentrification in the Antarctic stratosphere, *Nature*, **339**, 525, 1989.
- Sander, S. P., and R. T. Watson, Kinetics and mechanism of the disproportionation of BrO radicals, *J. Phys. Chem.*, **85**, 4000, 1981.
- Sander, S. P., and R. R. Friedl, Kinetics and product studies of ClO + BrO reaction: Implications for Antarctic chemistry, *Geophys. Res. Lett.*, **15**, 887, 1988.
- Sander, S. P., and R. R. Friedl, Kinetics and product studies of the reaction ClO + BrO using flash photolysis-ultraviolet absorption, *J. Phys. Chem.*, **90**, 4764, 1989.
- Sander, S. P., R. R. Friedl, and Y. L. Yung, Role of the ClO dimer in polar stratospheric chemistry: Rate of formation and implications for ozone loss, *Science*, **245**, 1095, 1989.
- Sanders, R. W., S. Solomon, M. A. Carroll, and A. L. Schmeltekopf, Visible and near-ultraviolet spectroscopy at McMurdo Station, Antarctica, 4. Overview and daily measurements of NO₂, O₃, and OClO during 1987, *J. Geophys. Res.*, **94**, 11381, 1989.
- Schmeltekopf, A. L., D. L. Albritton, P. J. Crutzen, P. D. Goldan, W. J. Harrop, W. R. Henderson, J. R. McAfee, M. McFarland, H. I. Schiff, T. L. Thompson, D. J. Hofmann, and N. T. Kjome, Stratospheric nitrous oxide altitude profiles at various latitudes, *J. Atmos. Sci.*, **34**, 729, 1977.
- Schmidt, U., R. Bauer, A. Khedim, E. Klein, G. Kulessa, and B. Schubert, In-situ observations of long-lived trace gases in the arctic stratosphere during winter, in *Proceedings of the Quadrennial Ozone Symposium*, 8-13 Aug, 1988, Gottingen, FRG, 1989.
- Schoeberl, M. R., A. J. Krueger, and P. A. Newman, The morphology of the Antarctic total ozone as seen by TOMS, *Geophys. Res. Lett.*, **13**, 1217, 1986.
- Schoeberl, M. R., R. S. Stolarski, and A. J. Krueger, The 1988 Antarctic ozone depletion. Comparison with previous year depletions, *Geophys. Res. Lett.*, **16**, 377-380, 1989.
- Schwentek, H., The sunspot cycle 1958/70 in ionospheric absorption and stratospheric temperature, *J. Atmos. Terr. Phys.*, **33**, 1829, 1971.
- Sekiguchi, Y., Antarctic ozone change correlated to the stratospheric temperature field, *Geophys. Res. Lett.*, **13**, 1202, 1986.
- Sekiguchi, Y., Ozone and stratospheric temperature change in Antarctica correlated to solar activity, *Proceedings of the Quadrennial Ozone Symposium*, Gottingen, FRG, 1989.

- Shi, G. Y., W. C. Wang, and M. K. W. Ko, Radiative heating due to stratospheric aerosols over Antarctica, *Geophys. Res. Lett.*, *13*, 1335, 1986.
- Shibasaki, K., N. Iwagami, and T. Ogawa, Stratospheric nitrogen dioxide observed by ground-based and balloon borne techniques at Syowa Station, *Geophys. Res. Lett.*, *13*, 1268, 1986.
- Shine, K. P., On the modelled thermal response of the Antarctic stratosphere to a depletion of ozone, *Geophys. Res. Lett.*, *13*, 1331, 1986.
- Shine, K. P., Comment on "Southern hemisphere temperature trends: A possible greenhouse effect," *Geophys. Res. Lett.*, *15*, 843–848, 1988.
- Simon, F. G., J. P. Burrows, W. Schneider, G. K. Moortgat, and P. J. Crutzen, Study of the reaction $\text{ClO} + \text{CH}_3\text{O}_2 \rightarrow \text{products}$ at 300 K, *J. Phys. Chem.*, in press, 1989.
- Simon, P. C., Solar irradiance between 120–400 nm and its variations, *Solar Phys.*, *74*, 273, 1981.
- Solomon, P. M., B. Connor, R. L. de Zafra, A. Parrish, J. Barrett, and M. Jaramillo, High concentrations of chlorine monoxide at low altitudes in the Antarctic spring stratosphere: Secular variation, *Nature*, *328*, 411, 1987.
- Solomon, S., The mystery of the Antarctic ozone hole, *Rev. Geophys.*, *26*, 131, 1988.
- Solomon, S., and R. R. Garcia, Simulation of NO_x partitioning along isobaric parcel trajectories, *J. Geophys. Res.*, *88*, 5497, 1983.
- Solomon, S., R. R. Garcia, F. S. Rowland, and D. J. Wuebbles, On the depletion of Antarctic ozone, *Nature*, *321*, 755, 1986.
- Solomon, S., G. H. Mount, R. W. Sanders, and A. L. Schmeltekopf, Visible spectroscopy at McMurdo Station, Antarctica, 2. Observations of OClO, *J. Geophys. Res.*, *92*, 8329, 1987.
- Solomon, S., G. H. Mount, R. W. Sanders, R. O. Jakoubek, and A. L. Schmeltekopf, Observations of the nighttime abundance of OClO in the winter stratosphere above Thule, Greenland, *Science*, *242*, 550, 1988.
- Solomon, S., R. W. Sanders, M. A. Carroll, and A. L. Schmeltekopf, Visible and near-ultraviolet spectroscopy at McMurdo Station, Antarctica, 5. Observations of the diurnal variations of OClO and BrO, *J. Geophys. Res.*, *94*, 11393, 1989.
- Stanford, J. L., and J. S. Davis, A century of stratospheric cloud reports: 1870–1972, *Bull. Am. Met. Soc.*, *55*, 213, 1974.
- Steele, H. M., P. Hamill, M. P. McCormick, and T. J. Swissler, The formation of polar stratospheric clouds, *J. Atmos. Sci.*, *40*, 2055, 1983.
- Stolarski, R. S., and R. J. Cicerone, Stratospheric chlorine: A possible sink for ozone, *Can. J. Chem.*, *52*, 1610, 1974.
- Stolarski, R. S., A. J. Krueger, M. R. Schoeberl, R. D. McPeters, P. A. Newman, and J. C. Alpert, Nimbus 7 satellite measurements of the springtime Antarctic ozone decrease, *Nature*, *322*, 808, 1986.
- Stolarski, R. S., and M. R. Schoeberl, Further interpretation of satellite measurements of Antarctic total ozone, *Geophys. Res. Lett.*, *13*, 1210, 1986.
- Stordal, F., I. S. A. Isaksen, and K. Hornveth, A diabatic circulation two-dimensional model with photochemistry: Simulations of ozone and long-lived tracers with surface sources, *J. Geophys. Res.*, *90*, 5757, 1985.
- Sze, N. D., M. K. W. Ko, D. K. Weisenstein, J. M. Rodriguez, R. S. Stolarski, and M. R. Schoeberl, Antarctic ozone hole: possible implications for ozone trends in the Southern Hemisphere, *J. Geophys. Res.*, *94*, 11521, 1989.
- Tarasenko, D. A., Structure and circulation of the stratosphere and mesosphere in the Northern Hemisphere, pp. 287, Hydrometizdat, Leningrad, 1988.
- Thomas, R. J., K. H. Rosenlof, R. T. Clancy, and J. M. Zawodny, Stratospheric NO_2 over Antarctica as measured by the Solar Mesosphere Explorer during austral spring, 1986, *J. Geophys. Res.*, *93*, 12561, 1988.

POLAR OZONE

- Tolbert, M. A., M. J. Rossi, R. Malhotra, and D. M. Golden, Reaction of chlorine nitrate with hydrogen chloride and water at Antarctic stratospheric temperatures, *Science*, 238, 1258, 1987.
- Tolbert, M. A., M. J. Rossi, and D. M. Golden, Heterogeneous interactions of ClONO₂, HCl, and HNO₃ with sulfuric acid surfaces at stratospheric temperatures, *Geophys. Res. Lett.*, 15, 851–854, 1988a.
- Tolbert, M. A., M. J. Rossi, and D. M. Golden, Antarctic ozone depletion chemistry: Reactions of N₂O₅ with H₂O and HCl on ice surfaces, *Science*, 240, 1018, 1988b.
- Toohey, D. W., W. H. Brune, and J. G. Anderson, Chemistry of the Antarctic stratosphere: Reactions of ClO and BrO. Paper presented at the Eighteenth International Symposium on Free Radicals, Oxford, England, September 10–15, 1987.
- Toohey, D. W., and J. G. Anderson, On the formation of BrCl in the reaction of BrO with ClO, *J. Phys. Chem.*, 92, 1705, 1988.
- Toon, G. C., and C. B. Farmer, Detection of HOCl in the Antarctic stratosphere, *Geophys. Res. Lett.*, 16, 1375, 1989.
- Toon, G. C., C. B. Farmer, L. L. Lowes, P. W. Schaper, J.-F. Blavier, and R. H. Norton, Infrared measurements of stratospheric composition over Antarctica during September 1987, *J. Geophys. Res.*, 94, 16571, 1989a.
- Toon, G. C., C. B. Farmer, P. W. Schaper, J.-F. Blavier, and L. L. Lowes, Ground-based infrared measurements of tropospheric source gases over Antarctica during 1986 austral spring, *J. Geophys. Res.*, 94, 11613, 1989b.
- Toon, O. B., P. Hamill, R. P. Turco, and J. Pinto, Condensation of HNO₃ and HCl in the winter polar stratosphere, *Geophys. Res. Lett.*, 13, 1284, 1986.
- Toon, O. B., R. Turco, and J. Jordan, Physical processes in polar stratospheric ice clouds. *Polar Ozone Workshop Abstracts*, 90–94, NASA Conference Publications 10014, 1988.
- Toon, O. B., R. P. Turco, J. Jordan, J. Goodman, and G. Ferry, Physical processes in polar stratospheric ice clouds, *J. Geophys. Res.*, 94, 11359, 1989.
- Trenberth, K. E., and J. G. Olson, Temperature trends at the South Pole and McMurdo Sound, in press, *J. Climate*, 1989.
- Trodahl, H. J., and R. G. Buckley, Ultraviolet levels under sea ice during the Antarctic spring, *Science*, 245, 194, 1989.
- Trolier, M., R. L. Mouldin, and A. R. Ravishankara, The rate coefficient for the termolecular channel of the self-reaction of ClO, submitted to *J. Phys. Chem.*, 1989.
- Tuck A. F., Synoptic and chemical evolution of the Antarctic vortex in late winter and early spring, 1987: An ozone processor, *J. Geophys. Res.*, 94, 11687, 1989.
- Tuck, A. F., R. T. Watson, E. P. Condon, and J. J. Margitan, The planning and execution of ER-2 and DC-8 aircraft flights over Antarctica, August and September, 1987, *J. Geophys. Res.*, 94, 11182, 1989.
- Tung, K. K., On the relationship between the thermal structure of the stratosphere and the seasonal distribution of ozone, *Geophys. Res. Lett.*, 13, 1308, 1986.
- Tung, K. K., M. K. W. Ko, J. M. Rodriguez, and N. D. Sze, Are Antarctic ozone variations a manifestation of dynamics or chemistry?, *Nature*, 333, 811, 1986.
- Tung, K. K., and H. Yang, Dynamic variability of column ozone, *J. Geophys. Res.*, 93, 11123, 1988a.
- Tung, K. K., and H. Yang, Dynamical component of seasonal and year-to-year changes in Antarctic and global ozone, *J. Geophys. Res.*, 93, 12537, 1988b.
- Turco, R. P., R. C. Whitten, and O. B. Toon, Stratospheric aerosols: Observations and theory, *Rev. Geophys. Space Phys.*, 20, 233, 1982.
- Turco, R. P., O. B. Toon, and P. Hamill, Heterogeneous physicochemistry of the polar ozone hole, *J. Geophys. Res.*, 94, 16493, 1989.
- Vaida, V., S. Solomon, E. C. Richard, E. Ruehl, and A. Jefferson, Photoisomerisation of OCIO: A polar ozone depletion mechanism, *Nature*, 342, 405, 1989.

- van Loon, H., and K. Labitzke, The southern oscillation, Part V: The anomalies in the lower stratosphere of the Northern Hemisphere in winter and a comparison with the quasi-biennial oscillation, *Mon. Wea. Rev.*, *115*, 357, 1987.
- Wahner, A., G. Tyndall, and A. R. Ravishankara, Absorption cross sections for OCIO as a function of temperature in the wavelength range from 240–480 nm, *J. Chem. Phys.*, *91*, 2734, 1987.
- Wahner, A., R. O. Jakoubek, G. H. Mount, A. R. Ravishankara, and A. L. Schmeltekopf, Remote sensing of daytime column NO₂ during the airborne Antarctic ozone experiment, *J. Geophys. Res.*, *94*, 16619, 1989a.
- Wahner, A., R. O. Jakoubek, G. H. Mount, A. R. Ravishankara, and A. L. Schmeltekopf, Remote sensing observations of nighttime OCIO column during the airborne Antarctic ozone experiment, *J. Geophys. Res.*, *94*, 11405, 1989b.
- Watson, L. R., J. M. Van Doren, P. Davidovits, D. R. Worsnop, M. S. Zahniser, and C. E. Kolb, Uptake of HCl molecules by aqueous sulfuric acid droplets as a function of acid concentration, submitted to *J. Geophys. Res.*, 1989.
- Watterson, I.G., and A.F. Tuck, A comparison of the longitudinal distributions of polar stratospheric clouds, total column ozone and temperatures for the 1987 Antarctic spring, *J. Geophys. Res.*, *94*, 16511, 1989.
- Williams, W. J., J. J. Kusters, and D. G. Murcray, Nitric acid column densities over Antarctica, *J. Geophys. Res.*, *87*, 8976, 1982.
- WMO, Atmospheric Ozone 1985: Assessment of Our Understanding of the Processes Controlling Its Present Distribution and Change, *WMO Report No. 16*, Sponsored by WMO, NASA, NOAA, FAA, UNEP, CEC, and BMFT, Washington, D.C., 1986.
- Wofsy, S. C., Temporal and latitudinal variations of stratospheric trace gases: A critical comparison between theory and experiment, *J. Geophys. Res.*, *83*, 364, 1978.
- Wofsy, S. C., M. J. Molina, R. J. Salawitch, L. E. Fox, and M. B. McElroy, Interactions between HCl, NO_x and H₂O ice in the Antarctic stratosphere: implications for ozone, *J. Geophys. Res.*, *93*, 2442–2450, 1988.
- Wolff, E. W., R. Mulvaney, and K. Oates, Diffusion and location of hydrochloric acid in ice: Implications for polar stratospheric clouds and ozone depletion, *Geophys. Res. Lett.*, *16*, 487, 1989.
- Wuebbles, D. J., F. M. Luther, and J. E. Penner, Effect of coupled anthropogenic perturbations on stratospheric ozone, *J. Geophys. Res.*, *88*, 1444, 1983.
- Yamazaki, K.: Observations of stratospheric final warmings in the two hemispheres, *J. Met. Soc. Japan*, *65*, 51–65, 1987.
- Yung, Y. L., J. P. Pinto, R. T. Watson, and S. P. Sander, Atmospheric bromine and ozone perturbations in the lower stratosphere, *J. Atmos. Sci.*, *37*, 339, 1980.
- Zawodny, J. M., Short-term variability of nitrogen dioxide in the winter stratosphere, *J. Geophys. Res.*, *91*, 5439, 1986.
- Zeller, E. J., G. A. M. Dreschoff, and C. M. Laird, Nitrate flux on the Ross ice shelf, Antarctica, and its relation to solar cosmic rays, *Geophys. Res. Lett.*, *13*, 1264, 1986.